PHYSICO-CHEMICAL CHARACTERIZATION OF ATROPINESTERASE FROM PSEUDOMONAS PUTIDA

A comparison with other serine hydrolases

STELLINGEN

1. De suggestie van Mueller en Burchard dat het verschil in de afmetingen van fibrinogeen, zoals die zijn bepaald enerzijds door middel van lichtverstrooiing en anderzijds met behulp van andere technieken, kan worden toegeschreven aan de binding van Ca^{2+}-ionen, is niet juist.

Mueller, M. en Burchard, W. (1978) Biochim. Biophys. Acta 537, 208.
Van der Drift, A.C.M., Poppema, A., Haverkate, F. en Nieuwenhuizen, W. (1983) in Fibrinogen. Structure, functional aspects, metabolism. (Haverkate, F., Henschen, A., Nieuwenhuizen, W. en Straub, P.W., Eds.) p. 3, Walter de Gruyter, Berlin.

2. De conclusies van Russell en Bennett met betrekking tot de relatieve sterkte van -35 en -10 gebieden van de door hen onderzochte promotoren zijn voorbarig.

Russell, D.R. en Bennett, G.N. (1982) Gene 20, 231.
De Boer, H.A., Comstock, L.J. en Vasser, M. (1983) Proc. Natl. Acad. Sci. USA 80, 21.
Enger-Valk, B.E. (1981) Proefschrift, Landbouwhogeschool Wageningen.

3. Bij de bestudering van het effect van glycoproteïnen op de permeabiliteit van modelmembranen houden Neitchev en Desbals onvoldoende rekening met mogelijke fusie- en aggregatieverschijnselen.

Neitchev, V.Z. en Desbals, B.P. (1983) Int. J. Biochem. 15, 159.

4. Ten onrechte noemen Brossmer et al. hun affiniteitschromatografische zuiveringsmethode selectief voor neuraminidase.

Brossmer, R., Ziegler, D. en Keilich, G. (1977) Hoppe-Seyler's Z. Physiol. Chem. 358, 397.

5. De bewijsvoering die door Meise-Gresch en Müller-Warmuth wordt gebruikt om de door hen gevonden positieve Li-DNP-versterkingsfactoren in het systeem Li-o-dimesitoylbenzeen/$LiBH_4$ toe te schrijven aan een interne beweging in het Li-o-dimesitoylbenzeen-ionenpaar is hoogst aanvechtbaar.

Meise-Gresch, K. en Müller-Warmuth, W. (1979) Ber. Bunsenges. physik. Chem. 83, 586.

6. De door Okon et al. beschreven arylering van pyridine-2-aldoxim in ether met behulp van 2,4-dinitrobenzeen is niet juist.

Okon, K., Grochowski, J.W., Waclawek, W. en Zieba, J. (1963) Biul. Wojskowej Akad. Tech. 12(130), 25.

7. De conclusie van Clement dat de veroudering van met soman geremd acetylcholinesterase in het diafragma van de rat relatief langzaam verloopt, wordt onvoldoende door de experimentele resultaten ondersteund.

Clement, J.G. (1982) Biochem. Pharmac. 31, 1283.

8. De door Allenmark et al. gerapporteerde zuivering van lysophospholipase is in tegenspraak met de door hen verstrekte experimentele gegevens.

Allenmark, S., Sjödahl, E., Sjödahl, R. en Tagesson, C. (1980) Prep. Biochem. 10(4), 463.

9. De experimentele resultaten, op grond waarvan Marguerie en Ardaillou concluderen dat de twee C-terminale uiteinden van de Aα-ketens van fibrinogeen betrokken zijn bij de binding van een Ca^{2+}-ion, zijn onvoldoende om deze conclusie te rechtvaardigen.

Marguerie, G. en Ardaillou, N. (1982) Biochim. Biophys. Acta 701, 410.
Nieuwenhuizen, W. en Gravesen, M. (1981) Biochim. Biophys. Acta 668, 81.

10. De conclusie van Wiltzius et al. dat in de beginfase van de fibrine-polymerisatie de monomeren slechts "end-to-end"-associatie vertonen, is aanvechtbaar.

Wiltzius, P., Hofmann, V., Straub, P.W. en Känzig, W. (1981) Biopolymers 20, 2035.
Wiltzius, P., Dietler, G. Känzig, W., Häberli, A. en Straub, P.W. (1982) Biopolymers 21, 2205.

11. Het verdient aanbeveling om het geneeskundig onderzoek door een arts, dat verplicht is voor 60-jarigen en ouderen om verlenging van hun rijbewijs te kunnen krijgen, te vervangen door een rijvaardigheidstest met een verkeerssimulator.

12. Het dragen van klompen door parlementariërs tijdens kamerdebatten zal in belangrijke mate aan de politieke duidelijkheid ten goede komen.

Stellingen behorend bij het proefschrift "Physico-chemical characterization of Atropinesterase from Pseudomonas putida. A comparison with other serine hydrolases".

A.C.M. van der Drift

Utrecht, 8 juni 1983

PHYSICO-CHEMICAL CHARACTERIZATION OF ATROPINESTERASE FROM PSEUDOMONAS PUTIDA

A comparison with other serine hydrolases

PROEFSCHRIFT

TER VERKRIJGING VAN DE GRAAD VAN DOCTOR IN DE WISKUNDE EN NATUURWETENSCHAPPEN AAN DE RIJKSUNIVERSITEIT TE UTRECHT, OP GEZAG VAN DE RECTOR MAGNIFICUS PROF. DR. O.J. DE JONG, VOLGENS BESLUIT VAN HET COLLEGE VAN DECANEN IN HET OPENBAAR TE VERDEDIGEN OP WOENSDAG 8 JUNI 1983 DES NAMIDDAGS TE 4.15 UUR

DOOR

ALPHONSUS CORNELIS MARIE VAN DER DRIFT

GEBOREN OP 29 OKTOBER 1940 te OEGSTGEEST

1983
DRUKKERIJ J.H. PASMANS B.V., 's-GRAVENHAGE

Promotores: Prof. Dr. G.H. de Haas
Prof. Dr. Ir. J. Smidt (Technische Hogeschool Delft)
Prof. Dr. C. Veeger (Landbouwhogeschool Wageningen)

In herinnering aan mijn vader

Aan mijn moeder

Voor Mieke

„Que sçay-je?"

M. de Montaigne

CONTENTS

CHAPTER 5
COMPARISON OF THE ACTIVE SITES OF ATROPINESTERASE AND SOME SERINE PROTEASES BY SPIN LABELLING

CHAPTER 6
^{31}P NMR AND MASS SPECTROMETRY OF ATROPINESTERASE AND SOME SERINE PROTEASES PHOSPHORYLATED WITH A TRANSITION-STATE ANALOGUE

Since the various chapters have been written as separate papers to be submitted for publication in journals, they are mentioned in the lists of references with the names of all authors.

CONCISE LIST OF SYMBOLS AND ABBREVIATIONS (not explained in the text)

Amino acids

Ala - alanine
Asn - asparagine
Asp - aspartic acid
Glu - glutamic acid
Gly - glycine
His - histidine
Leu - leucine
Met - methionine
Ser - serine
Thr - threonine
Trp - tryptophan

A_{280} - absorbance of 1.0 at 280 nm

B - static magnetic field

D - Debye unit

EC - number given by the Commission on Enzymes
ESR - electron spin resonance
EtOAc - ethyl acetate
$E^{0.1\%}_{280}$ - extinction coefficient (cm^{-1}) at 280 nm of an aqueous solution containing 1 mg of protein/ml

GHz - gigahertz

Hz - hertz

IR - infrared

K - Kelvin
kHz - kilohertz

M - molecular weight
MHz - megahertz
mp - melting point
mT - millitesla

NMR - nuclear magnetic resonance

OEt - ethyl ester group
^{32}P - radioactive isotope of phosphorus
ppm - parts per million

R_F - retardation factor
r.p.m. - revolutions per minute

s.e.(m.) - standard error (of the mean)

UV - ultraviolet
v/v - on the basis of volumes

GENERAL INTRODUCTION

Enzymic Catalysis

Enzymes are proteins which function as catalysts of biochemical reactions. Analogous to non-enzymic catalysts they shift the pathway of a particular reaction to a more favourable one with a lower standard free energy of activation (Westley, 1969). However, the pathway of a biochemical reaction is different for catalysis by an enzyme and catalysis by another type of catalyst (Kosower, 1962). Compared with non-enzymic catalysts an enzyme is more efficient and very specific for its substrate, i.e. the molecule to be chemically modified (Mahler and Cordes, 1966; Westley, 1969). These special features of enzymes are due to specific interactions between the enzyme molecule and its substrate, which are determined by the chemical and the spatial properties of both components.

To explain this so-called structure-activity relationship of enzymes, a variety of theories has been proposed in which the molecular complementarity or matching of enzyme and substrate is viewed as due to either static or dynamic properties of the conformation of one or both components (Kosower, 1962; Jencks, 1969; Westley, 1969; Koshland, 1973; Johnson et al., 1974). Most of the proposals have a limited validity as they over-emphasize one particular factor of the catalytic process. A generally applicable conceptual framework for the description of the molecular dynamics underlying the relation between the structure of an enzyme and its activity is provided by the transition-state theory (Lienhard, 1973; Kraut, 1977). Basically, this theory states that a chemical reaction, while progressing along the path of the lowest attainable potential energy, proceeds through an activated complex, a transient molecular adduct of the reactants in the state of the highest potential energy along the reaction coordinate. In this so-called transition state the activated complex is in an unstable or quasi-equilibrium with the reactants in their normal states (Wolfenden, 1972; Lienhard, 1973; Johnson et al., 1974; Kraut, 1977). According to this description the catalytic efficiency and the

specificity of an enzyme are due to special features of its three-dimensional structure or conformation which promote it to act as a matrix for stabilizing the activated complex of enzyme and substrate, by various types of interactions. Apart from structural factors, this facilitation of binding of the substrate in the transition state may also be promoted by the solvent (Lienhard, 1973). The resulting stabilization of the activated complex increases its lifetime and thus its effective concentration, leading to an enhancement of the reaction rate (Johnson et al., 1974; Kraut, 1977). The limited domain of the protein structure directly involved in this transient binding and the chemical transformation is situated at the protein surface and is generally called the active site or active centre of the enzyme (Kosower, 1962). Topologically, various subsites can be discerned within this region, each involved in a specific interaction during the catalytic process.

Serine Proteases and Serine Esterases

Enzymes may be classified according to the type of reaction they catalyse (Mahler and Cordes, 1966; IUB, 1979). The class of hydrolases includes all enzymes catalysing the hydrolysis of chemical bonds. On the basis of the type of bond hydrolysed various subclasses can be distinguished, like the peptide hydrolases acting on peptide bonds in peptides and proteins and the ester hydrolases or esterases acting on ester bonds. A further refinement of this classification can be made when bonds in particular substrates are taken into account. Sometimes, however, such a sharp distinction cannot be made since various enzymes may act on more than one type of bond (IUB, 1979).

Proteinases (also called proteases) are peptide hydrolases acting on proteins as their natural substrates (Fruton, 1975). Within this sub-sub-class the so-called serine proteases form a large group. These proteolytic enzymes are widely spread in nature with a diversity of functions (Hartley, 1970[b]; Walsh and Wilcox, 1970; Walsh, 1975; Blow, 1976). Besides their proteolytic activity they show esterolytic activity towards appropriate esters (Glazer, 1967; Walsh and Wilcox, 1970;

IUB, 1979). They are characterized by the presence of one particular serine residue at the active site (the so-called active serine). Presumably because of its proper orientation, the hydroxyl group in the side chain of this serine behaves as an unusually strong nucleophile (Hartley, 1960; Matthews et al., 1977). It can specifically react with various types of electrophilic reagents leading to its transient acylation when substrates are involved (Balls and Wood, 1956; Oosterbaan and Van Adrichem, 1958) or to a more permanent phosphorylation (Dixon and Webb, 1964; Baker, 1975) or sulphonylation (Hartley and Massey, 1956; Fahrney and Gold, 1963), resulting in inhibition of the hydrolase activity. Under appropriate conditions some of these covalently bound groups can be displaced from the active site, leading to restoration of enzymic activity, i.e. reactivation (Cf. Berends, 1964; de Jong, 1978).

Within the group of serine proteases several sub-groups, called families, can be distinguished the members of which usually show more than 50% homology in their primary structure and consequently also an appreciable resemblance in their three-dimensional structure (Dayhoff, 1969; Walsh and Wilcox, 1970; Dayhoff et al., 1978). A homology of 20% or more between enzymes with a comparable function is generally considered to indicate the descent from a common ancestral prototype enzyme as the result of a divergent molecular evolution. Because of such an evolutionary relationship, some families have been grouped together into so-called superfamilies (Dayhoff et al., 1978). At present two superfamilies of serine proteases are known. The superfamily of the prothrombin-related serine proteases includes digestive enzymes such as trypsin, α-chymotrypsin and their parent inactive precursors (zymogens or pro-enzymes) trypsinogen and chymotrypsinogen and enzymes involved in blood coagulation and fibrinolysis such as thrombin and plasmin. The other superfamily comprises the bacterial subtilisins, e.g. subtilisin A (Subtilisin Carlsberg). Members of these two superfamilies have been extensively studied (Stroud et al., 1975; Blow, 1976; Kraut, 1977; Markley, 1979). As a result the relation between

their three-dimensional structure and catalytic activity is known in much more detail than for any other group of enzymes.

Analogous to the serine proteases there are also serine esterases with a highly reactive serine side chain at the active site, for example various cholinesterases and carboxylesterases. These enzymes are less well investigated than the serine proteases, mainly due to their limited availability. The same electrophilic reagents that inhibit the serine proteases may also inhibit the esterases due to specific reaction with the serine side chain. In particular the phosphorylation by stoichiometric reaction with diisopropyl phosphorofluoridate (DFP) is considered a typical identification criterion for serine proteases and serine esterases (Hartley, 1960).

Serine proteases and serine esterases are connoted collectively as serine hydrolases or, sometimes, as serine enzymes (Hartley et al., 1972).

Reaction Sequence of the Hydrolysis by Serine Proteases

Despite the absence of homology in primary structure among the two superfamilies of serine proteases, the mechanisms of their proteolytic and esterolytic activity show close resemblance because of a similarity in certain features of their otherwise different three-dimensional structure (Hartley et al., 1972; Stroud et al., 1975). A general scheme for the sequence of reactions and the various intermediates involved in the hydrolysis of peptide and ester bonds by these enzymes is shown in Figure 1 (Stroud et al., 1975; Kraut, 1977). Two mutually symmetric series of events can be distinguished: the acylation and deacylation. As a first step in the acylation, enzyme and substrate reversibly associate after encounter to a stable so-called Michaelis complex with a dissociation constant $K = k_{-1}/k_{+1}$. The subsequent formation of a covalent bond between the carbonyl carbon atom of the bond to be hydrolysed in the substrate and the $O\gamma$ atom of the serine side chain by nucleophilic substitution proceeds through the tetrahedral transition-state intermediate in which a proton is partially transferred from the $O\gamma$ to the leaving group X of the

substrate. After completion of this proton transfer the tetrahedral intermediate breaks down into the acylated enzyme and HX. The subsequent regeneration of the active enzyme by deacylation of the acyl-enzyme is mechanistically the reverse of the acylation except that a water molecule replaces HX. The net result of acylation and deacylation consists of an acyl transfer from substrate to water (IUB, 1979).

Structural Basis of the Catalytic Activity of Serine Proteases

The evidence for the scheme in Figure 1 comes in particular from kinetic and structural investigations of the proteases trypsin, α-chymotrypsin and their zymogens trypsinogen and α-chymotrypsinogen, as well as of subtilisin A (Cf. Stroud et al., 1975). The results of these studies strongly suggest (Blow, 1976; Kraut, 1977) that serine proteases catalyse proteolytic and esterolytic reactions because their

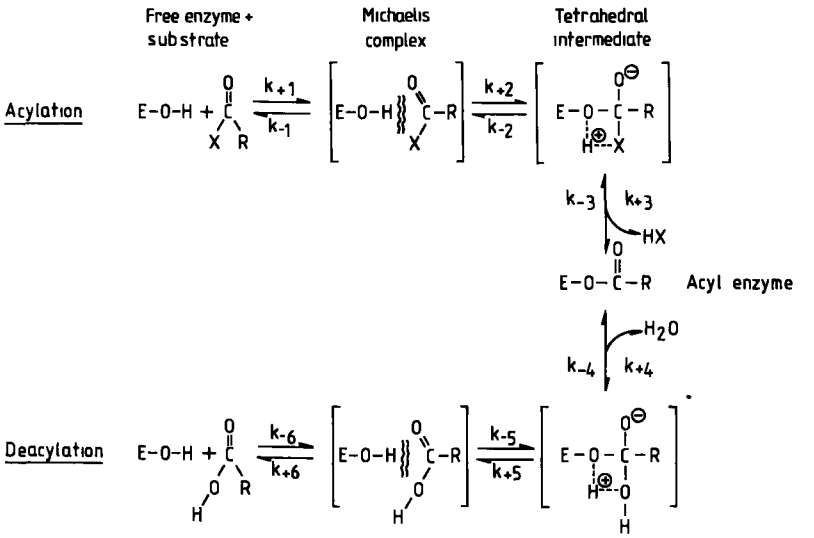

FIGURE 1: General scheme for the reaction sequence of serine proteases (Cf. Kraut, 1977). The enzyme is represented by E-O-H, where -O-H denotes the hydroxyl group of the side chain of the active serine. The substrate is denoted by $\overset{X}{\underset{R}{\diagdown}}C{=}O$, where X is the leaving group.

three-dimensional structure allows them to act as a transient mould for fixing the so-called tetrahedral intermediate, the activated complex occurring during the acyl transfer, in which the covalently bound carbonyl carbon atom is in a tetrahedral configuration. This rate-limiting stabilization of the tetrahedral intermediate is assumed to be due to the concerted action of a restricted number of structural elements in the active-site region, which serve as "binding sites" for the substrate during the catalytic process (Blow, 1976; Kraut, 1977).

Studies on both active and inhibited enzymes show that the active serine is part of a so-called charge-relay system (Blow, 1976; Kraut, 1977). This catalytic unit, schematically represented in Figure 2, participates in the electronic rearrangements leading to hydrolysis of the substrate's covalent bond; it consists of an invariable triad of amino-acid residues, i.e. an aspartic acid, a histidine and the active serine, which are relatively far apart along the amino-acids backbone (primary structure) but the side chains of which are within hydrogen-bonding distances in the tertiary structure. For α-chymotrypsin and closely related enzymes these residues are Ser(195), His(57) and Asp(102) (Blow et al., 1969), whereas for subtilisin these are Ser(221), His(64) and Asp(32) (Wright et al., 1969; Alden et al., 1970). An unprotonated imidazole side chain of the histidine is considered a prerequisite for enzymic activity (Cf. Glazer, 1967), as serine proteases are inactive at low pH when this site is fully protonated. In the cases studied so far a strong hydrogen bond with normal geometry is found between the Nδ1 (also denoted as Nπ or N1) of this imidazole side chain and an oxygen of the β-carboxyl group of the aspartic acid residue which is buried in a mainly hydrophobic environment shielded from the solvent. In general, hydrogen bonding between the solvent-exposed Nε2 (also denoted as Nτ or N3) of the histidine and the Oγ of the serine seems unlikely in native enzymes; whether in particular cases the binding of a substrate or ligand may promote the formation of such a hydrogen bond is not clear yet (Cruickshank and Kaplan, 1975; Matthews et al., 1977; Huber and Bode, 1978). During acylation the proton of the serine hydroxyl group is transferred to

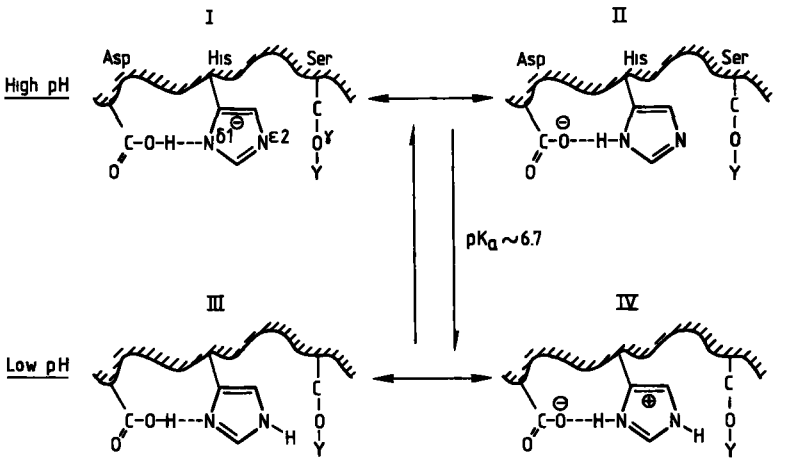

FIGURE 2: Ionization scheme of the charge-relay system in serine proteases (Cf. Cruickshank et al., 1975). I and II denote the canonical forms of the deprotonated system, III and IV that of the protonated system. Y = H in the native enzyme, and Y = $_{R}\!\!>$C=O in the acyl-enzyme. The pK$_a$ indicated is that found for α-chymotrypsin and subtilisin at room temperature (Cf. Cunningham and Brown, 1956; Glazer, 1967).

the leaving group via temporary binding by the Nε2 of the histidine-aspartic acid couple; in the deacylation this unit transfers a proton from the attacking nucleophile, a water molecule, to the leaving serine via a tetrahedral intermediate. The contributions of the various canonical forms of the charge-relay system (Figure 2) to catalysis are still a matter of some dispute (Cf. Cruickshank and Kaplan, 1975). Originally it has been suggested that the histidine-aspartic acid couple, while temporarily acting as binding site for the transferable proton, provides the "charge relay" by a concomitant proton transfer from Nδ1 to the aspartic acid, leaving the histidine unionized (Hunkapiller et al., 1973; Koeppe and Stroud, 1976). However, evidence is accumulating that the histidine may act as a transient cationic acid (Cruickshank and Kaplan, 1975; Bachovchin and Roberts, 1978; Kossiakoff and Spencer, 1981).

In the nearly inactive precursors trypsinogen and α-chymotrypsinogen the charge-relay system is found in a form more favourable to

hydrogen bonding between Nε2 and Oγ than in the corresponding active enzymes. Therefore, other structural elements must be essential to enzymic catalysis which are different for enzyme and proenzyme (Blow, 1976). These are the substrate binding site and the oxy-anion hole, the two main elements involved in the primary interaction between enzyme and substrate.

The substrate binding site immediately adjacent to the active serine provides for the proper binding of the amino-acid residues P_1-P_2-P_3 next to the bond to be cleaved in the acylating part of the polypeptide substrate (P_1 being the residue preceding the scissile bond). This part extends from the bond to be hydrolysed towards the NH_2-terminus. The main types of interactions involved in this acyl-binding are hydrophobic interaction and hydrogen bonding of P_1-P_2-P_3 with three amino-acid residues of the enzyme, denoted as S_1-S_2-S_3, but sometimes also ionic (electrostatic) interactions may contribute substantially. The interaction of the side chain of P_1 with the enzyme is always the dominant contribution and provides largely for the proper orientation of the hydrolysable bond with respect to the charge-relay system. In both superfamilies of serine proteases this binding of the P_1-side chain occurs in a rigid, well-developed crevice in the enzyme surface, the primary substrate specificity pocket, one side of which is formed by the planar arrangement of the peptide bonds of the amino-acid residues S_1-S_2-S_3, e.g. Ser(214)-Trp(215)-Gly(216) in α-chymotrypsin and Ser(125)-Leu(126)-Gly(127) in subtilisin A (Kraut, 1977). Depending on the size and charge of this apolar pocket, hydrophobic and/or ionic interactions contribute to this binding. Effective hydrophobic interaction occurs only with the side chains of certain hydrophobic amino-acid residues preceding the scissile bond. The geometry of the pocket thus determines mainly the specificity of the enzyme (Hartley, 1970[a]; Walsh and Wilcox, 1970; Stroud et al., 1975). In α-chymotrypsin the specificity pocket is geometrically well-defined and preferentially accommodates planar aromatic side chains, in subtilisin it is less defined and binds other types of side chains at P_1 equally well. Therefore, subtilisin is generally less specific towards sub-

strates than α-chymotrypsin which primarily catalyses the hydrolysis of peptide and ester bonds adjacent to the carbonyl group of aromatic amino-acid residues (Walsh and Wilcox, 1970; Fruton, 1975). The preference of trypsin for peptide bonds following the positively charged side chains of arginine and lysine is due to the presence of a negatively charged aspartate residue at the bottom of the specificity pocket which otherwise resembles that of chymotrypsin (Hartley, 1970[a]). One of the main differences between proenzymes and their corresponding active enzymes resides in a less well-developed specificity pocket of the substrate binding site (Freer et al., 1970. Kossiakoff et al., 1977).

Apart from permitting hydrophobic and possible ionic interactions in the specificity pocket, the folding of the enzyme backbone at the substrate binding site effects the formation of an antiparallel β-pair hydrogen-bonded structure with the backbone of the acylating polypeptide chain of the substrate. The number of hydrogen bonds involved and the length of the hydrogen-bonded structure vary from enzyme to enzyme. In trypsin and α-chymotrypsin the residues S_1 and S_3 form 2 and 3 hydrogen bonds, respectively; in subtilisin not only the backbone chain segment S_1-S_2-S_3 but also 2 or 3 other amino-acid residues are involved (Blow, 1976; Kraut, 1977). In general these hydrogen-bonding interactions between enzyme and substrate are of minor importance and give a final adjustment of the orientation of the hydrolysable bond with respect to the charge-relay system (Cf. Stroud et al., 1975). Only when the specificity pocket is small, as for elastase, these interactions may dominate the hydrophobic interactions (Blow, 1976).

An important contribution to the stabilization of the transition-state complex is ascribed to the "oxy-anion binding hole". From X-ray data on acyl-enzymes and enzyme-substrate complexes it was concluded that in the tetrahedral configuration, when the carbonyl carbon atom is covalently attached to the Oγ of the active serine, the carbonyl oxygen fits into a hole where it is fixed by bifurcated hydrogen bonding with the enzyme backbone, resulting in stabilization of the negative charge on the oxygen. Therefore, this binding site was termed

"oxy-anion binding hole". In α-chymotrypsin the two hydrogen bonds to the carbonyl oxygen are provided by the backbone N-H groups of Gly(193) and Ser(195), in subtilisin by the N-H of Ser(221) and the side-chain amino group of Asn(155) (Kraut, 1977). In the pancreatic zymogens the hydrogen bond to the backbone N-H of Gly(193) is either severely distorted or absent, due to an improper orientation of this donor (Freer et al., 1970; Kossiakoff et al., 1977). For various types of inhibitors which specifically react with the active serine, e.g. phenylsulphonyl fluoride, phenylmethanesulphonyl fluoride and diisopropyl phosphorofluoridate, it has been established that the inhibiting group assumes a tetrahedral geometry in the adduct with one oxygen atom fixed by similar hydrogen bonding in the oxy-anion binding hole (Kraut, 1977). Because of this structural resemblance with the transition state these so-called transition-state analogues can be used for studying the tetrahedral intermediate.

At the side of the leaving group as well, the enzyme molecule has some sites for interaction with the substrate. However, these structural elements are less well-defined since here the strength of the interactions and the specificity are much smaller than at the side of the acyl group (Kraut, 1977; Stroud et al., 1975).

The presence of these common structural elements for catalysis in the tertiary structure of serine proteases from different superfamilies strongly suggests convergent molecular evolution within this group of hydrolases, i.e. the tendency towards the development of similar structures for comparable functions (Hartley, 1970[b]). At present, because of insufficient structural data it is not established whether such an evolutionary trend also includes the serine esterases.

Atropinesterase, a Bacterial Serine Esterase

Almost two decades ago a new bacterial serine enzyme was isolated from Pseudomonas putida strain L of the biotype A (strain PMBL-1*;

* This notation refers to the culture collection of the Medical Biological Laboratory TNO.

Berends et al., 1967; Stevens, 1969; Oosterbaan and Berends, 1971; Rörsch et al., 1971). This enzyme specifically catalyses the hydrolysis of (-)-atropine (hyoscyamine) to (-)-tropic acid and tropine (Figure 3). It is an inducible enzyme that enables the bacteria to

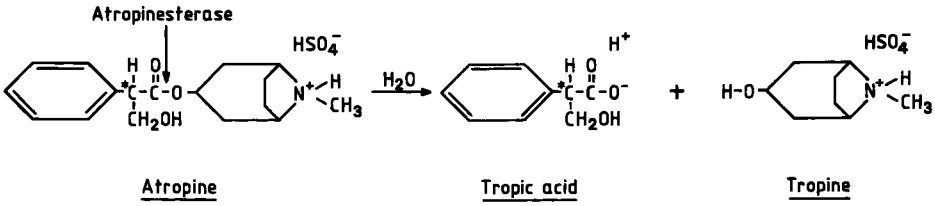

FIGURE 3: Esterolysis of atropine to tropic acid and tropine by atropinesterase at physiological pH. *C = asymmetric carbon atom.

grow on atropine, by providing for the first step in the catabolic breakdown of this carbon source. Consequently, it was named atropinesterase (AtrE). In contrast to other serine hydrolases such as α-chymotrypsin and subtilisin it has no proteolytic activity and therefore it can be considered a true esterase. The further characterization of the primary and tertiary structure of this enzyme was taken up for the following reasons (Berends et al., 1967):

- The specificity of this enzyme indicated a particular interaction of the active-site region with atropine. Atropine can be applied as an antidote against intoxications with anti-cholinergic substances like organophosphorus insecticides. This therapeutic action is ascribed to the high affinity of atropine towards muscarinic receptors, a particular type of the cholinergic receptors. The mode of this interaction and the various structural features involved were (and are) still unknown because this type of receptor, in contrast to nicotinic cholinergic receptors, is only recognizable as such in situ; consequently, it is hardly accessible to structural analysis by means of biochemical and biophysical methods, which require isolation in vitro. Since it is not unreasonable to assume that the specific interactions of

atropine with the muscarinic receptor and with AtrE show, at least to some extent, a structural similarity, AtrE was chosen as a model for the muscarinic receptor (Rörsch et al., 1971).

- As a true esterase and also in some aspects of enzyme kinetics, AtrE resembled acetylcholinesterase rather than the serine proteases. Acetylcholinesterase plays a crucial role in neuromuscular transmission as it catalyses the hydrolysis of the neurotransmitter acetylcholine at the neuromuscular junction. Its rapid inactivation by poisonous organophosphates is the predominant cause of the high toxicity of these agents. However, acetylcholinesterase is poorly accessible to biochemical and biophysical techniques; it was hoped, therefore, that AtrE - as a well accessible, mechanistically related model esterase - might be a useful substitute of this interesting enzyme.
- AtrE was thought to be a suitable protein for sequence studies, to investigate whether homology may exist between serine esterases and serine proteases.
- The bacterial origin of this enzyme opened the possibility to obtain variants differing in primary structure from mutant bacteria, which might be used for investigation of the effects of specific alterations in the amino-acid sequence on its structure and function.

The determination of the primary structure has been completed recently and will be presented elsewhere (Hessing, 1983). The protein consists of a single polypeptide chain of 272 amino-acid residues. The amino-acid sequence around the active serine is found to be Gly-His-Ser-Met-Gly, i.e. different from that of the chymotrypsin and the subtilisin families for which it is Gly-Asp-Ser-Gly-Gly and Gly-Thr-Ser-Met-Ala, respectively (Dayhoff, 1969; Ottesen and Svendsen, 1970; Wilcox, 1970; Hartley, 1972). No evidence has been found for significant homology with other known serine enzymes. The active serine is located at position 110, i.e. at about 40% from the NH_2-terminus; in the chymotrypsin and the subtilisin families the active serine is located at about 80% from the NH_2-terminus. The lack of homology suggests that

also the secondary and tertiary structure of AtrE will be different. However, it does not preclude that characteristic structural elements such as involved in the catalytic activity of the chymotrypsin and subtilisin types of serine proteases are also present in this serine esterase. Therefore, a further characterization of the tertiary structure of AtrE has been attempted in order to supplement the information on the primary structure.

Aim and Outline of the Present Investigation

The objective of this study was to characterize the conformation of AtrE, in particular to explore whether and, if so, to what extent the molecular architecture of its active-site region shows a structural resemblance to that of the serine proteases. The most detailed information on the structure of a protein is obtained by means of X-ray analysis on crystallized material. However, as attempts to obtain suitable crystals of AtrE have not been successful, such a direct determination of the detailed geometry of its structure was not feasible. Therefore, indirect methods have been used to investigate the three-dimensional structure of AtrE.

For the characterization of the overall conformation (size, shape and hydration) of AtrE in solution, velocity and equilibrium sedimentation techniques performable with the analytical ultracentrifuge were chosen. These methods are theoretically well-founded and require only small quantities of material. The evaluation of the molecular size from sedimentation data is unambiguous; with respect to the determination of the shape and hydration, however, interpretation is only possible in terms of a restricted number of geometrically simple model particles which can be applied to describe the hydrodynamic behaviour of the protein but which, within certain limits, may differ in shape and hydration from the real molecule. The estimates of the molecular dimensions derived in this way for globular proteins compare rather well with data obtained by other methods such as electron microscopy.

Spectroscopic and kinetic methods were used to characterize the active-site region of AtrE in more detail, in particular with respect

to the earlier-mentioned structural elements which underlie the catalytic activity of serine proteases. As these methods do not give direct structural information and as much depends on the interpretability of the data, the characterization of the active-site region of this esterase was performed by a comparison with serine hydrolases, the active-site structure of which is known in detail, viz. α-chymotrypsin (Chymo) and subtilisin A (Sub) as representatives of the prothrombin-related and subtilisin superfamilies of serine proteases, respectively.

For the spectroscopic investigation NMR, ESR and fluorescence spectrometry have been applied. Apart from reasons of specificity and sensitivity, this combination of techniques was chosen because the structural information obtainable with each of these methods may, in principle, supplement and confirm that of the others. In this way the uncertainty inherent in the interpretation of the data obtained with each of these indirect techniques may be reduced.

The comparison of the enzymes with different spectroscopic techniques was performed by specific labelling of the active-site region with various fluorescent, paramagnetic and nuclear magnetic reporter groups that give information on characteristic features of their immediate environment. Labels were chosen that were expected to provide information on a charge-relay system, an oxy-anion hole or a specificity pocket near the active serine, if present. Suitable reporter groups for this comparative study were selected on the basis of various criteria. Firstly, the labelling should be specific, i.e. the reporter group should become attached to the active centre at a well-known position, and no label should be bound elsewhere in the protein. Secondly, each reporter group should respond to its environment in an interpretable manner. Thirdly, the introduction of the label should perturb the native structure of the protein as little as possible. The first criterion was met by selecting or designing labelling agents that reacted exclusively with the active-serine residue as to become covalently attached to the oxygen atom in its side chain. Fulfilment of the interpretability criterion in some cases necessitated rather extended additional studies on model compounds, in order to establish

the response of the reporter group to specific changes in its direct environment. Nevertheless, some uncertainty remained on the question whether the group in the labelled enzymes would respond in exactly the same manner as in the model systems. With regard to the third criterion, it was expected that the outlined approach of using different reporter groups and a variety of techniques would make it possible to distinguish the relevant information on the structure of the active centre from data possibly resulting from artificial responses of the system due to the labelling.

The results obtained with the various techniques are presented in this thesis. The characterization of the size and shape of AtrE by means of various ultracentrifugal techniques is described in chapter 1. In chapter 2 results are presented of a comparative study by fluorescence spectrometry of the active sites of the three enzymes, labelled with the fluorescent dansyl group. The interpretation of the observed variations in the excitation and emission spectrum of the serine-bound dansyl group was based on the results obtained in a study of model systems, which are given and discussed in chapter 3. An investigation of the kinetics of inhibition of AtrE and Chymo by dansyl fluoride, which was used for the fluorescent labelling, is described in chapter 4. The results of a comparative study of the active sites of AtrE, Chymo and Sub by means of electron spin resonance (ESR) spectrometry is presented in chapter 5. Chapter 6 deals with a comparative nuclear magnetic resonance (^{31}P NMR) study of the active sites of the three enzymes and of the proenzyme α-chymotrypsinogen after introduction of a diisopropyl phosphoryl group. Furthermore, in this chapter information is given on the mechanism that governs specific dealkylation of this group, as obtained by mass spectrometry. A general survey of the results obtained with the different techniques and of the conclusions that have been drawn with respect to the tertiary structure of AtrE is given in the summary.

REFERENCES

Alden, R.A., Wright, C.S., and Kraut, J. (1970) Phil. Trans. Roy. Soc. (London) B 257, 119.

Bachovchin, W.W., and Roberts, J.D. (1978) J. Am. Chem. Soc. 100, 8041.

Baker, B.R. (1975) Design of Active-Site-Directed Irreversible Enzyme Inhibitors. Rober E. Krieger Publishing Company, Huntington N.Y.

Balls, A.K., and Wood, J.H. (1956) J. Biol. Chem. 219, 245.

Berends, F. (1964) Ph.D. Thesis, University of Leiden.

Berends, F., Rörsch, A., and Stevens, W.F. (1967) in Proceedings of the Conference on Structure and Reactions of DFP Sensitive Enzymes (Heilbronn, E., Ed.) p. 45, Försvarets Forskningsanstalt, Stockholm.

Blow, D.M. (1976) Acc. Chem. Res. 9, 145.

Blow, D.M., Birktoft, J.J., and Hartley, B.S. (1969) Nature (London) 221, 337.

Cruickshank, W.H. and Kaplan, H. (1975) Biochem. J. 147, 411.

Cunningham, L.W., and Brown, C.S. (1956) J. Biol. Chem. 221, 433.

Dayhoff, M.O. (1969) Atlas of Protein Sequence and Structure, National Biomedical Research Foundation, Silver Spring.

Dayhoff, M.O., Barker, W.C., and Hunt, L.T. (1978 in Atlas of Protein Sequence and Structure, Vol. 5, Suppl. 3 (Dayhoff, M.O., Ed.) p. 9. National Biomedical Research Foundation, Washington D.C.

Dixon, M., and Webb, E.C. (1964) Enzymes, Longmans, London.

Fahrney, D.E., and Gold, A.M. (1963) J. Am. Chem. Soc. 85, 997.

Freer, S.T., Kraut, J., Robertus, J.D., Wright, H.T., and Xuong, Ng.H. (1970) Biochemistry 13, 1302.

Fruton , J.S. (1975) in Proteases and Biological Control (Reich, E., Rifkin, D.B., and Shaw, E., Eds.) p. 33, Cold Spring Harbor Laboratory.

Glazer, A.N. (1967) J. Biol. Chem. 242, 433.

Hartley, B.S. (1960) Ann. Rev. Biochem. 29, 45.

Hartley, B.S. (1970[a]) Phil. Trans. Roy. Soc. (London) B 257, 77.

Hartley, B.S. (1970[b]) in Homologies in Enzymes and Metabolic Pathways; Metabolic Alterations in Cancer (Whelan, W.J., and Schultz, J., Eds.) p. 191, North-Holland Publishing Company, Amsterdam.

Hartley, B.S., Burleigh, B.D., Midwinter, G.G., Moore, C.H., Morris, H.R., Rigby, P.W.J., Smith, M.J., and Taylor, S.S. (1972) in Proceedings 8e FEBS Meeting, Amsterdam, Enzyme, Structure and Function 29, p. 151.

Hartley, B.S., and Massey, V. (1956) Biochim. Biophys. Acta 21, 58.

Hessing, J.G.M. (1983) Ph.D. Thesis, University of Leiden.

Huber, R., and Bode, W. (1978) Acc. Chem. Res. 11, 114.

Hunkapiller, M.W., Smallcombe, S.H., Whitaker, D.R., and Richards, J.H. (1973) Biochemistry 12, 4732.

IUB (1979) Enzyme Nomenclature 1978, Acad. Press, New York.

Jencks, W.P. (1969) Catalysis in Chemistry and Enzymology, McGraw-Hill Book Company, New York.

Johnson, F.H., Eyring, H., and Stover, B.J. (1974) The Theory of Rate Processes in Biology and Medicine, John Wiley and Sons, New York.

Jong, L.P.A. de (1978) Ph.D. Thesis, University of Leiden.

Koeppe II, R.E., and Stroud, R.M. (1976) Biochemistry 15, 3450.

Koshland, D.E. (1973) Sci. Am. 229, 52.

Kosower, E.M. (1962) Molecular Biochemistry, McGraw-Hill Book Company Inc., New York.

Kossiakoff, A.A., Chambers, J.L., Kay, L.M., and Stroud, R.M. (1977) Biochemistry 16, 654.

Kossiakoff, A.A., and Spencer, S.A. (1981) Biochemistry 20, 6462.

Kraut, J. (1977) Ann. Rev. Biochem. 46, 331.

Lienhard, G.E. (1973) Science 180, 149.

Mahler, H.R., and Cordes, E.H. (1966) Biological Chemistry, Harper and Row, New York.

Markley, J.L. (1979) in Applications of Magnetic Resonance (Shulman, R.G., Ed.) p. 397, Academic Press, New York.

Matthews, D.A., Alden, R.A., Birktoft, J.J., Freer, S.T., and Kraut, J. (1977) J. Biol. Chem. 252, 8875.

Oosterbaan, R.A., and Berends, F. (1971) Proc. Koninkl. Nederl. Akademie van Wetenschappen, Series C, Vol. 74, No. 2, 158.
Oosterbaan, R.A., and Van Adrichem, M.E. (1958) Biochim. Biophys. Acta 27, 423.
Ottesen, M., and Svendsen, I. (1970) in Methods in Enzymology Vol. XIX, (Perlman, G.E., and Lorand, L., Eds.), p. 199, Academic Press, New York.
Rörsch, A., Berends, F., Bartlema, H.C., and Stevens, W.F. (1971) Proc. Koninkl. Nederl. Akademie van Wetenschappen, Series C, Vol. 74, No. 2, 132.
Stevens, W.F. (1969) Ph.D. Thesis, University of Leiden.
Stroud, R.M., Krieger, M., Koeppe II, R.E., Kossiakoff, A.A., and Chambers, J.L. (1975) in Proteases and Biological Control (Reich, E., Rifkin, D.B., and Shaw, E., Eds.) p. 13, Cold Spring Harbor Laboratory.
Walsh, K.A. (1975) in Proteases and Biological Control (Reich, E., Rifkin, D.B., and Shaw, E., Eds.) p. 1, Cold Spring Harbor Laboratory.
Walsh, K.A., and Wilcox, P.E. (1970) in Methods in Enzymology Vol. XIX, (Perlman, G.E., and Lorand, L., Eds.) p. 31, Academic Press, New York.
Westley, J. (1969) Enzymic Catalysis, Harper and Row, New York.
Wilcox, P.E. (1970) in Methods in Enzymology Vol. XIX, (Perlman, G.E., and Lorand, L., Eds.), p. 64, Academic Press, New York.
Wolfenden, (1972) Acc. Chem. Res. 5, 10.
Wright, C.S., Alden, R.A., and Kraut, J. (1969) Nature (London) 221, 235.
Young, C.L., Barker, W.C., Tomaselli, C.M., and Dayhoff, M.O. (1978) in Atlas of Protein Sequence and Structure, Vol. 5, Suppl. 3 (Dayhoff, M.O., Ed.) p. 73. National Biomedical Research Foundation, Washington D.C.

CHAPTER 1

HYDRODYNAMIC CHARACTERIZATION OF THE SIZE AND SHAPE OF ATROPINESTERASE FROM PSEUDOMONAS PUTIDA

ABSTRACT: Atropinesterase (AtrE) from Pseudomonas putida PMBL-1 is a serine esterase which specifically catalyses the hydrolysis of (-)-atropine to (-)-tropic acid and tropine. Size and shape of this enzyme have been investigated by means of different ultracentrifugal methods under native and various denaturing conditions. The following quantities were determined: sedimentation coefficient, translational diffusion and frictional coefficient, partial specific volume and molecular weight. These data were used to estimate the size, shape and hydration of AtrE in solution.

The results show that AtrE is a globular protein which consists of a single polypeptide chain with a molecular weight of about 30,000. In solution under non-denaturing conditions and at protein concentrations above 0.03 mg/ml it occurs mainly as a dimer which hydrodynamically behaves as a rigid impenetrable particle of ellipsoidal shape. By application of a prolate ellipsoidal model in order to estimate the extreme values of the dimensions and hydration of the dimer, a major axis of 61-125 Å, a minor axis of 34-61 Å and a hydration of 0-0.42 g/g protein are obtained (for an oblate ellipsoidal shape the axes are 61-82 Å and 21-61 Å, respectively). Under denaturing conditions dissociation into monomers takes place.

From the effects of sodium dodecyl sulphate on size and shape as studied by means of velocity and equilibrium sedimentation it is concluded that dimerization results from side-by-side association of two ellipsoidal monomers rather than from end-to-end association. Results obtained from an analysis of the monomer-dimer equilibrium at 9-25 °C suggest that the change in the standard Gibbs' free energy (ΔG) accompanying the dimerization does not appreciably vary with temperature in this range. The average value of ΔG found for one particular AtrE preparation was - 8.1 $\pm$ 0.5 kcal/mole.

INTRODUCTION

Atropinesterase (AtrE) from *Pseudomonas putida* strain L of the biotype A (strain PMBL-1) is a serine hydrolase which specifically catalyses the hydrolysis of (-)-atropine (hyoscyamine) to (-)-tropic acid and tropine (Berends et al., 1967; Stevens, 1969; Rörsch et al., 1971). Like other serine enzymes it is inactivated by various organophosphorus compounds (Berends et al., 1967; Oosterbaan and Berends,

1971; Rörsch et al., 1971) which specifically react with the side-chain hydroxyl group of Ser(110) at the active site (Stevens, 1969; Hessing, 1983).

With ^{32}P-labelled compounds it was found that one phosphorus was incorporated per relative molecular mass of about 30,000, suggesting a molecular weight for AtrE of this magnitude or a multiple (Hessing, 1983). From gel filtration on Sephadex G-100 columns the molecular weight was estimated to be 39,000 (Stevens, 1969). Thin-layer chromatography with various buffers on different types of Sephadex plates (Sephadex Superfine G-75, G-100, G-200) yielded values from 45,000 to 59,000; values in this range and sometimes even higher were also obtained in the presence of up to 4 M urea (Zwennis, 1972). With polyacrylamide gel electrophoresis in the presence of sodium dodecyl sulphate and urea (either with or without mercaptoethanol) values ranging from 30,000 to 34,000 were found (Zwennis, 1972).

The present hydrodynamic investigation by means of ultracentrifugal methods was performed to resolve these discrepancies and to characterize size and shape of AtrE in solution in more detail.

MATERIALS AND METHODS

a. Proteins and Other Chemicals

AtrE from Pseudomonas putida PMBL-1 was obtained according to the procedure of Rörsch et al. (1971) as modified by Oosterbaan et al. (1983). Three different batches of about the same purity and with specific activities of 530-550 units* per A_{280} at 25.0 ^{o}C, pH=7.0, were used. Polyacrylamide gel electrophoresis in SDS showed one component but with isoelectric focusing one main band and a few minor bands were observed.

Crystalline subtilisin (Sub) type Carlsberg (EC 3.4.21.14) was obtained from NOVO Industri A/S (Batch 70-4); crystalline and lyophi-

* 1 unit hydrolyses 1 μM of (-)-atropine per minute at the conditions indicated.

lized bovine serum albumin (BSA) was purchased from Sigma Chemical Company.

Highly purified sodium dodecyl sulphate (SDS) was obtained from Schwarz/Mann, urea p.a. from Union Chimique Belge, guanidine hydrochloride (GuHCl) from Fluka, deuterium oxide (D_2O) and the other chemicals, reagent grade, from Merck, unless indicated otherwise. Diisopropyl phosphorofluoridate (DFP) was obtained from the Prins Maurits Laboratory TNO. All chemicals were used without any further purification.

b. Preparation and Characterization of Protein Solutions

Proteins were dissolved in aqueous solution under various conditions. Unless stated otherwise, protein solutions always contained 10 mM phosphate buffer, pH=7.4, and 0.1 mM sodium azide to prevent growth of bacteria. Solutions containing in addition NaCl, GuHCl, urea or ammonium sulphate, were prepared by dialysis of 0.5-1.0 ml of protein solution at room temperature for at least 16 h against a large volume of buffer containing the particular compound. Protein-SDS solutions were prepared by adding a small volume of a concentrated SDS solution in buffer to the protein solution, followed by dialysis of this mixture at room temperature for 4 h against a large volume of solvent containing the same SDS concentration.

Enzyme activities in solutions of AtrE were determined at 25.0 ^{o}C and pH=7.0 according to the pH-stat method (Cf. Van der Drift et al., 1983) with (-)-atropine sulphate as substrate (Nutritional Biochemicals Corporation). Molar concentrations of total enzyme were determined spectrophotometrically at 280 nm (molecular extinction coefficient $\varepsilon_{280} = 5.55 \times 10^4\ M^{-1}cm^{-1}$).

To prevent autoproteolysis, samples of Sub were inactivated with DFP. To 1 ml of a solution of Sub in 10 mM phosphate buffer, pH=7.4, were added a few µl of a 0.1 M stock solution of DFP in dry, peroxide-free isopropanol to obtain a final concentration of 3-5 times that of the enzyme. After incubation for about 6 h at room temperature enzyme activity was no longer detectable as determined by pH-stat titration with N-acetyl-L-tyrosine ethyl ester (Merck) as substrate. Excess of

DFP was removed at 4 °C by extensive dialysis against buffer. Total Sub concentrations were determined spectrophotometrically by using $\varepsilon_{280} = 2.62 \times 10^4\ M^{-1}cm^{-1}$ (Cf. Ottesen and Svendsen, 1970).

For analysis of the ultracentrifugal data densities of solvents were determined by pycnometry at 20.0 °C by using the dialysate; viscosities required for correction of the sedimentation coefficients to standard conditions in buffer were measured with an Ostwald viscometer (Merrington, 1949; Bradbury, 1970).

c. Ultracentrifugal Methods

Sedimentation experiments were carried out with a Beckman Model E analytical ultracentrifuge equipped with an RTIC temperature regulator, an UV-absorption optical system in conjunction with a split-beam photo-electric scanner and mirror optics, and a schlieren optical system combined with a photographic system. Unless indicated otherwise, experiments were performed at 20.0 °C in a two-place aluminium An-D rotor, in a two-place An-H Ti rotor or in a six-place An-G Ti rotor; standard 12 mm Kel-F or charcoal-filled Epon double-sector centrepieces with plane sapphire windows were used.

For sedimentation experiments both the schlieren optical system and the UV-absorption scanning system were applied. In the latter case wavelengths in the range 270-300 nm were used for recording the sedimentation pattern. For diffusion measurements only the schlieren optical system was used. Photographs of schlieren patterns were taken automatically by employing Kodak metallographic plates (exposure time 8-10 s) which were developed with Kodak D-19 developer according to standard procedure (Cf. Chervenka, 1969).

c1. Equilibrium and Approach-to-Equilibrium Sedimentation

The molecular weight of AtrE under various conditions was determined by both conventional equilibrium sedimentation and the approach-to-equilibrium (Archibald) method (Schachman, 1959; Chervenka, 1969). Conventional equilibrium sedimentation was performed with 150-250 µl of a solution containing 0.1-0.3 mg of protein/ml at a rotor speed be-

tween 16,200 and 19,160 r.p.m. for 72-96 h. The equilibrium distribution of the protein was recorded by means of UV absorption.

From the equilibrium distribution in a solvent containing one or more low-molecular weight compounds which may interact with the protein, the buoyant density mass $M_w^a(c)\cdot(1 - \phi_s\rho_s)$ can be calculated from the relation

$$M_w^a(c)\cdot(1-\phi_s\rho_s)= (2RT/\omega^2)\cdot d\ln c(r)/dr^2 \qquad (1)$$

(Tanford et al., 1974; Fish, 1975; Eisenberg, 1976). $M_w^a(c)$ is the apparent weight-average molecular weight of the protein at concentration c, r is the distance in the cell with respect to the centre of rotation, ϕ_s is the effective partial specific volume of the protein including the effects of interactions with other components in solution, ρ_s is the density of the solvent mixture and ω the angular velocity. R and T are the universal gas constant and the absolute temperature, respectively.

For a monodisperse, i.e. non-associating, protein $M_w^a(c) = M^a(c)$, the apparent molecular weight of the anhydrous protein. At low protein concentrations, where contributions to thermodynamic non-ideality are negligible, $M^a(c) = M$, the true molecular weight of the anhydrous protein. For a thermodynamically ideal three components system consisting of a protein at low concentration in a dilute buffer which contains a low-molecular weight component that shows preferential binding to the protein, the buoyant density term $(1 - \phi_s\rho_s)$ can be approximated by (Casassa and Eisenberg, 1964; Fish, 1975; Eisenberg, 1976)

$$1-\phi_s\rho_s = 1-\bar{v}_p\rho_s + \delta_3\cdot(1-\bar{v}_3\rho_s) \qquad (2)$$

where δ_3 is the amount of the third component bound per gram of anhydrous protein, $\bar{v}_p$ is the partial specific volume of the protein under the particular conditions and $\bar{v}_3$ that of the third component when bound to the protein. Substitution of Equation (2) into Equation (1) shows that in case of a monodisperse protein, δ_3 can be estimated from the sedimentation equilibrium pattern when M, $\bar{v}_p$, ρ_s and $\bar{v}_3$ are known.

For a two components system consisting of a protein in dilute buffer with density ρ_b, $M_w^a(c)$ can be calculated from Equation (1) with $(1-\phi_s\rho_s)=(1-\bar{v}_p\rho_b)$. In the particular case of a monodisperse protein at low concentration, a plot of lnc(r) versus r^2 will be a straight line from which M can be calculated by the method of least squares.

The molecular weight of AtrE was also determined by the Archibald method by using the schlieren optical system. These experiments were performed according to the usual procedure (An-D rotor, double-sector capillary synthetic boundary centrepiece, 12 mm double-sector cell with schlieren window holders and sapphire windows; the sample-cell compartment contained 0.03 ml FC-43 fluorocarbon oil in order to obtain a sharp synthetic boundary at the bottom; Cf. Chervenka, 1969) at 20,400 r.p.m. Protein concentrations ranged from 3 to 11 mg/ml. Molecular weights were calculated from the concentration gradient both at the meniscus and at the bottom of the fluid column by standard procedure (Chervenka, 1969).

c2. Velocity Sedimentation

Sedimentation coefficients were determined by velocity sedimentation at various rotor speeds (47,660-52,600 r.p.m.) by measuring the displacement of the 50% point of the boundary with time by means of the UV-absorption system (Chervenka, 1969; Elias, 1969). Scans of 30 s were taken at 4 to 8 minutes intervals. Protein concentrations ranged from 0.07 to 0.5 mg/ml. Sedimentation coefficients thus obtained did not significantly differ from those obtained by measuring the displacement of the second moment or of the point of maximum gradient of the boundary gradient curve with the UV system or, at higher protein concentrations, with the schlieren optical system. Correction of sedimentation coefficients for small temperature deviations was performed according to standard procedures (Svedberg and Pedersen, 1940; Chervenka, 1969).

The sedimentation coefficient of a monodisperse protein (molecular weight M) in a particular solvent s at t ^{o}C obtained by extrapo-

lation to zero protein concentration, $s^0_{t,s}$, satisfies (Van Holde, 1971; Tanford, 1961)

$$s^0_{t,s} = M\cdot(1-\phi_s\rho_s)/Nf^0_{t,s} \qquad (3)$$

where $f^0_{t,s}$ is the translational frictional coefficient of the solvated protein molecule at the limit of zero protein concentration, and N is Avogadro's number.

As appears from Equations (1) and (3) for a monodisperse protein at low concentration ($M^a_w(c)=M$), $f^0_{t,s}$ can be computed from the combined results of velocity and equilibrium sedimentation experiments performed under the same conditions according to

$$f^0_{t,s} = (2kT/\omega^2 s^0_{t,s})\cdot d\ln c(r)/dr^2 \qquad (4)$$

where k is the Boltzmann constant.

c3. Diffusion Measurements

Free diffusion was measured in the ultracentrifuge at 20.0 °C with protein solutions of 2-10 mg/ml in 10 mM phosphate buffer, pH = 7.4, in 12 mm double-sector capillary-type synthetic boundary cells at rotor speeds up to 12,600 r.p.m. Translational diffusion coefficients were evaluated from photographs of the schlieren pattern, taken at 8 or 16 minutes intervals, according to the height-area method (Chervenka, 1969; Elias, 1969). Corrections for sedimentation were found to be negligible.

The translational diffusion coefficient in solvent s at t °C obtained by extrapolation to zero protein concentration, $D^0_{t,s}$, and the corresponding translational frictional coefficient $f^0_{t,s}$ of the solvated protein molecule are related according to

$$f^0_{t,s} = kT/D^0_{t,s} \qquad (5)$$

(Tanford, 1961; Van Holde, 1971).From Equations (3) and (5) follows

for a monodisperse protein at low concentration (Svedberg and Pedersen, 1940; Tanford, 1961)

$$M = RTs^0_{t,s}/(1-\phi_s\rho_s)\cdot D^0_{t,s} \qquad (6)$$

This relation is generally used to evaluate M from the experimental values of $s^0_{t,b}$ and $D^0_{t,b}$ obtained in dilute buffer for which $(1-\phi_s\rho_s)=(1-\bar{v}_p\rho_b)$.

c4. Determination of the Partial Specific Volume

Because of the limited amount of highly purified AtrE available, the partial specific volume of the protein, $\bar{v}_p$, was determined by equilibrium sedimentation at 20.0 °C in H_2O-D_2O solutions at 14,290-17,980 r.p.m. according to the method of Edelstein and Schachman (1973). The ratio k of the molecular weights of the protein in pure D_2O and H_2O, respectively, was assumed to be 1.0155, the value found for a large variety of proteins (Edelstein and Schachman, 1973).

RESULTS

The values of various quantities characterizing AtrE at 20.0 °C in 10 mM phosphate buffer, pH=7.4, under various conditions are shown in Table I. Since both the sedimentation coefficient and the diffusion coefficient did not systematically depend on protein concentration within the investigated ranges, the compiled values of $s^0_{20,b}$ and $D^0_{20,b}$ are averages of the measured values. The value of the partial specific volume obtained from equilibrium sedimentation was equal to that found from velocity sedimentation experiments in D_2O/H_2O mixtures (0.75 ± 0.03 ml/g), if it was assumed that replacement of H_2O by D_2O did not affect the shape of the protein. This value of 0.75 ml/g, used to determine the molecular weight of AtrE, is in good agreement with that of 0.74 ml/g which can be calculated on the basis of the amino-acid composition (Cf. Fish, 1975; Hessing, 1983).

TABLE I: Characteristic quantities of atropinesterase in various aqueous solutions at 20.0 °C.

Quantity (1)	Value (± s.e.)		Method and conditions (2)
$s^0_{20,b}$	4.36 ± 0.16	S	velocity sedimentation
$D^0_{20,b}$	$(6.9 \pm 0.4) \times 10^{-7}$	$cm^2\ s^{-1}$	free diffusion
$f^0_{20,b}$	$(5.9 \pm 0.3) \times 10^{-8}$	$g\ s^{-1}$	calculated from $D^0_{20,b}$
	$(5.5 \pm 0.2) \times 10^{-8}$	$g\ s^{-1}$	velocity and equilibrium sedimentation
$\bar{v}_p$	0.75 ± 0.01	$ml\ g^{-1}$	equilibrium sedimentation in D_2O/H_2O
M	57,800 ± 1000		conventional equilibrium sedimentation
	57,200 ± 2400 (3)		Archibald method
	61,600 ± 4250		calculated from $s^0_{20,b}$ and $D^0_{20,b}$
M	30,750 ± 1650		conventional equilibrium sedimentation in buffer + 3-4 M GuHCl (4)
M	30,400 ± 1450		conventional equilibrium sedimentation in buffer + 4.5-8.0 M urea

(1) $s^0_{20,b}$ = sedimentation coefficient (Svedberg units), $D^0_{20,b}$ = translational diffusion coefficient, $f^0_{20,b}$ = translational frictional coefficient (all three quantities at the limit of zero protein concentration). $\bar{v}_p$ = partial specific volume, M = molecular weight. For details, see text.

(2) In 10 mM phosphate buffer, pH=7.4, without any addition, unless indicated otherwise.

(3) Average of the values obtained from the gradients at the bottom and at the meniscus of the fluid column. Average value at meniscus: 56,300 ± 2400, average value at bottom: 58,600 ± 2300.

(4) With 1 mM 1,4-dithiothreitol.

In equilibrium sedimentation experiments under various conditions, AtrE at concentrations above 0.03 mg/ml generally behaved like a monodisperse system (see Discussion). This appeared from the linearity of plots of $\ln A_{280}^{1\ cm}$ versus r^2, an example of which is shown in Figure 1. The molecular weight in buffer given in Table I is an average of values calculated from such linear plots by the method of least squares. It was found to be independent of concentration in the range 0.03-0.2 mg of protein/ml. This value is in agreement with that calculated from $s^0_{20,b}$ and $D^0_{20,b}$ (Equation 6) and with that obtained by the Archibald method at higher protein concentrations (Table I). The values obtained with the latter method when applied to the meniscus data were not significantly different from those calculated for the concentration gradient at the bottom, which indicated that even at the higher concentrations mentioned non-ideality effects did not noticeably contribute to the mass distribution.

The molecular weight of AtrE in the presence of the denaturing agents GuHCl and urea (Table I) has also been calculated from sedimentation equilibrium distributions by linear regression according to the method of least squares with $\phi_s = \bar{v}_p = 0.75$ ml/g (Fish, 1975; see Discussion). It is substantially smaller than the value obtained under non-denaturing conditions, which suggests dissociation of AtrE upon denaturation.

In order to determine the stability of AtrE in more detail, the influence of the detergent SDS on the molecular size and shape has been investigated by means of velocity and equilibrium sedimentation at low protein concentrations. The dependence of the sedimentation coefficient and the buoyant density mass $M\cdot(1-\phi_s\rho_s)$ on the concentration of SDS is shown in Figures 2(A) and 3, respectively. Both quantities show a substantial decrease at a concentration of about 0.35 mM SDS. At concentrations in the range of 0.3-0.5 mM SDS the boundary in velocity sedimentation and, to a lesser extent, the protein gradient at sedimentation equilibrium reflected some molecular weight heterogeneity, which was ascribed to the presence of both monomers and dimers (see Discussion). As at 0.325 mM SDS this molecular heterogeneity

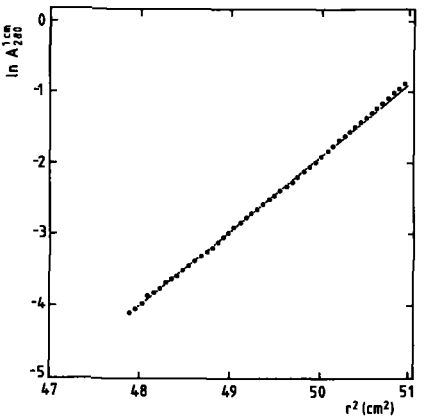

FIGURE 1: Distribution of atropinesterase in solution at sedimentation equilibrium. $A^{1\ cm}_{280}$ = absorbance at 280 nm for 1 cm light path; r = distance (cm) to the centre of the axis of rotation. The straight line was calculated according to the method of least squares. Experimental conditions: 17,980 r.p.m., 10 mM phosphate buffer, pH = 7.4, at 20.0 °C. Corresponding molecular weight: 57,480 ± 250.

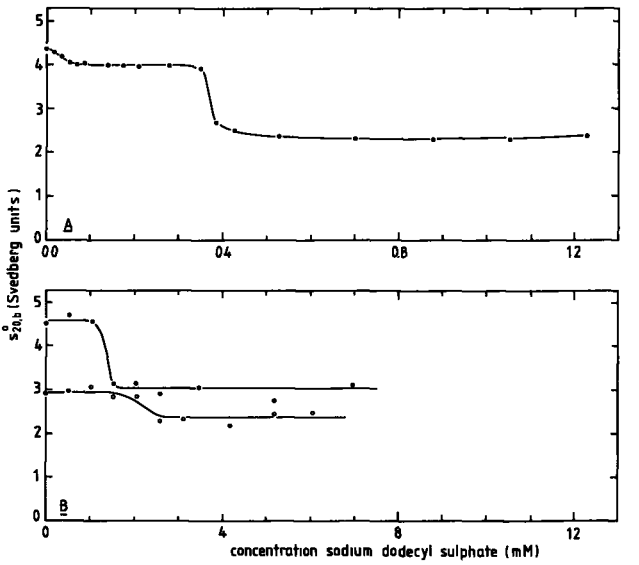

FIGURE 2: Influence of the concentration of sodium dodecyl sulphate (SDS) on the sedimentation coefficients, $s^0_{20,b}$, of atropinesterase (A, ●), subtilisin (B, ○) and bovine serum albumin (B, ●) in 10 mM phosphate buffer, pH = 7.4, at 20.0 °C. For atropinesterase, subtilisin and bovine serum albumin the average values (± s.e.) of $s^0_{20,b}$ at zero SDS concentration are 4.36 ± 0.16, 2.94 ± 0.09 and 4.51 ± 0.04, respectively, and at SDS concentrations beyond the transition 2.34 ± 0.03, 2.37 ± 0.12 and 3.02 ± 0.15, respectively.

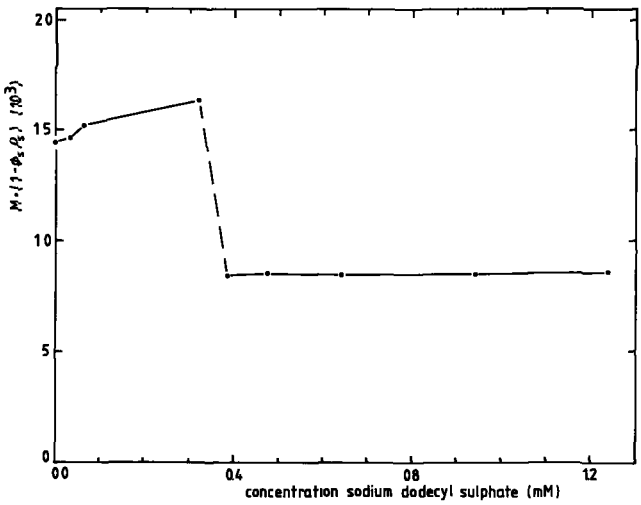

FIGURE 3: Influence of the concentration of sodium dodecyl sulphate on the buoyant density mass $M\cdot(1-\phi_s \rho_s)$, of atropinesterase. Equilibrium sedimentation at 20.0 °C in 10 mM phosphate buffer, pH = 7.4.

became noticeable at the lowest protein concentrations in the equilibrium gradient, the value of the buoyant density mass plotted in Figure 3 for this SDS concentration was obtained from the higher protein concentrations where the influence of molecular heterogeneity was negligible. For comparison, the effect of SDS on the sedimentation coefficient of DFP-inhibited Sub and BSA has also been investigated at low protein concentrations (Figure 2(B)). For both proteins the decrease in $s^0_{20,b}$ was smaller than for AtrE and occurred at higher SDS concentrations.

The presence of SDS led to a decrease in the catalytic activity of AtrE. This is shown in Figure 4 for the AtrE-SDS solutions subjected to the above sedimentation experiments.

DISCUSSION

The data in Table I show that the molecular weight of AtrE in solution is close to 60,000 under normal conditions, but amounts to about half this value under different denaturing conditions. This re-

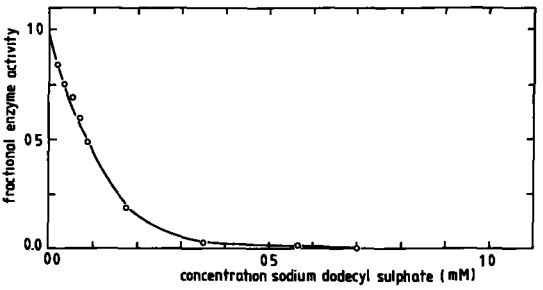

FIGURE 4: Influence of the concentration of sodium dodecyl sulphate (SDS) on the catalytic activity of atropinesterase. Small amounts of enzyme-SDS solutions as used in sedimentation experiments were added to substrate solutions containing SDS at the same concentrations. Activities were measured at 25.0 ^{o}C and pH=7.0.

duction has to be ascribed to dissociation as it is too large to result from a decrease in the effective partial specific volume ϕ_s of AtrE in the presence of the high concentrations GuHCl or urea used. On the contrary, the molecular-weight values suggest that ϕ_s does not appreciably differ from the value of 0.75 ml/g determined for $\bar{v}_p$ in dilute buffer. This was also found for BSA; by assuming $\phi_s = \bar{v}_p = 0.735$ ml/g, the molecular weight of the latter was found to be 69,200 $\pm$ 1400 in the presence of 2-6 M urea, which is not significantly different from the value of 68,700 $\pm$ 900, or 66,700 $\pm$ 1800 found at pH=7.4 in dilute phosphate buffer and ammonium sulphate solutions up to 2 M, respectively. Similar observations, reported for a large number of other proteins (Brouwer and Kuiper, 1973; Lee and Timasheff, 1974; Fish, 1975) also indicate that the assumption $\phi_s = \bar{v}_p$ at the concentrations urea and GuHCl used leads to molecular weights which could be at most 5-10% too high. Therefore, reduction of 60,000 to about 30,000 under denaturing conditions and in the presence or absence of the reducing agent 1,4-dithiothreitol indicates that the native particle consists of two non-covalently linked subunits of equal size, each containing a single polypeptide chain.

Since it has been found by using ^{32}P-labelled DFP that one DP group is bound per relative molecular mass of about 30,000 (Cf. Hessing, 1983), it can be concluded that, under the non-denaturing condi-

tions specified, AtrE exists as a dimer. In equilibrium sedimentation experiments this dimer was found to be stable in the pH-range 4-8 and at ionic strengths up to 0.2 M NaCl or 0.5 M ammonium sulphate; at higher concentrations of ammonium sulphate, up to about 2 M, the molecular weight showed a gradual decrease which may be ascribed to increased dissociation, as this was not found for Sub or BSA.

The values of $M_w^a(c)$ obtained by equilibrium sedimentation and the Archibald method in dilute buffer tended to be somewhat smaller than 60,000. Theoretically these values will result from the opposing effects of association and of the excluded-volume term in the second virial coefficient B_2 (Tanford, 1961; Fujita, 1975). Since a virial contribution due to excluded volume can be neglected at the investigated concentration range (estimated $B_2 \sim 10^{-4}$ mole ml g^{-2}; Cf. Tanford, 1961) a smaller value may reflect the contribution of monomers to $M_w^a(c)$. All batches of AtrE showed a systematic decrease in $M_w^a(c)$ with decreasing protein concentration but to a different extent. For two preparations the effect was too small in the range investigated to analyse it in terms of a monomer-dimer equilibrium. For unknown reasons the third batch differed from the other two in that it showed measurable dissociation under the same conditions, which allowed a detailed analysis according to a monomer-dimer equilibrium. The results, given in the Appendix, indicate that the change in the standard Gibbs' free energy corresponding with dimerization does not vary appreciably with temperature in the range 9-25 ^{o}C, the average value being -8.1 $\pm$ 0.5 kcal/mole. This value can at best be regarded as an upper limit.

Comparison of the sedimentation coefficient of AtrE with that of globular proteins of similar size (Cf. Smith, 1970) indicates that AtrE in aqueous solution behaves as a globular protein. Generally, the hydrodynamic behaviour of globular proteins as observed by means of ultracentrifugation can be satisfactorily explained in terms of a rigid impenetrable particle of spherical or ellipsoidal shape which is hydrated to a certain extent (Oncley, 1941; Schachman 1959; Tanford, 1961). According to this model the frictional ratio $f^0_{t,s}/f_o$, where f_o is the translational frictional coefficient of a spherical particle of

the same volume as the non-hydrated molecule, can be regarded as the product of a shape factor F_s and a hydration factor F_h. From F_s the axial ratio of the effective hydrodynamic particle can be estimated and from F_h the amount of bound water. For globular proteins the dimensions and hydration calculated for the corresponding model particle will approximate those of the molecule in solution (Schachman, 1959; Tanford, 1961). Since in general only $f^0_{t,s}/f_o$ can be obtained from experimental data and not the values of the individual factors, the size and hydration are usually estimated for the hypothetical limiting cases that 1) the equivalent model particle in solution is not hydrated, or 2) it is a hydrated sphere (Oncley, 1941; Tanford, 1961). In the former case F_h=1, its minimal value, so $F_s = f^0_{t,s}/f_o$ from which the maximal axial ratio can be estimated and consequently the dimensions if the molecular weight and the partial specific volume of the anhydrous protein are known. In the latter case F_s=1 and the maximal amount of bound water is estimated from $F_h = f^0_{t,s}/f_o$. It is generally accepted that the real dimensions and hydration of a globular protein will probably lie somewhere between these extremes (Oncley, 1941; Tanford, 1961).

For a protein in dilute buffer $f_o = 6\pi\eta_o(3M\bar{v}_p/4\pi N)^{1/3}$, where η_o is the viscosity of the solvent (Svedberg and Pedersen, 1940; Tanford, 1961). For the dimer M = 60,000, $f^0_{20,b} = 5.7\times10^{-8}$ g s^{-1} and $\bar{v}_p = 0.75$ ml/g (Table I), which yields $f^0_{20,b}/f_o = 1.16$. In the case of maximal asymmetry (no hydration) this corresponds with an axial ratio of 3.7 for a prolate ellipsoid of revolution and of 3.9 for an oblate ellipsoidal particle (Svedberg and Pedersen, 1940). In the former, anhydrous particle the major and minor axes are 125 Å and 34 Å and in the latter 82 Å and 21 Å, respectively. For spherical symmetry the maximally hydrated particle has a diameter of 61 Å and a hydration of 0.42 g of H_2O/g protein.

When AtrE is studied in the presence of increasing amounts of SDS, first the value of $s^0_{20,b}$ decreases from 4.36 to 4.00 at an increase of SDS concentration from 0 to about 0.05 mM, then it remains constant during a further increase with about 0.3 mM and subsequently

it drops from 4.00 to 2.34 at an SDS concentration of about 0.35 mM (Figure 2(A)). At low SDS concentrations the value of the sedimentation coefficient of AtrE is close to that of BSA, whereas at concentrations above 0.5 mM it resembles that of Sub at high SDS concentrations (Figure 2(B)). In view of the molecular weights of the three proteins (for BSA and AtrE see above; for Sub, with ϕ_s = 0.735 ml/g, M = 27,600 $\pm$ 1300 in phosphate buffer or ammonium sulphate solutions up to 2 M at 20 ^{o}C, pH=7.4.) this indicates the occurrence of dissociation of the AtrE dimer at SDS concentrations around 0.35 mM. This transition is accompanied with a concomitant drop in the buoyant density mass from about 16,300 to about 8500 (Figure 3).

The fact that for AtrE the transition of $s^{0}_{20,b}$ occurs at a lower SDS concentration than for the other proteins (Cf. Figure 2) shows that its conformation is less resistant towards denaturation by SDS than that of the monomeric proteins BSA, which contains various disulphide bridges, and Sub, a single polypeptide chain without disulphide bridges but which is known to be rather resistant towards denaturation (Ottesen and Svendsen, 1970). AtrE contains only one disulphide bridge which is not providing much conformational stability as it connects two adjacent cysteine residues (Hessing, 1983).

Dissociation around 0.35 mM SDS in AtrE-SDS solutions as used for sedimentation experiments is not accompanied by an analogous drop in the enzyme activity (Figure 4). Apparently, inactivation is largely completed before dissociation occurs. As investigations by means of fluorescence spectrometry point to a rather large apolar binding pocket near the active serine (Van der Drift et al., 1983), this might indicate some preferential interaction of SDS with the active-site region in AtrE.

From the sedimentation equilibrium data (Figure 3) the amount of SDS bound per gram of protein has been estimated by applying Equations (1) and (2) with $\bar{v}_3$=0.885 ml/g (Granath, 1953; Hersh and Schachman, 1958). The results (Figure 5) show that there is a gradual increase in the amount of bound of SDS with concentration to a maximum value of about 0.4 g of SDS/g protein. This value is equal to that found for other proteins after reduction of disulphide bridges (Tanford, 1973).

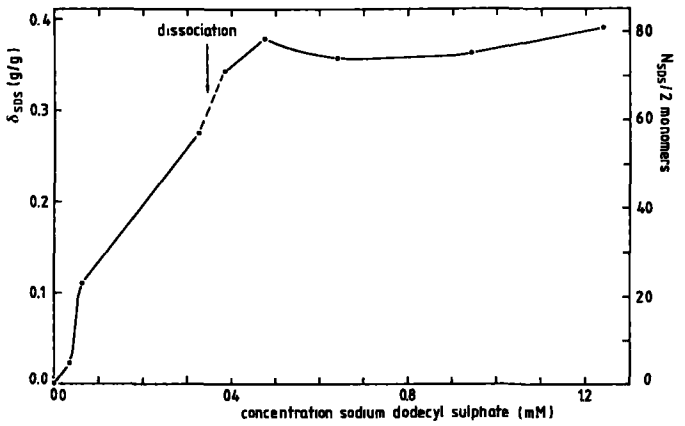

FIGURE 5: The influence of the concentration of sodium dodecyl sulphate (SDS) on the amount of SDS bound by atropinesterase in 10 mM phosphate buffer, pH = 7.4, at 20.0 °C. Left ordinate: amount of SDS, δ_{SDS}, per gram of protein. Right ordinate: number of SDS molecules, N_{SDS}, per atropinesterase dimer.

With $\bar{v}_3$=0.875 ml/g (Tanford et al., 1974) slightly smaller values were obtained. As Figures 3 and 5 show, after binding of about 57 SDS molecules per dimer, a further increase in binding of SDS causes dissociation. About 76 molecules of SDS are maximally bound per two AtrE monomers.

The value of the frictional ratio calculated for various concentrations of SDS from the data in Figures 2, 3 and 5 does not exceed 1.39; this is true for both the monomer and the dimer (no calculations are possible for the transition region because of the influence of heterogeneity, in particular on $s^0_{20,b}$). Both species can, therefore, be regarded as globular under the conditions employed (Tanford, 1961; Smith, 1970; Fish, 1975). The maximum values of the axial ratio and hydration have been estimated as outlined above for the unperturbed dimer, at various concentrations of SDS. The results for a prolate ellipsoid are plotted in Figures 6A,B. For an oblate ellipsoid of revolution comparable results were obtained. Although for the actual globular dimeric and monomeric species the values of the axial ratio and hydration will be smaller than those obtained for the two limiting hypothetical cases (Tanford, 1961), binding of SDS will affect both

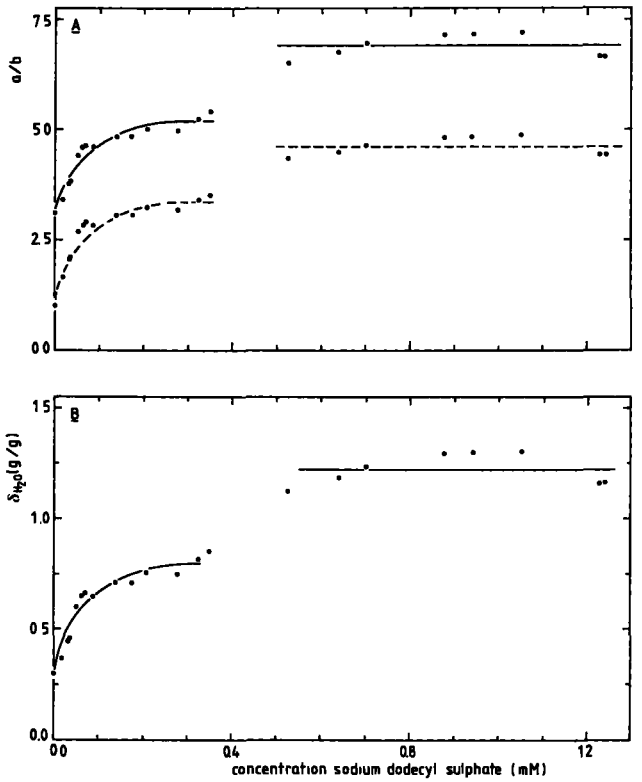

FIGURE 6A: Influence of sodium dodecyl sulphate (SDS) on the maximal axial ratio, a/b, of atropinesterase, by application of a prolate ellipsoidal model for the protein in solution (major axis 2a, minor axis 2b). Cases considered are: (———) the protein is not hydrated, and (- - -) the protein shows a gradual increase in hydration proportional to SDS binding such that the hydration per gram of protein-SDS complex remains equal to the maximum hydration of the unperturbed protein. The data points have been obtained from Figures 2(A) and 3, excluding the transition region (0.3 - 0.5 mM).

FIGURE 6B: Influence of sodium dodecyl sulphate (SDS) on the maximal hydration, δ_{H_2O}, of atropinesterase by application of a spherical model for the protein in solution. The data points have been obtained from Figures 2(A) and 5, excluding the transition region (0.3 - 0.5 mM).

these quantities qualitatively in a way shown in Figures 6A,B. However, in view of the lack of intramolecular cross-linking disulphide bridges in AtrE and the tendency of SDS to distribute uniformly along

a stretched polypeptide backbone, the contribution due to increased asymmetry will dominate (Cf. Reynolds and Tanford, 1970; Tanford, 1973; Bais et al., 1974). As an example this contribution for the case of a constant hydration per gram of protein-SDS complex, equal to the maximum hydration of the unperturbed protein, is represented in Figure 6A. Thus initially progressive binding of SDS leads to a rather gradual increase in the axial ratio of the dimer towards a constant value, until dissociation occurs at a concentration around 0.35 mM. The additional binding of about 9 SDS molecules per monomer (Figure 5) accompanying the transition results in an increase in the axial ratio which then remains constant at higher SDS concentrations.

For the association of the two AtrE monomers to a dimer various models can be devised. Two extreme cases are shown in Figure 7. If dimerization occurs by end-to-end association of the monomers, a de-

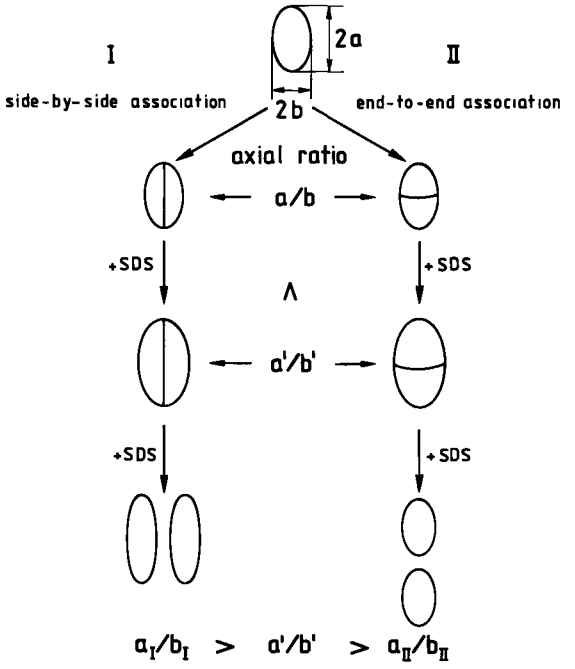

FIGURE 7: Schematic representation of two possible structures of the atropinesterase dimer and its dissociation due to interaction with SDS.

crease in the axial ratio upon dissociation would be expected, whereas in the case of side-by-side association an increase is likely to occur. The more or less sudden increase in the axial ratio in Figure 6A between 0.3 and 0.5 mM SDS suggests that the former model is less appropriate than the latter, i.e. dimerization of AtrE probably results from the side-by-side association of two ellipsoidal monomers.

APPENDIX: Analysis of the Monomer-Dimer Equilibrium of Atropinesterase.

The dimerization constant K_d (M^{-1}), the equilibrium constant of monomer-dimer association, may be related to $M_w^a(c)$ according to (Adams and Fujita, 1971; Williams, 1974)

$$2M_1/M_w^a(c) - 1 = (1 + 8K_dc)^{-\frac{1}{2}} + 2x10^{-3}\cdot B_2M_1^2c \qquad (7)$$

where M_1 is the molecular weight of the monomer, B_2 the second virial coefficient (mole ml g^{-2}) and c the total concentration expressed as moles of monomer per liter. In general, at low protein concentrations the second term on the right may be neglected ($M_w^a(c)=M_w(c)$) and K_d can be evaluated from the slope of the plot of $(M_w(c)/(2M_1-M_w(c)))^2 - 1$ versus c. The corresponding change in the standard Gibbs' free energy, ΔG, can be calculated from (Williams, 1971)

$$\Delta G = - RT \ln K_d \qquad (8)$$

Since the data obtained with samples of the batch that showed increased dissociation, did fit a monomer-dimer equilibrium (Figure 8), a value of K_d and of ΔG were estimated. At 20.0 °C, $K_d = (6.5 \pm 2.0) \times 10^5$ M^{-1}, corresponding with $\Delta G = -7.7 \pm 0.3$ kcal/mole. Figure 9 shows the dependence of ΔG on T for temperatures of 9-25 °C. Apparently, ΔG does not vary significantly within this temperature range, the average value being -8.1 ± 0.5 kcal/mole. The small temperature range does not allow a discrimination between enthalpic and entropic

contributions. As the other batches showed less dissociation, the value of -8.1 kcal/mole can at best be regarded as an upper limit of ΔG.

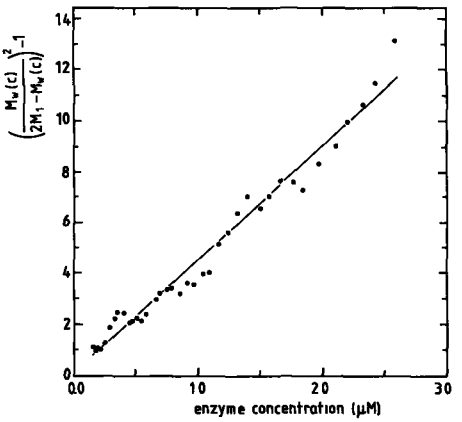

FIGURE 8: Example of a plot of $(M_w(c)/(2M_1-M_w(c)))^2-1$ as a function of total enzyme concentration (in moles of monomer/litre) for the batch of atropinesterase showing measurable dissociation, at 20.0 °C in 10 mM phosphate buffer, pH = 7.4, containing 0.15 M NaCl. The straight line was calculated by the method of least squares. Corresponding K_d = (5.6 ± 0.2) x 10^5 M^{-1}.

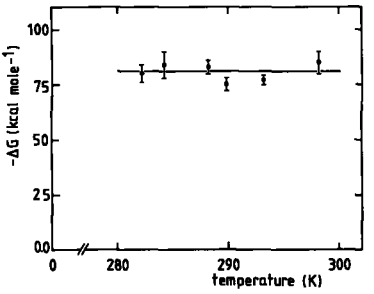

FIGURE 9: Change in the standard Gibbs' free energy of dimerization, ΔG, of atropinesterase as a function of temperature in the range 9.0-25.0 °C.

REFERENCES

Adams, Jr., E.T., and Fujita, H. (1963) in Ultracentrifugal Analysis (Williams, J.W., Ed.) p. 119, Academic Press, New York.

Bais, R., Greenwell, P., Wallace, J.C., and Keech, D.B. (1974) FEBS Lett. 41, 53.

Berends, F., Rörsch, A., and Stevens, W.F. (1967) in Proceedings of the Conference on "Structure and Reactions of DFP Sensitive Enzymes" (Heilbronn, E., Ed.) p. 45, Försvarets Forskningsanstalt, Stockholm.

Bradbury, J.H. (1970) in Physical Principles and Techniques of Protein Chemistry Part B (Leach, S.J., Ed.) p. 99, Academic Press, New York.

Brouwer, M., and Kuiper, H. (1973) Eur. J. Biochem. 35, 428.

Casassa, E.F., and Eisenberg, H. (1964) Adv. Protein Chem. 19, 287.

Chervenka, C.H. (1969) A Manual of Methods for the analytical ultracentrifuge. Spinco Division of Beckman Instruments, Inc., Palo Alto.

Edelstein, S.J., and Schachman, H.K. (1973) in Methods in Enzymology Vol. 27, Enzyme Structure, part D (Hirs C.H.W., and Timasheff, S.N., Eds.) p. 82, Academic Press, New York.

Elias, H.G. (1969) Ultrazentrifugen-Methoden, 3e Auflage, Beckman Instruments GmbH, München.

Eisenberg, H. (1976) Biological Macromolecules and Polyelectrolytes in Solution, Clarendon Press, Oxford.
Fish, W.A. (1975) in Methods in Membrane Biology Vol. 4, (Korn, E.D., Ed.), p. 189, Plenum Press, New York..
Fujita, H. (1975) Foundations of Ultracentrifugal Analysis (Chemical Analysis, Vol. 42) John Wiley and Sons, New York.
Granath, K. (1953) Acta Chem. Scand. 7, 297.
Hersh, R.T., and Schachman, H.K. (1958) Virology 6, 234.
Hessing, J.G.M. (1983) Ph.D. Thesis, University of Leiden.
Lee, J.C., and Timasheff, S.N. (1974) Arch. Biochem. Biophys. 165, 268.
Merrington, A.C. (1949) Viscometry, Edward Arnold and Co., London.
Oncley, J.L. (1941) Ann. N.Y. Acad. Sci. 41, 121.
Oosterbaan, R.A., and Berends, F. (1971) in Proc. Koninkl. Nederl. Akademie van Wetenschappen, Series C, Vol. 74, No. 2, 158.
Oosterbaan, R.A. et al. (1983) to be published.
Ottesen, M., and Svendsen, I. (1970) in Methods in Enzymology Vol. XIX, (Perlman, G.E., and Lorand, L., Eds.) p. 199, Academic Press, New York.
Reynolds, J.A., and Tanford, C. (1970) J. Biol. Chem. 245, 5161.
Rörsch, A., Berends, F., Bartlema, H.C., and Stevens, W.F. (1971) in Proc. Koninkl. Nederl. Akademie van Wetenschappen, Series C, Vol. 74, No. 2, 132.
Schachman, H.K. (1959) Ultracentrifugation in Biochemistry, Academic Press, New York.
Smith, M.H. (1970) in Handbook of Biochemistry, 2nd Edit. (Sober, H.A., Ed.) p. C-3, The Chemical Rubber Co., Cleveland.
Stevens, W.F. (1969) Ph.D. Thesis, University of Leiden.
Svedberg, T., and Pedersen, K.O. (1940) Die Ultrazentrifuge, Verlag von Theodor Steinkopff, Dresden.
Tanford, C. (1961) Physical Chemistry of Macromolecules, John Wiley and Sons, Inc., New York.
Tanford, C. (1973) The Hydrophobic Effect: Formation of Micelles and Biological Membranes, John Wiley and Sons, Inc., New York.
Tanford, C., Nozaki, Y., Reynolds, J.A., and Makino, S. (1974) Biochemistry 13, 2369.
Van der Drift, A.C.M., Roos, A.L.M., and Moes, G.W.H. (1983) This Thesis, Chapter 2; to be submitted for publication.
Van Holde, K.E. (1971) Physical Biochemistry, Prentice-Hall Inc., Englewood Cliffs, New Jersey.
Williams, J.W. (1972) Ultracentrifugation of Macromolecules, Academic Press, New York.
Zwennis, W.C.M. (1972) personal communication.

CHAPTER 2

COMPARISON OF THE ACTIVE SITES OF ATROPINESTERASE AND SOME SERINE PROTEASES BY FLUORESCENT LABELLING WITH A DANSYL GROUP

ABSTRACT: The active-centre region of atropinesterase (AtrE) from Pseudomonas putida PMBL-1 was compared with that of the serine proteases α-chymotrypsin (Chymo) and subtilisin A (Sub) by means of fluorescence spectrometry. This comparison has become possible because under appropriate conditions the active centre of these serine hydrolases can be specifically labelled with a dansyl (1-dimethylaminonaphthalene-5-sulphonyl) group by sulphonylation with dansyl fluoride. The labelling gives rise to a new low-energy band in both the absorption and emission spectrum of the enzymes. The spectral characteristics of these bands, such as the wave number of maximal absorption and the corresponding molecular extinction coefficient, the wave number of maximal emission ($\bar{\nu}_e^m$) and the quantum yield of fluorescence (ϕ^f), have been determined under various conditions. In order to be able to interpret these data, some dansylated low-molecular weight model compounds have also been studied in various solvents differing in Debye orientation polarization and hydrogen-bonding capacity.

Evidence has now been obtained that in the three enzymes the fluorescent reporter group is covalently attached to the oxygen of the side chain of the active serine and not to a histidine, as has been suggested by others. In all cases the dimethylamino group appears to be embedded in the protein structure; furthermore the carbon atom of the sulphonylated serine side chain is not accessible to nucleophilic attack by I^-. Notwithstanding these similarities the environment of the reporter group in AtrE differs from that in Chymo or Sub. On the basis of the enhancement of ϕ^f by deuterium oxide and the dependence of $\bar{\nu}_e^m$ and ϕ^f on the Debye orientation polarization factor, it is concluded that at pH 6.0-8.5 the dansyl label in the two proteases is mainly exposed to solvent whereas in AtrE the reporter group is embedded to an appreciable extent in the protein structure. The $\bar{\nu}_e^m$ and ϕ^f of the dansyl group in AtrE are very sensitive, therefore, to any changes in the protein structure in the immediate environment, e.g. due to variations in pH. From the effects of pH-alteration in the range 6-8.5 it is concluded that the active-site region of AtrE is sensitive to (de)-protonation of two histidines: a normal one with pK_a=6.5 and a histidine which forms part of a charge-relay system with pK_a=7.5. The presence of this particular histidine in combination with a hydrophobic binding site near the active serine points to a structural similarity between the active-site region of AtrE and that of serine proteases and consequently to a similar mechanism for enzymic activity.

Upon lowering the pH to values below 4 the enzymes undergo a conformational change. For Chymo and Sub this leads to an increased incorporation of the dansyl

label into the protein structure, whereas for AtrE mainly hydrogen bonding between label and environment in the excited state is lost. At low pH the environment of the dansyl label in AtrE resembles that in Sub more strongly than that in Chymo. At neutral pH the active sites of AtrE and of Chymo seem to be more sensitive to variation in ionic conditions than that of Sub.

INTRODUCTION

Serine proteases are hydrolases which catalyse the hydrolysis of peptide and ester bonds in proteins and particular esters (Walsh and Wilcox, 1970; Fruton, 1975). During this process one serine residue with an unusually strong nucleophilic hydroxyl group (the so-called active serine) plays a dominant role (Hartley, 1960). Two superfamilies are distinguishable among this type of enzyme: the prothrombin-related proteases, distributed mainly among the vertebrates, and the subtilisins, found in bacteria (Hartley, 1970; Walsh and Wilcox, 1970). For various members of each of these superfamilies, e.g. α-chymotrypsin (Kraut et al., 1967; Sigler et al., 1968; Steitz et al., 1969; Cohen et al., 1970; Birktoft et al., 1970; Birktoft and Blow, 1972; Wright et al., 1972) and subtilisin A (Wright et al., 1969; Alden et al., 1970, 1971), the detailed three-dimensional structure has been elucidated by means of X-ray diffraction. It was found that although the primary structures of members of different superfamilies show no homology, the tertiary structures of their active-site regions have some common features which form the structural basis of enzymic activity (Walsh, 1975; Kraut, 1977).

Some time ago a new serine hydrolase has been isolated from Pseudomonas putida PMBL-1 which specifically catalyses the hydrolysis of (-)-atropine to (-)-tropic acid and tropine (Berends et al., 1967; Stevens, 1969; Oosterbaan and Berends, 1971; Rörsch et al., 1971). In contrast to the above-mentioned proteases, this so-called atropinesterase has no proteolytic activity and thus can be regarded as a true esterase. Since the amino-acid sequence shows no homology with any of the known serine hydrolases (Hessing, 1983), it represents a new superfamily of these enzymes. To investigate whether the tertiary

structure of the active site of this enzyme nevertheless resembles that of serine proteases, a comparative study with α-chymotrypsin and subtilisin A has been performed by using different reporter groups specifically bound to the active sites and various spectroscopic techniques.

In order to enable the application of fluorescence spectrometry, various inhibitors reported to be suited for the covalent and specific binding of a fluorescent label to the active site of a serine enzyme were tried out. Most of these appeared to be useless for the present investigation. 1-Dimethylaminonaphthalene-5-sulphonyl chloride (DNS-Cl), for example, which can be used to label the active site of α-chymotrypsin (Hartley and Massey, 1956; Gundlach et al., 1962; Gold, 1965) is very reactive and, as a consequence, unstable in aqueous solution. Labelling has therefore to be performed with a large excess of DNS-Cl, leading also to non-specific reactions with other sites of the enzyme molecule (Hartley and Massey, 1956; Gold, 1965). Besides, atropinesterase does not endure the relatively high acetone concentration required for labelling with DNS-Cl. p-Nitrophenyl anthranilate, by means of which an anthraniloyl group can be specifically attached to the active site of α-chymotrypsin (Haugland and Stryer, 1967), did not show specific interaction with atropinesterase.

Himel et al. (1971) reported that various cholinesterases were inhibited by dansyl fluoride (DNS-F). Fluorescence studies by Vaz and Schoellmann (1976[a,b]) suggested that by inhibition with DNS-F a dansyl group can be specifically introduced at the active sites of α-chymotrypsin and subtilisin, presumably by sulphonylation at the active serine. DNS-F appeared to be a very useful probe for the present investigation. Besides inhibiting α-chymotrypsin and subtilisin it is also a good inhibitor of atropinesterase. As will be shown, under appropriate conditions a fluorescent reporter group can be covalently and specifically attached to the active serine of all three enzymes. As DNS-F is very stable in aqueous solution, labelling of the active site can be performed at low concentrations, thus minimizing non-specific side reactions. Apart from the high selectivity for the active site, the dansyl label meets other criteria required for a useful re-

porter group such as: 1) high sensivity to variations in the direct environment, and 2) absorption and emission spectrum distinct from that of the intrinsic fluorophores in the enzymes.

In the present paper results are presented of a comparative investigation of the fluorescence of atropinesterase, α-chymotrypsin and subtilisin A labelled by means of DNS-F. Results of an investigation of the steady-state kinetics of this inhibition will be presented elsewhere.

MATERIALS AND METHODS

a. Enzymes and Other Chemicals

Salt-free, crystalline α-chymotrypsin from bovine pancreas (EC 3.4.21.1; M = 24,800) was obtained from Sigma Chemical Company (Lot 40F-8051, 3x crystallized and lyophilized), crystalline subtilisin A (EC 3.4.21.14; M = 27,300) was purchased from NOVO Industri A/S (Batch 70-4). Atropinesterase (M = 30,300) was obtained according to the procedure of Rörsch et al. (1971) as modified by Oosterbaan et al. (1983).

1-Dimethylaminonaphthalene-5-sulphonyl fluoride (DNS-F), 1-dimethylaminonaphthalene-5-sulphonyl ethyl ester (DNS-OEt), 1-dimethylaminonaphthalene-5-sulphonic acid (DNS-OH), 1-dimethylaminonaphthalene-5-sulphonyl imidazole (DNS-Imid) and 1-dimethylaminonaphthalene-5-sulphonyl N-carbobenzoxy-DL-histidine (DNS-CBZ-His) were synthesized and characterized as described in the Appendix. Syntheses of these dansyl compounds were performed with reagent-grade chemicals, obtained from Merck, Aldrich and Fluka and used without further purification, unless indicated otherwise. The products were stored in the dark at -20 ^{o}C. For inhibition purposes solutions of DNS-F in dry acetone (1 and 10 mM) were used; these were kept in the dark at 4 ^{o}C. Diisopropyl phosphorofluoridate (DFP) was kindly provided by Mr. C. de Borst (Prins Maurits Laboratory TNO).

Dimethylformamide was spectroscopic grade. All other organic solvents used were reagent grade and were distilled shortly before use.

Dioxane and n-butanol were purchased from Union Chimique Belge, the other solvents, including deuterium oxide (D_2O; Uvasol), from Merck.

Sodium dodecyl sulphate (SDS) was purchased from Schwarz/Mann, potassium iodide (KI), potassium chloride (KCl), sodium sulphite (Na_2SO_3) - all analytical grade - and hydrogen peroxide (Perhydrol, 30% H_2O_2) from Merck.

b. Characterization of Enzymes

The amount of active α-chymotrypsin (Chymo) in the batch used was determined spectrophotometrically by titration with p-nitrophenyl acetate (Serva) in 67 mM phosphate buffer, pH=7.8, as described by Kézdy and Kaiser (1970). The purity was found to be 73%, in agreement with that found on the basis of the amount of phosphorus bound by inhibition with DFP (see below). Total enzyme concentrations were determined with $E_{280}^{0.1\%} = 2.04$ (Worthington Enzyme Manual, 1977).

Since the first method mentioned above is not applicable to subtilisin (Sub), the amount of active enzyme in the batch used was determined indirectly by inhibition of a certain amount of enzyme in solution with DFP followed by purification by either extensive dialysis or gel filtration on a Sephadex G-50 column, which showed a single protein peak. The total amount of protein-bound phosphorus in the purified sample, determined according to the method of Gerlach and Deuticke (1963) as modified by Kienhuis and Baar (1964), yielded a value of 50-60% active enzyme. Spectrophotometrically, by using $E_{280}^{0.1\%} = 0.96$ (Ottesen and Svendsen, 1970), the total amount of Sub was found to be 56% (Cf. Bender et al., 1966). On the basis of these data the amount of active Sub was assumed to be 56%.

Atropinesterase (AtrE) was almost pure as shown by polyacrylamide gel electrophoresis (1 band) and isoelectric focusing (1 main band and a few minor bands) (Cf. Hessing, 1983). Amounts of active AtrE were determined from the measured activity, by assuming a turnover number of 30,000 molecules of (-)-atropine (hyoscyamine) per minute per molecule AtrE (Rörsch et al., 1971). Total AtrE concentrations were determined spectrophotometrically with $E_{280}^{0.1\%} = 1.85$ (Cf. Hessing, 1983).

For inhibition all enzyme solutions were prepared in 10 mM phosphate buffer, pH=7.4, containing 0.1 mM sodium azide (Merck) to prevent growth of bacteria.

Enzyme activities were measured titrimetrically at 25.0 $\pm$ 0.1 ^{o}C in a Radiometer pH-stat equipment composed of a Titrator TTT 1c and a Titrigraph SBR 2c (Cf. Rörsch et al., 1971). N-acetyl-L-tyrosine ethyl ester (Merck) was used as a substrate for Chymo and Sub, and hyoscyamine sulphate (Nutritional Biochemicals Corporation) for AtrE. After pH and temperature equilibration of 12 ml of a substrate solution in the thermostatically controlled reaction vessel under CO_2-free air a few µl of enzyme solution were added. The acid-releasing reaction was followed by pH-stat addition of 0.0196 N NaOH for at least 5 min. Enzyme activities were evaluated graphically.

c. Labelling

Dansyl labelling was performed at room temperature (20-25 ^{o}C) by adding to 1-3 ml of enzyme solution (1-70 µM active enzyme) a small volume of 1 or 10 mM DNS-F in dry acetone, so that the concentration of DNS-F exceeded that of the enzyme by a factor of 3-4. After incubation in the dark for at least 24 h enzyme activity was below the detection limit (residual activity < 0.5%). Excess inhibitor was rapidly removed by gel filtration at room temperature on a Sephadex G-50 column. For preparations at pH $\geq$ 6 10 mM phosphate buffers were used as eluents, for preparations at pH < 6 10 mM phosphate/citrate buffers (all buffers contained 0.1 mM sodium azide). Labelled enzymes were eluted as single peaks, as measured by the absorbance at 280 nm. Only top fractions (residual activity < 1%) were used for fluorescence measurements. Solutions of labelled protein were stored in the dark at 4 ^{o}C and measured as soon as possible after isolation in order to minimize contamination by release of DNS-OH (see below).

Inhibition of the enzymes with DFP was performed at room temperature by adding a solution of DFP (0.1 M in dry, peroxide-free isopropanol) up to a concentration of about 20 times that of the enzyme. After about 4 h enzyme activity was below the detection limit and excess DFP was removed by gel filtration on a Sephadex G-50 column.

d. Spectrometry

Fully corrected emission and excitation spectra of samples thermostated at 20 °C were obtained with a modified double-beam differential absolute spectrofluorimeter, type Fica 55, equipped with a 450 W high pressure Xenon arc lamp (Osram, XBO 450 W) for excitation and a Hamamatsu R 928 photomultiplier (spectral response 200 - 800 nm) for detection. Automatic correction for intensity variation of the excitant light was performed with a thermostated (31 °C) rhodamine B solution (5 g, freshly recrystallized from absolute ethanol, per liter ethylene glycol) as quantum counter (White and Argauer, 1970). The variation in sensitivity of the detection unit with wavelength of the emitted light was automatically corrected by electric compensation of the photomultiplier voltage with an adjustable function potentiometer. For wavelengths above 400 nm calibration of this compensation was performed according to the standardized fluorescence method (White and Argauer, 1970) with the following, freshly crystallized dyes: quinine sulphate dihydrate (Lamers en Indemans B.V.), 3-aminonaphthalimide, m-nitrodimethylaniline and 4-dimethylamino-4'-nitrostilbene (all three from Eastman Kodak). Calibration for smaller wavelengths was done by reflection on barium sulphate (White Reflectance Coating, Lot 503-6A; Eastman Kodak Company).

For reasons of selectivity (see below) excitation was performed at wavelenghts above 395 nm, unless indicated otherwise. For excitation the bandwidth was $\leq$ 5 nm, for emission detection it was $\leq$ 7.5 nm. Quartz Suprasil half micro cuvettes with 4 mm effective path length (Hellma GmbH and Co.) were used in order to minimize corrections for inner filter effect. To facilitate comparison, all emission spectra of the proteins and model compounds presented have been normalized to a concentration of about 50 µM and are expressed in the same, arbitrary units. The spectra shown have been corrected for variations in the refractive indexes. Spectral characteristics, such as wave number of maximal emission ($\bar{\nu}_e^m$) or excitation ($\bar{\nu}_{ex}^m$), were determined from fully corrected spectra; relative quantum yields of fluorescence, ϕ^f, have been calculated according to

$$\phi^f = \phi^f_r * \frac{n_s^2}{n_r^2} * \frac{(1-10^{-\varepsilon cd})_r}{(1-10^{-\varepsilon cd})_s} * \frac{F_s}{F_r} \qquad (1)$$

where F is the area under the emission spectrum on wavelength scale, ε the molecular extinction coefficient at the wavelength of excitation, c the concentration (M), d the path length of the incident light in the effective emitting volume of the solution, and n the refractive index; s and r refer to sample and reference compound, respectively (Brand and Witholt, 1967; White and Argauer, 1970). Freshly prepared solutions of quinine sulphate dihydrate in 1 N sulphuric acid were used as reference (ϕ^f=0.55 at 365 nm excitation; White and Argauer, 1970). The optical densities of the solutions to be measured did not exceed 0.05 at the wavelength of excitation (for 1 cm path length). Since there were no indications of an oxygen effect on ϕ^f, no special precautions were taken to remove oxygen. In the case of DNS-OH the method outlined above yielded ϕ^f=0.36 which equals the value found by others (Chen, 1966; Himel and Mayer, 1970).

Absorption spectra were recorded at 20 °C with a double-beam spectrophotometer (Acta TM III; Beckman) by using standard cuvettes (1 cm path length). Wave number of maximal absorption ($\bar{\nu}^m_a$) and the corresponding molecular extinction coefficient (ε^m) were determined from these spectra. Refractive index measurements were performed at 20 °C at the sodium D-line (589.3 nm) with an Abbe-refractometer (Carl Zeiss). Oscillator strength f and natural life time τ_o (ns), were estimated from the absorption and emission spectra as described elsewhere (Van der Drift and Roos, 1983[c]).

RESULTS

a. Stoichiometry of Inhibition

Addition of a small excess of DNS-F to solutions with a low concentration of native Chymo, Sub or AtrE (Figure 1) resulted in complete inhibition of enzymic activity. After removal of excess inhibitor by gel filtration or by extensive dialysis at 4 °C, the enzymes re-

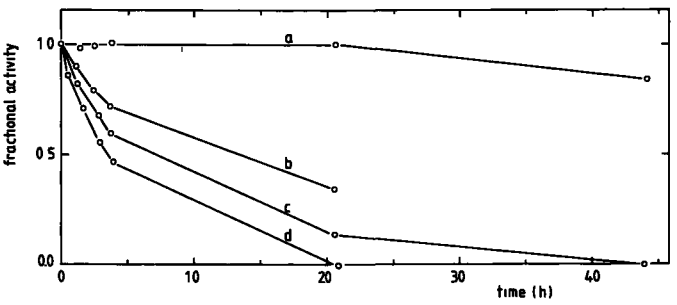

FIGURE 1: Inhibition of atropinesterase (AtrE) by low concentrations of dansyl fluoride (DNS-F). Experimental conditions: approx. 3 μM active AtrE in 10 mM phosphate buffer, pH = 7.4 at 25.0 °C; concentration DNS-F: a = 0 μM, b = 3 μM, c = 6 μM and d = 9 μM.

mained inhibited. A new low-energy band in the UV-absorption (Figure 2) and fluorescence emission spectra (Figure 3) was observed, the intensity of which - immediately after complete inhibition - was independent of excess inhibitor up to concentrations of at least 5 times that of the enzymes. The spectral characteristics of these bands (Table I) are typical for a 1-dimethylaminonaphthalene-5-sulphonate (Cf. Van der Drift and Roos, 1983[c]).

The values of ε^m in the new absorption bands, based on the initial amount of active enzyme (Table I), are of the same order of magnitude as those for dansylated model compounds (Tables II and III; Cf. Chen, 1968). Measurements with a fluoride-selective electrode (Orion) showed that during inhibition F^- was gradually released. The final concentration of F^- at complete inhibition and the amount of DNS-OH liberated from inhibited enzyme by treatment with 0.1 N NaOH (fluorescence measurement) were both 5-10% smaller than the initial concentration of active enzyme. Since at pH=7.4 and 20 °C in the dark decomposition of DNS-F into DNS-OH and F^- was less than 6% in 16 h and DNS-OH did not inhibit the enzymes, these observations indicated that only one dansyl group was covalently bound per enzyme molecule by reaction with DNS-F (Cf. Vaz and Schoellmann, 1976[a]). As enzymes inhibited by DFP showed no reaction with DNS-F, the dansyl group was very likely bound to a functional group at the active site of the enzyme.

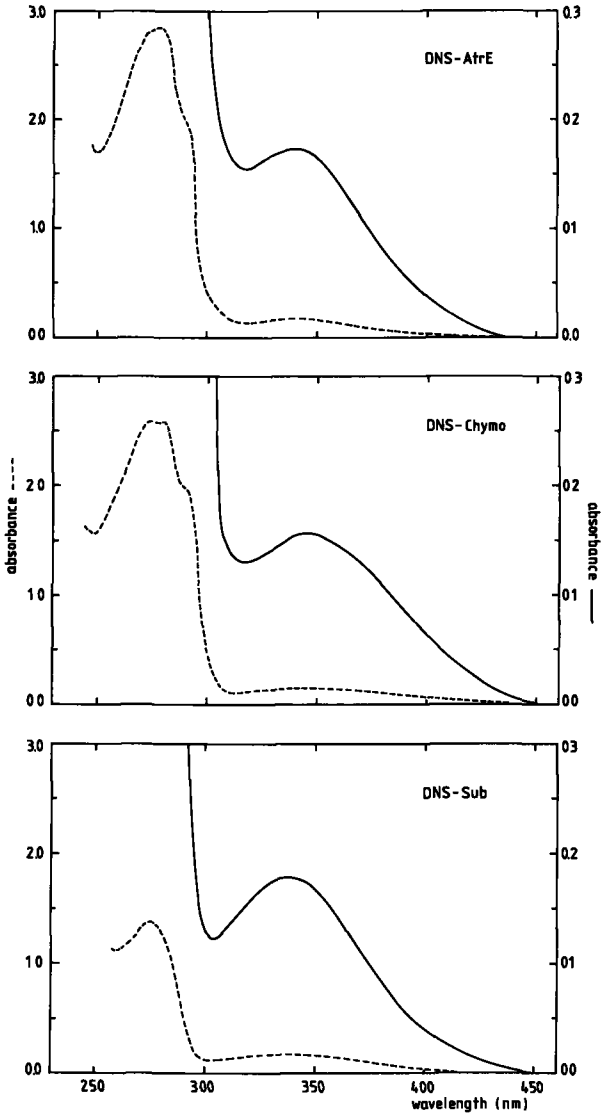

FIGURE 2: Absorption spectra (- - -) and expanded lowest energy bands (———) of dansylated atropinesterase (DNS-AtrE), α-chymotrypsin (DNS-Chymo) and subtilisin A (DNS-Sub). Conditions: approx. 50 μM labelled enzyme in 10 mM phosphate buffer, pH = 7.4, at 20 °C.

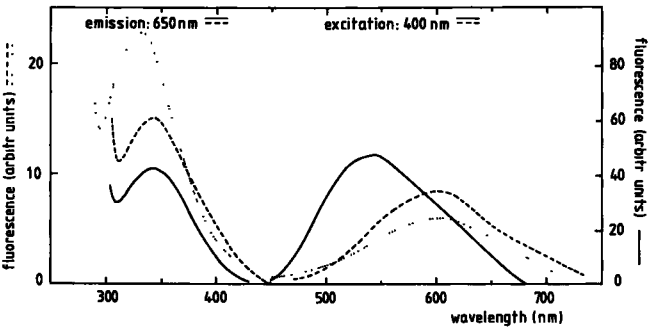

FIGURE 3: Corrected excitation spectra (left, emission at 650 nm) and emission spectra (right, excitation at 400 nm) of dansylated atropinesterase (———), α-chymotrypsin (- - -) and subtilisin A (.....). Conditions: approx. 50 μM labelled enzyme in 10 mM phosphate buffer, pH = 7.4, at 20 °C.

b. Origin of Spectral Differences

Under normal conditions,the emission spectrum of DNS-AtrE in buffer differed appreciably from that of the other dansylated enzymes (Figure 3), in particular with respect to the position of maximal emission and the quantum yield (Table I). In principle these differences may be due to attachment to a different functional group, to a different environment of the reporter group in the enzymes, or both.

Isolation of the dansyl-labelled amino acid after enzymic digestion or acid hydrolysis of the inhibited enzyme for the purpose of a direct identification of the functional group, e.g. by thin-layer

TABLE I: Characteristics of the lowest energy bands in the absorption and emission spectra of various dansylated serine enzymes in 10 mM phosphate buffer, pH = 7.4, at 20 °C. (1)

Enzyme	$\bar{\nu}_a^m$ (2)	ε^m	$\bar{\nu}_e^m$	ϕ^f	f	τ_o	ϕ_D^f/ϕ^f
Atropinesterase	2.916 (2.907)	3.46	1.838	0.180	0.077	39	1.07
α-Chymotrypsin	2.899 (2.915)	3.14	1.667	0.036	0.076	52	1.18
Subtilisin A	2.924 (2.994)	3.53	1.656	0.026	0.075	55	1.19

(1) $\bar{\nu}_a^m$ = wave number of maximum absorption (10^4 cm^{-1}), ε^m = molecular extinction coefficient at maximum absorption (10^3 $cm^{-1}M^{-1}$), $\bar{\nu}_e^m$ = wave number of maximum emission (10^4 cm^{-1}), ϕ^f = quantum yield of fluorescence, f = oscillator strength, τ_o = natural life time (ns), ϕ_D^f = quantum yield of fluorescence in the presence of D_2O/H_2O (50% v/v).

(2) Within parentheses, values of the wave number of maximum excitation (10^4 cm^{-1}).

TABLE II: *Characteristics of lowest energy bands in the absorption and emission spectra the model compounds* 1-dimethylaminonaphthalene-5-sulphonyl ethyl ester (DNS-OEt) and 1-dimethylaminonaphthalene-5-sulphonyl imidazole (DNS-Imid) in various pure solvents. (1)

Solvent	DNS-OEt						DNS-Imid					
	$\bar{\nu}_a^m$	ϵ^m	$\bar{\nu}_e^m$	ϕ^f	f	τ_o	$\bar{\nu}_a^m$	ϵ^m	$\bar{\nu}_e^m$	ϕ^f	f	τ_o
acetone	2.915	2.86	1.880	0.373	0.051	51	2.786	2.38	1.675	0.146	0.044	80
n-butanol	2.924	2.75	1.869	0.453	0.056	44	2.793	2.46	1.667	0.067	0.052	63
dimethylformamide	2.890	2.79	1.825	0.414	0.056	44	2.762	2.35	1.621	0.068	0.048	68
dioxane	2.924	2.91	1.961	0.657	0.056	36	2.809	2.54	1.805	0.466	0.053	47
ethanol	2.924	2.85	1.852	0.356	0.059	46	2.801	2.37	1.661	0.043	0.052	69
ethylene glycol	2.907	2.78	1.795	0.270	0.058	44	2.762	2.33	1.610	0.018	0.054	62
formamide	2.890	2.75	1.757	0.182	0.057	46	2.762	2.28	1.592	0.016	0.046	73
isopropanol	2.924	2.74	1.869	0.432	0.057	45	2.793	2.45	1.664	0.067	0.056	62
methanol	2.924	2.70	1.825	0.274	0.059	52	2.786	2.62	1.634	0.027	0.061	67
n-propanol	2.924	2.71	1.855	0.400	0.056	46	2.793	2.45	1.661	0.054	0.055	62
water	3.030	2.82	1.658	0.028	0.063	66	2.915	2.65	1.558	0.002	0.063	77

(1) For symbols and corresponding units, see footnote (1) of Table I.

TABLE III: Characteristics of the lowest energy bands in absorption and emission spectra of the model compounds 1-dimethylaminonaphthalene-5-sulphonyl ethyl ester (DNS-OEt) and 1-dimethylaminonaphthalene-5-sulphonyl imidazole (DNS-Imid) in various dioxane-water mixtures in the presence or absence of 10 mM SDS. (1)

Solvent composition (% v/v)		DNS-OEt						DNS-Imid					
dioxane	water	$\bar{\nu}_a^m$	ϵ^m	$\bar{\nu}_e^m$	ϕ^f	f	τ_o	$\bar{\nu}_a^m$	ϵ^m	$\bar{\nu}_e^m$	ϕ^f	f	τ_o
80	20	2.915	2.77	1.838	0.485	0.056	45	2.770	2.59	1.647	0.052	0.057	59
+10 mM SDS		2.915	2.77	1.842	0.477	0.055	45	2.770	2.54	1.647	0.053	0.054	61
60	40	2.924	2.78	1.808	0.290	0.060	46	2.793	2.51	1.616	0.023	0.057	64
+10 mM SDS		2.924	2.77	1.799	0.281	0.059	47	2.793	2.45	1.613	0.024	0.056	67
40	60	2.958	2.65	1.770	0.173	0.059	52	2.841	2.48	1.592	0.011	0.062	66
+10 mM SDS		2.950	2.82	1.776	0.180	0.063	48	2.833	2.48	1.595	0.011	0.061	66
20	80	3.003	2.80	1.709	0.083	0.061	59	2.874	2.64	1.572	0.005	0.064	69
+10 mM SDS		2.976	2.57	1.745	0.117	0.056	61	2.849	2.50	1.610	0.010	0.061	68
0	100	3.030	2.82	1.658	0.028	0.063	66	2.915	2.65	1.558	0.002	0.063	77
+10 mM SDS		2.976	2.72	1.745	0.119(2)	0.064	55	2.849	2.52	1.623	0.011	0.061	69

(1) For symbols and corresponding units, see footnote (1) of Table I.

(2) Replacement of 50% of the water by deuterium oxide leads to an increase of this value by a factor of 1.13.

chromatography, appeared to be impossible because DNS-OH was released rapidly by keeping protein solutions at higher temperatures and upon denaturation of the protein (pH < 1, 8 M urea or 6 M guanidine hydrochloride with 1 mM 1,4-dithiothreitol; Cf. Vaz and Schoellmann, 1976[a]). Consequently, an indirect identification procedure had to be followed.

Spectroscopically one can distinguish indirectly between the contributions of the environment and the functional group by minimizing any difference between the environment of the dansyl group in the three enzymes. This can be achieved by partial or complete denaturation of the protein leading to either an increased or a decreased solvent exposure of the label, depending on the type of denaturant used. In contrast to polar denaturants such as urea and guanidine hydrochloride which cause increased exposure to the solvent and a concomitant release of label, the detergent SDS, which shows a high affinity to apolar parts of proteins (Cf. Tanford, 1973), appeared to be a useful perturbant. Figure 4 shows the excitation and emission spectra of the labelled enzymes recorded 20-30 min after addition of 10 mM SDS; the corresponding values of the spectral parameters are compiled in Table IV.

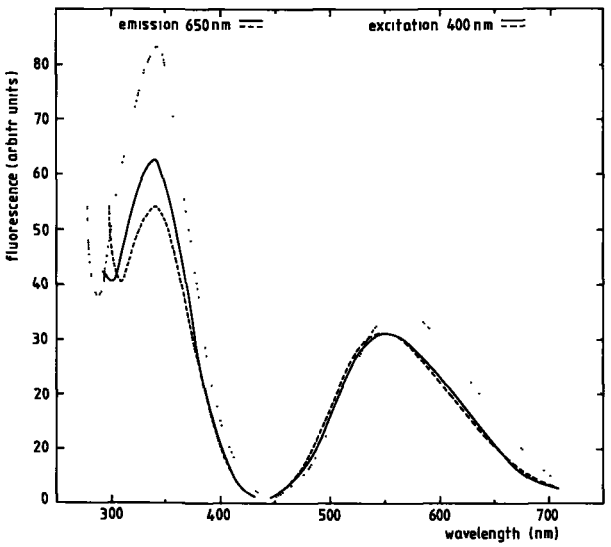

FIGURE 4: Corrected excitation spectra (left, emission at 650 nm) and emission spectra (right, excitation at 400 nm) of dansylated atropinesterase (————), α-chymotrypsin (- - -) and subtilisin A (.....) in the presence of sodium dodecyl sulphate (SDS). Conditions: approx 50 μM labelled enzyme and 10 mM SDS in 10 mM phosphate buffer, pH = 7.4, at 20 °C.

TABLE IV: Characteristics of the lowest energy bands in excitation and emission spectra of dansylated serine enzymes in various aqueous systems at 20 °C. (1),(2)

System	Atropinesterase			α-Chymotrypsin			Subtilisin A		
	$\bar{\nu}^m_{ex}$	$\bar{\nu}^m_e$	ϕ^f	$\bar{\nu}^m_{ex}$	$\bar{\nu}^m_e$	ϕ^f	$\bar{\nu}^m_{ex}$	$\bar{\nu}^m_e$	ϕ^f
Buffer (pH = 7.4) + 10 mM SDS	2.924	1.818	0.125	2.924	1.825	0.129	2.924	1.786	0.149
+ 3.4 M KI + 10 mM Na_2SO_3	2.907	1.908	0.174	2.933	1.859	0.114	2.967	1.645	0.027
+ 3.4 M KCl + 10 mM Na_2SO_3	2.915	1.905	0.172	2.933	1.664	0.041	2.985	1.647	0.029

(1) $\bar{\nu}^m_{ex}$ = wave number of maximum excitation (10^4 cm^{-1}), $\bar{\nu}^m_e$ = wave number of maximum emission (10^4 cm^{-1}), ϕ^f = quantum yield of fluorescence.

(2) Measurements were done 20-30 min after sample preparation.

Comparison between Figures 3 and 4 and between Tables I and IV shows that the presence of SDS leads to a considerable similarity in the spectral characteristics, indicating that the spectral differences between the unperturbed labelled enzymes can be ascribed to different environments of the probe. Higher concentrations of SDS had no appreciable additional effect on the spectra. In the presence of SDS there was a slow release of DNS-OH, which became spectroscopically inconvenient after 4-6 h. The small red shift in the excitation spectrum of Sub due to SDS can be ascribed to a reduction of the relative contribution of DNS-OH to emission (see Discussion).

c. Identification of the Functional Group

There is ample evidence, both direct and indirect, that inhibition of Chymo with phenylmethanesulphonyl fluoride (PMS-F) takes place via attachment of the PMS-group to the active serine (Gold and Fahrney, 1964; Gold, 1965; Matthews et al., 1967). Also, the inhibition of Chymo with 2-hydroxy-5-nitro-α-toluenesulphonic acid sultone (Heidema and Kaiser, 1967, 1968; Kézdy and Kaiser, 1970) or with DNS-Cl (Gold, 1965) is very likely due to sulphonylation of the side-chain hydroxyl group of the active serine. However, the results of Gundlach et al. (1962), obtained with dansyl chloride, point to sulphonylation of the imidazole side chain of a histidine. To discriminate between these two

possibilities, the spectral properties of the model compounds DNS-OEt, DNS-CBZ-His and DNS-Imid have been investigated. In spite of numerous attempts it has not been possible to synthesize DNS-serine with the dansyl group attached to the side-chain hydroxyl group. DNS-OEt, however, may be expected to have spectral characteristics similar to O-DNS-serine. As the spectral characteristics of DNS-CBZ-His did not differ significantly from those of DNS-Imid, only the results of the latter are presented.

The spectral characteristics of DNS-OEt and DNS-Imid in pure solvents of different polarity and hydrogen-bonding capacity are compiled in Table II. Comparison of the various sets of data with those of the labelled enzymes (Table I) shows that the characteristics of the labelled functional group in the enzymes can be approximated more closely by DNS-OEt than by DNS-Imid. The absorption and emission spectrum of DNS-OEt in buffer are shown in Figure 5. The spectral characteristics of DNS-OEt and DNS-Imid in water-SDS and dioxane-water-SDS mixtures (Table III), which may serve as a model system for the protein-water-SDS system (Table IV), support this observation. In particular the spectra of DNS-OEt in phosphate buffer with and without SDS (Figure 5(B), Table III) are quite similar to corresponding spectra of the labelled enzymes (Figures 3 and 4, Tables I and IV). For DNS-Imid such a similarity is not found. The spectral properties of DNS-F, DNS-CBZ-His and DNS-OH did not agree with those of the labelled enzymes either. These results strongly suggest that the dansyl group is bound to the side-chain oxygen of a serine at the active site of the enzymes. Addition of H_2O_2 in low concentrations (< 0.1 M) to the DNS-labelled enzymes caused some restoration of enzyme activity in all cases. This has also been reported for benzenesulphonyl Chymo (Gibian et al., 1969); it gives additional support to the conclusion that the dansyl group is bound to serine rather than to histidine.

d. Perturbation Studies on Labelled Enzymes and a Model Compound

In order to characterize the environment of the dansyl group in the enzymes in more detail, some perturbation studies have been performed in which the influences of changes in the medium on the spectra

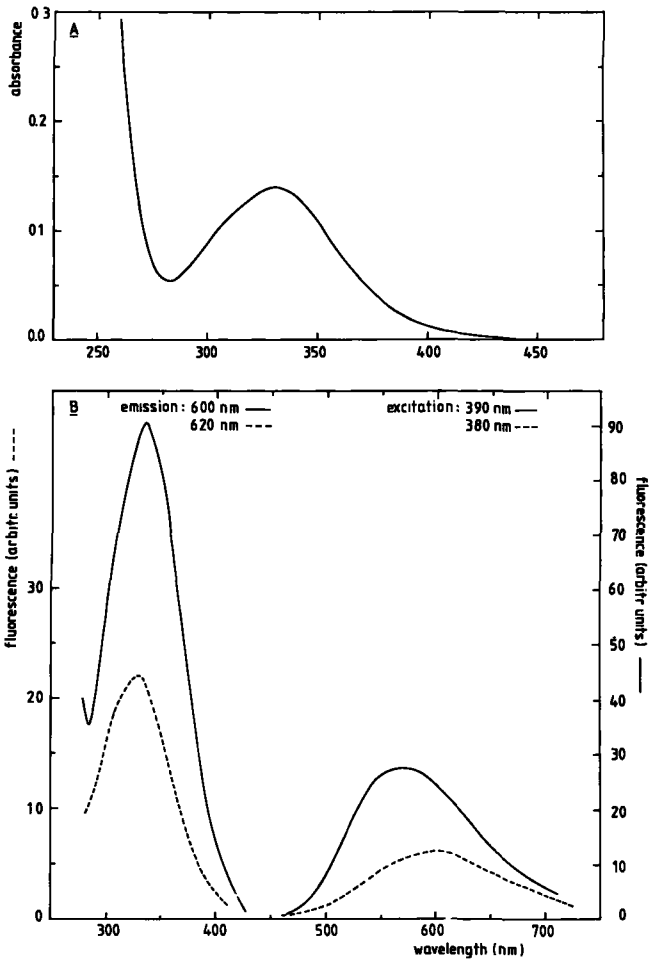

FIGURE 5: Spectral properties of 1-dimethylaminonaphthalene-5-sulphonyl ethyl ester (DNS-OEt) in 10 mM phosphate buffer, pH = 7.4, at 20 °C. Concentration: 50 µM DNS-OEt. A: lowest energy band of the absorption spectrum. B: corrected excitation spectrum (left, emission as indicated) and emission spectrum (right, excitation as indicated) without (- - -) or with (———) 10 mM sodium dodecyl sulphate.

of the labelled enzymes and of the model compound DNS-OEt were investigated. D_2O, which may enhance ϕ^f, and KI, which may quench fluorescence, were used to gain insight into the accessibility of the dansyl label in the proteins. To discriminate between a specific action of KI and a general salt effect, also the influence of KCl on the spectra

was studied. Furthermore, variation in pH was applied to investigate the sensitivity of the environment of the label to (de)protonation of particular groups.

For both DNS-OEt and the labelled enzymes, replacement of H_2O by D_2O was not found to have an obvious effect on $\bar{\nu}_a^m$ and $\bar{\nu}_e^m$, but it did increase ϕ^f. This is shown in Table I for the enzymes. The normalized values of ϕ^f of DNS-OEt in mixtures of dioxane and H_2O-D_2O (50%-50% v/v) and in phosphate-buffered H_2O-D_2O mixtures are shown in Figure 6.

Variation in pH within the range 2-8.5, was not found to have any significant effect on $\bar{\nu}_e^m$ and ϕ^f of DNS-OEt (Cf. Van der Drift and Roos, 1983[c]). Variations in $\bar{\nu}_e^m$ and ϕ^f were observed at pH > 8.5, but these could be attributed to formation of DNS-OH because of hydrolysis. With the labelled enzymes, however, alteration of pH did affect $\bar{\nu}_e^m$ and ϕ^f, as is shown in Figures 7 and 8, respectively. The most interesting pH-range in these figures is the region 6-8.5, where a striking difference is seen between AtrE and the two proteases: in the esterase both $\bar{\nu}_e^m$ and ϕ^f show an obvious dependence on pH, whereas in Chymo and Sub, there is hardly any pH-dependence. The spectra of the

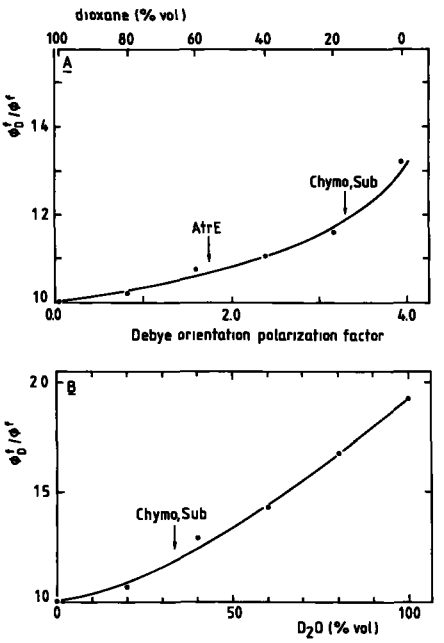

FIGURE 6: Influence of deuterium oxide (D_2O) on the relative quantum yield of fluorescence of 1-dimethylaminonaphthalene-5-sulphonyl ethyl ester in aqueous systems at 20 °C. A: increase in water-dioxane mixtures with different Debye orientation polarization factors by replacement of 50% of the water by D_2O. B: increase in aqueous solution by replacement of water by D_2O. ϕ_D^f and ϕ^f denote the quantum yield in the presence and in the absence of D_2O, respectively. The arrows indicate the values of ϕ_D^f/ϕ^f found for the dansylated enzymes.

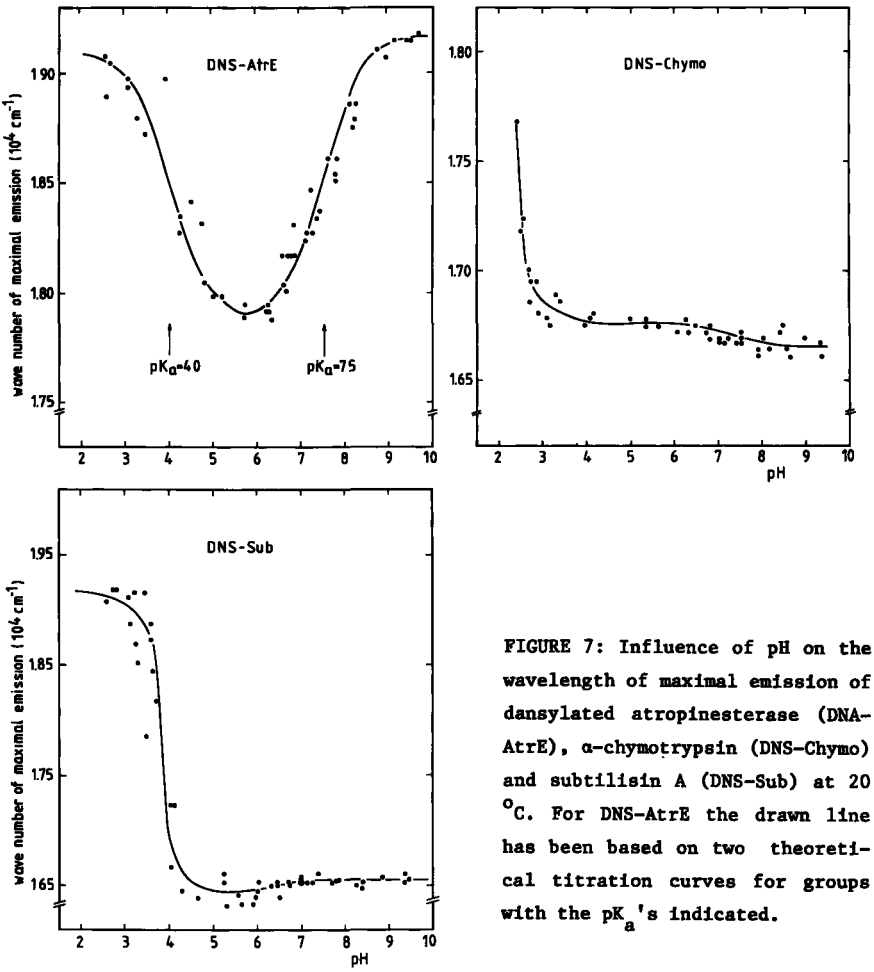

FIGURE 7: Influence of pH on the wavelength of maximal emission of dansylated atropinesterase (DNS-AtrE), α-chymotrypsin (DNS-Chymo) and subtilisin A (DNS-Sub) at 20 °C. For DNS-AtrE the drawn line has been based on two theoretical titration curves for groups with the pK$_a$'s indicated.

enzymes in the presence of 3.4 M KI (with 10 mM Na_2SO_3 in order to prevent the formation of I_3^-) and 3.4 M KCl (also with 10 mM Na_2SO_3) are shown in Figure 9; the relevant spectral parameters of the labelled enzymes are summarized in Table IV. The results obtained from these perturbation studies will be considered in more detail in the discussion.

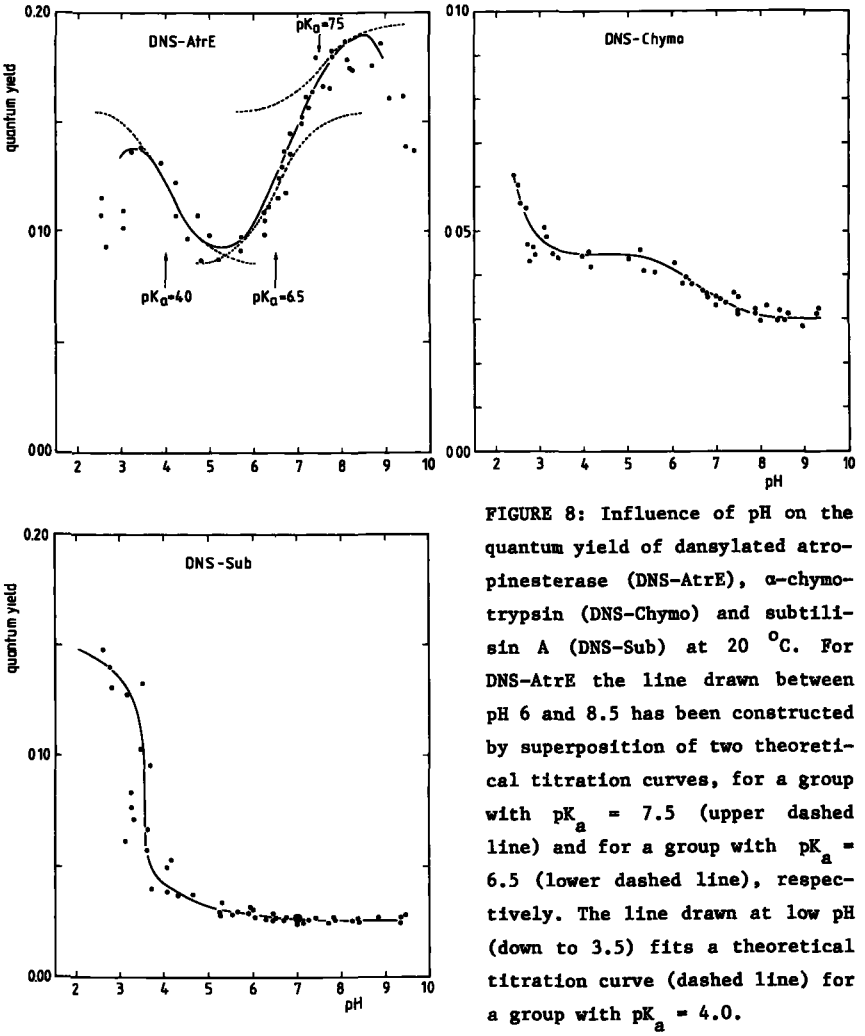

FIGURE 8: Influence of pH on the quantum yield of dansylated atropinesterase (DNS-AtrE), α-chymotrypsin (DNS-Chymo) and subtilisin A (DNS-Sub) at 20 °C. For DNS-AtrE the line drawn between pH 6 and 8.5 has been constructed by superposition of two theoretical titration curves, for a group with pK_a = 7.5 (upper dashed line) and for a group with pK_a = 6.5 (lower dashed line), respectively. The line drawn at low pH (down to 3.5) fits a theoretical titration curve (dashed line) for a group with pK_a = 4.0.

DISCUSSION

a. Release of DNS-OH from the Labelled Enzymes

Evidence has been presented that the inhibition of AtrE, Chymo and Sub by DNS-F results from covalent labelling of the active serine with a dansyl group. Since sulphonyl inhibitors may be easily released from serine enzymes by hydrolytic desulphonylation (Fahrney and Gold,

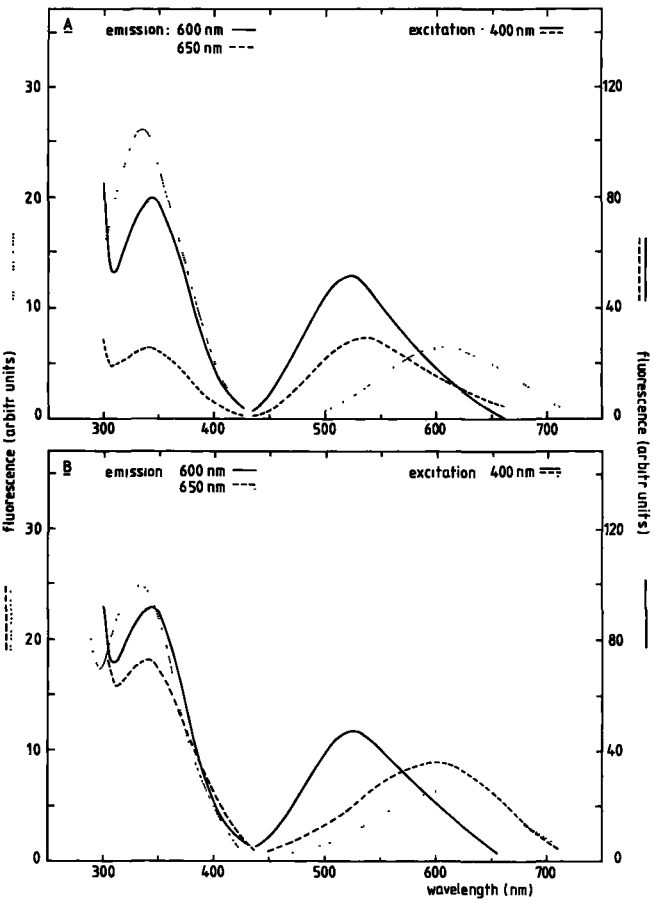

FIGURE 9: Effects of potassium iodide (KI) and sodium chloride (KCl) on the emission spectra of dansylated enzymes. The figures show the corrected excitation spectra (left, emission as indicated) and emission spectra (right, excitation as indicated) of dansylated atropinesterase (————), α-chymotrypsin (- - -) and subtilisin A (.....) in 10 mM phosphate buffer, pH = 7.4, at 20 °C. A: approx. 50 μM dansylated enzyme with 3.4 M KI. B: approx. 50 μM dansylated enzyme with 3.4 M KCl. In both cases 10 mM Na_2SO_3 was present (see text).

1963; Gold, 1965), DNS-OH is expected to occur as a contaminant in solutions of the dansylated enzymes, causing a shift of $\bar{\nu}_a^m$ to larger values whereas $\bar{\nu}_e^m$ and ϕ^f become dependent on the wavelength of excitation. As the absorption spectrum shows (Figure 10(A)), at excitation above 395 nm the contribution of DNS-OH to the emission spectrum will

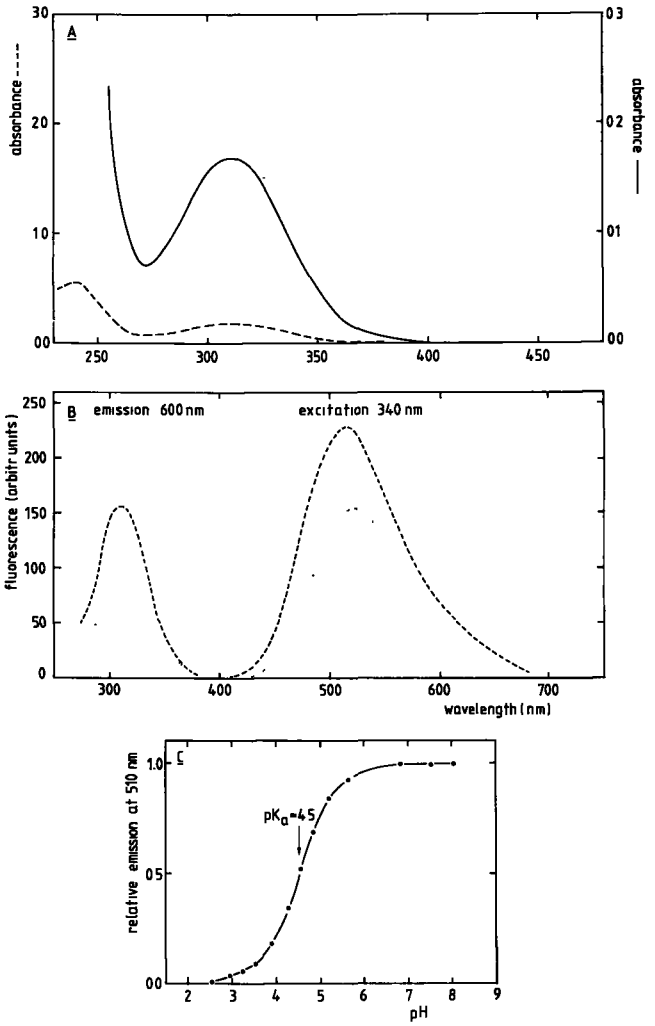

FIGURE 10: Spectral properties of 1-dimethylaminonaphthalene-5-sulphonic acid (DNS-OH) in aqueous systems. A: Absorption spectrum (- - -) and expanded lowest energy band (———). Conditions: 50 µM DNS-OH in 10 mM phosphate buffer, pH = 7.4, at room temperature. $\bar{\nu}_a^m$ = 3.205x10^4 cm^{-1}; ε^m = 3.35x10^3 cm^{-1} M^{-1}. B: Corrected excitation spectra (left, emission as indicated) and emission spectra (right, excitation as indicated) in the absence (- - -) or presence (.....) of potassium iodide (+ 10 mM Na_2SO_3). Conditions: 50 µM DNS-OH in 10 mM phosphate buffer, pH = 7.4, at 20 °C ($\bar{\nu}_e^m$ = 1.93x10^4 cm^{-1}; ϕ^f = 0.36) with 3.4 M KI (ϕ^f = 0.24). C: Influence of pH on the relative emission intensity at 510 nm . Solid line is theoretical titration curve for a group with pK$_a$ = 4.5.

be negligible; at excitation below 370 nm the presence of DNS-OH will lead to an increase in $\bar{\nu}_e^m$ and ϕ^f with decreasing wavelength of excitation (Figure 10(B)). Below pH 6.5 the contribution of DNS-OH will decrease with decreasing pH (Figure 10(C)).

Under non-denaturing conditions and at low temperatures (4 °C) the bond between the dansyl group and the enzymes was fairly stable and spectroscopically desulphonylation interfered seriously only after days. Denaturation and pH < 3 resulted in an increased release of DNS-OH. Excitation of dansylated enzyme below 370 nm at room temperature showed an emission spectrum which apparently reflected an increasing contamination with DNS-OH with time. After dialysis of the sample at low temperatures, this effect was temporarily reduced. Similar observations were also reported by Bridge and Johnson (1973). This suggests that at room temperature under non-denaturing conditions DNS-OH may be easily formed by hydrolysis. For AtrE and Chymo this release appeared to be slower than for Sub. To avoid perturbation of the emission spectra by DNS-OH, excitation was performed at wavelengths above 395 nm with small bandwidths and samples were measured as soon as possible after preparation.

The excitation spectra of Chymo and AtrE for emission above 590 nm (Figure 3) coincide with the corresponding absorption bands (Figure 2), but for freshly prepared solutions of Sub (Figure 3) there was always a slight shift to smaller wavelenghts relative to the absorption spectrum (Figure 2). This suggests some release of DNS-OH by photolytic desulphonylation in the case of Sub.

b. Characterization of the Environment of the DNS-Label in the Enzymes

As shown above, the differences between the absorption (excitation) and emission spectra of the labelled enzymes under various conditions can be ascribed to variations in the interaction of the dansyl group with its direct environment. Investigations on the spectral properties of the model compound DNS-OEt in a large number of different media showed that the capability to act as donor in hydrogen bonding

with the dansyl-sulphonyl moiety and the Debye orientation polarization factor are the main environmental parameters to be considered for these differences (Van der Drift and Roos, 1983[c]). These results will be used in the discussion below.

b1. Labelled Enzymes in Buffer at pH 6-8.5

Replacement of H_2O by D_2O at pH=7.4 led to an increase in the quantum yield of the DNS-enzymes (Table I). This implies (Cf. Van der Drift and Roos, 1983[c]) that in the excited state the hydrogen bond acceptor site of the reporter group is accessible to the solvent for hydrogen bonding. Comparison of the values of ϕ_D^f/ϕ^f (Table I) with Figure 6(A) suggests a Debye orientation polarization factor of about 1.8 for AtrE and of about 3.3 for Chymo and Sub. These values are minimal values; only if all water molecules involved in hydrogen bonding with the probe in the excited state are freely exchangeable with D_2O they are equal to the real orientation polarization factor.

In the pH-range 6-8.5 the variations in $\bar{\nu}_e^m$ and ϕ^f with pH were different for the three enzymes. In the case of Chymo and Sub these variations were small (Figures 7 and 8) indicating absence of changes in hydrogen bonding and only minor changes in the polarity of the environment of the probe and in spin-orbit coupling associated with (de)protonation of particular groups in the enzyme (Cf. Van der Drift and Roos, 1983[c]). Figures 7 and 8 suggest the presence of a titratable group in Chymo with a pK_a in the pH-range under consideration. This group might be His(57) which is known to be part of the charge-relay system and to be located within hydrogen-bonding distance from the sulphonyl label (Cf. Cruickshank and Kaplan, 1972, 1974; Kraut, 1977). For Sub neither plot (Figures 7 and 8) gives indications of environmental changes due to protonation of the histidine of the charge-relay system.

Because of absence of changes in hydrogen bonding, $\bar{\nu}_e^m$ and ϕ^f from Table I can be used to characterize the environment of the probe in Chymo and Sub in the pH-range 6-8.5 in more detail.

Comparison with other data (Figures 3(B) and 4(B) in Van der Drift and Roos, 1983[c]) shows that for Chymo the values of $\bar{\nu}_e^m$ and

$(\phi^f/1-\phi^f)^{\frac{1}{2}}$ coincide with those of DNS-OEt in aliphatic OH-type solvents at an orientation polarization factor of 3.6-3.8. For Sub a slightly higher value of 3.8-4.0 is found. Although proteins contain highly polar groups (e.g. the electric dipole moment associated with the peptide bond is estimated to be 3-5 D, Cf. Wada (1962)) their rigidity and three-dimensional structure will probably exclude such a high contribution to the orientation polarization of the immediate environment of the probe in the excited state. Since the Debye orientation polarization factor of water is about 3.9, the above-mentioned values of 3.6-4.0 suggest that in Chymo and Sub the dansyl probe (in the excited state) is almost fully exposed to solvent in the pH-range 6-8.5. Therefore, the difference between the value of 3.6-4.0 and the one of 3.3 derived from Figure 6(A) may indicate that either a part of the water molecules involved in hydrogen bonding with the probe may not be freely exchangeable with the solvent or that the conformation of the active-site region in the presence of D_2O is different from that in water. Since the former possibility is the most likely, on the basis of Figure 6(B) it can be estimated that in both Chymo and Sub about 35% of the water molecules participating in hydrogen bonding with the dansyl probe in the excited state are not rapidly exchangeable with the solvent. This in turn points to a particular interaction between the dansyl probe and the protein due to which some solvent is "locked". The primary binding pocket has to be considered as the site of this interaction (see below). Similar studies by others (Haugland and Stryer, 1967; Vaz and Schoellmann, 1976[a,b]) also point to a highly polar environment of the label in Chymo and Sub with a polarity close to that of water. However, these authors attributed this high polarity to the protein backbone and not to partly bound and partly free solvent. Also, the present investigation points to a rather equally restricted accessibility of the dansyl probe in Chymo and Sub to solvent, whereas Vaz and Schoellmann (1976[b]) suggest a significantly lower accessibility in the case of Chymo.

In the case of AtrE $\bar{\nu}_e^m$ changes appreciably with pH in the range 6-8.5 according to a theoretical titration curve for a group with

pK_a=7.5 (Figure 7). The spectral change upon protonation of this group corresponds to the transfer of the reporter group from a non-hydrogen-bonding environment with an orientation polarization factor of about 1.8 to an aliphatic OH-type hydrogen-bonding environment of the same orientation polarization (Van der Drift and Roos, 1983[c]). This value of the orientation polarization factor is equal to that obtained from the partial replacement of H_2O by D_2O at pH=7.4 (Figure 6(A)). It can be concluded, therefore, that the reporter group in AtrE resides in a significantly less polar environment than in Chymo and Sub and that the transition due to pH does not affect this polarity but only the hydrogen-bonding interactions of the dansyl group in the excited state.

In the same pH-region ϕ^f of DNS-AtrE decreases from about 0.18 to 0.10 according to a composite theoretical titration curve with two pK_a's at 7.5 and 6.5 (Figure 8), indicating the influence of a second titratable group on the environment of the label. The values of $(\phi^f/1-\phi^f)^{\frac{1}{2}}$ at high and low pH are about half the values to be expected at an orientation polarization factor of 1.8, indicating that in AtrE ϕ^f is not only determined by hydrogen bonding but also by interactions between the protein and the reporter group which affect the spin-orbit coupling (Cf. Van der Drift and Roos, 1983[c]). The decrease in ϕ^f upon transfer from a non-hydrogen-bonding to an aliphatic OH-type hydrogen-bonding environment (Cf. Van der Drift and Roos, 1983[c]) of the same orientation polarization accompanying protonation of the group with pK_a=7.5 is smaller than expected if hydrogen bonding was the only interaction involved. This indicates a partial compensation due to decreased spin-orbit interactions. On the other hand, the decrease in ϕ^f accompanying the protonation of the second group (pK_a=6.5) mainly results from an appreciable increase in the spin-orbit interactions.

The lower polarity of its environment and the reduction in ϕ^f by spin-orbit coupling indicates that in AtrE the dansyl group is much more shielded from the solvent and interacts more strongly with the protein moiety than in Chymo and Sub. This points to the presence of an apolar binding site near the active serine in AtrE which allows a

stronger binding of the bulky dansyl group to the protein than the apolar substrate specificity pockets known to be present in Chymo and Sub (Cf. Kraut, 1977).

b2. Perturbations at pH=7.4

The result above is supported by the effect of excess SDS on the spectra of the labelled enzymes (Figure 4 and Table IV). Under the conditions employed this anionic detergent shows excessive binding to proteins which results in a coating of the available protein surface with an apolar layer (Tanford, 1973). As expected, upon addition of SDS emission spectra of Chymo and Sub show a transfer of the dansyl group from a highly polar to a much less polar environment with an orientation polarization factor of 1.4-2.0, about equal to that of AtrE; the emission spectrum of DNS-AtrE is only slightly perturbed by SDS. The excitation spectra of AtrE and Chymo do not change; the red shift in the case of Sub can be attributed to the larger contribution of the bound label in an apolar environment than that of released DNS-OH, the spectrum of which (Figure 10(B)) is not influenced by SDS.

Like for native DNS-AtrE ϕ^f of the DNS-enzymes in the presence of SDS (Table IV) is appreciably smaller than expected for an orientation polarization factor of 1.4-2.0 (Cf. Van der Drift and Roos, 1983[c]). Such a smaller value of ϕ^f is also found for DNS-OEt in SDS micelles. From the value of $\bar{\nu}_e^m$ in the presence of SDS (Table III, Figure 3(B) in Van der Drift and Roos, 1983[c]) and from the effect of the partial replacement of H_2O by D_2O on ϕ^f under these conditions (ϕ_D^f/ϕ^f = 1.13; Figure 6(A)) an orientation polarization factor of 2.6-2.7 is found for the environment of the dansyl group of DNS-OEt in SDS micelles. The experimental value of ϕ^f (0.12) is smaller than expected (0.15; Figure 4(B) in Van der Drift and Roos, 1983[c]) for this orientation polarization factor. Since the viscosity of SDS micelles at 20 °C (about 19 centipoise; Cf. Zachariasse, 1978) is significantly higher than that of water, the additional reduction in ϕ^f might be ascribed to a reduced motility of the label as a result of a decreased fluidity of the environment (Cf. Vaz and Schoellmann, 1976[b]).

In view of the $1\text{-}a_{\pi}$ nature of the electronic transition involved and the apparent intersystem crossing from S_1 to a nearby triplet (Cf. Van der Drift and Roos, 1983[c]) external heavy ions such as I^- may cause quenching of fluorescence (Becker, 1969). A study of the effect of I^- on the fluorescence of DNS-enzymes in comparison with the model compound was not possible as in the presence of KI DNS-OEt was completely converted into DNS-OH within a few minutes as judged from the spectral changes. DNS-OH was quenched to about 30% in 3.4 M KI (Figure 10(B)). Also in the presence of high concentrations of sodium thiosulphate such a rapid desulphonylation was found. Since I^- is a soft nucleophile, the desulphonylation of the model compound is expected to proceed via a nucleophilic attack on the carbon atom of the ester bond (Cf. Jencks, 1969; Bender, 1971). The labelled enzymes did not show such an increased desulphonylation in the presence of KI (Figure 9(A)), which suggests that the carbon of the serine side chain is shielded from I^- in solution. However, KI may induce conformational changes which are different for the three enzymes. The values of $\bar{\nu}_e^m$ and ϕ^f (Table IV) show that at pH=7.4 in the presence of KI the environment of the dansyl group in AtrE is similar to that at pH 8-8.5 without KI, i.e. similar to a non-hydrogen-bonding environment with an orientation polarization factor of about 1.8. This conformational change is not specific for KI since it also occurred in the presence of KCl (Figure 9(B)). In Chymo KI led to a transfer of the dansyl probe into a less polar environment (Figure 9(A); orientation polarization factor < 3), but KCl did not induce such an effect (Figure 9(B)). The emission spectra of Sub were not significantly affected by KI nor by KCl (Figure 9; Table IV). At the concentration used KI caused an immediate reduction in the enzymic activity of uninhibited AtrE and Chymo to a few per cent, whereas the activity of Sub was only slightly affected. This observation suggests that a direct interaction of particular anions, e.g. I^-, may perturb the active-site region in AtrE and Chymo but not in Sub.

b3. Effect of Low pH

Figures 7 and 8 indicate that the three enzymes underwent a conformational transition at low pH, which resulted in an increased shielding of the dansyl probe from the solvent. As the transition is shifted towards lower pH in the sequence AtrE>Sub>Chymo, the stability of the active-site region at low pH seems to increase in this order.

Between pH 5 and 3.5 AtrE showed a transition similar to that at high pH: the transfer of the dansyl moiety from a hydrogen-bonding environment of the aliphatic OH-type to a non-hydrogen-bonding environment of the same orientation polarization. The titration curves in Figures 7 and 8 suggest that a titratable group with a pK_a=4.0 is involved, presumably a carboxyl group (Cf. Edsall and Wyman, 1958; Brill, 1977). Below pH 3.5 the fit to a single titration curve becomes less, indicating that more titratable groups become involved in the transition.

Sub showed a comparable transition at low pH (Figures 7 and 8). In this case the curves do not fit to a simple titration graph. The values of $\bar{\nu}_e^m$ and ϕ^f at pH=3 indicate that this transition around pH 3.5 is accompanied by a transfer of the dansyl probe from a nearly aqueous environment to a less polar, non-hydrogen-bonding environment at low pH with an orientation polarization factor of about 1.8, similar to AtrE. For Chymo the data in Figures 7 and 8 point to an analogous transition at pH< 3.5.

In contrast to $\bar{\nu}_e^m$ and ϕ^f the value of $\bar{\nu}_a^m$ (or $\bar{\nu}_{ex}^m$) of the dansyl group was not immediately affected by variation in pH; at low pH $\bar{\nu}_{ex}^m$ is about 2.907×10^4 cm^{-1} for the three enzymes, not substantially different from the values of $\bar{\nu}_{ex}^m$ at pH=7.4. As shown elsewhere for DNS-OEt (Figure 1 in Van der Drift and Roos, 1983[c]), protonation of the dimethylamino group, pK_a about 3.5, leads to the disappearance of the original low-energy absorption band of the dansyl group. For the dansylated enzymes prolonged keeping at low pH leads to a gradual decrease in this band. Therefore, the absence of any "blue" shift of $\bar{\nu}_{ex}^m$ and the increase in ϕ^f upon lowering pH indicate that in the three enzymes the dimethylamino group is initially not titratable at low pH,

i.e. is shielded from the solvent. In view of the appreciable electric dipole moment of the dimethylamino group (1-2 D) binding of this group at the protein surface by dipole-dipole interaction is feasible (Purcell et al., 1964). The apparent red shift of $\bar{\nu}^{m}_{ex}$ observed for Sub in going from pH 7.4 to 3.5 must be mainly attributed to the decreased contribution of contaminating DNS-OH due to protonation of the dimethylamino group (Figure 10(C)).

c. Comparison of the Active Sites

Owing to an unusually high nucleophilicity the side-chain hydroxyl group of the active serine in serine proteases can be specifically labelled with DFP and particular sulphonyl fluorides (Hartley, 1970). AtrE has a similar serine at the active centre since it reacts specifically with various organophosphorus compounds (Oosterbaan and Berends, 1971; Rörsch et al., 1971, Hessing, 1983) and, as the present results show, with DNS-F, like Chymo and Sub. Besides, like Chymo and Sub (Cf. Kraut et al., 1971; Robertus et al., 1972; Blow, 1974), AtrE seems to have a hydrophobic binding site near the active serine which interacts with the dansyl group, but the interactions involved differ from those in the proteases.

In all three enzymes the dimethylamino group is shielded from the solvent whereas the accessibility of the serine-dansyl bond is limited, indicating at least a partial incorporation of the dansyl probe into the protein.

The large Debye orientation polarization factor of the environment of the probe in Chymo and Sub, closely resembling that of water, and the smaller enhancement of ϕ^{f} by D_2O than expected, indicate that in these proteases the group may still extensively interact with both bound and rapidly exchangeable solvent. Although model-building studies suggested that the dansyl moiety may just fit into the primary substrate binding pocket (Vaz and Schoellmann, 1976[b]), the present results indicate that in Chymo the dansyl group is not completely but only partially inserted into this pocket, or bound outside the pocket while covering the crevice and thus locking some solvent molecules.

This is consistent with recent NMR investigations on tosylated Chymo in solution, which indicate that also the smaller tosyl group which is known to fit very well in this binding hole *is not* immobilized but has a considerable degree of motional freedom with respect to the protein (Ando et al., 1982). According to the results above in Sub the dansyl group is obviously bound in the same way.

The smaller orientation polarization factor found for DNS-AtrE and the enhancement of ϕ^f by D_2O according to expectation indicate that in AtrE the dansyl probe interacts less with solvent and more strongly with the protein moiety than in the two proteases. This suggests that in the esterase the dansyl group is more embedded in the protein structure than in Chymo and Sub, but apparently without locking solvent like in the two proteases. This points to a larger size of the hydrophobic binding pocket in AtrE than in Chymo or Sub. This picture is consistent with ESR results (Van der Drift et al., 1981; 1983[b]). If hydrolysis of the ester bond in (-)-atropine by AtrE proceeds analogously to esterolysis by Chymo or Sub, the presence of a large apolar binding pocket near the active serine in the esterase may be understood in the light of the bulky size and the mainly apolar character of the tropic acid moiety which will require specific binding during catalysis.

In principle the above conclusions based on the emission data concern the final equilibrium situation of the excited state resulting from interactions between the probe and its environment after electronic excitation, and not the ground state. This should be stressed as long as the molecular dynamics underlying the relaxation towards this situation are not clear. If the probe has a fixed position in the protein, the final situation results from molecular rearrangements in its immediate environment and thus fluorescence reflects the properties of the environment of the non-excited probe. However, if the probe has some motility with respect to the protein, increased dipole-dipole interactions, for instance between the excited probe and the protein, may lead to an increased association and the environment of the probe in the excited state may differ from that in the ground state.

X-ray diffraction data indicate that protonation of the charge-relay histidine at Nε2 in Sub and Chymo has no appreciable effect on the active-site structure (Mavridis et al., 1974; Cf. Huber and Bode, 1977; Matthews et al., 1977). This and a weak interaction of the dansyl group with the protein may explain why variation in pH between 6.0 and 8.5 has no appreciable effect on the emission spectra of dansylated Chymo and Sub. On the other hand, due to a stronger interaction with the protein, the emission spectrum of the dansyl group in AtrE appears to be more susceptible to conformational changes due to pH-variations in the above range. This provides evidence for the presence of two titratable groups which influence the environment of the dansyl probe in AtrE at pH 6.0-8.5. The pK_a-values estimated are characteristic for two different types of histidines: a normal one (pK_a=6.5; Cf. Edsall and Wyman, 1958; Meadows, 1972) which may correspond with His(109) positioned adjacent to the active serine in the primary structure (Hessing, 1983) and a particular one with pK_a=7.5, i.e. within the range characteristic for the histidine of a charge-relay system in inhibited serine proteases (Markley, 1979). Other evidence for the presence of such a particular histidine near the active serine in AtrE is provided by the investigation of DFP-inhibited AtrE by means of ^{31}P NMR (Van der Drift et al., 1983[a]). This result strongly suggests the presence of a charge-relay system in AtrE, analogous to the situation in Chymo and Sub.

The indications of the presence of a charge-relay system in combination with those of a hydrophobic binding site near the active serine suggest a structural resemblance of the active-centre regions of AtrE and the serine proteases.

APPENDIX: Syntheses of Dansylated Compounds

a. 1-Dimethylaminonaphthalene-5-sulphonyl fluoride (DNS-F)

1.0 g of DNS-Cl (3.7 mmole; Fluka A.G., puriss.) was dissolved in 10 ml of dry acetone and, after removal of the insoluble dimethylaminonaphthalene-5-sulphonic acid (DNS-OH) by filtration, 1.5 g (40

mmole) of dry powdered ammonium fluoride was added. The mixture was refluxed for 2 h under continuous stirring and, after cooling and removal of excess ammonium fluoride and precipitated ammonium chloride by filtration, the volume was reduced by evaporation under reduced pressure to about 2 ml. Addition of 25 ml of distilled water resulted in the separation of a yellow oil, which solidified on stirring. The yellow solid was collected by filtration, recrystallized from acetone/water at room temperature and dried. Yield: 800 mg (3.16 mmole; 85%). Freshly prepared or purified DNS-Cl gave almost quantitative yields of DNS-F.

Analyses

- m.p.: 50-52 °C
- elementary analysis:

	Found (%)	Calculated (%)
C	56.87-56.96	56.90
H	4.79- 4.84	4.78
Cl	< 0.03	0.00

- The infrared spectrum was in agreement with the expected structure (wavenumbers SO_2F (cm^{-1}): 1401, 1210); no free sulphonic acid was found.
- Thin-layer chromatography (Merck Silicagel, F 254 Fertigplatten) with different solvents* showed one fluorescent spot (excitation at 254 nm and 360 nm).

* R_F values observed in $CHCl_3$/EtOAc/CH_3OH/ (30/50/20 v/v) acidified with 1 volume per cent acetic acid (A) and $CHCl_3/CCl_4$ (1/3 v/v) (B)

	R_F(A)	R_F(B)
DNS-Cl	0.72	0.30
DNS-F	0.72	0.25
DNS-OH	0.20	0.00

b. 1-Dimethylaminonaphthalene-5-sulphonyl ethyl ester (DNS-OEt)

1.0 g of DNS-Cl (3.7 mmole; Fluka) was dissolved in 50 ml of dry acetone and the insoluble DNS-OH was removed by filtration. A solution of 136 mg of Na in 2.5 ml of dry ethanol was added dropwise in 5 min under continuous stirring at 0-5 °C. The yellow colour of the mixture became pale and NaCl precipitated. After stirring for 1 h at 0 °C the mixture was kept in the dark for about 16 h at 5 °C. After evaporation of the solvent at 30 °C and reduced pressure the residue was dissolved in 50 ml of ether and the solution washed with 10 ml portions of ice-cold water until the water layer remained colourless and had neutral pH. The ether layer was dried over magnesium sulphate, stirred with activated charcoal and, after filtration, evaporated in vacuo. About 1.5 ml of a yellow oil remained. Thin-layer chromatography showed that the fluorescent product contained various strongly fluorescent contaminants. The oil was dissolved in the minimum amount of ether and applied to 3 preparative thin-layer chromatographic plates (Merck Silicagel 60 F 254, 20x20 cm^2, thickness 2 mm). After development over a distance of 19 cm in CH_2Cl_2 the ester bands were extracted with 500 ml of ether, and the combined extracts were evaporated at 20 °C under vacuum. The residue was thoroughly degassed under a pressure of 10^{-3} mm Hg. A clear yellow-green oil resulted (300 mg, 29%), which did not crystallize*.

Analyses

- On thin-layer chromatography the oil appeared as a single spot with R_F=0.24 in $CCl_4/CHCl_3$ (3/1 v/v) and R_F=0.44 in CH_2Cl_2.
- The ^{1}H-NMR spectrum in CCl_4 was in agreement with the structure of DNS-OEt (chemical shift -O-CH_2 quartet: 3.96 ppm).

* The compound is reported to be a solid, mp 40-41 °C (Vaz and Schoellmann, 1976[a]). However, the R_F=0.43 in CH_2Cl_2 reported is in agreement with the present investigation. Due to the instability of the compound attempts to recrystallize the product from various solvents were unsuccessful and only resulted in the formation of the original impurities.

c. 1-Dimethylaminonaphthalene-5-sulphonic acid (DNS-OH)

DNS-OH was prepared from DNS-Cl (Fluka) by hydrolysis with NaOH in acetone-water. The DNS-OH precipitated as a white solid and was dried after collection by filtration and extensive washing with water and acetone, respectively.

d. 1-Dimethylaminonaphthalene-5-sulphonyl imidazole (DNS-Imid)

136 mg of imidazole (2 mmole; Aldrich) dissolved in 6 ml of H_2O saturated with sodium bicarbonate was added to 540 mg (2 mmole) of DNS-Cl (Fluka) dissolved in a mixture of 15 ml of acetone and 8 ml of H_2O. After stirring shortly the mixture was kept in the dark at room temperature for about 20 h. Then the acetone was removed by evaporation at 40 °C and under reduced pressure and the aqueous residue, containing a yellow oil, was acidified to pH=6 with 2 N hydrochloric acid. The yellow oil was extracted with ether, the ether solution dried over magnesium sulphate and, after filtration, the ether was removed by evaporation. A yellow oil remained which solidified after addition of some petroleum ether. The product was recrystallized from ether/petroleum ether and a pale yellow fluorescent solid was obtained. Yield: 260 mg (43%).

Analyses

- mp 98.5-99.0 °C
- Thin-layer chromatography (Merck Silicagel F 254 Fertigplatten) showed the product to be homogeneous (R_F=0.64 in $CHCl_3$/EtOAc/CH_3OH, 30/50/20 v/v acidified with 1 volume per cent acetic acid).
- ^{1}H-NMR (in $CDCl_3$) and infrared spectra were in agreement with DNS-Imid.

e. 1-Dimethylaminonaphthalene-5-sulphonyl N-carbobenzoxy-DL-histidine (DNS-CBZ-His)

540 mg (2 mmole) of DNS-Cl (Fluka) was dissolved in 15 ml of acetone. After removing solid DNS-OH by filtration, 8 ml of H_2O was added. Then 500 mg (1.7 mmole) of N-carbobenzoxy-DL-histidine (Sigma

Chemical Company), dissolved in 6 ml of H_2O saturated with sodium bicarbonate, was added and under continuous stirring the pH of the mixture was brought to 8-9 with 2 N sodium hydroxide. The reaction was completed in about 90 min, during which time the pH was checked every 5 min and adjusted to 8-9 if necessary. The deep yellow colour of the solution became pale and after about 0.5 h precipitation of sodium chloride occurred. After evaporation of the acetone at 40 °C and reduced pressure, the remaining yellow solution was washed 3 times with 30 ml of ether in order to remove excess DNS-Cl. After adjustment of the pH to 6 with 2 N hydrochloric acid the reaction mixture, containing a yellow oil, was extracted 3 times with 30 ml of ethyl acetate. The combined extracts were dried over magnesium sulphate, treated with activated charcoal for about 30 min, filtered and evaporated under reduced pressure. The yellow glassy residue was dried under vacuum at 20 °C. Yield:730 mg (81%).

Analyses

- m.p.: 60-83 °C.
- Thin-layer chromatography with various types of mobile phase showed one main component (R_F=0.61 in $CHCl_3/C_6H_5CH_2OH$, 70/30 v/v acidified with 3 volume per cent acetic acid) and very small amounts of some contaminants, possibly resulting from decomposition on the layer.
- NMR, IR and mass spectrometry indicated that the product was DNS-CBZ-His.

REFERENCES

Alden, R.A., Wright, C.A., and Kraut, J. (1970) Phil. Trans. Roy. Soc. B257, 119.

Alden, R.A., Birktoft, J.J., Kraut, J., Robertus, D.J., and Wright, C. (1971) Biochem. Biophys. Res. Comm. 45, 355.

Ando, M.E., Gerig, J.T., and Weigand, E.F. (1982) J. Am. Chem. Soc. 104, 3172.

Becker, R.S. (1969) Theory and Interpretation of Fluorescence and Phosphorescence, Wiley Interscience, New York.

Bender, M.L. (1971) Mechanism of Homogeneous Catalysis from Protons to Proteins, Wiley Interscience, New York.

Bender, M.L., Begué-Cantón, M.L., Blakeley, R.L., Brubacker, L.J., Feder, J., Gunter, C.R., Kézdy, F.J., Kilheffer Jr., J.V., Marshall, T.H., Miller, C.G., Roeske, R.W., and Stoops, J.K. (1966) J. Am. Chem. Soc. 88, 5890.

Berends, F., Rörsch, A., and Stevens, W.F. (1967) in Proceedings of the Conference on "Structure and Reactions of DFP sensitive Enzymes" (Heilbronn, E., Ed.) p. 45, Försvarets Forskningsanstalt, Stockholm.

Birktoft, J.J., and Blow, D.M. (1972) J. Mol. Biol. 68, 187.
Birktoft, J.J., Blow, D.M., Henderson, R., and Steitz, T.A. (1970) Phil. Trans. Roy. Soc. B257, 67.
Blow, D.M. (1974) Isr. J. of Chem. 12, 483.
Brand, L., and Witholt, B. (1967) in Methods in Enzymology Vol. XI, (Hirs, C.W., Ed.) p. 776, Acad. Press, New York.
Bridge, J.B., and Johnson, P. (1973) Eur. Polym. J. 9, 1327.
Brill, A.S. (1977) Transition Metals in Biochemistry, Springer Verlag, Berlin.
Chen, R.F. (1966) Nature 209, 69.
Chen, R.F. (1968) Anal. Biochem. 25, 412.
Cohen, G.H., Matthews, B.W., and Davies, D.R. (1970) Acta Crystallogr. B26, 1062.
Cruickshank, W.H., and Kaplan, H. (1972) Biochem. J. 130, 1125.
Cruickshank, W.H., and Kaplan, H. (1974) J. Mol. Biol. 83, 267.
Edsall, J.T., and Wyman, J.(1958) Biophysical Chemistry Vol. I, Academic Press, New York.
Fahrney, D.E., and Gold, A.M. (1963) J. Am. Chem. Soc. 85, 997.
Fruton, J.S. (1975) in Proteases and Biological Control (Reich, E., Rifkin, D.B., and Shaw, E., Eds.) Cold Spring Harbor Conferences on Cell Proliferation, Vol. 2, p. 33, Cold Spring Harbor Laboratory.
Gerlach, E., and Deuticke, B. (1963) Biochem. Z. 337, 477.
Gibian, M.J., Elliott, D.L., and Hardy, W.R. (1969) J. Am. Chem. Soc. 91, 7528.
Gold, A.M. (1965) Biochemistry 4, 897.
Gold, A.M., and Fahrney, D. (1964) Biochemistry 3, 783.
Gundlach, G., Kohne, C., and Turka, F. (1962) Biochem. Z. 336, 215.
Hartley, B.S. (1960) Ann. Rev. Biochem. 29, 45.
Hartley, B.S. (1970) in Homologies in Enzymes and Metabolic Pathways and Metabolic Alterations in Cancer (Whelan, W.J., and Schultz, J., Eds.) p. 191, North-Holland Publishing Company, Amsterdam.
Hartley, B.S., and Massey, V. (1956) Biochim. Biophys. Acta 21, 58.
Haugland, R.P., and Stryer, L. (1967) in Conformation of Biopolymers Vol. 1, (Ramachandran, G.N., Ed.) p. 321, Academic Press, New York.
Heidema, J.H., and Kaiser, E.T. (1967) J . Am. Chem. Soc. 89, 460.
Heidema, J.H., and Kaiser, E.T. (1968) J. Am. Chem. Soc. 90, 1860.
Hessing, J.G.M. (1983) Ph.D. Thesis, University of Leiden.
Himel, C.M., Aboul-Saad, W.G., and Uk, S. (1971) J. Agr. Food Chem. 19, 1175.
Himel, C.M., and Mayer, R.T. (1970) Anal. Chem. 42, 130.
Huber, R., and Bode, W. (1977) in NMR in Biology (Dwek, R.A., Campbell, I.D., Richards, R.E., and Williams, R.J.P., Eds.) p. 1, Academic Press, New York.
Jencks, W.P. (1969) Catalysis in Chemistry, McGraw Hill Book Company, New York.
Kézdy, E.J., and Kaiser, E.T. (1970) in Methods in Enzymology Vol. XIX, (Perlmann, G.E., and Lorand, L., Eds.) p. 3, Academic Press, New York.
Kienhuis, H., and Baar, J.A.J. (1964) Internal Report, Prins Maurits Laboratory TNO, Rijswijk.
Kraut, J. (1977) Ann. Rev. Biochem. 46, 331.
Kraut, J., Wright, H.T., Kellerman, M., and Freer, S.T. (1967) Proc. Nat. Acad. Sci. 58, 304.
Kraut, J., Robertus, J.A., Birktoft, J.J., Alden, R.A., Wilcox, P.E., and Powers, J.C. (1971) Cold Spring Harbor Symp. Quant. Biology 36, 111.
Markley, J.L. (1979) in Biological Applications of Magnetic Resonance (Shulman, R.G., Ed.) p. 397, Academic Press, New York.
Matthews, D.A., Alden, R.A., Birktoft, J.J., Freer, S.T., and Kraut, J. (1977) J. Biol. Chem. 252, 8875.
Matthews, B.W., Sigler, P.B., Henderson, R., and Blow, D.M. (1967) Nature 214, 652.
Mavridis, A., Tulinski, A., and Liebman, M.N. (1974) Biochemistry 13, 3661.
Meadows, D.H. (1972) in Methods in Enzymology Vol. XXVI, (Hirs, C.H.W., and Timasheff, S.N., Eds.) p. 638, Academic Press, New York.
Oosterbaan, R.A., and Berends, F. (1971) Proc. Koninkl. Nederl. Akademie van Wetenschappen, Series C, Vol. 74, No. 2, 158.
Oosterbaan, R.A. et al. (1983) to be published.
Ottesen, M., and Svendsen, I. (1970) in Methods in Enzymology Vol. XIX, (Perlmann, G.E., and Lorand, L., Eds.) p. 199, Academic Press, New York.

Purcell, W.P., Beasley, J.G., and Quintana, R.P. (1964) Biochim. Biophys. Acta 88, 233.

Robertus, J.D., Alden, R.A., Birktoft, J.J., Kraut, J., Powers, J.C., and Wilcox, P.E. (1972) Biochemistry 11, 2439.

Rörsch, A., Berends, F., Bartlema, H.C., and Stevens, W.F. (1971) Proc. Koninkl. Nederl. Akademie van Wetenschappen, Series C, Vol. 74, No. 2, 132.

Sigler, P.B., Blow, D.M., Matthews, B.W., and Henderson, R. (1968) J. Mol. Biol. 35, 143.

Steitz, T.A., Henderson, R., and Blow, D.M. (1969) J. Mol. Biol. 46, 337.

Stevens, W.F. (1969) Ph.D. Thesis, University of Leiden.

Tanford, C. (1973) The Hydrophobic Effect: Formation of Micelles and Biological Membranes, Wiley-Interscience, New York.

Van der Drift, A.C.M., Beck, H.C., Dekker, W.H., Hulst, A.H., and Wils, E.R.J. (1983[a]) This Thesis, Chapter 6; to be submitted for publication.

Van der Drift, A.C.M., Moes, G.W.H., Van der Drift, E., and Rousseeuw, B.A.C. (1983[b]) This Thesis, Chapter 5; to be submitted for publication.

Van der Drift, A.C.M., and Roos, A.L.M. (1983[c]) This Thesis, Chapter 3; to be submitted for publication.

Van der Drift, A.C.M., Rousseeuw, B.A.C., and Van der Drift, E. (1981) Bull. Magn. Res. 2 (1-4), 208.

Vaz, W.L.C., and Schoellmann, G. (1976[a]) Biochim. Biophys. Acta 439, 194.

Vaz, W.L.C., and Schoellmann, G. (1976[b]) Biochim. Biophys. Acta 439, 206.

Wada, A. (1962) in Polyamino Acids, Polypeptides and Proteins (Stahmann, M.A., Ed.) p. 131, The University of Wisconsin Press, Madison.

Walsh, K.A., and Wilcox, P.E. (1970) in Methods in Enzymology Vol. XIX, (Perlmann, G.E., and Lorand, L., Eds.) p. 31, Academic Press, New York.

Walsh, K.A. (1975) in Proteases and Biological Control (Reich, E., Rifkin, D.B., and Shaw, E., Eds.) Cold Spring Harbor Conferences on Cell Proliferation, Vol. 2, p. 1, Cold Spring Harbor Laboratory.

White, C.E., and Argauer, R.J. (1970) Fluorescence Analysis. A Practical Approach, Marcel Dekker, New York.

Worthington Enzyme Manual (1977), Worthington Biochemical Corporation, Freehold (New Jersey).

Wright, C.S., Alden, R.A., and Kraut, J. (1969) Nature 221, 235.

Wright, C.S., Hess, G.P., and Blow, D.M. (1972) J. Mol. Biol. 63, 295.

Zachariasse, K.A. (1978) Ber. Bunsenges. Phys. Chem. 82, 950.

CHAPTER 3

FLUORESCENCE OF 1-DIMETHYLAMINONAPHTHALENE-5-SULPHONYL ETHYL ESTER IN SOLUTION

ABSTRACT: In order to interpret spectral differences between various serine hydrolases fluorescently labelled with a dansyl group at the active serine, the absorption and corrected fluorescence emission spectrum of the model compound 1-dimethylaminonaphthalene-5-sulphonyl ethyl ester (DNS-OEt) have been measured in a variety of solvents with different polarity and hydrogen-bonding capacity. From the lowest energy band in the absorption spectrum the maximum value of the molecular extinction coefficient, ε^m, and the corresponding wave number of maximal absorption, $\bar{\nu}_a^m$, were determined; from the emission spectra the wave number of maximal emission, $\bar{\nu}_e^m$, and the quantum yield of fluorescence, ϕ^f, were obtained. A semi-empirical formalism based on the classical dipole model including Debye orientation polarization was used to analyse the experimental data.

From ε^m and the estimated values of the oscillator strength and natural lifetime, it is concluded that the lowest energy absorption band in all solvents corresponds with an $1\text{-}a_\pi$ transition.

Analysis of the experimental data shows that differences between emission spectra of DNS-OEt in various media can be explained in terms of variations in both the molecular electric dipole moment of DNS-OEt and the orientation polarization and hydrogen-bonding capacity of the medium. $\bar{\nu}_a^m$, $\bar{\nu}_e^m$ and $(\phi^f/1\text{-}\phi^f)^{\frac{1}{2}}$ were found to be linearly dependent on the Debye orientation polarization factor of the solvent. Hydrogen bonding appears to be stronger in the excited state than in the ground state. Estimates of the value of the molecular electric dipole moment of DNS-OEt in the relaxed first excited singlet state, a nearby Franck-Condon triplet state and the relaxed ground state showed a decrease in this order. The energy separation between the first two states in DNS-OEt was estimated to be 3.2 kcal.

The present analysis suggests that the linear dependence of $\bar{\nu}_a^m$, $\bar{\nu}_e^m$ and $(\phi^f/1\text{-}\phi^f)^{\frac{1}{2}}$ on the Debye orientation polarization factor can be used to characterize an environment of DNS-OEt in more detail.

INTRODUCTION

Aminonaphthalenesulphonates have been widely used as fluorescent probes in biochemistry and biophysics (Edelman and McClure, 1968; Azzi, 1975; Radda, 1975; Chen and Edelhoch, 1976; Waggoner, 1976;

Wehry, 1976) because the characteristics of their fluorescence emission spectrum, like quantum yield, wavelength of maximal emission and bandwidths, are sensitive to the immediate environment (Seliskar and Brand, 1971[a]). The influences of environmental parameters like polarity, viscosity, pH and solvent deuteration on the fluorescence characteristics of these compounds have been the object of numerous experimental investigations (Stryer, 1966; Seliskar et al., 1969; Brand et al., 1971; Seliskar and Brand, 1971[b]; Kosower et al., 1975; Dodiuk and Kosower, 1977; Kosower and Dodiuk, 1978; Kosower et al., 1978). Various correlations between spectral and solvent parameters have been proposed (Grunwald and Winstein, 1948; Kosower, 1958; Sinanoglu, 1967; Mataga and Kubota, 1970; Nicol, 1974; Reeves et al., 1974). In many cases, however, the theoretical description of experimental data, mostly in terms of both macroscopic and molecular parameters like dielectric constant, refractive index and electric dipole moment, appears insufficient as it holds only for one spectral characteristic in a small number of rather apolar and pure solvents (Turner and Brand, 1968; Ainsworth and Flanagan, 1969). In other investigations the proposed correlations have an empirical basis rather than a theoretical one, emphasizing the lack of understanding of the phenomena observed.

In a comparative study of the active sites of some serine hydrolases, specifically labelled with a dansyl group at their active serine, 1-dimethylaminonaphthalene-5-sulphonyl ethyl ester (DNS-OEt) was used as a model compound (Van der Drift et al., 1983). To explain the influence of the environment on the emission spectra of the bound dansyl probe, the spectral characteristics of DNS-OEt have been investigated in various types of protic and non-protic solvents of different polarity. This paper shows that the environmental effects on emission can be reasonably explained by analysing the data according to a classical dipole model including Debye orientation polarization.

THEORETICAL PART

a. Wave-number Shifts

The wave-number shifts observed in the fluorescence emission

spectra and the UV-absorption spectra of molecules in solution at low concentration may result from various types of interactions between solute and solvent, such as dipolar interactions and hydrogen bonding, and from intramolecular charge transfer (Cf. Seliskar and Brand, 1971[a]; Kosower et al., 1975, 1978). The dipolar contribution is generally described in terms of a classical dipole model in which the polarizable or otherwise permanent electric dipole of the solute interacts with a medium in which it is embedded according to the Onsager reaction field formalism (Mataga and Kubota, 1970; Nicol, 1974). In this model a shift $\Delta\bar{\nu}_e^m$ of the wave number of maximal emission, $\bar{\nu}_e^m$, with respect to that of the isolated molecule corresponds with a change $\Delta E_{1\to 0}$ of the energy difference between the relaxed first excited singlet state S_r^1 and the Franck-Condon ground state S_{FC}^o given by

$$\Delta E_{1\to 0} = hc\Delta\bar{\nu}_e^m = (\vec{M}_{FC} - \vec{M}_r^*)\cdot\vec{R}^* \qquad (1)$$

where h is Planck's constant and c the velocity of light, $\vec{M}_{FC}$ and $\vec{M}_r^*$ are the permanent parts of the dipole moment vector of the solute molecule in S_{FC}^o and S_r^1, respectively, and $\vec{R}^*$ is the reaction field (vector) caused by the dipole moment of the solute molecule in S_r^1. $\vec{R}^*$ can be estimated in various ways, depending on whether the medium is considered as continuous or discrete.

If $\vec{R}^*$ results from the interaction of a polarizable point dipole with a continuous medium of static dielectric constant ε_o (Böttcher, 1952)

$$R^* = \frac{2(\varepsilon_o - 1)}{(2\varepsilon_o + n^{*2})} \frac{(n^{*2}+2)}{3} \frac{\vec{M}_r^*}{a^3} \qquad (2)$$

where n^* is the refractive index of the solute in the excited state and a is the Onsager spherical cavity radius. Usually it is assumed that n^* can be replaced by n, the refractive index of the solute in the ground state. In many cases $\vec{R}^*$ can be approximated sufficiently accurate by

$$R^* \simeq \frac{(\varepsilon_o-1)}{(\varepsilon_o+2)} \frac{(n^2+2)}{3} \frac{\vec{M}_r^*}{a^3} \qquad (3)$$

If the contribution of the solvent to the dipolar interactions with the solute is determined by the orientation of permanent dipoles according to Debye, $(\varepsilon_o-1)/(\varepsilon_o+2)$ in Equation 3 can be replaced by the orientation polarization factor $P = 4\pi N\mu^2/9kT$ (Böttcher, 1952), μ being the magnitude of the permanent dipole moments of the solvent molecules, N the number of solvent dipoles per cm^3, k the Boltzmann constant and T the Kelvin temperature. This leads to

$$\Delta E_{1\to 0} = \frac{(n^2+2)}{3} \frac{\vec{M}_r^* \cdot (\vec{M}_{FC}-\vec{M}_r^*)}{a^3} \frac{4\pi N\mu^2}{9kT} \qquad (4)$$

For the change $\Delta E_{0\to 1}$ in the energy difference between the first excited Franck-Condon state S_{FC}^1 and the relaxed ground state S_r^o due to orientation polarization of the environment, an analogous relation can be derived

$$\Delta E_{0\to 1} = hc\Delta\bar{\nu}_a^m = \frac{(n^2+2)}{3} \frac{\vec{M}_r \cdot (\vec{M}_r-\vec{M}_{FC}^*)}{a^3} \frac{4\pi N\mu^2}{9kT} \qquad (5)$$

where $\Delta\bar{\nu}_a^m$ is the shift of the wave number of maximal absorption, $\bar{\nu}_a^m$.

If the mean, isotropic polarizability of the solute is assumed to be $a^3/2$ (Cf. Mataga and Kubota, 1970) the same equations will result except that $(n^2+2)/3$ in Equations (4) and (5) is replaced by 2. This result is also obtained if the reaction field of the solute molecule is assumed to result from interactions of an ideal non-polarizable permanent point dipole with a discrete medium consisting of permanent dipoles which orient according to Debye. Thus various approximative treatments essentially lead to the same result except for a numerically small factor.

It is generally assumed that the dipole moment vector in the Franck-Condon state equals that in the corresponding relaxed state ($\vec{M}_{FC} = \vec{M}_r \equiv \vec{M}$) (Mataga and Kubota, 1970). With this assumption and by using Equations (4) and (5) the difference M^2-M^{*2} can be obtained from

the slopes of the plots of $\bar{\nu}_a^m$ and $\bar{\nu}_e^m$ versus P if n is known. Moreover if the angle θ between $\vec{M}$ and $\vec{M}^*$ is known, their magnitudes M and M^* can be calculated and vice versa (Mataga and Kubota, 1970; Exner, 1975).

b. Quantum Yield

The quantum yield of fluorescence ϕ^f satisfies (Guilbault, 1973)

$$\phi^f = \frac{k_e}{k_e + \Sigma_i k_i} \tag{6}$$

k_e is the radiative transition probability and $\Sigma_i k_i$ the sum of the transition probabilities of the various radiationless processes. For two close electronic states n and m (Mataga and Kubota, 1970; Seliskar et al., 1969; Seliskar and Brand, 1971[b])

$$k_i = \frac{A_{nm}}{(E_m - E_n)^2} \tag{7}$$

A_{nm} depends on the type of interaction causing the transition process, e.g. spin-orbit coupling in the case of intersystem crossing or vibronic interaction in the case of internal conversion, E_m and E_n ($E_m > E_n$) are the energies of the unperturbed states.

If, as is generally the case with aromatic molecules, intersystem crossing from S_r^1 (energy E_1^o) to a nearby triplet state T_{FC} (energy $E_T < E_1^o$) and internal conversion from S_r^1 to S_{FC}^o (energy E_o) are the only radiationless processes significantly competing with fluorescence emission it follows from Equations (6) and (7) that

$$\left[\frac{\phi^f}{1-(1+B)\phi^f}\right]^{\frac{1}{2}} = \left[\frac{k_e}{A_{ST}}\right]^{\frac{1}{2}} \cdot (E_1^o - E_T) \tag{8}$$

with $B = A_{SS}/k_e(E_1^o - E_o)^2$. For a sufficiently large energy separation $E_1^o - E_o$ may be approximated by $hc\bar{\nu}_e^m$, giving $B = C(\text{onstant})/\bar{\nu}_e^{m2}$. If only intersystem crossing competes appreciably with fluorescence ($B \ll 1$), the left-hand side of Equation (8) reduces to $(\phi^f/1-\phi^f)^{\frac{1}{2}}$. Since $E_1^o - E_T$ will depend on solute-solvent interactions

$$\left[\frac{\phi^f}{1-(1+B)\phi^f}\right]^{\frac{1}{2}} = \left[\frac{k_e}{A_{ST}}\right]^{\frac{1}{2}} \cdot (E_1^{oo}-E_T^o+\Sigma_i \Delta E_{ST}^i) \qquad (9)$$

where $\Sigma_i \Delta E_{ST}^i$ represents the various contributions of these interactions to $E_1^o-E_T$. E_1^{oo} and E_T^o are the energies of S_r^1 and T_{FC} of the isolated molecule. For ΔE_{ST}^D, the contribution of the interaction of the solute dipole with the permanent dipoles of the solvent molecules, an expression analogous to Equation (4) can be derived

$$\Delta E_{ST}^D = X \cdot \frac{\vec{M}_r^* \cdot (\vec{M}_{FC}^T - \vec{M}_r^*)}{a^3} \cdot \frac{4\pi N\mu^2}{9kT} \qquad (10)$$

where $X = (n^2+2)/3$ or 2, depending on whether the medium is regarded as continuous or discrete (see above), $\vec{M}_{FC}^T$ is the dipole moment of the solute in the Franck-Condon triplet state. Inserting (10) into (9) leads to

$$\left[\frac{\phi^f}{1-(1+B)\phi^f}\right]^{\frac{1}{2}} = \left[\frac{k_e}{A_{ST}}\right]^{\frac{1}{2}} \cdot \left[E_1^{oo}-E_T^o+\Delta E_{ST}+X \cdot \frac{\vec{M}_r^* \cdot (\vec{M}_{FC}^T - \vec{M}_r^*)}{a^3} \cdot \frac{4\pi N\mu^2}{9kT}\right] \qquad (11)$$

ΔE_{ST} represents the contributions of other types of interactions such as hydrogen bonding between solute and solvent.

On the basis of Equation (11) a plot of $(\phi^f/1-(1+B)\phi^f)^{\frac{1}{2}}$ versus P is expected to yield a straight line for a series of solvents of the same type. Since in general the constant C in the expression for B is not known, in practice this line can be obtained by varying C and taking the plot for which the slope and intercept have a minimal standard deviation. If $E_1^{oo}-E_T^o + \Delta E_{ST}$ (or $(k_e/A_{ST})^{\frac{1}{2}}$) and M_r^* are known, then $M_{FC}^T \cos\theta^1$ (in which θ^1 is the angle between $\vec{M}_r^*$ and $\vec{M}_{FC}^T$) and $(k_e/A_{ST})^{\frac{1}{2}}$ (or $E_1^{oo}-E_T^o+\Delta E_{ST}$) can be evaluated from the slope and intercept of such a linear plot. On the other hand if $M_{FC}^T \cos\theta^1$ and M_r^* are known then $E_1^{oo}-E_T^o+\Delta E_{ST}$ and $(k_e/A_{ST})^{\frac{1}{2}}$ can be calculated.

MATERIALS AND METHODS

Purified 1-dimethylaminonaphthalene-5-sulphonyl ethyl ester (DNS-OEt) and 1-dimethylaminonaphthalene-5-sulphonic acid (DNS-OH)

were obtained as described elsewhere (Van der Drift et al., 1983). All organic solvents (Merck) were reagent grade and were distilled before use, phenol shortly before use. Deuterium oxide (D_2O) was spectroscopic grade (Uvasol; Merck).

The spectrofluorimeter, the spectrophotometer and the Abbe-refractometer were identical to those described elsewhere and were used in the same way (Van der Drift et al., 1983). All measurements were done at 20 ^{o}C. Excitation of DNS-OEt for emission measurements occurred in the lowest energy absorption band at wavelengths not below 390 nm, unless indicated otherwise. For the determinations of relative quantum yields freshly prepared solutions of quinine sulphate dihydrate (Lamers en Indemans B.V.) in 1.0 M sulphuric acid were used as a standard (ϕ^f = 0.55, for excitation at 365 nm; Melhuish, 1960, 1964; Dawson and Windsor, 1968). Since there were no indications of oxygen effects, no special precautions were taken to keep oxygen away.

RESULTS

The parameters characterizing the lowest energy band in the absorption and emission spectrum of DNS-OEt in various pure protic and non-protic solvents, in several mixtures and in D_2O-containing solvents are compiled in Tables IA,B,C, respectively. According to the functional group acting as proton donor in hydrogen bonding (Cf. Pimentel and McClellan, 1960) the solvents have been classified as non-proton donating (np), proton donating via an aliphatic (OH-al) or aromatic OH-group (OH-ar) and proton donating via an aliphatic (NH_2-al) or via an aromatic NH_2-group (NH_2-ar).

$\bar{\nu}_a^m$ and the corresponding molecular extinction coefficient, ε^m, were determined from the lowest energy band in the absorption spectrum. The oscillator strength, f, was obtained from (Birks, 1970)

$$f = \frac{4.319}{n_s} \times 10^{-9} \cdot \int \varepsilon d\bar{\nu} \qquad (12)$$

where n_s is the refractive index of the solvent. The integral was approximated by 1.0645 x ε^m x $\Delta\bar{\nu}_{\frac{1}{2}}$, where $\Delta\bar{\nu}_{\frac{1}{2}}$ represents the half-width of the absorption band on wave-number scale (Sandorfy, 1964).

TABLE IA: Characteristics of the lowest energy band in the absorption and emission spectrum of 1-dimethylaminonaphthalene-5-sulphonyl ethyl ester in various pure solvents at 20 °C. (1)

Solvent	type	$\bar{\nu}_a^m$	ϵ^m	$\bar{\nu}_e^m$	ϕ^f	f	τ_o	index
acetone	np	2.915	2.86	1.880	0.373	0.051	51	1
acetonitrile	"	2.907	2.95	1.825	0.334	0.065	45	2
benzene	"	2.915	2.78	2.004	0.524	0.052	31	3
chlorobenzene	"	2.882	2.78	1.968	0.605	0.051	31	4
dimethylformamide	"	2.890	2.79	1.825	0.414	0.056	44	5
dimethylsulfoxide	"	2.865	2.84	1.786	0.385	0.058	40	6
dioxane	"	2.924	2.91	1.961	0.657	0.056	36	7
acetic acid	OH-al	3.021	1.55	1.852	0.401	0.033	84	17
n-butanol	"	2.924	2.75	1.869	0.453	0.056	44	18
ethanol	"	2.924	2.85	1.852	0.356	0.059	46	19
ethylene glycol	"	2.907	2.78	1.795	0.270	0.058	44	20
isopropanol	"	2.924	2.74	1.869	0.432	0.057	45	21
methanol	"	2.924	2.70	1.825	0.274	0.059	52	22
n-propanol	"	2.924	2.71	1.855	0.400	0.056	46	23
water	"	3.030	2.82	1.658	0.028	0.063	66	24
formamide	NH_2-al	2.890	2.75	1.757	0.182	0.057	46	34
aniline	NH_2-ar	2.890	2.46	1.825	0.273	0.043	42	41

(1) $\bar{\nu}_a^m$ = wave number of maximal absorption (10^4 cm^{-1}), ϵ^m = molecular extinction coefficient at maximal absorption (10^3 cm^{-1} M^{-1}), $\bar{\nu}_e^m$ = wave number of maximal emission (10^4 cm^{-1}), ϕ^f = quantum yield of fluorescence; f = oscillator strength, τ_o = natural lifetime of excited state (ns). For type of solvent, see text. The indices are used in Figures 2, 3 and 4.

TABLE IC: Characteristics of the lowest energy band in the absorption and emission spectrum of 1-dimethylaminonaphthalene-5-sulphonyl ethyl ester in various solvents containing D_2O at 20 °C. (1),(2)

Solvent composition (% v/v)			$\bar{\nu}_a^m$	ϵ^m	$\bar{\nu}_e^m$	ϕ^f	f	τ_o
I	D_2O	H_2O						
	1	4	3.030	2.76	1.664	0.030	0.062	67
	2	3	3.030	2.64	1.661	0.036	0.057	74
	3	2	3.030	2.67	1.664	0.040	0.059	71
	4	1	3.030	2.76	1.667	0.047	0.062	67
	5	0	3.030	2.41	1.664	0.054	0.054	77
II	D_2O	dioxane						
	1	4	2.915	2.72	1.838	0.513	0.055	46
	2	3	2.924	2.72	1.808	0.355	0.056	50
	3	2	2.959	2.73	1.770	0.226	0.059	53
	4	1	3.003	2.85	1.709	0.122	0.064	57

(1) For symbols and corresponding units, see footnote (1) of Table IA.

TABLE IB: Characteristics of the lowest energy band in the absorption and emission spectrum of 1-dimethylaminonaphthalene-5-sulphonyl ethyl ester in various mixtures at 20 °C. (1)

Solvent composition (% v/v)		type	$\bar{\nu}_a^m$	ε^m	$\bar{\nu}_e^m$	ϕ^f	f	τ_o	index
benzene-acetonitrile									
88.9	11.1	np	2.899	2.84	1.931	0.486	0.056	32	8
83.3	16.7	"	2.899	2.81	1.923	0.524	0.055	34	9
50.0	50.0	"	2.899	2.77	1.869	0.421	0.056	41	10
33.3	66.7	"	2.899	2.81	1.859	0.403	0.060	42	11
12.5	87.5	"	2.899	2.88	1.838	0.341	0.062	45	12
benzene-chlorobenzene									
50	50	np	2.924	2.86	1.980	0.565	0.051	32	13
chlorobenzene-acetonitrile									
88.9	11.1	np	2.890	2.76	1.927	0.585	0.053	33	14
80.0	20.0	"	2.890	2.79	1.905	0.544	0.054	34	15
dimethylformamide-benzene									
66.7	33.3	np	2.899	2.84	1.855	0.440	0.059	38	16
benzene-acetic acid									
50	50	OH-al	2.950	2.46	1.912	0.526	0.044	50	25
dioxane-water									
80	20	OH-al	2.915	2.77	1.838	0.485	0.056	45	26
60	40	"	2.924	2.78	1.808	0.290	0.060	46	27
40	60	"	2.958	2.65	1.770	0.173	0.059	52	28
20	80	"	3.003	2.80	1.709	0.083	0.061	59	29
phenol in benzene									
2.87 M		OH-ar	2.941	2.72	1.835	0.511	0.053	38	30
3.82 M		"	2.959	2.80	1.828	0.480	0.056	37	31
5.74 M		"	2.976	2.86	1.808	0.437	0.059	35	32
7.63 M		"	2.985	2.79	1.802	0.379	0.061	34	33
dioxane-formamide									
80	20	NH_2-al	2.899	2.83	1.835	0.490	0.057	42	35
75	25	"	2.899	2.88	1.828	0.435	0.061	40	36
60	40	"	2.890	2.81	1.808	0.373	0.059	42	37
50	50	"	2.899	2.82	1.799	0.338	0.060	42	38
40	60	"	2.890	2.71	1.792	0.310	0.057	44	39
20	80	"	2.890	2.71	1.770	0.245	0.057	45	40
benzene-aniline									
50	50	NH_2-ar	2.882	2.83	1.855	0.285	0.045	40	42
formamide aniline									
11.1	88.9	NH_2-ar	2.907	2.78	1.799	0.222	0.051	38	43

(1) For type of solvent see text. For symbols and corresponding units, see footnote (1) of Table IA.

The radiative (or natural) lifetime τ_o (ns) was estimated by using

$$1/\tau_o = 2.88 \times 10^{-9} \cdot n_s^2 \cdot (\bar{\nu}_e^m)^3 \cdot \int \varepsilon' d\ln\bar{\nu} \qquad (13)$$

based on the Strickler-Berg equation (Birks, 1970), which for the present data was found to give values not substantially different from

that calculated with the original, more laborious equation. The integral in Equation (13) was approximated similarly to that in Equation (12). The values of f and τ_o thus obtained serve the purpose of the present investigation.

$\bar{\nu}_e^m$ and ϕ^f were determined from fully corrected emission spectra as described elsewhere (Van der Drift et al., 1983). Refractive indexes required for correction were obtained from literature (Riddick and Bunger, 1970; West, 1974) or, if not available as for the mixtures, were determined at 20 °C by using the D-line of sodium (589.3 nm). The index numbers of the solvents in Tables IA,B,C correspond with those in Figures 2 through 4.

In order to test the above procedure the lifetime of the excited state, τ, of DNS-OH was determined. From the absorption and emission spectrum of DNS-OH a value of 44 ns for τ_o was obtained by using Equation (13). ϕ^f was found to be 0.36, so that according to $\tau = \phi^f \tau_o$ (Guilbault, 1973) a value of 16 ns was found for τ, in agreement with the values 13-14 ns in literature (Chen et al., 1967; Bridge and Johnson, 1973).

The influence of pH on the low-energy band of the absorption and emission spectrum of DNS-OEt in aqueous solution is shown in Figure 1. The data indicate that the low-energy absorption band is displaced to smaller wavelengths upon lowering pH but that the emission band does not shift.

The data in Tables IA,B have been analysed according to the model outlined in the theoretical section. The solvent parameters relevant for the analysis, i.e. electric dipole moment, molecular weight and density, were obtained from literature (Riddick and Bunger, 1970; Steffen, 1970; West, 1974). The Debye orientation polarization factor P was calculated according to the formula given above. The plots of $\bar{\nu}_a^m$ and $\bar{\nu}_e^m$ versus P for the various types of solvents (Figures 2 and 3, respectively) are linear in agreement with Equations (4) and (5). Analysis of the quantum yield data according to Equation (11) showed that $B \ll 1$, so that the approximation $B = 0$ was sufficiently accurate. The linear plots of $(\phi^f/1-\phi^f)^{\frac{1}{2}}$ versus P are given in Figure 4. The values of the slopes and intercepts of the straight lines in Figures 2, 3 and

4 were calculated by the method of least squares and are compiled in Table II.

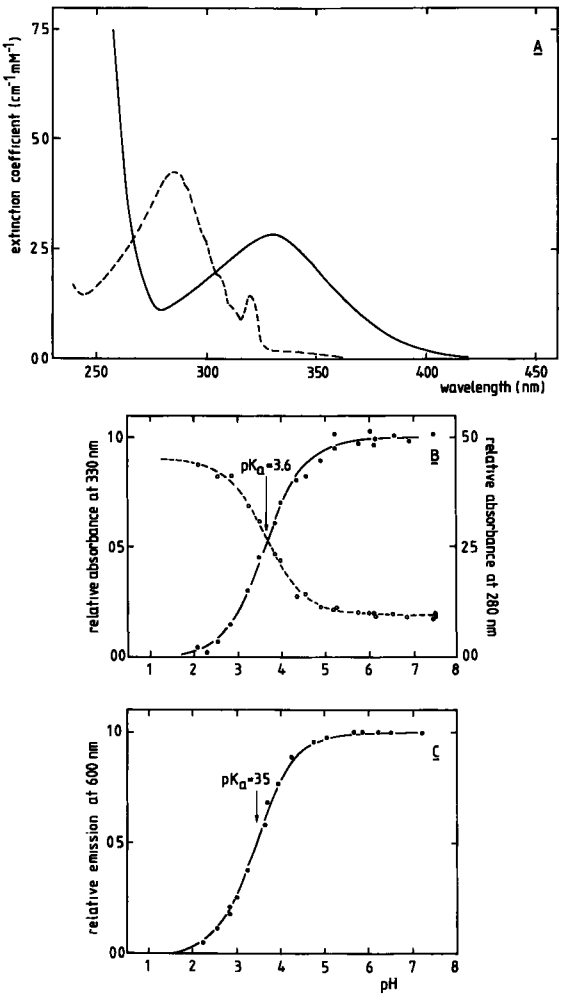

FIGURE 1: Influence of pH on the spectral properties of 1-dimethylaminonaphthalene-5-sulphonyl ethyl ester in aqueous solution at 20.0 °C. A: lowest energy band in the absorption spectrum at pH = 7.4 (———) and pH = 0.5 (- - -). B: effect of pH on the relative absorption at 280 nm (O, right scale) and 330 nm (●, left scale). The lines are theoretical titration curves for a group with pK_a = 3.6. C: effect of pH on the relative emission at 600 nm. Solid line is a theoretical titration curve for a group with pK_a = 3.5.

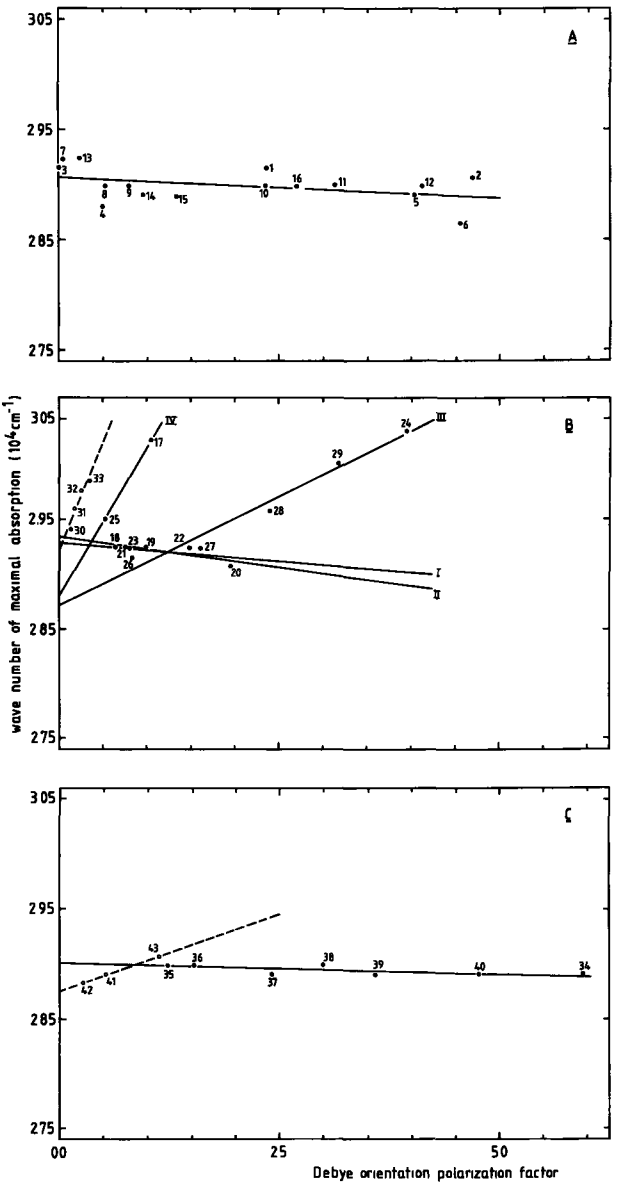

FIGURE 2: Dependence of the wave number of maximal absorption of 1-dimethylamino-naphthalene-5-sulphonyl ethyl ester in the lowest energy absorption band ($\tilde{\nu}_a^m$) on the Debye orientation polarization factor (P) for different classes of solvents at 20.0 °C. Values of $\tilde{\nu}_e^m$ were plotted versus calculated values of P. A: non-hydrogen-bonding solvents. B: hydrogen-bonding solvents with aliphatic (●) or aromatic OH (○). C: hydrogen-bonding solvents with aliphatic (●) or aromatic NH_2 (○). Indices refer to solvents listed in Tables IA,B and to Table II. Straight lines were calculated by the method of least squares; values of slopes and intercepts are given in Table II.

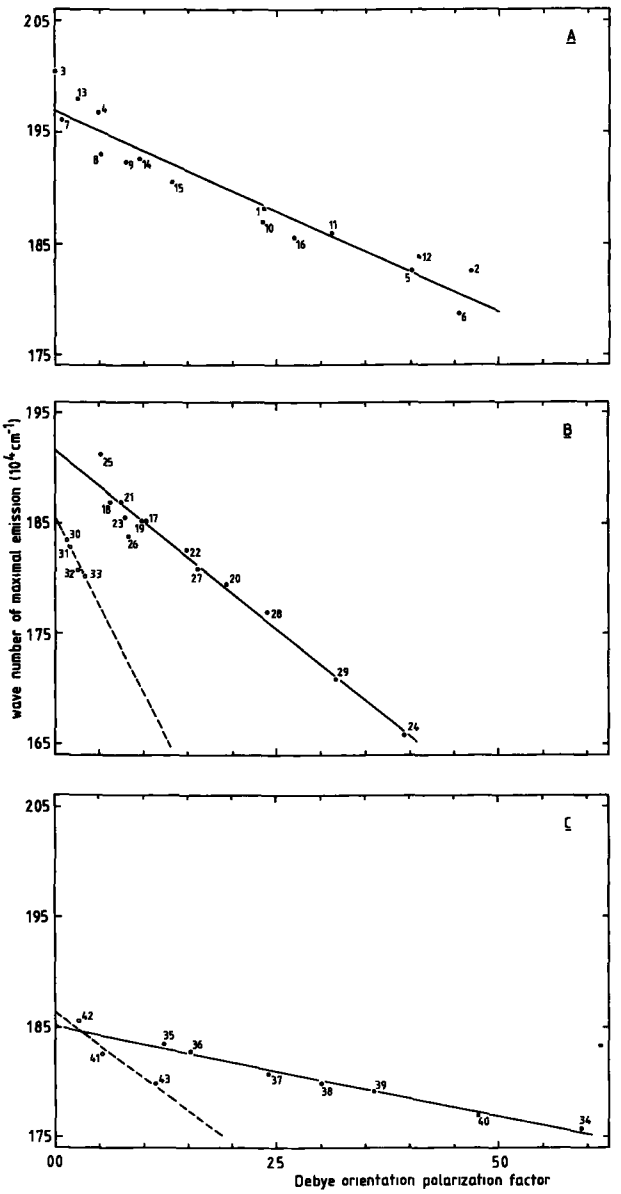

FIGURE 3: Dependence of the wave number of maximal emission ($\bar{\nu}_e^m$) of 1-dimethylamino-naphthalene-5-sulphonyl ethyl ester on the Debye orientation polarization factor (P) for different classes of solvents at 20.0 °C. Values of $\bar{\nu}_e^m$ were plotted versus calculated values of P. For further details, see legend to Figure 2.

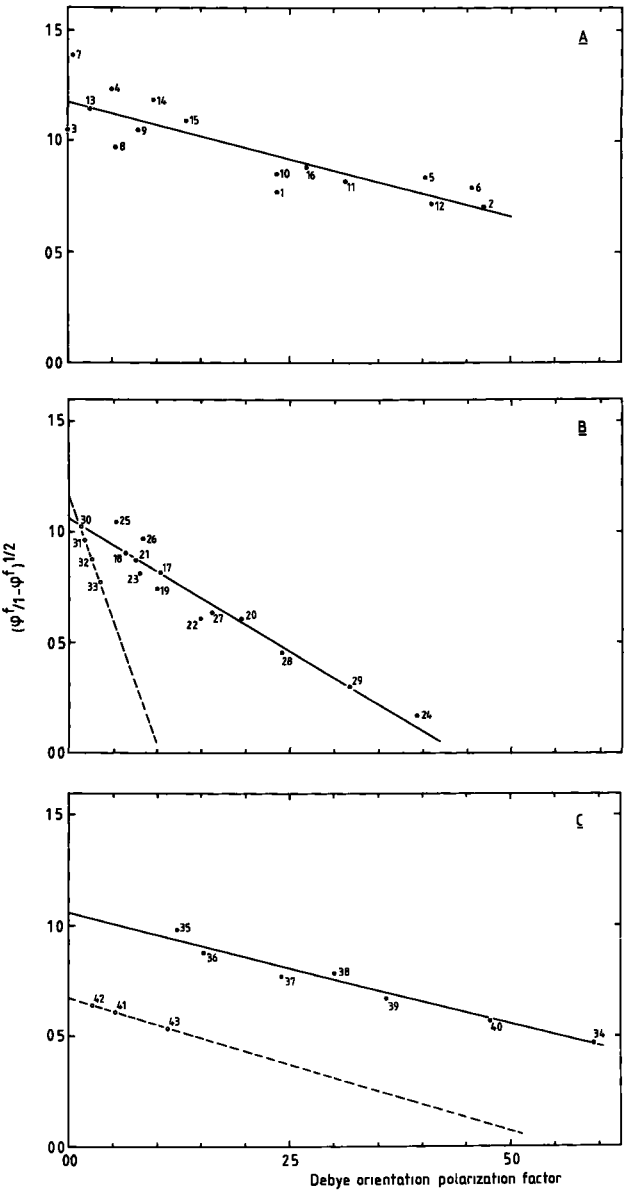

FIGURE 4: Dependence of the quantum yield of fluorescence (ϕ^f) of 1-dimethylamino-naphthalene-5-sulphonyl ethyl ester on the Debye orientation polarization factor (P) for different classes of solvents at 20.0 °C. Values of $(\phi^f/1-\phi^f)^{\frac{1}{2}}$ were plotted versus calculated values of P. For further details, see legend to Figure 2.

TABLE II: Values of the slopes and intercepts (± s.e.) calculated from the linear plots in Figures 2, 3 and 4 by the method of least squares.

Type of solvent	Figure 2(A,B,C)		Figure 3(A,B,C)		Figure 4(A,B,C)	
	intercept ($10^4 cm^{-1}$)	slope (cm^{-1})	intercept ($10^4 cm^{-1}$)	slope (cm^{-1})	intercept (10^{-1})	slope (10^{-2})
np	2.907 ± 0.006	- 38 ± 22	1.969 ± 0.007	- 362 ± 28	11.8 ± 0.4	- 10.2 ± 1.7
OH-al (1) I	2.928 ± 0.006	- 68 ± 46				
II	2.933 ± 0.005	-109 ± 43				
III	2.871 ± 0.011	397 ± 44	1.916 ± 0.006	- 650 ± 35	10.6 ± 0.3	- 23.9 ± 1.8
IV	2.879	1385				
OH-ar	2.921 ± 0.009	2031 ± 388	1.855 ± 0.006	-1666 ± 261	11.6 ± 0.1	-112.7 ± 5.2
NH_2-al	2.900 ± 0.003	- 20 ± 9	1.852 ± 0.003	- 166 ± 9	10.6 ± 0.3	- 10.1 ± 0.9
NH_2-ar	2.875 ± 0.000	289 ± 0	1.862 ± 0.012	- 611 ± 168	6.7 ± 0.1	- 12.1 ± 1.0
All solvents (2)	2.915 ± 0.004	- 53 ± 15				

(1) I = all aliphatic alcohols and the dioxane-water mixtures Nos. 26 and 27, II = aliphatic alcohols only, III = dioxane-water mixtures and water only, IV = the acetic acid-containing solvents only.

(2) All solvents except the Nos. 17, 24, 25, 26, 27, 28, 29, 30, 31, 32, 33, 42 and 43.

In order to examine some implications of the present analysis on their physical meaning the values of various molecular parameters have been estimated from the above plots for both a continuous and a discrete medium. Since both calculations yielded similar results, only the values for a continuous medium have been tabulated. The various assumptions on which these approximative calculations are based will be discussed afterwards.

The minimum and maximum values of $\vec{M}$ and $\vec{M}^*$ of DNS-OEt in the non-protic solvents which can be derived from the corresponding slopes of Figures 2 and 3 are given in Table IIIA. As for these solvents the dependence of $\bar{v}_a^m$ on the Debye orientation polarization is small, the cases of no dependence and of a somewhat larger dependence have also been considered in order to estimate the extreme values of $\vec{M}$ and $\vec{M}^*$. In the latter case all solvents were taken into account except those which obviously deviated presumably owing to particular solvent effects. The values of $\vec{M}$ and $\vec{M}^*$ derived for these two cases are also given in Table IIIA. The extreme values of $\vec{M}_r^*$ in the various types of

TABLE IIIA: Extreme values and difference between squared values of the ground-state and the excited-state dipole moment of 1-dimethylaminonaphthalene-5-sulphonyl ethyl ester in non-protic solvents. (1)

	cosθ=1		cosθ=0	
M^2-M^{*2}	$\vec{M}$	$\vec{M}^*$	$\vec{M}$	$\vec{M}^*$
-4.84	0.23	2.21	$\sim$ 0	2.09
-5.02 (2)	0.33	2.26	$\sim$ 0	2.09
-4.38 (3)	0	2.09	$\sim$ 0	2.09

(1) Estimated from the slopes of plots of $\bar{\nu}_a^m$ and $\bar{\nu}_e^m$ versus the Debye orientation polarization factor (Table II) by application of the classical dipole model including equal dipole moments in the Franck-Condon and relaxed states. $\vec{M}$ = electric dipole moment in ground state (D), $\vec{M}^*$ = electric dipole moment in the first excited singlet state (D), θ = angle between $\vec{M}$ and $\vec{M}^*$.

(2) Based on the slope for all solvents (see footnote (2) of Table II).

(3) Based on the assumption that $\bar{\nu}_a^m$ is independent of the orientation polarization factor.

TABLE IIIB: Extreme values of the excited-state dipole moment of 1-dimethylaminonaphthalene-5-sulphonyl ethyl ester in various types of solvents. (1)

Type of solvent	$\vec{M}_r^*$
np	2.1 - 2.3
OH-al	2.8 - 3.0
OH-ar	4.5 - 4.7
NH_2-al	1.4 - 1.6
NH_2-ar	2.7 - 2.9

(1) Estimated from the slopes of the plots of $\bar{\nu}_e^m$ versus the Debye orientation polarization factor (Table II) by application of the classical dipole model for a continuous medium, including $0 \leq \vec{M}_{FC} \leq 0.3$ D (Table IIIA) where $\vec{M}_{FC}$ is the dipole moment in the Franck-Condon ground state. $\vec{M}_r^*$ = electric dipole moment in the relaxed first excited singlet. For type of solvent, see text.

solvents, estimated from Figure 3 by assuming that the minimum and maximum values of $\vec{M}_{FC}$ equal those of $\vec{M}$ in Table IIIA, are compiled in Table IIIB.

The value of the Onsager cavity radius (4.5 Å) of DNS-OEt was estimated in the usual way from the specific density (1.21 g) and the molecular weight (279.36), assuming dense packing by spherical particles. This value may also be expected on the basis of molecular bond lengths. The refractive index of DNS-OEt is 1.5843.

As indicated above $E_1^{oo}-E_T^o+\Delta E_{ST}$ can be evaluated from the plots in Figure 4 for $M_{FC}^T\cos\theta^1 = 0$ if M_r^* is known. The limiting values of $E_1^{oo}-E_T^o+\Delta E_{ST}$ compiled in Table IV have been calculated by using the extreme values of $\vec{M}_r^*$ in Table IIIB.

On the other hand if M_r^* is known, $M_{FC}^T\cos\theta^1$ can be calculated for any value of $E_1^{oo}-E_T^o+\Delta E_{ST}$. For some values within the range to be expected the results of such a calculation, based on the values of $\vec{M}_r^*$ in Table IIIB, are given in Table V.

TABLE IV: Estimates of the minimum and maximum values of the energy separation $E_1^{oo}-E_T^o+\Delta E_{ST}$ for $M_{FC}^T\cos\theta^1=0$ by application of the classical dipole model for a continuous medium. (1)

Type of solvent	$E_1^{oo}-E_T^o+\Delta_{ST}$ (kcal)
np	12.1 - 14.5
OH-al	8.2 - 9.4
OH-ar	4.9 - 5.4
NH_2-al	4.9 - 6.4
NH_2-ar	9.5 - 11.0

(1) $E_1^{oo}-E_T^o+\Delta E_{ST}$ = energy difference between the relaxed first excited singlet (dipole moment $\vec{M}_r^*$) and a nearby Franck-Condon triplet (dipole moment $\vec{M}_{FC}^T$) including the contribution of various types of interactions except diple-dipole interactions. θ^1 = angle between $\vec{M}_r^*$ and $\vec{M}_{FC}^T$. Calculations are based on the minimum and maximum values of $\vec{M}_r^*$ in Table IIIB. For type of solvent, see text.

TABLE V: Estimates of the minimum and maximum values of $M_{FC}^{T}\cos\theta^{1}$ (D) for various values of the energy separation $E_1^{oo}-E_T^{o}+\Delta E_{ST}$ by application of the classical dipole model. (1)

Type of solvent	$M_{FC}^{T}\cos\theta^{1}$ (D)			
	$E_1^{oo}-E_T^{o}+\Delta E_{ST}$ (kcal)			
	2	3	4	5
np	1.8 - 2.0	1.6 - 1.8	1.4 - 1.7	1.2 - 1.5
OH-al	2.1 - 2.4	1.8 - 2.0	1.4 - 1.7	1.1 - 1.4
OH-ar	2.7 - 3.0	1.8 - 2.1	0.8 - 1.2	-0.1 - 0.3
NH_2-al	0.8 - 1.1	0.5 - 0.8	0.2 - 0.6	0 - 0.3
NH_2-ar	2.1 - 2.4	1.9 - 2.1	1.6 - 1.8	1.3 - 1.6

(1) For symbols and further details, see footnote (1) of Table IV.

DISCUSSION

a. Characterization of the Lowest Energy Absorption Band

Comparison of the values of ε^{m}, f and τ_o in Tables IA,B,C with that of the molecular electronic transition f-number scale (Kasha, 1967; Kasha and Rawls, 1968) indicates that in the present solvents the electronic transition in the lowest energy absorption band of DNS-OEt is of the $1\text{-}a_{\pi}$ type.

The displacement of the absorption band to smaller wavelengths at low pH (Figure 1(A,B)) can be ascribed to protonation of the dimethylamino group in the ground state (pK_a = 3.6). In the excited state the pK_a of this group is smaller and becomes negative as can be estimated from the shift in $\bar{\nu}_a^{m}$ (Schulman, 1976). Thus in the excited state deprotonation of the dimethylamino group is expected to occur. Since from the relative emission intensity versus pH a pK_a of 3.5 is obtained (Figure 1(C)), ϕ^{f} can be regarded as independent of pH within the range investigated indicating that this deprotonation is completed within a time interval obviously shorter than the lifetime of the

excited state (Schulman, 1976). In these aspects DNS-OEt resembles N-arylaminonaphthalenesulphonates (Seliskar et al., 1969; Seliskar and Brand, 1971[b]) for which the lowest energy absorption band corresponds also with the promotion of an l-electron localized on N to an anti-bonding π-like orbital of the naphthalenesulphonyl moiety.

b. Hydrogen Bonding

According to the present investigation dipole-dipole interactions and hydrogen bonding between DNS-OEt and solvent are the main factors determining $\bar{\nu}_a^m$ and $\bar{\nu}_e^m$ (Cf. Seliskar and Brand, 1971[a]).

On the basis of the Förster cyclus the difference $\Delta\bar{\nu}_e^m$ between the intercepts of the plots of $\bar{\nu}_e^m$ versus P for non-hydrogen-bonding and hydrogen-bonding solvents obeys (Pimentel, 1957; Mataga and Kubota, 1970; Schulman, 1976)

$$\Delta\bar{\nu}_e^m = \Delta E_H^* - \Delta E_H^o + \delta\varepsilon_H^o \qquad (14)$$

where ΔE_H^* and ΔE_H^o denote the energy due to hydrogen bonding in the relaxed first excited singlet and in the ground state, respectively, whereas $\delta\varepsilon_H^o$ is the additional destabilization energy of the Franck-Condon ground state resulting from hydrogen bonding . Similarly

$$\Delta\bar{\nu}_a^m = \Delta E_H^* - \Delta E_H^o - \delta\varepsilon_H^1 \qquad (15)$$

where $\delta\varepsilon_H^1$ denotes the additional Franck-Condon destabilization energy of the excited state. The quantities on the right-hand side of Equations (14) and (15) are positive (Pimentel, 1957; Mataga and Kubota, 1970).

For all types of protic solvents the intercepts of the plots of $\bar{\nu}_e^m$ versus P are significantly smaller than those of the non-protic solvents (Table II), the difference ranging from about 1.5 kcal for OH-al to about 3.3 kcal for NH_2-al. According to Equation (14) this indicates that

$$\Delta E_H^* > \Delta E_H^o - \delta\varepsilon_H^o \qquad (16)$$

On the other hand the intercepts of the plots of $\bar{\nu}_a^m$ versus P hardly differ for protic and non-protic solvents (Table II), with the possible exception of the more strongly hydrogen-bonding solvents water, water-dioxane, acetic acid and aniline which show somewhat smaller intercepts corresponding with a difference of about 0.9 kcal. Thus according to Equation (15)

$$\Delta E_H^* \geq \Delta E_H^o + \delta\varepsilon_H^1 \qquad (17)$$

From Equations (16) and (17) it may be concluded that in protic solvents $\Delta E_H^* > \Delta E_H^o$, i.e. the hydrogen-bonding energy in the excited state is larger than in the ground state. Since upon excitation electronic charge is transferred from the $-N(CH_3)_2$ group to the dansylsulphonyl moiety, the former will become a weaker proton acceptor and so one would expect $\Delta E_H^* < \Delta E_H^o$. This suggests that in protic solvents another site becomes stronger involved in hydrogen bonding in the excited state. Although a site on the naphthalene ring cannot be excluded (Cf. Dodiuk and Kosower, 1977) the $-SO_2-O-C_2H_5$ group seems also a likely candidate since due to its electron-withdrawing power it will acquire an increased electronic charge upon excitation.

The fact that neither $\bar{\nu}_e^m$ nor ϕ^f is clearly influenced by pH in the range 2-7.5 (see Figure 1(B,C)), whereas the replacement of H_2O by D_2O leads to a significant increase in the quantum yield (Tables IB,C) also emphasizes that hydrogen bonding and not protonation determines the spectral parameters. The straight lines obtained in Figure 3 indicate that the processes of disruption and formation of hydrogen bonds are fast compared with the lifetime of the excited state. At concentrations of H-bond donors below that used in the present investigation plots of $\bar{\nu}_e^m$ and $(\phi^f/1-\phi^f)^{\frac{1}{2}}$ versus P showed an upward curvature. Such a concentration dependence may be expected for a diffusion-controlled hydrogen bond formation between the electronically excited DNS-OEt as acceptor and a donor at low concentration.

c. Dipole Moments

The differences in slopes of the plots in Figures 2, 3 and 4 can be ascribed to differences in dipole moments. For the estimate of dipole moments in non-protic solvents, the assumption, $\vec{M}_{FC} = \vec{M}_r \equiv \vec{M}$ is acceptable from a physical point of view. Table IIIA shows that for these solvents $M^2 - M^{*2} < 0$, i.e. electronic excitation of DNS-OEt gives rise to an increased dipole moment. For the $1\text{-}a_\pi$ type of transition this is to be expected (Seliskar et al., 1969; Seliskar and Brand, 1971[b]). Quantitatively this is more clear from the extreme values of $\vec{M}$ and $\vec{M}^*$. For the allowed values of $\cos\theta$ ($\frac{\pi}{2} \geq \theta \geq 0$), $0 \leq M \leq 0.3$ D and $2.1 \leq M^* \leq 2.3$ D (Table IIIA).

For protic solvents such an analysis seems unreliable since the assumption that the dipole moment in the Franck-Condon state equals that in the corresponding relaxed state is rather questionable because of hydrogen bonding. This is supported by the signs of the slopes of $\bar{\nu}_a^m$ and $\bar{\nu}_e^m$ versus the orientation polarization factor, in particular for the aliphatic OH-type of solvents (Table II). However, an estimate of M_r^* seems possible according to the following arguments. Figure 2(B) shows that the solvent effect on the absorption spectrum of DNS-OEt in the aliphatic alcohols is not substantially different from that in the non-protic solvents (Figure 2(A)) and is mainly determined by the orientation polarization of the alcohols. This implies that M_r is not affected by hydrogen bonding and equals that in the non-protic solvents. It may, therefore, be assumed that analogous to the non-protic solvents M_{FC} will not differ substantially from M_r in these alcohols. On the other hand Figure 3(B) indicates that the value of $M_{FC}\cos\theta$ is the same for aliphatic OH-type solvents that differ in their influence on the absorption spectrum. These facts lead to the conclusion that M_{FC} and the angle θ between $\vec{M}_r^*$ and $\vec{M}_{FC}$ do not depend very much on hydrogen bonding with the solvent. Therefore, in first instance it may be assumed that for all solvents M_{FC} equals M_r in non-protic solvents (Table IIIA) and $0 \leq \cos\theta \leq 1$. The extreme values of $\vec{M}_r^*$ calculated for the various types of solvents on the basis of these considerations (Table IIIB) point to a substantial, solvent-dependent dipole moment of S_r^1.

d. Intersystem Crossing from S_r^1

In view of the large energy gap between S^1 and S^o in DNS-OEt and the $1\text{-}a_\pi$ nature of the electronic transition the contribution of internal conversion to the depopulation of S_r^1 will be negligibly small compared with that of fluorescence emission and intersystem crossing between S_r^1 and a nearby triplet that occur in this type of naphthalene derivates (Wehry, 1967; Becker, 1969; Seliskar and Brand, 1971[b]; Seliskar et al., 1974; Kosower et al., 1975). The estimated values of τ_o (Tables IA,B,C) indicate that k_e is rather insensitive to the type of solvent. The validity of these considerations is confirmed by the analysis of the quantum yield data which satisfies Equation (11) for B = 0 (Figure 4). Thus a decrease in ϕ^f and, consequently, in $(\phi^f/1\text{-}\phi^f)^{\frac{1}{2}}$ indicates an increased intersystem crossing between S_r^1 and T_{FC}. Theoretically this is caused by a decreased energy separation of the two levels and/or by increased spin-orbit interactions depending on the various ways of coupling between solute and solvent (Becker, 1969; Mataga and Kubota, 1970; Seliskar et al., 1974). The intercepts and slopes of Figure 4 will reflect these coupling mechanisms as they are determined by $(k_e/A_{st})^{\frac{1}{2}}$ and $(E_1^{oo}\text{-}E_T^o\text{+}\Delta E_{ST})$. On the basis of theoretical considerations and because the data did not give any indication of distinct molecular species resulting from intramolecular charge transfer (Cf. Kosower et al., 1975, 1978) ΔE_{ST} will only depend on the hydrogen-bonding interactions with the solvent whereas $(k_e/A_{st})^{\frac{1}{2}}$ may also depend on other factors than hydrogen bonding that influence spin-orbit interactions (Seliskar et al., 1974).

Table II shows that the intercepts of the OH-al, OH-ar and NH_2-al types of solvents do not significantly differ from that of the np-type. Comparison of corresponding results with D_2O (Table IC) and water (Tables IA,B) indicates that the "stronger" hydrogen-bonding interactions in H_2O lead to a small decrease of about 0.08 in the intercept which can be attributed to an increase in A_{ST} (Pimentel and McClellan, 1960). These small variations in intercepts between the different types of solvents indicate that hydrogen-bonding interactions may have only small effects on the values of $E_1^{oo}\text{-}E_T^o\text{+}\Delta E_{ST}$ and

$(k_e/A_{st})^{\frac{1}{2}}$. The significantly smaller intercept of the NH_2-ar type of solvent can therefore not be attributed solely to increased spin-orbit interactions due to H-bonding (Cf. Wehry, 1967; Seliskar et al., 1974). The additional coupling between solute and solvent predominantly affects A_{ST} since k_e is rather insensitive to the type of solvent.

The magnitude of the slopes in Figure 4 is determined by both $(k_e/A_{st})^{\frac{1}{2}}$ and $M_r^*(M_{FC}^T\cos\theta^1-M_r^*)$. Since there are no significant differences in the values of $(k_e/A_{st})^{\frac{1}{2}}$, the smaller slopes of OH-al and OH-ar compared to np-solvents may be attributed to differences in $M_r^*(M_{FC}^T\cos\theta^1-M_r^*)$. The transition from np to NH_2-al does not influence this factor since the slope obviously remains the same. On the other hand the transition from np to NH_2-ar is accompanied by a decrease in $M_r^*(M_{FC}^T\cos\theta^1-M_r^*)$ since $(k_e/A_{st})^{\frac{1}{2}}$ is decreased whereas the slope is only slightly smaller.

These qualitative conclusions concerning $M_r^*(M_{FC}^T\cos\theta^1-M_r^*)$ can be refined and formulated in a more quantitative way. The value of $E_1^{oo}-E_T^o+\Delta E_{ST}$ can be estimated from M_r^* and the corresponding slope and intercept of Figure 4 without any further information if $M_{FC}^T\cos\theta^1 = 0$. Since $M_{FC}^T = 0$ is highly improbable in view of the substantial extreme values of $\vec{M}_r^*$ (Table IIIB), this would mean that $\cos\theta^1 = 0$, i.e. $\vec{M}_r^*$ and $\vec{M}_{FC}^T$ are mutually perpendicular. The limiting values of $E_1^{oo}-E_T^o+\Delta E_{ST}$ have been evaluated for this case by using the data of Table IIIB. The results (Table IV) have the correct order of magnitude but are generally too large and show too much variation between the different protic solvents for this type of transition. For molecules showing $n-\pi^*$ transitions, for example, one may expect a maximum value of about 5-6 kcal (Becker, 1969; Badley, 1976). Other data indicate that this applies also for substituted aminonaphthalenesulphonates (Seliskar and Brand, 1971[b]; Seliskar et al., 1974). Therefore, the assumption $M_{FC}^T\cos\theta^1 = 0$ apparently does not hold for DNS-OEt.

On the other hand if the value of $E_1^{oo}-E_T^o+\Delta E_{ST}$ is known, one may calculate the values of $M_{FC}^T\cos\theta^1$. The results of such a calculation by using the data in Table IIIB are compiled in Table V for some energy separations within the range to be expected. The differences between

the solvents are minimal for $E_1^{oo}-E_T^o+\Delta E_{ST}$ ≈3 kcal and the values are nearly the same for the np, OH-al, OH-ar and NH_2-ar types. On the basis of the values of $\vec{M}_r^*$ in Table IIIB small differences may be expected. Moreover, these values of $M_{FC}^T\cos\theta^1$ lie reasonably well between those of $\vec{M}_r$ and $\vec{M}_r^*$, in agreement with other results (Seliskar et al., 1969; Seliskar and Brand, 1971[b]). Therefore, in view of the conclusion above that $E_1^{oo}-E_T^o+\Delta E_{ST}$ is rather insensitive to the type of solvent, the results in Table V suggest that for DNS-OEt in solution this energy difference is about 3 kcal. and that for the np, OH-al, OH-ar and NH_2-ar types of solvents $M_{FC}^T\cos\theta^1$ has the approximately same value of 1.6-2.1 D, whereas for the NH_2-al-type of solvent this value is smaller, lying between 0.5 and 0.8 D. A graphical analysis of the data of the first four solvents leads to the same conclusion. By using the mean of the extreme values of $\vec{M}_r^*$ from Table IIIB the plot of the ratios of slope and intercept from Figure 4, divided by the mean of M_r^*, versus the mean M_r^* is a straight line for these types of solvents (Figure 5). From the slope and the intercept calculated by the method of least squares one finds $E_1^{oo}-E_T^o+\Delta E_{ST}$ = 3.2 kcal and $M_{FC}^T\cos\theta^1$ = 1.8 D. By using the value of 3.2 kcal one obtains for the NH_2-al solvents $M_{FC}^T\cos\theta^1$ = 0.5 D.

These results suggest that the decrease in $M_r^*(M_{FC}^T\cos\theta^1-M_r^*)$ in going from the np-type of solvent to the OH-al, OH-ar and NH_2-ar types of solvents is primarily due to an increase in M_r^*. The constancy of $M_r^*(M_{FC}^T\cos\theta^1-M_r^*)$ upon transition from np to HN_2-al, however, seems to result from a compensation of a decrease in M_r^* by a corresponding larger decrease in $M_{FC}^T\cos\theta^1$.

e. Some Remarks on the Analysis

The present investigation indicates that the spectral properties of DNS-OEt in a large variety of protic and non-protic solvents of different polarity can be described by a classical dipole model including Debye orientation polarization. Although the assumption of Debye orientation polarization of solvent molecules around the solute may be disputable, the numerical results of approximative calculations of

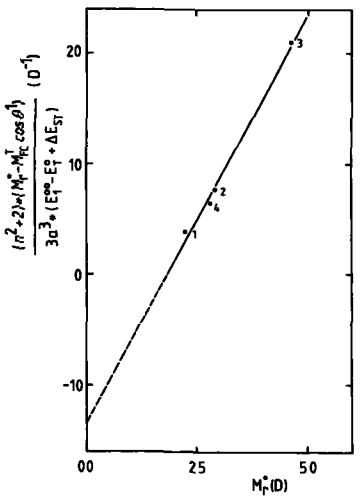

FIGURE 5: Estimate of the difference between the relaxed first excited singlet and a nearby triplet of 1-dimethylaminonaphthalene-5-sulphonyl ethyl ester with respect to energy content and electric dipole moment. (Slope/intercept) of the lines in Figure 4 (Table II) divided by the mean of M_r^* (Table IIIB) were plotted versus the mean M_r^* for different classes of solvents. 1 = np, 2 = OH-al, 3 = OH-ar, 4 = NH_2-ar (see text). Straight line was calculated by the method of least squares. Calculated values: $M_{FC}^T \cos\theta^1$ = 1.8 D; $E_1^{00} - E_T^0 + \Delta E_{ST}$ = 3.2 kcal.

various molecular parameters are acceptable from a physical point of view. This suggests that at least a qualitative physical meaning can be attributed to the description of the effects of various intermolecular interactions on the spectral characteristics, which can be given on the basis of the presented analysis.

The spectral properties of DNS-OEt can be explained in terms of at least three types of interactions between solute and solvent, dipole-dipole and hydrogen-bonding interactions being the common ones. The contributions of these interactions to the spectral parameters $\bar{\nu}_a^m$, $\bar{\nu}_e^m$ and ϕ^f are distinguishable and can be analysed in more detail. Shifts of $\bar{\nu}_e^m$ and $\bar{\nu}_a^m$ depend on the one hand on molecular quantities as dipole moment and energy separation of the electronic states involved, both sensitive to hydrogen bonding, and on the other on the Debye orientation polarization factor and the hydrogen-bonding capacity of the solvent as the main environmental parameters. Intersystem crossing from S_1 to a lower triplet is the main process influencing ϕ^f. Changes in the molecular quantities M_r^* and $M_{FC}^T \cos\theta^1$ due to hydrogen bonding in the excited state which affect the energy separation of the levels, together with changes in A_{ST} due to interactions different from mere hydrogen bonding lead to variations of ϕ^f.

Another consequence of the analysis presented in this paper is

that by comparing observed values of $\bar{\nu}_a^m$, $\bar{\nu}_e^m$ and ϕ^f with Figures 2, 3 and 4 an unknown environment of DNS-OEt can be characterized in more detail. In principle from the values of $\bar{\nu}_a^m$ and $\bar{\nu}_e^m$ (both depending only on the orientation polarization and hydrogen-bonding interactions) the Debye orientation polarization factor and the type of hydrogen bond donor can be determined. From the corresponding value of ϕ^f it can be concluded whether additional interactions influencing spin-orbit coupling are also present. As shown elsewhere (Van der Drift et al, 1983) this procedure allows one to get more detailed information about the environment of the dansyl reporter group specifically bound to the active serine in some serine hydrolases.

REFERENCES

Ainsworth, S., and Flanagan, M.F. (1969) Biochim. Biophys. Acta 194, 213.

Azzi, A. (1975) Quart. Rev. of Biophysics 8, 237.

Badley, R.A. (1976) in Modern Fluorescence Spectroscopy Vol. 2 (Wehry, E.L., Ed.) p. 91, Heyden, London.

Becker, R.S. (1969) Theory and Interpretation of Fluorescence and Phosphorescence, Wiley Interscience, New York.

Birks, J. (1970) Photophysics of Aromatic Molecules, Wiley Interscience, London.

Böttcher, C.J.F. (1952) Theory of Electric Polarization, Elsevier, Amsterdam.

Brand, L., Seliskar, C.J., and Turner, D.C. (1971) in Probes of Structure and Function of Macromolecules and Membranes Vol. 1 (Chance, B., Lee, C.P., and Blaisie, J.K., Eds.) p. 17, Academic Press, New York.

Bridge, J.B., and Johnson, P. (1973) Eur. Polym. J. 9, 1327.

Chen, R.F., and Edelhoch, H. (Eds.) (1976) Biochemical Fluorescence Vol. 2 Marcel Dekker Inc., New York.

Chen, R.F., Vurek, G.G., and Alexander, N. (1967) Science 156, 949.

Dawson, W.R., and Windsor, M.W. (1968) J. Phys. Chem. 72, 3251.

Dodiuk, H., and Kosower, E.M. (1977) J. Am. Chem. Soc. 99, 859.

Edelman, G.M., and McClure, W.O. (1968) Acc. Chem. Res. 1, 65.

Exner, O. (1975) Dipole Moments in Organic Chemistry, Thieme, G., Stuttgart.

Grunwald, E., and Winstein, S. (1948) J. Am. Chem. Soc. 70, 846.

Guilbault, G.G. (1973) Practical Fluorescence, Theory, Methods and Techniques, Marcel Dekker, Inc., New York.

Kasha, M. (1967) in Fluorescence, Theory, Instrumentation and Practice (Guilbault, G.G., Ed.) p. 201, Marcel Dekker, Inc., New York.

Kasha, M., and Rawls, H.R. (1968) Photochem. Photobiol. 7, 561.

Kosower, E.M. (1958) J. Am. Chem. Soc. 80, 3253.

Kosower, E.M., and Dodiuk, H. (1978) J. Am. Chem. Soc. 100, 4173.

Kosower, E.M., Dodiuk, H., and Kanety, H. (1978) J. Am. Chem. Soc. 100, 4179.

Kosower, E.M., Dodiuk, H., Tanizawa, K., Ottolenghi, M., and Orbach, N. (1975) J. Am. Chem. Soc. 97, 2167.

Mataga, M., and Kubota, T. (1970) Molecular Interactions and Electronic Spectra, Marcel Dekker, Inc., New York.

Melhuish, W.H. (1960) J. Phys. Chem. 64, 762; (1961) 65, 229.

Melhuish, W.H. (1964) J. Opt. Soc. Amer. 54, 183.

Nicol, M.F. (1974) Appl. Spect. Reviews 8(2), 183.

Pimentel, G.C. (1957) J. Am. Chem. Soc. 79, 3325.

Pimentel, G.C., and McClellan, A.L. (1960) The Hydrogen bond, W.H. Freeman and Company, San Francisco.

Radda, G.K. (1975) in Methods in Membrane Biology Vol. 4 (Korn, E.D., Ed.) p. 97, Plenum Press, New York.
Reeves, R.L., Maggio, M.S., and Costa, L.F. (1974) J. Am. Chem. Soc. 96, 5917.
Riddick, J.A., and Bunger, W.B. (1970) Organic Solvents, 3th Edition (Techniques of Chemistry, Vol. II), Wiley Interscience, New York.
Sandorfy, C. (1964) Electronic Spectra and Quantum Chemistry, Printice Hall Inc., Englewood Cliffs.
Schulman, S.G. (1976) in Modern Fluorescence Spectroscopy Vol. 2 (Wehry, E.L., Ed.) p. 239, Plenum Press, New York.
Seliskar, C.J., and Brand, L. (1971[a]) Science 171, 799.
Seliskar, C.J., and Brand, L. (1971[b]) J. Am. Chem. Soc. 93, 5405, 5414.
Seliskar, C.K., Khalil, O.S., and Mc Glynn, S.P. (1974) in Excited States Vol. I (Lim, E.C., Ed.) p. 231, Academic Press, New York.
Seliskar, C.J., Turner, D.C., Gohlke, J.R., and Brand, L. (1969) in Molecular Luminescence (Lim, E.C., Ed.) p. 677, W.A. Benjamin Inc., New York.
Sinanoglu, O. (1967) in Molecular Associations in Biology (B. Pullman, Ed.) p. 427, Academic Press, New York.
Steffen, M. (1970) Ber. Bunsenges. Phys. Chem. 74, 505.
Stryer, L. (1966) J. Am. Chem. Soc. 88, 5708.
Turner, D.C., and Brand, L. (1968) Biochemistry 7, 3381.
Van der Drift, A.C.M., Roos, A.L.M., and Moes, G.W.H. (1983) This Thesis, Chapter 2; to be submitted for publication.
Waggoner, A. (1976) in Enzymes of the Biological Membranes Vol. 1 (Martonosi, A., Ed.) p. 119, Plenum Press, New York.
Wehry, E.L. (1967) in Fluorescence, Theory, Instrumentation and Practice (Guilbault, G.G., Ed.) p. 37, Marcel Dekker, New York.
Wehry, E.L. (Ed.) (1976) Modern Fluorescence Spectroscopy Vol. 2, Heyden, London.
West, R.C. (Ed.) (1974) Handbook of Chemistry and Physics, 55th Edition, C.R.C. Press, Cleveland.

CHAPTER 4

KINETICS OF THE INHIBITION BY DANSYL FLUORIDE

ABSTRACT: Inactivation of the serine hydrolases atropinesterase (AtrE) and α-chymotrypsin (Chymo) by dansyl fluoride (DNS-F) results from the covalent attachment of a dansyl group to the side chain of the active serine. The kinetics of this irreversible inhibition with various concentrations of excess DNS-F has been studied at different temperatures (range: 15-37 ^{o}C) and pH's (range: 4.5-8.5). In all cases first-order kinetics was observed.

For both enzymes the inactivation proceeds via two steps: formation of a reversible enzyme-inhibitor complex in rapid equilibrium with the free components and a subsequent sulphonylation reaction. The dissociation constants of the complexes K_I and the monomolecular rate constants of sulphonylation k_2 have been calculated from Lineweaver-Burk, Hofstee and Eadie plots. From the temperature dependence of K_I and k_2 the corresponding changes in the enthalpy and entropy were estimated. The different values of these quantities for the two enzymes are attributed to a different structure and solvation of the active-site region: a larger binding pocket near the active serine in AtrE allows a larger amount of solvent to become entrapped in and subsequently to be released from the enzyme during complex formation and sulphonylation than in the case of Chymo.

The variation in the inhibition with pH is also different for both enzymes and can be attributed to an effect on k_2, K_I being almost insensitive to changes in pH. For Chymo the effect can be ascribed to the involvement of a single titratable histidine in sulphonylation, whereas the results for AtrE point to an antagonistic influence of at least two titratable groups on this reaction.

INTRODUCTION

In a previous paper it has been shown that the serine hydrolases atropinesterase, α-chymotrypsin and subtilisin A can be specifically labelled at the so-called active serine with a fluorescent reporter group by sulphonylation with dansyl fluoride (Van der Drift et al., 1983[c]). This opened the possibility of a comparative investigation of these enzymes by means of fluorescence spectrometry. According to the fluorescence data the direct environment of the bound dansyl group in atropinesterase appeared to differ from that in chymotrypsin and sub-

tilisin, i.e. in the esterase the label is more extensively embedded in the protein structure than in the two proteases. The aim of the present investigation was to examine whether this difference in the environment of the active serine is also reflected in the process of irreversible inhibition (inactivation) of the enzymes by dansyl fluoride.

To this end the kinetics of the inactivation of atropinesterase and chymotrypsin by dansyl fluoride have been investigated by means of steady-state methods. Also, the effects of temperature and pH on the dissociation constant of the enzyme-inhibitor complex and on the rate constant of sulphonylation have been determined. From these data thermodynamic parameters have been calculated which indicate particular changes in the active-site regions of these enzymes during inactivation.

MATERIAL AND METHODS

a. Enzymes and Other Chemicals

Purified atropinesterase from Pseudomonas putida PMBL-1 (AtrE) was obtained according to the procedure of Rörsch et al. (1971) as modified by Oosterbaan et al. (1983). The specific activity of the batches used varied from 530-550 units* per A_{280} at 25.0 °C, pH = 7.0 (see Inhibition). Salt-free α-chymotrypsin (Chymo; EC 3.4.21.1) from bovine pancreas was purchased from Sigma Chemical Company (Lot 40 F-8051, 3x crystallized and lyophilized). 1-Dimethylaminonaphthalene-5-sulphonyl fluoride (dansyl fluoride; DNS-F) was prepared as described elsewhere (Van der Drift et al., 1983[c]). For inhibition, stock solutions of DNS-F in freshly distilled and dried acetone were prepared at various concentrations (1-10 mM). Other chemicals were commercial products of analytical grade, unless stated otherwise.

* 1 unit hydrolyses 1 μM of (-)-atropine per minute at the conditions indicated.

b. Inhibition

Enzyme solutions of pH 6-8.5 were prepared in 10 mM phosphate buffer; for solutions with pH $\leq$ 6 10 mM phosphate-citric acid buffer was used. All buffers contained 0.1 mM sodium azide (Merck) as a bacteriostatic. Inhibition of the enzyme was performed at constant temperature ($\pm$0.1 °C) and started by addition of a small volume of a stock solution of DNS-F to a pre-thermostated enzyme solution (concentration of active enzyme $\leq$ 3 µM) giving a final concentration of DNS-F of 0.01-0.20 mM. The use of higher concentrations was hampered by the restricted solubility of DNS-F in the buffer (about 0.25 mM at 20 °C). The initial inhibition was followed by taking at intervals 1-5 µl samples from the reaction mixture which were assayed for enzyme activity. Enzyme activities were measured titrimetrically at pH=7.0 and at 25.0 $\pm$ 0.1 °C with a Radiometer pH-stat equipment (Titrator TTT 1c combined with a Titrigraph SBR 2c). N-acetyl-L-tyrosine ethyl ester (Merck; 16.7 mM in 0.1 M KCl) or hyoscyamine sulphate (Nutritional Biochemicals Corporation; 0.4 mM in 0.1 M KCl and 0.02% saponine) was used as a substrate for Chymo and AtrE, respectively. After pH and temperature equilibration of 12 ml of a substrate solution in the thermostatically controlled reaction vessel under a continuous flow of N_2, in order to prevent uptake of CO_2, an enzyme sample was added and the acid release was followed by pH-stat addition of standardized NaOH (0.0195 N) for at least 5 minutes. Spontaneous hydrolysis of substrate was negligible. Enzyme activities were evaluated graphically.

RESULTS

The inhibition of AtrE and Chymo by excess DNS-F can be described by the reaction scheme which is often applicable to the irreversible inhibition of enzymes (Westley, 1969; Davies et al., 1970; Bender, 1971; Wold, 1971)

$$E + I \underset{k_{-1}}{\overset{k_1}{\rightleftharpoons}} E \cdot I \xrightarrow{k_2} EI + \text{Products} \qquad (1)$$

E, I, E.I and EI denote the native enzyme, the inhibitor, the reversi-

ble enzyme-inhibitor complex (Michaelis complex) and the inactivated enzyme, respectively. On the basis of this scheme inhibition by an excess of inhibitor proceeds according to first-order kinetics in the case of rapid equilibrium, i.e. $k_2 \ll k_{-1}$ (Cf. Davies et al., 1970). Examples of first-order plots derived from the initial inhibition data of AtrE and Chymo are given in Figure 1.

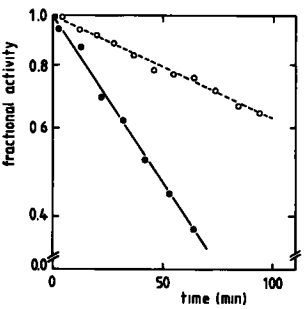

FIGURE 1: Inhibition of atropinesterase (O) and α-chymotrypsin (●) by an excess of dansyl fluoride (DNS-F) at 20.0 °C, pH = 7.3. Semi-logarithmic plot of enzyme activity versus time. Concentrations: about 3 μM enzyme and 0.1 mM DNS-F. The lines were calculated by the method of least squares. Corresponding $k_{obs.}$: (4.73 ± 0.16) x 10^{-3} min^{-1} and (15.4 ± 0.6) x 10^{-3} min^{-1} for atropinesterase and α-chymotrypsin, respectively.

Values of the (pseudo) first-order reaction rate constant, k_{obs}, were obtained from the slopes of such plots. Slopes and intercepts of these and other linear plots mentioned in the present paper were calculated by the method of least squares.

For scheme (1) it can be shown that

$$k_{obs} = \frac{k_2 [I]}{K_I + [I]} \qquad (2)$$

where $K_I = k_{-1}/k_{+1}$ is the dissociation constant of the enzyme-inhibitor complex and [I] the concentration of inhibitor (Cf. Davies et al., 1970). For both AtrE and Chymo values of k_{obs} determined at various concentrations of DNS-F but under otherwise identical conditions obey Equation (2). By fitting Equation (2) to a set of k_{obs}, [I] data according to the linear plots of Lineweaver and Burk (1934), Hofstee (1952) or Eadie (1942), the kinetic parameters K_I and k_2, the monomolecular rate constant of the sulphonylation reaction, were evaluated from the slopes and intercepts. As examples of such plots the results for AtrE and Chymo at 15.0 °C are shown in Figure 2.

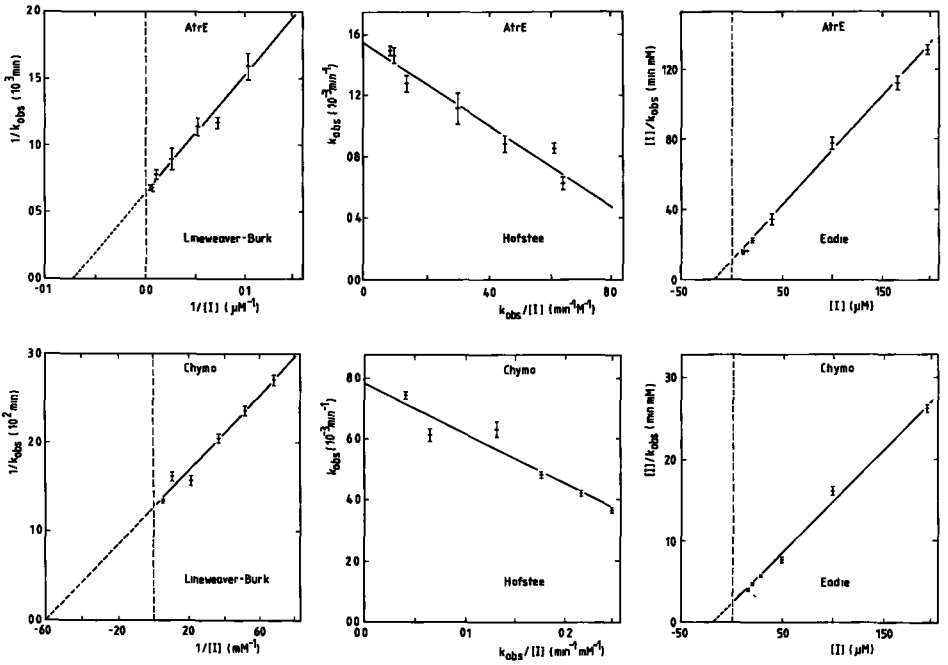

FIGURE 2: Kinetic analysis of the inhibition of atropinesterase (AtrE) and α-chymotrypsin (Chymo) by an excess of dansyl fluoride at 15.0 °C, pH = 7.3. The observed first-order rate constants (k_{obs}) of the inhibition, determined at different concentrations of inhibitor ([I]), were plotted according to Lineweaver and Burk, Hofstee and Eadie. The lines were calculated by the method of least squares. From these plots the dissociation constant K_I of the reversible enzyme-inhibitor complex and the monomolecular rate constant of the sulphonylation reaction k_2 were calculated; the values are given in Tables IA,B and IIA,B, respectively.

In order to examine the effect of temperature, similar inhibition experiments were carried out at 5 different temperatures, at pH=7.3. Since AtrE showed some spontaneous inactivation at 37 °C and higher temperatures, experiments with this enzyme were performed up to 35.0 °C where the effect was not observed. The values of K_I for AtrE and Chymo obtained from these data are compiled in Tables IA and IB, respectively; the corresponding values of k_2 are given in Tables IIA and IIB. The three methods of determining K_I and k_2 lead to about the same values.

TABLE IA: Dissociation constant K_I (± s.e.) of the reversible enzyme-inhibitor complex evaluated from the inhibition of atropinesterase by an excess of dansyl fluoride at pH = 7.3 as a function of temperature, and the corresponding changes in enthalpy (ΔH) and entropy (ΔS) upon association.

Temperature (°C)	K_I (μM)		
	Lineweaver-Burk	Hofstee	Eadie
15	13.8 ± 1.2	13.4 ± 1.5	16.1 ± 2.4
20	22.5 ± 1.9	20.6 ± 2.3	19.5 ± 1.3
25	28.7 ± 2.6	26.4 ± 4.4	26.5 ± 3.7
30	33.8 ± 2.7	34.3 ± 3.1	32.1 ± 2.7
35	51.4 ± 16.0	49.0 ± 10.9	44.1 ± 11.1
ΔH (kcal/mole)	-10.8 ± 1.1	-11.0 ± 0.6	-8.8 ± 0.5
ΔS (cal/mole K)	-15.3 ± 3.5	-15.8 ± 2.0	-8.7 ± 1.6

TABLE IIA: The monomolecular rate constant of sulphonylation k_2 (± s.e.) of atropinesterase by an excess of dansyl fluoride at pH = 7.3 as a function of temperature, and the values of the enthalpy ($\Delta H^{\neq}$) and entropy of activation ($\Delta S^{\neq}$) at 20.0 °C.

Temperature (°C)	k_2 (10^{-3} min^{-1})		
	Lineweaver-Burk	Hofstee	Eadie
15	1.55 ± 0.08	1.54 ± 0.06	1.60 ± 0.04
20	6.04 ± 0.37	5.83 ± 0.27	5.72 ± 0.09
25	10.30 ± 0.75	9.96 ± 0.74	9.95 ± 0.62
30	16.15 ± 1.14	16.33 ± 0.85	15.84 ± 0.49
35	40.37 ± 11.83	40.48 ± 5.19	38.42 ± 3.95
$\Delta H^{\neq}$ (kcal/mole)	26.0 ± 3.0	26.2 ± 2.8	25.6 ± 2.6
$\Delta S^{\neq}$ (cal/mole K)	11.2 ± 10.0	12.0 ± 9.2	9.7 ± 8.7

K_I and k_2 obey an exponential temperature dependence in the range investigated since for both enzymes the plots of $-RlnK_I$ and $-lnk_2$ versus 1/T, where R is the universal gas constant and T the absolute temperature, are linear (Figure 3). From a plot of $-RlnK_I$ versus 1/T the difference in enthalpy (ΔH) and entropy (ΔS) between the reversible

TABLE IB: Dissociation constant K_I (± s.e.) of the reversible enzyme-inhibitor complex evaluated from the inhibition of α-chymotrypsin by an excess of dansyl fluoride at pH = 7.3 as a function of temperature, and the corresponding changes in enthalpy (ΔH) and entropy (ΔS) upon association.

Temperature (°C)	K_I (μM)		
	Lineweaver-Burk	Hofstee	Eadie
15	16.8 ± 1.7	16.4 ± 2.6	18.1 ± 4.0
20	23.5 ± 1.9	22.0 ± 2.6	18.4 ± 3.8
25	25.5 ± 3.4	27.7 ± 3.9	25.1 ± 4.5
30	28.9 ± 2.1	30.7 ± 2.6	30.0 ± 2.7
37	35.6 ± 4.5	39.0 ± 5.2	47.4 ± 5.9
ΔH (kcal/mole)	-5.6 ± 0.7	-6.8 ± 0.6	-8.0 ± 1.2
ΔS (cal/mole K)	+2.2 ± 2.5	-1.8 ± 2.1	-5.9 ± 3.9

TABLE IIB: The monomolecular rate constant of sulphonylation k_2 (± s.e.) of α-chymotrypsin by an excess of dansyl fluoride at pH = 7.3 as a function of temperature, and the values of the enthalpy ($\Delta H^{\neq}$) and entropy of activation ($\Delta S^{\neq}$) at 20.0 °C.

Temperature (°C)	k_2 (10^{-3} min^{-1})		
	Lineweaver-Burk	Hofstee	Eadie
15	7.87 ± 0.43	7.82 ± 0.42	7.98 ± 0.34
20	17.75 ± 1.16	17.27 ± 0.98	16.30 ± 0.67
25	20.21 ± 2.20	21.20 ± 1.53	20.47 ± 0.97
30	30.68 ± 1.88	31.75 ± 1.45	31.49 ± 0.89
37	70.69 ± 7.91	74.80 ± 5.83	82.11 ± 4.76
$\Delta H^{\neq}$ (kcal/mole)	15.8 ± 1.9	16.4 ± 1.7	17.1 ± 1.7
$\Delta S^{\neq}$ (cal/mole K)	-21.4 ± 6.4	-19.3 ± 5.7	-17.0 ± 5.8

complex E.I and the free components E and I can be obtained according to

$$-R \ln K_I = -\frac{\Delta H}{T} + \Delta S \qquad (3)$$

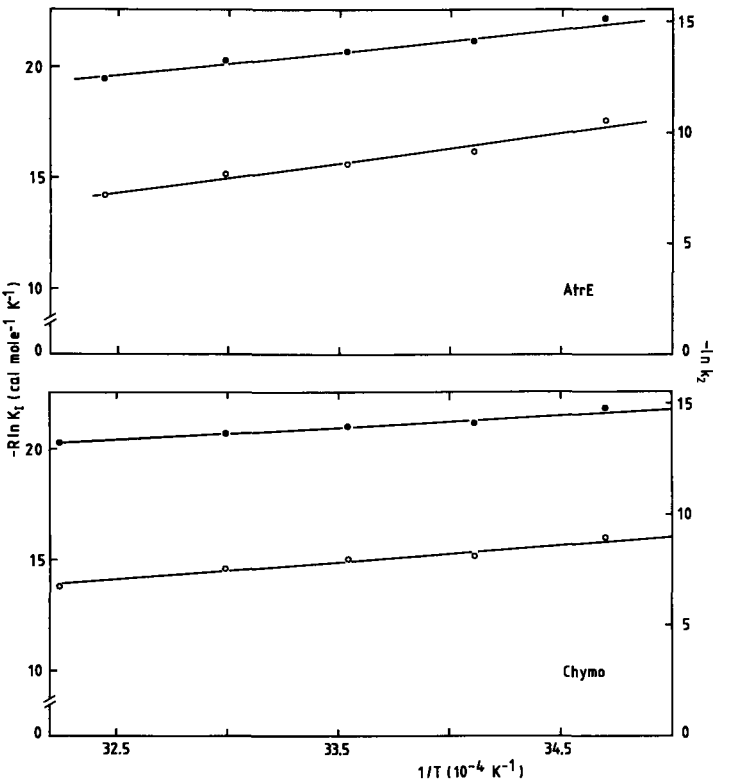

FIGURE 3: Temperature dependence of the dissociation constant of the reversible enzyme-inhibitor complex K_I (●; left scale) and the monomolecular rate constant of sulphonylation k_2 (○; right scale) for atropinesterase (AtrE) and α-chymotrypsin (Chymo). Solid lines were calculated by the method of least squares.

The values of ΔH and ΔS thus calculated are given in Tables IA and IB.

Since the relation between k_2 and T is expressed by the Arrhenius equation

$$k_2 = A\, e^{-E_a/RT} \qquad (4)$$

where E_a is the activation energy and A a frequency factor, the slope and intercept of a plot of $-\ln k_2$ versus 1/T yield E_a and $-\ln A$, respectively. With these quantities the enthalpy of activation ($\Delta H^{\neq}$) and the

entropy of activation ($\Delta S^{\neq}$) associated with the sulphonylation reaction, were calculated according to (Jencks, 1969; Westley, 1969)

$$\Delta H^{\neq} = E_a - RT \qquad (5a)$$

$$\Delta S^{\neq} = R \left[\ln A - \ln\left(\frac{kT}{h}\right) \right] - R \qquad (5b)$$

where k is the Boltzmann constant and h Planck's constant. The values of $\Delta H^{\neq}$ and $\Delta S^{\neq}$ are given in Tables IIA and IIB.

For both enzymes the influence of pH on K_I and k_2 has been investigated at 25.0 °C. For different pH's between 4.5 and 8.5, K_I and k_2 were evaluated from k_{obs} according to the procedure of Lineweaver and Burk. The values obtained are depicted in Figure 4.

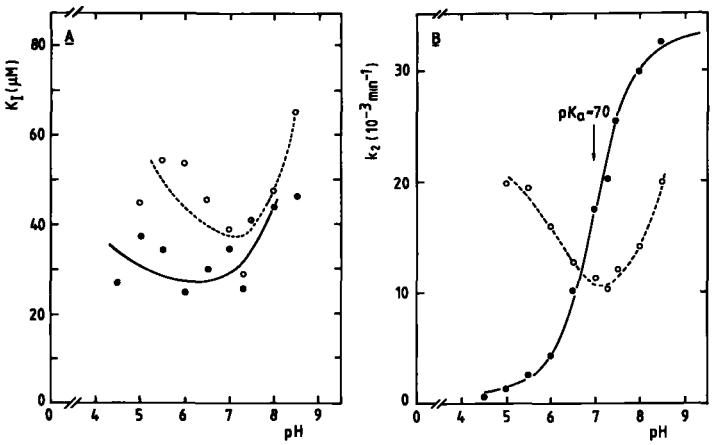

FIGURE 4: pH-Dependence of the dissociation constant of the reversible enzyme-inhibitor complex K_I (A) and the monomolecular rate constant of sulphonylation k_2 (B), obtained from Lineweaver-Burk plots. O = atropinesterase, ● = α-chymotrypsin. Temperature: 25 °C. The solid line for k_2 of Chymo corresponds with a theoretical titration curve of a group with pK_a = 7.0.

DISCUSSION

The above analysis shows that the irreversible inhibition of AtrE and Chymo by an excess of DNS-F can be described by reaction scheme (1). Apparently, during inactivation of both enzymes two processes can be distinguished kinetically: 1) the formation of a reversible association complex in rapid equilibrium with the free components, characterized by K_I, and 2) the subsequent relatively slow chemical modification of the side chain of the active serine, characterized by k_2. Such a kinetic similarity may reflect a structural similarity between the active-site regions of both enzymes. The linear relationships of $-RlnK_I$ and $-lnk_2$ with 1/T for AtrE and Chymo (Figure 3) indicate that - in the temperature range studied - the structure of the active-site region of the enzymes is not affected by abrupt conformational changes which appreciably influence either one or both steps of the inhibition process and that therefore such a structural similarity if present will be maintained. Investigations by means of NMR (Van der Drift et al., 1983[a]), ESR (Van der Drift et al., 1981[b], 1983[b]) and fluorescence spectrometry (Van der Drift et al., 1983[c]) have already indicated that the tertiary structure of the active-site region of AtrE has some characteristic features in common with that of serine proteases, in particular the presence of a binding pocket near the active serine. However, these studies also point to differences in structure of this binding site in AtrE and in Chymo or subtilisin A. The kinetic results presented are consistent with such a difference.

The small values of K_I in the temperature range investigated indicate tight binding of the DNS-F to the active-site region of both enzymes. The changes in the Gibbs' free energy (ΔG) upon complexation is about the same for both enzymes and the value of -6.0 to -6.5 kcal/mole is in agreement with other observations on the inhibition of Chymo by association with aromatic compounds (Miles et al., 1963; Wallace et al., 1963; Hymes et al., 1965; Garel and Labouesse, 1970; Rajender et al., 1970). The binding tends to decrease at higher temperatures, since the association is mainly enthalpy-driven as the values of ΔH and ΔS show (Tables IA,B). In particular the negative values of

ΔH indicate that the reversible association of DNS-F with both enzymes can be ascribed mainly to non-classical hydrophobic binding, as might occur between two moderately polar components in aqueous solutions (Jencks, 1969; Tanford, 1973).

On the basis of other investigations (Bender and Kézdy, 1965; Bender, 1971) and the structure of the active-site region in Chymo (Sigler et al., 1968; Steitz et al., 1969; Henderson, 1970; Blow, 1976) the interaction of DNS-F with this enzyme can be expected to be hydrophobic. The favourable enthalpy of association and the small entropic contribution point to some increase in mobile solvent as a driving force in this binding (Jencks, 1969). As the negative values of ΔH and ΔS for AtrE are appreciably larger than for Chymo (Cf. Tables IA,B), the immobilization of the label by the former enzyme will be accompanied by some decrease rather than by an increase in solvent mobility (Jencks, 1969; Page and Jencks, 1971).

Although for both enzymes the Gibbs' free energy of activation associated with k_2 is about 22 kcal/mole, $\Delta H^{\neq}$ and $\Delta S^{\neq}$ are different. For Chymo the values of $\Delta H^{\neq}$ and $\Delta S^{\neq}$ (Table IIB) do not differ substantially from those found for the hydrolysis of apolar substrates (Page and Jencks, 1971; Laidler and Peterman, 1979). The negative value of $\Delta S^{\neq}$ strongly suggests an increased ordering of the components (inhibitor, solvent, protein) in going from the Michaelis complex to the transition state, as has been found for various substrates (Wedler et al., 1975; Laidler and Peterman, 1979). For AtrE, on the contrary, there is an increase in entropy upon activation of the complex to the transition state, indicating an increased overall disorder of its components. Since activation will be accompanied by increased binding between enzyme and inhibitor, this increase in entropy is probably due to the displacement of "bound water" from the enzyme-inhibitor complex during the positioning of the inhibitor for sulphonylation.

The results of the kinetic analysis are consistent with previous fluorescence studies (Van der Drift et al., 1983[c]). These investigations indicate that after sulphonylation the rather apolar dansyl group is more embedded in the protein structure in AtrE than in Chymo. This is confirmed by ESR mobility studies by using spin-labelling

techniques, which point to the presence of a binding pocket near the active serine in AtrE that can bind large aromatic groups more strongly than the pocket in Chymo (Van der Drift et al., 1981[b]; 1983[b]). Since the binding pocket in AtrE is apparently more accessible to large apolar groups, it is expected to contain a larger amount of bound solvent in the native enzyme than in Chymo. As penetration of the dansyl group into the pocket will start during formation of the Michaelis complex and will be optimized subsequently during sulphonylation, it is conceivable that in AtrE a larger amount of solvent will be immobilized by entrapment in the first process and subsequently removed in the second step than in Chymo. The thermodynamic parameters associated with the two processes (Tables IA,B and IIA,B) suggest that these differences between the two enzymes are attended with entropy-enthalpy compensation (Lumry and Rajender, 1970).

The effect of pH on k_{obs} suggests that the active sites of the two enzymes have a different sensitivity to variations in pH. Figure 4 shows that for Chymo the increase in k_{obs} with increasing pH in the range 4.5 to 8.5 is due to an increase in k_2 since K_I does not change appreciably (Cf. Equation 2). Such a pH-effect has also been found for the enzymatic hydrolysis of aspecific substrates (Cuppett and Canady, 1970; Rajender et al., 1970; Hardman et al., 1971). The plot of k_2 versus pH fits a theoretical titration curve for a single group with a pK_a=7.0, which is characteristic for a histidine. The simple pH-dependence of k_2 indicates that the reversible association of enzyme and DNS-F does not significantly affect the pK_a of this histidine (Cf. Tipton and Dixon, 1979). Probably this is His(57) which is known to be present in the active site of Chymo as part of the charge-relay system (Cf. Kraut, 1977). The above pK_a-value is only slightly smaller than that found for DFP-inhibited Chymo (pK_a=7.2) by means of ^{31}P NMR spectrometry (Van der Drift, 1981[a]; Van der Drift et al., 1983[a]).

Apparently, the active serine in Chymo shows reactivity towards the inhibitor when the Nε2 of His(57) is in the non-protonated form. There are two explanations for this increased nucleophilic reactivity. From X-ray diffraction data on native and inhibited serine proteases it has been concluded that the reactivity of the active serine must be

ascribed to a favourable position of the Oγ in the side chain with respect to the electrophilic centre of the substrate or inhibitor and not to an unusually high intrinsic nucleophilicity (Matthews et al., 1977). On the other hand, the reactivity of the active-site serine in Chymo towards substitution of the hydroxyl group has been ascribed to induction of a hydrogen bond between this group and the Nε2 of His(57) by the binding of substrate or particular ligands, resulting in an increased nucleophilicity of Oγ (Cruickshank and Kaplan, 1975). If the latter explanation were correct, the pK_a of the histidine in the Michaelis complex would be substantially smaller than that in the free enzyme ($pK_a \sim 7.0$) because of stabilization of the dissociated form of histidine by hydrogen bonding. Since this is not the case, the present data support the former explanation.

Figure 4(A) shows that in the case of AtrE the pH-dependence of K_I is about the same as for Chymo. The variation in k_2 with pH, however, is different for both enzymes (Figure 4(B)). For AtrE the maximum variation in k_2 with pH is about a factor of two, whereas for Chymo it is about 30. Thus, the inhibition of AtrE by DNS-F agrees with that of Chymo in that the formation of the Michaelis complex is almost pH-independent. However, in contrast with Chymo an increase in pH does not simply lead to increased inactivation of AtrE resulting from a more favourable orientation of the serine side chain as the only factor. Figure 4(B) suggests that this different sensitivity of the active-site region in AtrE to a change in pH results from the involvement of at least two different titratable groups whose (de)protonation has an opposite effect on the inactivation. At the moment, further characterization of these groups is not possible because the present data do not allow a reliable determination of the corresponding pK_a-values.

REFERENCES

Bender, M.L. (1971) Mechanisms of Homogeneous Catalysis from Protons to Proteins, Wiley-Interscience, New York.
Bender, M.L., and Kézdy, F.J. (1965) Ann. Rev. Biochem. 34, 49.
Blow, D.M. (1976) Acc. Chem. Res. 9, 145.
Cruickshank, W.H., and Kaplan, H. (1975) Biochem. J. 147, 411.
Cuppett, C.C., and Canady, W.J. (1970) J. Biol. Chem. 245, 1069.
Davies, J.H., Campbell, W.R., and Kearns, C.W. (1970) Biochem. J. 117, 221.

Eadie, G.S. (1942) J. Biol. Chem. 146, 85.
Garel, J.R., and Labouesse, B. (1970) J. Mol. Biol. 47, 41.
Hardman, M.J., Valenzuela, P., and Bender, M.L. (1971) J. Biol. Chem. 246, 5907.
Henderson, R. (1970) J. Mol. Biol. 54, 341.
Hofstee, B.H.J. (1952) Science 116, 329.
Hymes, A.J., Robinson, D.A., and Canady, W.J. (1965) J. Biol. Chem. 240, 134.
Jencks, W.P. (1969) Catalysis in Chemistry and Enzymology, McGraw-Hill, New York.
Kraut, J. (1977) Ann. Rev. Biochem. 46, 331.
Laidler, K.J., and Peterman, B.F. (1979) in Enzyme Kinetics and Mechanism. Part A. Methods in Enzymology. Vol. 63 (D.L. Purich, Ed.) p. 234. Academic Press, New York.
Lineweaver, H., and Burk, D. (1934) J. Am. Chem. Soc. 56, 658.
Lumry, R., and Rajender, S. (1970) Biopolymers 9, 1125.
Matthews, D.A., Alden, R.A., Birktoft, J.J., Freer, S.T., and Kraut, J. (1977) J. Biol. Chem. 252, 8875.
Miles, J.L., Robinson, D.A., and Canady, W.J. (1963) J. Biol. Chem. 238, 2932.
Oosterbaan, R.A. et al. (1983) to be published.
Page, M.I., and Jencks, W.P. (1971) Proc. Natl. Acad. Sci. (USA) 68, 1678.
Rajender, S., Han, M. and Lumry, R. (1970) J. Am. Chem. Soc. 92, 1378.
Rörsch, A., Berends, F., Bartlema, H.C., and Stevens, W.F. (1971) Proc. Koninkl. Nederl. Akademie van Wetenschappen, Series C, vol. 74, No. 2, 132.
Sigler, P.B., Blow, D.M., Matthews, B.W., and Henderson, R. (1968) J. Mol. Biol. 35, 143.
Steitz, T.A., Henderson, R., and Blow, D.M. (1969) J. Mol. Biol. 46, 337.
Tanford, C. (1973) The Hydrophobic Effect: Formation of Micelles and Biological Membranes, J. Wiley and Sons, New York.
Tipton, K.F., and Dixon, H.B.F. (1979) in Enzyme Kinetics and Mechanism. Part A. Methods in Enzymology. Vol. 63 (D.L. Purich, Ed.) p. 183. Academic Press, New York.
Van der Drift, A.C.M. (1981[a]) Zweites deutsch-niederländisches Symposium "Schutz vor hochtoxischen Substanzen" p. 347, TNO, Rijswijk.
Van der Drift, A.C.M., Beck, H.C., Dekker, W.H., Hulst, A.H., and Wils, E.R.J. (1983[a]) This Thesis, Chapter 6; to be submitted for publication.
Van der Drift, A.C.M., Moes, G.W.H., Van der Drift, E., and Rousseeuw, B.A.C. (1983[b]) This Thesis, Chapter 5; to be submitted for publication.
Van der Drift, A.C.M., Roos, A.L.M., and Moes, G.W.H. (1983[c]) This Thesis, Chapter 2; to be submitted for publication.
Van der Drift, A.C.M., Rousseeuw, B.A.C., and Van der Drift, E. (1981[b]) Bull. Magn. Res. 2, 208.
Wallace, R.A., Kurtz, A.N., and Niemann, C. (1963) Biochemistry 2, 824.
Wedler, F.C., Uretsky, L.S., McClune, G., and Cencula, J. (1975) Arch. Biochem. Biophys. 170, 476.
Westley, J. (1969) Enzymic Catalysis, Harper and Row, New York.
Wold, F. (1971) Macromolecules: Structure and Function, Prentice Hall, Inc., Englewood Cliffs, N.J..

CHAPTER 5

COMPARISON OF THE ACTIVE SITES OF ATROPINESTERASE AND SOME SERINE PROTEASES BY SPIN LABELLING

ABSTRACT: The side chain of the serine in the active centre of the hydrolases atropinesterase from Pseudomonas putida PMBL-1 (AtrE), α-chymotrypsin (Chymo) and subtilisin A (Sub) was specifically labelled with a paramagnetic reporter group. Two groups of different size were used (label I or II, respectively) by sulphonylation with N-(3-fluorosulphonylphenyl)-2,2,5,5-tetramethylpyrroline-1-oxyl-3-carboxamide or 2-N-(6-fluorosulphonylnaphthyl)-2,2,5,5-tetramethylpyrroline-1-oxyl-3-carboxamide. ESR spectrometry was applied on the labelled proteins to compare the environment of the active serine in AtrE with that in the well-known structures of Chymo and Sub.

ESR spectra of labelled enzymes in 10 mM phosphate buffer, pH=7.4, were measured at temperatures between 133 K and 298 K by using a home-built spectrometer operating in the absorption mode at 10 kHz field modulation. The spectra, in particular those at 276 K - 298 K, were analysed by computer simulation of the overall line shape according to the methods developed by Freed and coworkers, based on eigenfunction expansion.

In the case of AtrE for both labels the best agreement between experimental and simulated solution spectra was obtained with only one mobility component showing anisotropic, axially symmetric reorientation according to the Egelstaff jump diffusion model. The axis of preferential reorientation was found to lie in the XZ-plane at a polar angle of about 30° with the X-axis. The corresponding rotational correlation time ($\tau_{\parallel}$) did not show appreciable viscosity (η)/temperature (T) dependence but had a constant value of 4.4 and 2.2 ns for label I and II, respectively. The rotational correlation time associated with rotation around the axes perpendicular to that of preferential reorientation ($\tau_{\perp}$) showed the usual η/T dependence and had a value of 22.0 ns at 276 K for both labels. The above results strongly suggest that in AtrE both apolar reporter groups reside in a pocket near the active serine.

Contrary to the situation in AtrE, the overall mobility of the -N-O$^{\cdot}$ fragments in Chymo and Sub was found to result from contributions of at least two distinct motional states, a strongly and a weakly immobilized. In going from label I to II the relative contribution of the latter state increases at the expense of that of the former. This is ascribed to an equilibrium between a relatively free state of the aromatic cores and a firmly bound position in the specificity pocket of these proteases.

The apparently more rigorous embedding of the spin labels in the enzyme structure of AtrE suggests that the size of the apolar binding pocket in the active-centre region of this esterase allows a deeper penetration of the aromatic portions of the labels than is possible for the specificity pocket of Chymo or Sub.

INTRODUCTION

Stable nitroxide radicals (Cf. Rozantsev, 1970) have been widely applied as spin labels in enzymology (Berliner, 1974, 1978; Morrisett, 1976) and in biomedical research (Chignell, 1979; Piette and Hsia, 1979) because they have proven to be useful reporter groups for probing the structure of specific sites in a biomolecular environment. Their ESR spectra reflect both the effect of interactions between label and biomolecule on the mobility of the -N-O· fragment and the polarity of the direct environment (Berliner, 1974, 1978; Griffith et al., 1974; Jost and Griffith, 1978). This information may supplement the results obtained by other methods such as X-ray diffraction, NMR and fluorescence spectrometry.

Serine proteases may be irreversibly inhibited by different alkyl and aromatic sulphonyl fluorides by sulphonylation of their active serine (Fahrney and Gold, 1963; Sigler et al., 1966; Wright et al., 1969). With spin-labelled phenylsulphonyl fluorides, analogues of the inhibitor tosyl fluoride, structurally different nitroxide spin labels may be specifically attached to the active serines of both α-chymotrypsin and trypsin (Berliner and Wong, 1974; Wong et al., 1974). This approach allows a more detailed comparison of the spatial structure of the environment of this amino-acid residu in different enzymes than the usual one with only one spin label.

Atropinesterase from Pseudomonas putida strain L of the biotype A (strain PMBL-1) is a serine esterase which specifically catalyses the hydrolysis of (-)-atropine to (-)-tropic acid and tropine (Berends et al., 1967; Stevens, 1969; Rörsch et al., 1971; Hessing, 1983). Within the scope of the physico-chemical characterization of this enzyme by means of various techniques (Van der Drift et al., 1983 [a,b]; Van der Drift and Sluyter, 1983[c]), the environment of its active serine (at position 110) has been compared with that of the well-known serine proteases α-chymotrypsin and subtilisin A by using nitroxide spin labels of different size as reporter groups. All three enzymes are irreversibly inhibited by spin-labelled phenylsulphonyl fluoride (I) and

spin-labelled naphthylsulphonyl fluoride (II) (Figure 1) by specific sulphonylation of the side chain of the active serine. Label I was used to allow comparison with other investigations (Berliner and Wong, 1974) whereas label II was suggested by fluorescence investigations on these enzymes labelled with a dansyl group (Van der Drift et al., 1983[b]). Contrary to related work on chymotrypsin and trypsin (Berliner and Wong, 1974) detailed spectrum simulation by using the rigorous theory for slowly tumbling spin labels (Freed et al., 1971; Freed, 1972, 1976) has been attempted for the interpretation of the experimental ESR spectra. This quantitative approach allows a more detailed characterization of the active-site region of these enzymes than the qualitative methods used by Hoff et al. (1971).

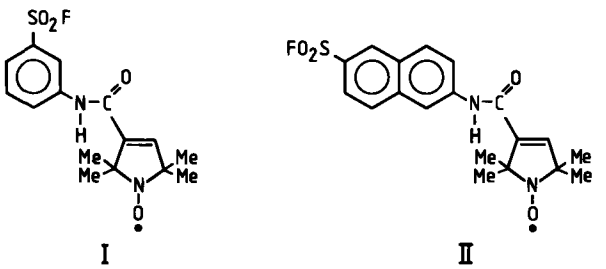

FIGURE 1: Molecular structures of N-(3-fluorosulphonylphenyl)-2,2,5,5-tetramethylpyrroline-1-oxyl-3-carboxamide (Label I) and 2-N-(6-fluorosulphonylnaphthyl)-2,2,5,5-tetramethylpyrroline-1-oxyl-3-carboxamide (Label II).

MATERIALS AND METHODS

a. Enzymes

Salt-free α-chymotrypsin (M = 24,800; EC 3.4.21.1) from bovine pancreas (3 x crystallized and lyophilized) was purchased from Sigma Chemical Company (Lot C-4129). Dialysed and lyophilized subtilisin A (M = 27,300; EC 3.4.21.14) was obtained from NOVO Industri A/S (Batches 73-1, A 8003-75, A 9001-75). Atropinesterase (M = 30,300) was isolated from Pseudomonas putida PMBL-1 and purified according to the procedure of Rörsch et al. (1971) as modified by Oosterbaan et al.

(1983). Enzyme activities were determined by acidimetric titration according to the pH-stat method described elsewhere (Van der Drift et al., 1983[b]) with N-acetyl-L-tyrosine ethyl ester (Merck) as a substrate for α-chymotrypsin and subtilisin A and with (-)-atropine sulphate (Nutritional Biochemicals Corporation) for atropinesterase. Total enzyme concentrations were determined spectrophotometrically at 280 nm with $E_{280}^{0.1\%}$ = 2.04, 0.96 and 1.85 for α-chymotrypsin (Chymo), subtilisin A (Sub) and atropinesterase (AtrE), respectively (Cf. Van der Drift et al., 1983[b]).

b. Nitroxide Spin Labels

The fluorosulphonyl radicals N-(3-fluorosulphonylphenyl)-2,2,5,5-tetramethylpyrroline-1-oxyl-3-carboxamide and 2-N-(6-fluorosulphonylnaphthyl)-2,2,5,5-tetramethylpyrroline-1-oxyl-3-carboxamide (Figure 1) were synthesized as described in the Appendix. 10 mM solutions in dry acetone were used for the inhibition. These solutions were kept at 277 K in the dark. All commercially available chemicals used were reagent grade, unless stated otherwise.

c. Preparation of Spin-labelled Enzymes

To 1.0. ml of an enzyme solution (about 0.1 mM in 10 mM sodium phosphate buffer, pH=7.4, containing 0.1 mM sodium azide to prevent growth of bacteria) 35 µl of a solution of radical I or II was added. The mixture was incubated at room temperature in the dark for 12-16 h, until inhibition was complete (residual enzyme activity less than 1% of the original activity). Since the solubility of the radicals, in particular of label II, in water was very limited ($\leq$ 0.3 mM) some precipitate of excess radical was always present during incubation. After inhibition this precipitate was removed by centrifugation. Subsequently the protein solution was dialysed for 48-72 h at 277 K in the dark against frequently renewed 150 ml of phosphate buffer. Increase in enzyme activity during dialysis was negligible. In order to check homogeneity, solutions of labelled enzymes were routinely subjected to gel filtration at 277 K on a Sephadex Superfine G-50 column. All enzy-

mes were eluted as a single peak as measured by absorbance at 280 nm. Spectroscopically no difference was observed between the various fractions of the protein peak. Protein solutions were kept in the dark and investigated by ESR as soon as possible after completion of the dialysis in order to minimize contamination by any release of spin label (see below). To improve the signal-to-noise ratio in some cases solutions were concentrated at 277 K by means of Minicon Macrosolute concentrators, type A 25 (Amicon). Protein solutions were 0.05 - 0.2 mM.

d. ESR Spectrometry

Electron spin resonance measurements of the enzyme preparations were taken at X-band (9 GHz) on a home-built spectrometer (Mehlkopf, 1970; Mehlkopf et al., 1972) operating in the absorption mode at 10 kHz field modulation. The microwave field was kept below the level of observable saturation. Similarly the amplitude of the field modulation was small compared with the line widths in order to prevent spectrum distortion. Samples were contained in thin pyrex glass capillaries (1 mm inner diameter) centred along the symmetry axis of the cylindrical TE 011 cavity. Measurements were done at various temperatures ($\pm$ 0.5 K) in the range 133 K - 298 K.

e. Spectral Analysis

Spectral analysis was achieved by computer simulation of the overall line shape according to the methods developed by Freed and co-workers (Freed et al., 1971; Freed, 1972, 1976), based on eigenfunction expansion. For that purpose the principal values of the nuclear hyperfine coupling tensor ($\bar{\bar{A}}$) and the Zeeman interaction tensor ($\bar{\bar{g}}$), which in principle can be obtained from an analysis of the rigid limit spectra, have to be known. For labels I and II these values are not available in the literature, whereas the resolution in the centre of the rigid limit spectra is too small to allow an accurate direct determination of the X- and Y-components of these tensors. An example of the rigid limit spectra of the labelled enzymes at low temperatures is given in Figure 2. In the present analysis the accurate principal values of $\bar{\bar{g}}$ determined for di-t-butyl nitroxide (DTBN; Libertini and

FIGURE 2: Comparison between the experimental rigid limit spectrum of label II bound to subtilisin (Sub) at 213 K (———) and the corresponding simulated spectrum (.....). $2A_{zz}$ equals the distance between the outer extrema. Best agreement was obtained with α = 0.3 mT and β = 0.05 mT for the angle-dependent residual line width.

TABLE I: Principal values of the Zeeman interaction tensor ($\bar{\bar{g}}$) and the nuclear hyperfine coupling tensor ($\bar{\bar{A}}$) used in the present analysis.

Tensor		X-axis	Y-axis	Z-axis
$\bar{\bar{g}}$	(1)	2.0088	2.0062	2.0027
$\bar{\bar{A}}$ (mT)	(2)	0.623	0.623	3.596

(1) Obtained from Libertini and Griffith (1971).

(2) Obtained from rigid limit and solution spectra.

Griffith, 1970) were used for both spin labels (Table I). In single host crystals spectra of DTBN were reported to be very similar to those of 2,2,5,5-tetramethyl-3-oxopyrrolidine-1-oxyl (Griffith et al., 1965), which in turn are considered to be very similar to those of the pyrrolinyl spin labels. It is assumed that in solution the similarity between DBTN and the pyrrolinyl spin labels is unaltered.

The value of A_{zz} was obtained directly from the distance between the extrema at low and high magnetic field in the rigid limit spectrum (Figure 2). Since in free nitroxide radicals $\bar{\bar{A}}$ is found to be almost axially symmetric around the Z-axis, the values of A_{xx} and A_{yy} were assumed to be equal and were obtained from the isotropic hyperfine splitting $a_{iso} = (A_{xx} + A_{yy} + A_{zz})/3 = 1.614$ mT, observed in buffer, and the value of A_{zz}. These principal values of $\bar{\bar{A}}$ are also listed in Table I. Within experimental accuracy no differences were found between the two labels bound to the three enzymes. For free nitroxide radicals the principal axes of $\bar{\bar{A}}$ and $\bar{\bar{g}}$ can be assumed to coincide (Libertini and Griffith, 1970).

In order to verify the above assumptions, the experimental spectrum in Figure 2 has been reconstructed via the program of Polnaszek (1976) by using the values of Table I. This simulation required an angle-dependent residual line width $\alpha + \beta \cos^2\theta$, where θ is the polar angle between the external magnetic field and the principal Z-axes of $\bar{\bar{A}}$ and $\bar{\bar{g}}$ and α and β are constants to be assessed. The best agreement between experimental and simulated spectrum was obtained with $\alpha = 0.3$ mT and $\beta = 0.05$ mT. Figure 2 shows that agreement is satisfactory.

Variables related to the reorientation of the -N-O˙ fragment which remain to be assessed via spectrum simulation are: principal values of the rotational diffusion tensor $\bar{\bar{R}}$ (or of the corresponding correlation times τ), including the position of its principal axes in the molecular frame, the reorientation model, e.g. Brownian, free or jump diffusion and the rotationally invariant line width (Cf. Bruno, 1973; Freed, 1976; Polnaszek, 1976). Unless stated otherwise, the latter parameter could be set to zero. Figure 3 shows the molecular reference frame as usually defined for nitroxide radicals and to which the components of $\bar{\bar{A}}$ and $\bar{\bar{g}}$ are related (Smith, 1972).

The computer program used for slowly tumbling simulations (Polnaszek, 1982) was a more rapid and corrected version of that given elsewhere (Polnaszek, 1976) and is confined to axially symmetric rotational diffusion with the option of non-coinciding Z-axes for $\bar{\bar{R}}$ and for $\bar{\bar{A}}$ and $\bar{\bar{g}}$.

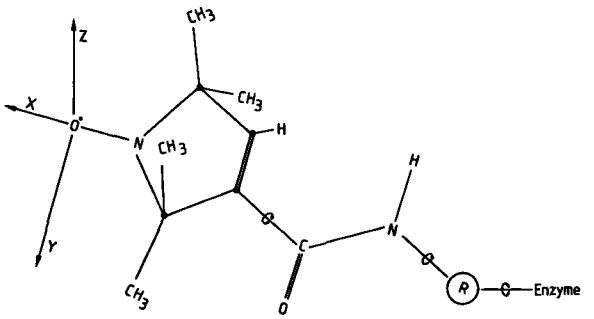

FIGURE 3: Molecular reference frame as defined for nitroxide radicals and the internal rotations around atomic bonds in the side chain connecting the -N-O· fragment with the enzyme. R = sulphonylated aromatic moiety. The molecular Z-axis is perpendicular to the pyrrolinyl ring.

RESULTS

ESR spectra of the labelled enzymes at 276 K and 298 K are shown in Figures 4 and 5, respectively. When the enzymes were inhibited with diisopropyl phosphorofluoridate (DFP), i.e. when a diisopropyl phosphoryl group was covalently attached to the active serine (Cf. Baker, 1975), before treatment with spin label no ESR signal was observed. In view of this and investigations on specific sulphonylation of serine hydrolases (Fahrney and Gold, 1963; Gold and Fahrney, 1964; Gold, 1965; Cardinaud and Baker, 1970) it may be assumed that after treatment with spin label the enzyme molecule contains just one spin probe bound to the active serine.

The spectra with label I invariably revealed the presence of unbound label. The concentration of this rapidly reorienting component showed a gradual increase with time and temperature and was reduced temporarily by dialysis at 277 K. This phenomenon was also reported by

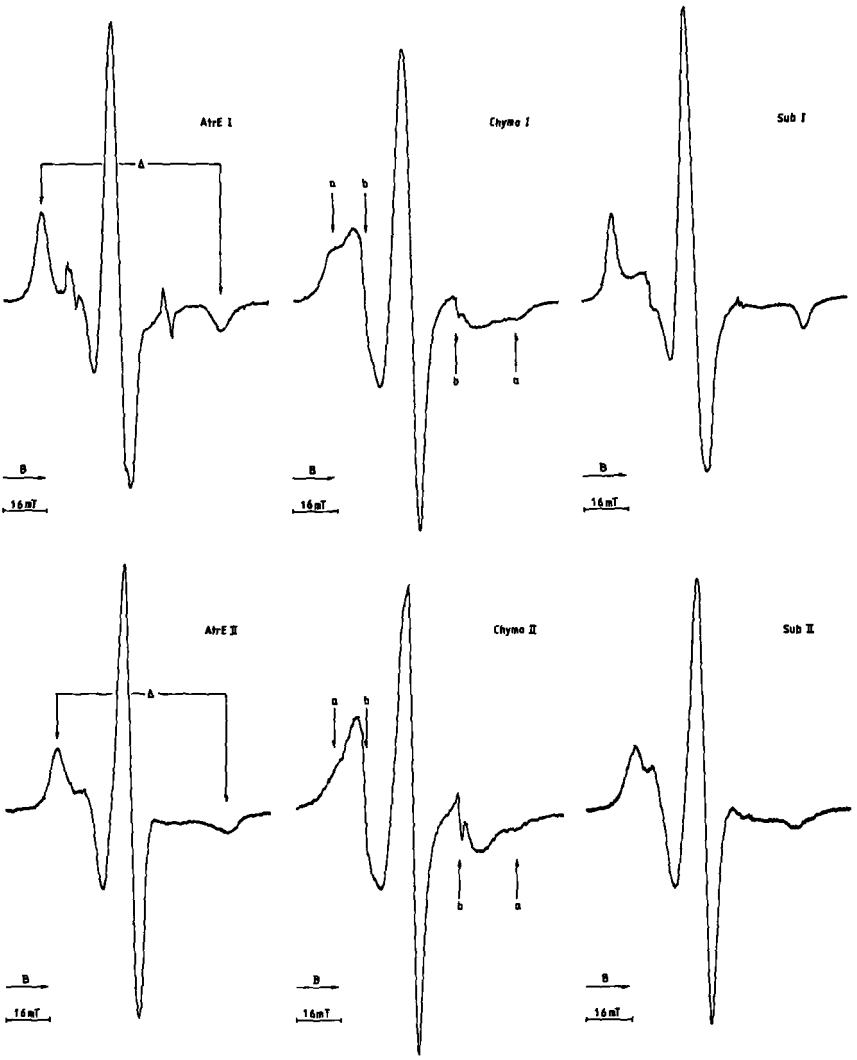

FIGURE 4: Experimental spectra of atropinesterase (AtrE), α-chymotrypsin (Chymo) and subtilisin A (Sub) with label I (upper row) and II at 276 K in 10 mM phosphate buffer, pH = 7.4. Δ = distance between the outer extrema. Outer extrema of the slow and more rapid motional components discernible in the spectra of Chymo are indicated by a and b, respectively. The very sharp satellite lines on either side of the central line are due to unbound label.

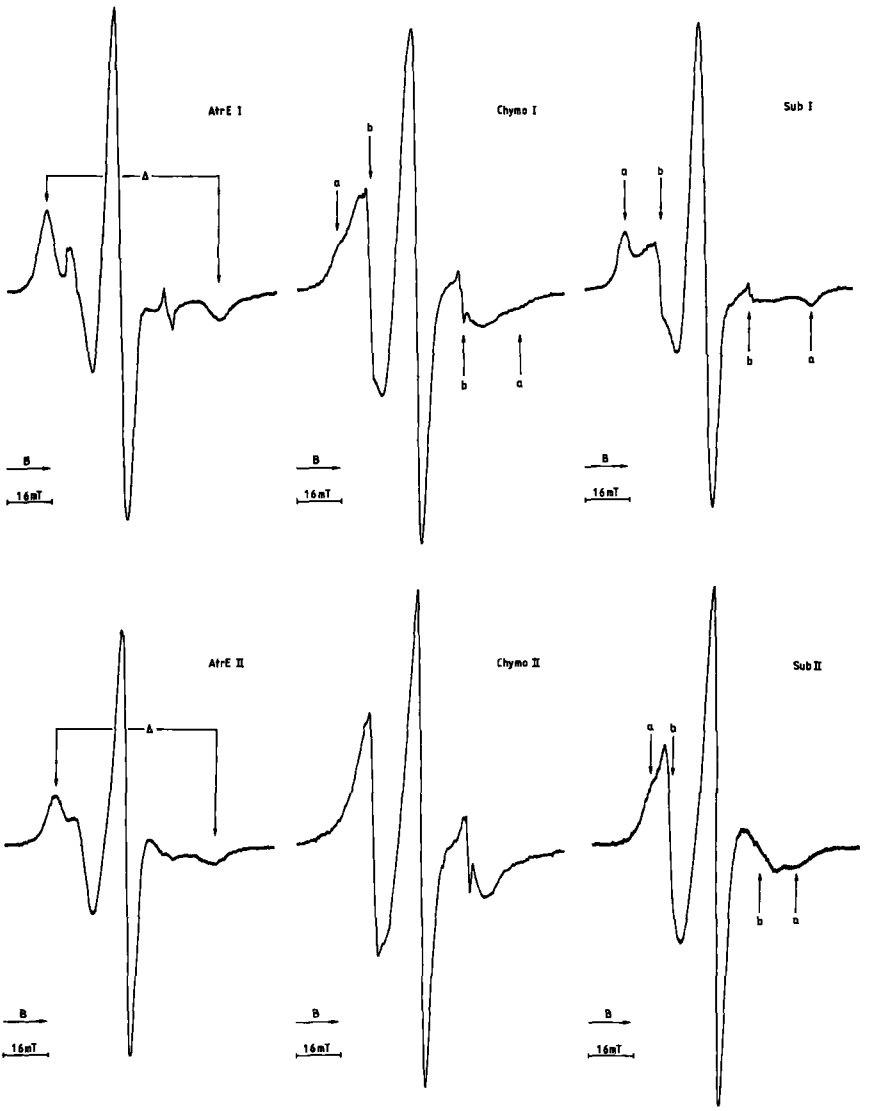

FIGURE 5: Experimental spectra of atropinesterase (AtrE), α-chymotrypsin (Chymo) and subtilisin A (Sub) with label I (upper row) and II at 298 K in 10 mM phosphate buffer, pH = 7.4. Δ = distance between the outer extrema. Outer extrema of the slow and more rapid components discernible in the spectra of Chymo and Sub are indicated by a and b, respectively. The very sharp satellite lines on either side of the central line are due to unbound label.

other investigators and can be ascribed to either hydrolytic desulphonylation of the reporter group from the enzyme (Fahrney and Gold, 1963; Gold, 1965) or to intramolecular hydrolysis of the label (Wong et al., 1974). By measuring the ESR spectra as soon as possible after dialysis at 277 K contamination was kept small: for AtrE maximally 1% of the overall ESR absorption, for the other enzymes somewhat more. Label II was found to be released to a lesser extent at all temperatures.

In general, the spectra of AtrE, Chymo and Sub at 276 K (Figure 4) and 298 K (Figure 5) clearly showed a distance Δ between the extrema at low and high magnetic field which exceeded the value of $2a_{iso}$ = 3.23 mT appreciably (Table II). This points to the presence of labelled enzyme molecules with the mobility of the -N-O$^{\cdot}$ fragment in the slow motional region. In addition most spectra of Chymo (Figures 4 and 5) suggested the presence of at least one more rapidly reorienting component with $\Delta \approx 2a_{iso}$. For Sub the spectral indications for such a mixture of mobility components were hardly observable at 276 K (Figure 4) but obvious at 298 K (Figure 5). The spectra of AtrE are attributable to only one mobility component. For the latter enzyme, as for the slow motional species of Sub, the value of Δ for label I is larger than that for label II (Table II), which indicates that the -N-O$^{\cdot}$ fragments have a different mobility under similar conditions. For Chymo such a difference was not observed at 276 K (Table II). These qualitative characteristics of the experimental solution spectra in terms of one or more components with a characteristic mobility have been analysed in more detail by spectrum simulation.

TABLE II: Distance ($\pm$ s.e.; mT) between outer extrema in solution spectra of various serine hydrolases with label I and II at 276 K and 298 K.

	Label I		Label II	
	276 K	298 K	276 K	298 K
Atropinesterase	6.52 $\pm$ 0.04	6.20 $\pm$ 0.04	6.16 $\pm$ 0.08	5.68 $\pm$ 0.12
α-Chymotrypsin	6.60 $\pm$ 0.12	6.36 $\pm$ 0.32	6.60 $\pm$ 0.32	(1)
Subtilisin	6.92 $\pm$ 0.04	6.68 $\pm$ 0.04	5.72 $\pm$ 0.06	5.33 $\pm$ 0.16

(1) slow motional component not discernible.

a. Reconstruction of the Spectra of Atropinesterase

Detailed reconstruction of the slow motional spectra of labelled AtrE was started by assuming reorientation of a single mobility component by isotropic Brownian rotational diffusion. Simulations of the experimental spectra at 276 K (Figure 6(A,B)) were obtained by adjusting the rotational correlation time τ_R to approximate the line positions as close as possible. The best values of τ_R were 15.0 and 6.7 ns for label I and label II, respectively.

The experimental spectra at 298 K were simulated with τ_R = 7.9 ns for label I and τ_R = 3.5 ns for label II (Figure 6(C,D)). These values were calculated from those at 276 K by imposing the usual viscosity (η) / temperature (T) dependence for isotropic rotational diffusion.

For both labels, but in particular for label II, the simulated overall line shapes in Figure 6 deviate substantially from those of the experimental spectra. Nevertheless, some conclusions relevant for further analysis can be drawn:

1) As it may be assumed that the essential features of the reorientation process are the same for label I and label II, the significantly smaller Δ of label II at 276 K (Table II) is a strong indication that the -N-O$^{\cdot}$ fragment of this larger label has a definite motional freedom relative to the enzyme moiety. This is supported by the comparison of the best value of τ_R of label II with the theoretical lower limits of 16 and 32 ns, respectively, estimated on the basis of the Stokes-Einstein relation (Cf. Carrington and McLachlan, 1967) for an anhydrous monomer or dimer (Cf. Van der Drift and Sluyter, 1983[c]) at this temperature.
2) In contrast to label I, extension of the simulations to 298 K for label II leads to a substantially smaller Δ than experimentally observed (Figure 6(D)). This points to contributions to the orientation of the -N-O$^{\cdot}$ fragment which are not hydrodynamically (η/T) controlled.

These conclusions suggest that the mobility of the -N-O$^{\cdot}$ fragment in label II results from reorientation of the enzyme in solution and from internal rotations around atomic bonds connecting the ESR-sensi-

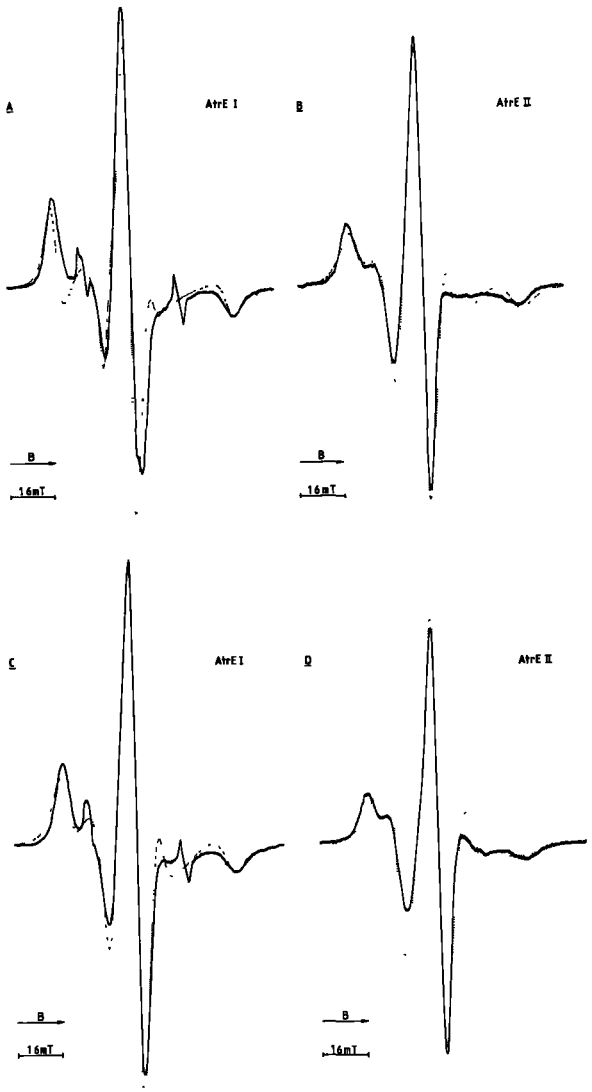

FIGURE 6: Comparison of the experimental solution spectra (———) and corresponding optimized computer simulations (.....) for atropinesterase (AtrE) with label I and II at 276 K (A,B) and 298 K (C,D). Simulations are based on the isotropic Brownian rotational diffusion model. Best values of τ_R at 276 K and 298 K: for label I 15.0 and 7.9 ns, for label II 6.7 and 3.5 ns, respectively.

tive group to the enzyme (Cf. Buchachenko and Wasserman, 1982). Although for label I the evidence of such a composite mobility is less pronounced, the similarity of the molecular structures of both labels (Figure 1) justifies the assumption that this more general mobility concept applies to this label as well. Any difference between comparable spectra of label I and II can then be ascribed to the effect of a different aromatic core on the internal mobility of the side chains. Because of the anisotropic nature of these specific internal rotations (Figure 3), some anisotropy may be anticipated for the composite motion of the -N-O˙ fragment.

A rough test for the validity of the anisotropic model is shown in Figure 7 where simulations for AtrE with label II at 276 K are given, based on axially symmetric Brownian rotational diffusion. In this model the anisotropic mobility is described by two rotational diffusion coefficients, $R_{\parallel}$ and $R_{\perp}$,with $R_{\parallel}$ accounting for preferential reorientation (i.e. $R_{\parallel} > R_{\perp}$) around some axis and $R_{\perp}$ for reorientation around axes perpendicular to this symmetry axis. The corresponding rotational correlation times are defined as $\tau_{\parallel} = 1/6R_{\parallel}$ and $\tau_{\perp} = 1/6R_{\perp}$. In Figure 7 simulations with the axis of preferential reorientation collinear with the molecular X-, Y- or Z-axis (Figure 3) are compared. The anisotropy factor $N = R_{\parallel}/R_{\perp}$ was chosen to be 10 and the individual values of $R_{\parallel}$ and $R_{\perp}$ were adjusted to approximate the experimental line positions as close as possible. Obviously, preferential reorientation around the molecular Y-axis ($\tau_{\parallel}$ = 3.75 ns) leads to less agreement with the experimental spectrum than that around the X- ($\tau_{\parallel}$ = 3.0 ns) or Z-axis ($\tau_{\parallel}$ = 0.6 ns). Preferential reorientation around an axis collinear with the -N-O˙ bond (X-axis: Figure 3) leads to the best reconstruction because in this case the difference between the measured and the simulated absorption next to the high-field side of the central line is minimal, whereas the other parts of the spectrum remain in fair agreement with the experimental line shape. Physically, this outcome is not unreasonable in view of the internal rotational modes of the side chain (Figure 3), the contributions of which to $R_{\parallel}$ will be larger than to $R_{\perp}$. In further refinement of the simulations this result has to be taken into account.

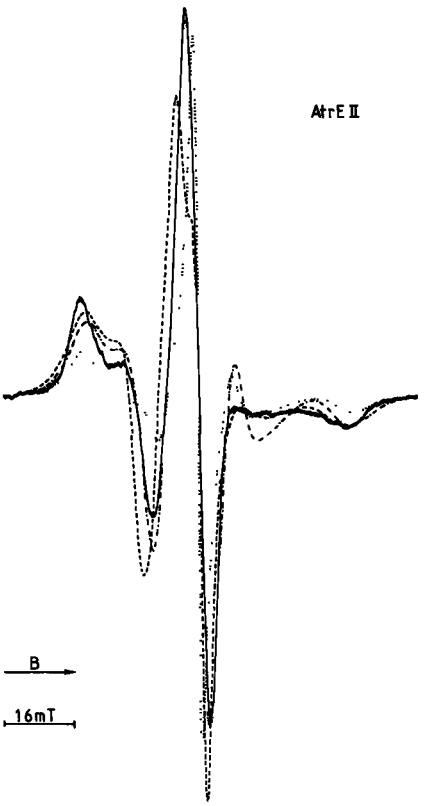

FIGURE 7: Comparison between the experimental (———) and simulated spectrum for atropinesterase (AtrE) with label II at 276 K. Simulations were performed on the basis of anisotropic reorientation (anisotropy factor = 10) according to axially symmetric Brownian rotational diffusion with preferential reorientation around the molecular X- (- - -), Y- (.....) and Z-axis (.-.-.-).

In view of the numerous degrees of motional freedom in the composite reorientation of the -N-O˙ fragments and the limited possibilities to account for this properly in the available theories for label reorientation in the slow motional region, the ultimate reconstructions of the spectra at different temperatures were inevitably approximative and were based on assumptions inferred from the above results:

1) The superposition of two types of motion governing reorientation, i.e. the continuous process of Brownian rotational diffusion of

the enzyme and the jump-like character of the internal rotations around atomic bonds in the side chain, were approximated by a single jump-rotational diffusion process accounting for deviations from the Brownian limit of infinitesimally small jumps (Egelstaff jump diffusion model, Cf. Bruno, 1973; Polnaszek, 1976).

2) The anisotropic reorientation process was assumed to be axially symmetric, i.e. describable by diffusion coefficients $R_{\parallel}$ and $R_{\perp}$.

3) In view of the physical principles underlying the anisotropic reorientation process, $R_{\perp}$ will be mainly determined by the tumbling of the enzyme, i.e. governed by η/T. The preferential reorientation, $R_{\parallel}$, will be mainly determined by the more rapid internal rotations of the side chain, negligibly dependent on η/T but rather on the enzyme structure.

The final reconstructions of the spectra of AtrE under these assumptions yield the results in Figure 8. For 276 K the various parameters were adjusted until the best agreement with the experimental overall line shape was obtained. For both labels the axis of preferential reorientation ($R_{\parallel}$) was found to lie in the molecular XZ-plane at a polar angle of about 30° with the X-axis. The correlation times $\tau_{\parallel}$ and $\tau_{\perp}$ corresponding with the best $R_{\parallel}$ and $R_{\perp}$, respectively, are compiled in Table III. $\tau_{\parallel}$ is larger for label I than for label II whereas $\tau_{\perp}$ is the same for both. The deviation from the Brownian model of infinitesimally small jumps results in a mean jump angle of about 12°.

TABLE III: Values of the rotational correlation times of atropinesterase with label I and II at different temperatures as obtained from optimized simulations according to the anisotropic jump diffusion model. (1)

Correlation times (ns) (2)	Label I		Label II	
	276 K	298 K	276 K	298 K
$\tau_{\parallel}$	4.4	4.4	2.2	2.2
$\tau_{\perp}$	22.0	11.6	22.0	11.6

(1) For details, see text.

(2) $\tau_{\parallel}$ = correlation time of preferential rotation around the symmetry axis, $\tau_{\perp}$ = correlation time of rotation around axes perpendicular to the symmetry axis.

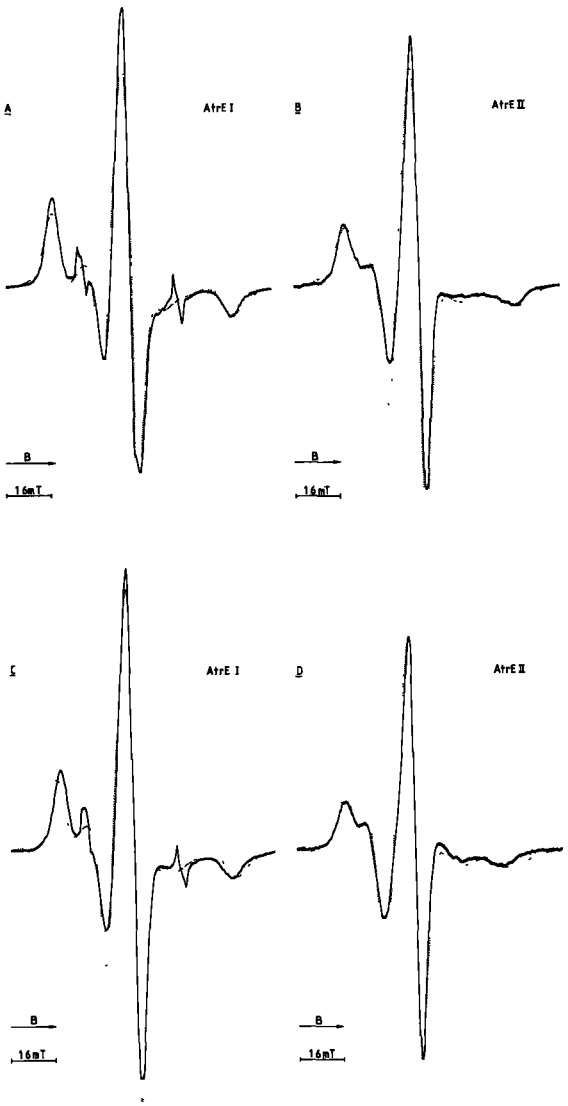

FIGURE 8: Comparison between experimental solution spectra (———) and optimized simulations (.....) for atropinesterase (AtrE) with label I and II at 276 K (A,B) and 298 K (C,D). Simulations are based on the anisotropic jump diffusion model as described in the text.

Reconstructions at 298 K were performed similarly by applying the third assumption above. Since no appreciable conformational change of the active-site region is expected to occur upon increasing the temperature from 276 K to 298 K, the polar angle and the mean jump angle were taken equal to those at 276 K. Restricted variation of $R_{\parallel}$, $R_{\perp}$ and the polar angle did not improve the results but rather worsened the agreement, which supports the assumptions underlying the present approach.

Notwithstanding the inevitably approximative character of this approach and the obvious imperfections in the agreement between reconstructed and experimental spectra in Figure 8, the anisotropic reorientation model with a different temperature dependence for $R_{\parallel}$ and $R_{\perp}$ is a substantial improvement in comparison with the isotropic model (Figure 6), particularly for label II. This is stressed even more by $\tau_1 = 22$ ns at 276 K for both labels, which is in the range of the theoretical lower limits of 16 and 32 ns for AtrE as either an anhydrous monomer or dimer. This value is smaller than the overall correlation time of 37 ns estimated in a rather qualitative way for AtrE inhibited with 1-oxyl-2,2,6,6-tetramethyl-4-piperidinyl methylphosphonofluoridate, assuming isotropic reorientation (Hoff et al., 1971).

b. Reconstruction of the Spectra of α-Chymotrypsin and Subtilisin A.

A similar mobility analysis of the spectra of Chymo and Sub is practically impossible because the important regions on both sides of the central line, at a distance of about 1.3 mT, are largely obscured by overlap with the spectra resulting from other mobility components. However, less detailed line-shape simulations are feasible which are consistent with the presence of a mixture of components with different mobilities. This is illustrated in Figure 9 which shows simulations for Chymo based on Brownian rotational diffusion for a mixture of two components. With an agreement comparable to that obtained for AtrE it was possible to simulate the spectra of both labels with the same two mobility components in different proportions. The best reconstructions were obtained with anisotropic reorientation of the -N-O$^{\cdot}$ fragment with preferential reorientation around the molecular X-axis for the

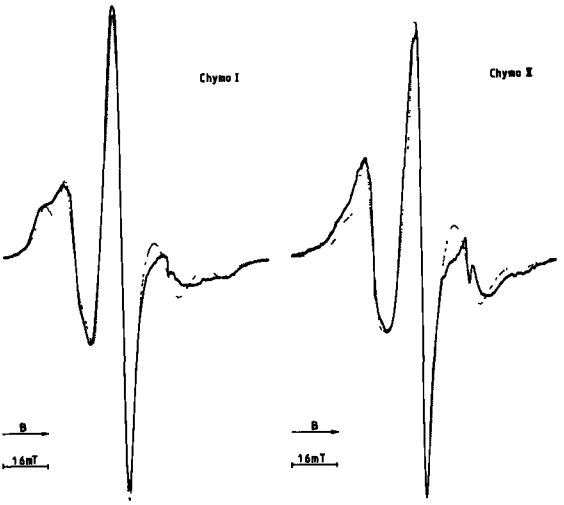

FIGURE 9: Comparison of the experimental solution spectra (———) and corresponding simulations (.....) for α-chymotrypsin (Chymo) with label I and II at 276 K. Simulations are based on the presence of a mixture of two mobility components, the ratio of which is different for Chymo I and Chymo II, respectively.

slowest component ($\tau_{\parallel}$ = 4 ns; $\tau_{\perp}$ = 40 ns; rotationally independent line width 0.05 mT) and around the molecular Y-axis for the more rapidly reorienting component ($\tau_{\parallel}$ = 0.75 ns; $\tau_{\perp}$ = 7.5 ns; rotationally independent line width 0.15 mT). The fraction of the slowest component was about 0.55 for label I and 0.30 for label II. In view of the uncertainties about the number of mobility components and the type of reorientation process, these simulations can only serve as a demonstration of the principle of superposition. No physical meaning should be attributed to the characteristics of the single components.

The spectra of Sub at higher temperatures (Figure 5), which clearly indicate the presence of different mobility components, can also be analysed with Brownian rotational diffusion of two single mobility components showing anisotropic reorientation of the -N-O˙ fragment. From a limited number of simulations in the case of Sub with label I at 298 K the fraction of the slower component was about 0.8. For Sub with label II this fraction was estimated at 0.3 because of the great similarity of this spectrum with that of Chymo with label II

at 276 K. In contrast to the situation in Chymo the mobility of the slower component of label I bound to Sub was different from that of label II as can be concluded from the different value of Δ (Table II). In this respect Sub resembles AtrE more than Chymo.

DISCUSSION

The results obtained by reconstructions according to the above model of anisotropic motion with some jump diffusion character and separate contributions of enzyme tumbling and atomic bond rotations to $R_\perp$ and $R_\parallel$, e.g. the values of $\tau_\perp$ and $\tau_\parallel$ at different temperatures (Table III), strongly suggest that in AtrE at least the apolar aromatic portions of the spin labels are situated in a pocket-like structure near the active serine. The values of $\tau_\parallel$ (Table III) indicate that the -N-O˙ fragment of label II has more degrees of freedom for internal rotations of the side chain and thus a higher mobility than that of the smaller label I; so, most likely, it protrudes farther outside the protein structure.

Evidence for an apolar pocket-like structure near the active serine in AtrE was also obtained from fluorescence data on a dansyl group bound to the active serine (Van der Drift et al., 1983[b]). Also, the large downfield shift of the ^{31}P resonance observed by NMR upon ageing of AtrE phosphorylated with diisopropyl phosphorofluoridate points to a crevice-like structure close to the active serine (Van der Drift et al., 1983[a]). In this respect AtrE resembles Chymo and Sub for which X-ray diffraction studies revealed a so-called primary substrate specificity pocket at the acyl-group side, adjacent to the active serine, which preferentially binds the apolar side chain of the amino acid residue preceding the hydrolysable bond of the substrate (Cf. Blow, 1974; Kraut, 1977).

Notwithstanding the fact that the results for Chymo and Sub are quantitatively less interpretable, they do show that in these enzymes - in contrast to AtrE - the -N-O˙ fragment may be in at least two distinct motional states: a strongly immobilized and a rather mobile (weakly immobilized) one. As only one spin label is present per enzyme

molecule specifically bound to the active serine, this indicates that the mobility of the -N-O˙ fragment is subjected to an equilibrium between different conformational states. Data obtained by others with Chymo and trypsin (Berliner and Wong, 1974) also indicated that there may be several interconvertible modes of immobilizing a spin label at the active serine. For labels I and II the mobility of the -N-O˙ fragment in the strongly immobilized state is comparable to that found with AtrE. This state appears to be favoured when the size of the aromatic portion of the side chain is smaller. Therefore, it may reflect a kind of incorporation of the side chain into the enzyme structure.

Due to the composite nature of the reorientation of the -N-O˙ fragment any difference between spectra of label I and II can be ascribed to different internal mobilities of the side chain. However, the equality of Δ for the strongly immobilized component of the labels when bound to Chymo (Table II) points to a more or less complete immobilization of the aromatic parts of the side chains. For Sub, Δ of the slowest component of label I is larger than that of label II (Table II), indicating that the naphthyl core of the latter is appreciably less tightly bound to the enzyme than the phenyl core of label I, which allows more degrees of freedom for internal rotations of the side chain to be effective in the reorientation of the -N-O˙ fragment.

These differences between Chymo and Sub can be understood in the light of the difference in structure of the substrate binding site of these enzymes. In Chymo this hydrophobic site is a geometrically well-defined slit-shaped pocket, consisting of two planar and parallel sides between which only planar, preferentially aromatic groups of particular size and shape can be sandwiched; for Sub it is a less well-defined shallow crevice being planar only on one side and irregular on the other, which, therefore, imposes less stringent geometrical requirements on size and shape of the interacting group (Kraut et al., 1971; Robertus et al., 1972; Blow, 1974). For the strongly immobilized fractions of Chymo and Sub with label I or II, the plane aromatic portion of the side chain will, at least partly, be wedged in the binding pocket. In Chymo this interaction will leave at most a few degrees of

freedom and thus lead to a rather complete immobilization of that section of the side chain for both labels. On the other hand, the geometry of the pocket in Sub will allow the naphthyl group somewhat more motional freedom than the smaller phenyl core.

According to this point of view the occurrence of strongly and weakly immobilized fractions for Chymo and Sub labelled with I or II may be traced back to an equilibrium between free and specifically bound aromatic cores at the substrate specificity pocket. This is a more specific model than that formulated thus far (Berliner and Wong, 1974). The increase in the strongly immobilized fraction of label I and several other labels in Chymo upon addition of indole at pH=3.5 observed by Berliner and Wong (1974) might therefore point to a decreased mobility of the aromatic core due to increased binding in the specificity pocket rather than to a displacement of the label to another stronger binding site at the protein surface near the active serine (Berliner and Wong, 1974).

Apparently, the embedding of the spin label in the enzyme structure is much more rigorous in AtrE than in Chymo and Sub as a more rapidly reorienting component does not occur in AtrE. The better fit in the AtrE structure suggests a deeper penetration of the aromatic portions of the labels into the binding pocket of AtrE than in that of the other enzymes. This is consistent with results of a comparative study of these enzymes labelled with a fluorescent inhibitor (Van der Drift et al., 1983). The difference may be ascribed to larger dimensions of the binding pocket in AtrE, e.g. a greater depth and/or width. In AtrE the pocket is presumably deeper than in Sub because of the shallow nature of the primary substrate binding site in the latter. As in Sub, however, immobilization of the naphthyl core in AtrE is less complete than that of the phenyl core, whereas in Chymo such a difference between labels I and II does not exist. This indicates that, similar to the situation in Sub, the width of the binding pocket in AtrE may be larger than that of the slit-shaped pocket in Chymo.

The indications of a pocket-like binding site in AtrE near the active serine, in combination with those for an oxy-anion hole and a

charge-relay system (Van der Drift et al., 1983[a], 1983[b]) point to a close structural resemblance of the active-site regions of this esterase and proteases of the prothrombin-related and the subtilisin superfamilies (Cf. Kraut, 1977). This indicates a similar mechanism of catalysis by these enzymes. In analogy with other serine hydrolases, it is therefore expected that the tropic acid moiety in the substrate (-)-atropine requires a specific binding site in AtrE during the acylation step of the hydrolysis of the ester bond. In view of the bulky size of this group and its apolar character, the presence of a large hydrophobic binding pocket adjacent to the active serine in AtrE can thus be understood.

APPENDIX: Syntheses of Spin Labels

a. N-(3-fluorosulphonylphenyl)-2,2,5,5-tetramethylpyrroline-1-oxyl-3-carboxamide (Label I).

Synthesis of this meta-compound was partly based on the procedure of Wong et al. (1974) for the ortho-analogue. 1.84 g (10 mmole) of 3-carboxy-2,2,5,5-tetramethylpyrroline-1-oxyl, prepared according to Rozantsev (1970), was dissolved in a mixture of 30 ml of benzene and 2 ml of pyridine. Dropwise addition of excess thionyl chloride (1 ml) at room temperature resulted in a deep yellow solution and a white precipitate of pyridine-HCl. After stirring for about 30 min at 20 ^{o}C, 2.43 g (13.9 mmole) of m-aminobenzenesulphonyl fluoride, prepared by treating m-aminobenzenesulphonyl fluoride-HCl salt (Aldrich) in tetrahydrofuran with excess pyridine, in 20 ml of benzene was added. Another 2 ml of pyridine was added in order to maintain a basic reaction mixture.

After stirring for 1 h, 200 ml of water was added which resulted in a three-phase system of benzene, water and a precipitate. The latter was collected by filtration, washed with water, dried and redissolved in acetone. The solution was filtered and evaporated to dryness in vacuo. The residue was recrystallized from acetone/water and the

solid material was stirred with 20 ml of boiling toluene. After cooling to room temperature the solid material was collected by filtration. This extraction procedure was repeated 4 times. Yield of the yellowish product: 2.08 g (60%).

Analyses

- m.p. = 218-219 ^{o}C
- Thin-layer chromatography (T.L.C.) was carried out on Merck Silicagel F 254 Fertigplatten with a mixture of ethyl acetate and methylene chloride (50/50 v/v) as the mobile phase. One spot (R_F = 0.70) was detected by fluorescence (excitation at 254 and 360 nm) and iodination. No product was found in benzene or water.
- Characteristic infrared wavenumbers (cm^{-1}): 3370 (-NH); 1672 (C = O); 1424, 1404, 1205 (SO_2); 778 (SF); 750, 690 (m-subst.).
- The mass spectrum (M = 341) was in accordance with the molecular structure of label I.

The above method differs from that of Wong et al. (1974) in that thionyl chloride is used (Cf. Krinitskaya et al., 1966) instead of isobutyl chloroformate. This modification yielded appreciably better results. Moreover, chromatographic purification of the spin label can be omitted since pure products are obtained.

b. 2-N-(6-fluorosulphonylnaphthyl)-2,2,5,5-tetramethylpyrroline-1-oxyl-3-carboxamide (Label II).

Synthesis of label II was analogous to that of label I except that the m-aminobenzenesulphonyl fluoride solution was replaced by 2.25 g (10 mmol) of 2-aminonaphthalene-6-sulphonyl fluoride (see below) in 20 ml of acetone/benzene (50/50 v/v). After stirring for 1 h the mixture was shaken with 400 ml of a saturated sodium bicarbonate solution and the yellow precipitate was collected by filtration and washed with water and benzene. Purification of the product was similar to that of label I by recrystallization from water/acetone and repeated extraction with toluene. Yield: 1.87 g (46%).

Analyses

- m.p. = 233 °C
- T.L.C. was carried out as with label I; R_F = 0.70. No impurities were found.
- Characteristic infrared wavenumbers (cm^{-1}): 3385 (NH), 1677, 1533, 1288 (amide), 1400, 1193 (SO_2).
- The mass spectrum (M = 391) was in accordance with the molecular structure of label II.

2-aminonaphthalene-6-sulphonyl fluoride was prepared (Cf. British patent, 1956) by slowly adding 10 ml (173 mmole) of fluorosulphonic acid (Aldrich) to 7.7 g (34 mmole) of 2-aminonaphthalenesulphonic acid (technical grade, Pfaltz and Bauer). With continuous stirring the mixture was heated to 140-150 °C, allowed to cool slowly to room temperature and then poured onto 200 ml of crushed ice. After melting of the ice the white precipitate was collected by filtration. A second batch of product was obtained by neutralization of the filtrate with solid sodium bicarbonate and filtration of the precipitate. The combined fractions were thoroughly washed on a glass filter with 200 ml of a saturated sodium bicarbonate solution (3 x) and 50 ml of water (3 x) and, finally, recrystallized from acetone/water and dried in a vacuum desiccator. Yield of the white product: 2.43 g (33%).

Analyses

- m.p. = 148 -148.5 °C.
- Elementary analysis: $C_{10}H_8FNO_2S$ M = 225.25.

	Calculated (%)	Found (%)
C	53.22	53.33-53.38
H	3.58	3.47- 3.52
F	8.44	8.42- 8.45
N	6.22	6.19- 6.25
S	14.24	14.23-14.24

- T.L.C. as described above showed one spot, R_F = 0.50 with fluorescence detection (excitation at 254 and 360 nm).
- Characteristic infrared wavenumbers (cm^{-1}): 3475, 3375 (NH_2), 1632 (NH_2 + arom.), 1399 (SO_2 asym. + NH_2), 1192 (SO_2 sym.), 865, 819 (subst. arom.)

REFERENCES

Baker, B.R. (1975) Design of Active-Site-Directed Irreversible Enzyme Inhibitors, Robert E. Krieger Publishing Company, Huntington.

Berends, F., Rörsch, A., and Stevens, W.F. (1967) in Proceedings of the Conference on Structure and Reactions of DFP Sensitive Enzymes (Heilbronn, E., Ed.), p. 45, Försvarets Forskningsanstalt, Stockholm.

Berliner, L.J. (1974) Prog. Bioorg. Chem. 3, 1.

Berliner, L.J. (1978) in Methods in Enzymology Vol. XLIX, Enzyme Structure Part G (Hirs C.H.W., Timasheff S.N., Eds.) p. 418, Academic Press, New York.

Berliner, L.J., and Wong, S.S. (1974) J. Biol. Chem. 249, 1668.

Blow, D.M. (1974), Isr. J. of Chem. 12, 483.

Bruno, G.V. (1973) Ph.D. Thesis, Cornell University.

British patent (1956), No. 819664.

Buchachenko, A.L., and Wasserman, A.M. (1982) Pure and Appl. Chem. 54(2), 507.

Cardinaud, R., and Baker, B.R. (1970), J. Med. Chem. 13, 467.

Carrington, A. and McLachlan, A.D. (1967), Introduction to Magnetic Resonance, Harper and Row, New York.

Chignell, C.F. (1979) in Spin Labeling II. Theory and Applications (Berliner, L.J., Ed.), p. 223, Academic Press, New York.

Fahrney, D.E., and Gold, A.M. (1963) J. Am. Chem. Soc. 85, 997.

Freed, J.H. (1972) in Electron Spin Relaxation in Liquids (Muus, L.T., and Atkins, P.W., Eds.) p. 165, Plenum Press, New York.

Freed, J.H. (1976) in Spin Labeling. Theory and Applications (Berliner, L.J., Ed.), p. 53, Academic Press, New York.

Freed, J.H., Bruno, G.V., and Polnaszek, C.F. (1971) J. Phys. Chem. 75, 3385.

Gold, A.M. (1965) Biochemistry 4, 897.

Gold, A.M., and Fahrney, D.E. (1964) Biochemistry 3, 783.

Griffith, O.H., Cornell, D.W., and McConnell, H.M. (1965) J. Chem. Phys 43, 2909.

Griffith, O.H., Dehlinger, P.J., and Van, S.P. (1974) J. Membr. Biol. 15, 159.

Hessing, J.G.M. (1983) Ph.D. Thesis, University of Leiden.

Hoff, A.J., Oosterbaan, R.A., and Deen, R. (1971) FEBS Lett. 14, 17.

Jost, P.C., and Griffith, O.H. (1978) in Methods in Enzymology Vol. XLIX, Enzyme Structure Part G, (Hirs C.H.W., and Timasheff S.N., Eds.) p. 369, Academic Press, New York.

Kraut, J.(1977) Ann. Rev. Biochem. 46, 331.

Kraut, J. Robertus, J.A., Birktoft, J.J., Alden, R.A., Wilcox, P.E., and Powers, J.C. (1971), Cold. Spring Harbor. Symp. Quant. Biology 36, 117.

Krinitskaya, L.A., Rozantsev, E.G., and Neiman, M.B. (1966), Z. Org. Khimii 2(7), 1301.

Libertini, L.J., and Griffith, O.H. (1970), J. Chem. Phys. 53, 1359.

Mehlkopf, A.F. (1970), Internal Report, Department of Applied Physics, University of Technology, Delft.

Mehlkopf, A.F., Smidt, J., and Tiggelman, T.A. (1972), Rev. Sci. Inst. 43, 693.

Morrisett, J.D. (1976) in Spin Labeling. Theory and Applications (Berliner, L.J., Ed.) p. 273, Academic Press, New York.

Oosterbaan, R.A., et al. (1983) to be published.

Piette, L.H., and Hsia, J.C. (1979) in Spin Labeling II. Theory and Applications (Berliner, L.J., Ed.), p. 247, Academic Press, New York.

Polnaszek, C. (1976), Ph.D. Thesis, Cornell University.

Polnaszek, C. (1982), Personal communication.

Robertus, J.D., Alden, R.A., Birktoft, J.J., Kraut, J. Powers, J.C., and Wilcox, P.E. (1972), Biochemistry 11, 2439.

Rörsch, A., Berends, F., Bartlema, H.C., and Stevens, W.F. (1971), Proc. Koninkl. Nederl. Akademie van Wetenschappen, Series C, 74, No. 2, 132.

Rozantsev, E.G. (1970), Free Nitroxyl Radicals, Plenum Press, New York.

Sigler, P.B., Jeffrey, B.A., Matthews, B.W., Blow, D.M. (1966), J. Mol. Biol. 15, 175.

Smith, I.C.P. (1972) in Biological Applications of Electron Spin Resonance, (Swartz H., Bolton J.R., and Borg D., Eds.) p. 483, Wiley, New York.

Stevens, W.F. (1969), Ph.D. Thesis, University of Leiden.

Van der Drift, A.C.M., Beck, H.C., Dekker, W.H., Hulst, A., and Wils, E.R.J. (1983[a]) This Thesis, Chapter 6; to be submitted for publication.
Van der Drift, A.C.M., Roos, A.L., and Moes, G.W.H. (1983[b]) This Thesis, Chapter 2; to be submitted for publication.
Van der Drift, A.C.M., and Sluyter, W. (1983[c]) This Thesis, Chapter 1; to be submitted for publication.
Wong, S.S., Quiggle, K., Triplett, C., and Berliner, L.J. (1974) J. Biol. Chem. 249, 1678.
Wright, C.S., Alden, R.A., and Kraut, J. (1969) Nature 221, 235.

CHAPTER 6

^{31}P NMR AND MASS SPECTROMETRY OF ATROPINESTERASE AND SOME SERINE PROTEASES PHOSPHORYLATED WITH A TRANSITION-STATE ANALOGUE

ABSTRACT: The side chain of the serine in the active centre of atropinesterase from Pseudomonas putida PMBL-1 (AtrE), α-chymotrypsin (Chymo), subtilisin A (Sub) and of the corresponding serine in the zymogen α-chymotrypsinogen (Chymogen) can be specifically phosphorylated with a diisopropyl phosphoryl (DP) group by incubation with diisopropyl phosphorofluoridate (DFP). In the present investigation the active-site region of DP-AtrE was compared with that of the other DP-proteins by means of ^{31}P NMR and mass spectrometry with special attention to the conversion of the DP-group into a monoisopropyl phosphoryl (MP) group due to "ageing".

^{31}P NMR spectra of DP- and MP-proteins in buffered solutions of various pH's were measured at 4 °C and under different denaturing conditions at 25 °C. To interpret the variations between these spectra, e.g. the variation in chemical shift, the phosphorylated model peptides Gly-Ser(DP) and Gly-Glu-Ser(DP)-Gly-OEt and diisopropyl hydrogen phosphate have been investigated under similar conditions and in other solvents with different hydrogen-bonding capacity.

The increase in the chemical shift (i.e. a downfield displacement of the ^{31}P line in the NMR spectrum) according to a simple titration curve observed for all DP-proteins upon lowering the pH from 8.5 to 5.0 is ascribed to protonation of a histidine residue in the active-centre region which forms a hydrogen bond with the oxygen of a nearby isopropoxy group. The values of the chemical shift in this pH-range show that for AtrE hydrogen bonding at the phosphoryl oxygen dominates the interaction between substituent and protein, whereas for the other DP-proteins non-bonding interactions become more dominant in the sequence Chymogen<Chymo<Sub. From the change in the chemical shift it is concluded that upon ageing of the DP-enzymes there is an increase in the non-bonding interaction of the remaining isopropyl group with the protein in the sequence Chymo<Sub<AtrE.

By using ^{31}P NMR it was demonstrated that DP-AtrE, DP-Chymo and DP-Sub show ageing according to first-order kinetics. From the pH-dependence of the reaction rate constant k_a it appeared that this process is catalysed by the same protonated histidine which is also responsible for the downfield shift in the NMR spectrum of the DP-enzymes. The maximum value of k_a obtained when the histidine is fully protonated (k_a^m) increased in the order Chymo<Sub<AtrE.

Mass-spectrometric analysis of the products resulting from ageing in the presence of $H_2{}^{18}O$ showed that in all cases ageing occurs by C-O fission. During the process both isopropanol and propene are formed. The amount of isopropanol decreased and that

of propene increased in the order Chymo<Sub<AtrE. In view of these data the increase in k_a^m has been interpreted as a shift in the character of ageing from mainly S_N2 for Chymo to considerably S_N1 for AtrE and Sub.

The results indicate that the active-centre region near the serine in AtrE is characterized by the same structural elements that are also found in serine proteases for which they are essential to the hydrolytic activity, i.e. a charge-relay system, an oxy-anion hole and a hydrophobic binding pocket. This suggests that esterolysis by AtrE will proceed according to essentially the same mechanism as proteolysis by Chymo or Sub.

INTRODUCTION

Serine proteases and serine esterases are hydrolases characterized by an extremely nucleophilic serine residue at the active site, which is essential to the catalytic activity. A generally accepted criterion for identification of these enzymes is the inhibition by diisopropyl phosphorofluoridate (DFP) (Hartley, 1960) which results from covalent binding of a diisopropyl phosphoryl (DP) group to the oxygen atom in the side chain of the active serine residue (Schaffer et al., 1953, 1954; Cohen et al., 1955; Oosterbaan et al., 1955).

This selective introduction of a phosphorus-containing substituent at the active site opened the possibility of using ^{31}P NMR spectrometry to study serine hydrolases (Gorenstein and Findlay, 1976; Reeck et al., 1977; Markley, 1979). Since the magnetic properties of a substituted ^{31}P nucleus depend on its electronic configuration as determined by the substituents and their bonding and non-bonding interactions with the immediate environment (Letcher and Van Wazer, 1967; Ionin, 1968; Mavel, 1973), the DP-group may be suitable to compare the structure of the active-site region in different serine hydrolases by means of ^{31}P NMR. Various investigations on DP-serine proteases (Cf. Markley, 1979; Steitz and Shulman, 1982) have already shown that the chemical shift of the ^{31}P nucleus is a sensitive criterion for the detection of variations in the interaction between the DP-group and its environment but the data are still insufficient to allow a detailed correlation between differences in chemical shift and the interactions involved.

There are two other considerations which make the DP-group attractive as a nuclear spin probe in comparative studies on serine hydrolases. Firstly, the catalytic activity of these enzymes towards hydrolysis of peptide or ester bonds is based on their ability to act as a mould for binding and stabilizing the so-called tetrahedral intermediate (Kraut, 1977). In this transition state of the enzyme-substrate complex, the carbonyl carbon of the scissile bond in the substrate has a tetrahedral configuration and is covalently linked to the Oγ of the active serine, while the carbonyl oxygen resides in the "oxy-anion hole" on the enzyme surface, stabilized by hydrogen bonding with the protein (Kraut, 1977). Many inhibitors of serine hydrolases also form tetrahedral adducts which, presumably, closely resemble this transient intermediate (Kraut, 1977). The DP-group is considered to be such a transition-state analogue (Stroud et al., 1974; Kraut, 1977), and thus the magnetic properties of the ^{31}P nucleus may reflect interactions that stabilize the transition-state geometry of the enzyme-substrate complex.

Secondly, phosphorylated serine hydrolases in solution may be converted into a non-reactivatable form by a process called ageing (Cf. Usdin, 1970). As was shown for α-chymotrypsin and butyrylcholinesterase, ageing of DP-enzymes involves the conversion of the tertiary phosphate ester into a secondary ester, i.e. the DP-group loses one isopropyl group and becomes a monoisopropyl phosphoryl (MP) group (Berends, 1964). It has been suggested that elements of the enzyme structure which are responsible for the catalytic activity also play an essential role in ageing (Berends, 1964). Because of its negative charge and its geometry the MP-group may be regarded as an even better transition-state analogue than the DP-group (Kossiakoff and Spencer, 1981). Since alterations in the interactions with the protein resulting from such a change in transition-state analogue will affect the magnetic properties of the ^{31}P nucleus, investigation of this conversion by ^{31}P NMR may give additional information about the various interactions in the transition state and about the role of the structural elements involved in ageing. Besides, investigation of the mechanism by mass-spectrometric characterization of the products form-

ed during ageing may supplement the structural information obtained with ^{31}P NMR.

In previous studies of this series the active-site region of atropinesterase from Pseudomonas putida PMBL-1 was compared with that of α-chymotrypsin and subtilisin A with respect to inhibition kinetics (Van der Drift and Roos, 1983[b]), by fluorescence (Van der Drift et al., 1983[c]) and ESR spectrometry (Van der Drift et al., 1981; 1983[a]). These investigations gave strong indications that some of the structural elements which are known to form the basis of the catalytic activity of chymotrypsin and subtilisin, i.e. a primary substrate binding site and a particular histidine as part of a charge-relay system, are also present in atropinesterase. The subject of the present paper concerns a comparative study of the phosphorylated active sites of these enzymes and of α-chymotrypsinogen, the inactive precursor of α-chymotrypsin, by means of ^{31}P NMR and mass spectrometry. Special attention has been devoted to the conversion of the DP-group into an MP-group due to ageing. The aim was to supplement the previous investigations on the structural resemblance between the active site of atropinesterase and of other serine hydrolases.

MATERIALS AND METHODS

a. Proteins and Model Compounds

Salt-free α-chymotrypsin (Chymo; EC 3.4.21.1) from bovine pancreas (3x crystallized and lyophilized; Lots 58C-8135; 40F-8051; 49C-8015) and salt-free α-chymotrypsinogen A (Chymogen) from bovine pancreas (6x crystallized; type II; Lot 29C-8010) were obtained from Sigma Chemical Company. Dialysed and lyophilized subtilisin A (Sub; EC 3.4.21.14) was purchased from NOVO Industri A/S (Batches 70-4; 73-1; A 8003-75; A 9001-75; A 9005-75). Atropinesterase (AtrE) was obtained from Pseudomonas putida PMBL-1 according to the procedure of Rörsch et al. (1971) as modified by Oosterbaan et al. (1983). Characterization of the enzymes and determination of enzyme activities were performed as described elsewhere (Van der Drift et al., 1983[c]).

The phosphorylated model peptides Gly-Ser(DP) and Gly-Glu-

Ser(DP)-Gly-OEt were kindly provided by Dr. H. Kienhuis (Prins Maurits Laboratory TNO), diisopropyl hydrogen phosphate and diisopropyl phosphorofluoridate (DFP) were obtained from Mr. C. de Borst (Prins Maurits Laboratory TNO).

b. Chemicals

All chemicals were reagent grade and commercially available. Organic solvents (Merck) were distilled shortly before use. Deuterium oxide (D_2O; 99.8% isotopically pure; Uvasol, Merck), $H_2{}^{18}O$ (91% isotopically pure, Ventron), citric acid (Merck), sodium citrate (Merck), Tris (J.T. Baker Chemicals B.V.), urea (Union Chimique Belge, s.a.), sodium dodecyl sulphate (SDS; specially purified for biochemical work, British Drug House), guanidine hydrochloride (GuHCl; Fluka, AG) and 1,4-dithiothreitol (Merck) were used without further purification.

Buffers for calibration of pH meters were obtained from Radiometer A/S and Beckman.

c. Labelling with a DP-Group

Chymo, Chymogen or Sub (30-90 mg) was dissolved in 1 ml of 0.1 M Tris-HCl, pH=7.6, resulting in a protein concentration of 1-3 mM. AtrE solutions of this concentration were prepared at 4 °C from stock solutions of 0.01-0.10 mM active enzyme by concentrating with Amicon magnetically stirred cells (models 202 and 52) equipped with a PM 10 filter, followed by a further concentration with Minicon macrosolute concentrators (Type A-25, Amicon).

To achieve complete inhibition (> 99.9%), 20 µl of 0.5 M DFP in dry, peroxide-free isopropanol was added (final DFP concentration 10 mM) and the mixture was incubated at room temperature for about 6 h or, in the case of AtrE and Chymogen, for 20 h. Non-specific labelling was not observed under these conditions. Sometimes, e.g. at high concentrations of AtrE, a slight precipitate was formed. After inhibition this was removed by centrifugation.

The remaining DFP and its hydrolysis product were removed by dialysis at 4 °C against 140 ml buffer for at least 36 h, under continu-

ous stirring and frequent renewal. Finally, the sample was dialysed against 12 ml of buffer containing about 20% D_2O as internal standard for field-frequency locking. Buffers employed were 0.1 M Tris-HCl pH $\geq$ 7.6 and 0.1 M citric acid-sodium citrate pH < 7.6. Concentrations of phosphorylated proteins were measured by determination of the amount of phosphorus according to a modified method of Gerlach and Deuticke (Gerlach and Deuticke, 1963; Kienhuis and Baar, 1964). To improve the signal-to-noise ratio dialysed protein solutions were sometimes concentrated at 4 °C by means of Minicon macrosolute concentrators (Type A-25, Amicon). Usually, concentrations ranged from 1.5-3.0 mM.

d. Ageing and Denaturation

Unless stated otherwise, 0.5 ml of DP-enzyme was allowed to age at 36 °C in a dialysis tube to remove released low-molecular weight materials. After a specific time interval the sample was rapidly cooled to 4 °C to stop the reaction and brought to the conditions required for NMR measurements as described above.

For mass-spectrometric analysis of reaction products, ageing of 0.5 ml samples (mostly in a dialysis tube) was run to completion in closed glass capillaries under the same conditions but in the presence of about 50% $H_2{}^{18}O$ (introduced into the tube by dialysis).

Denaturations were carried out with 0.2 M SDS, 8 M urea or 6 M GuHCl , containing 10 mM 1,4-dithiothreitol. In the first case 1.0 M SDS in a buffer containing 20% D_2O was added to the protein solution (4 °C) and the mixture was slowly (4-8 h) brought to room temperature at which it was kept for at least 24 h before NMR measurements were done. In the other two cases the solutions were dialysed at 4-8 °C during 24 h and subsequently at room temperature for at least 48 h against 140 ml of buffer containing the denaturant, followed by dialysis for at least 24 h against 12 ml of the same solution containing D_2O. By following these denaturation procedures, additional ageing sometimes observed at the very beginning of denaturation was avoided.

e. NMR Spectrometry

^{31}P NMR spectra were recorded at a frequency of 40.5 MHz in the

Ser(DP)-Gly-OEt were kindly provided by Dr. H. Kienhuis (Prins Maurits Laboratory TNO), diisopropyl hydrogen phosphate and diisopropyl phosphorofluoridate (DFP) were obtained from Mr. C. de Borst (Prins Maurits Laboratory TNO).

b. Chemicals

All chemicals were reagent grade and commercially available. Organic solvents (Merck) were distilled shortly before use. Deuterium oxide (D_2O; 99.8% isotopically pure; Uvasol, Merck), $H_2{}^{18}O$ (91% isotopically pure, Ventron), citric acid (Merck), sodium citrate (Merck), Tris (J.T. Baker Chemicals B.V.), urea (Union Chimique Belge, s.a.), sodium dodecyl sulphate (SDS; specially purified for biochemical work, British Drug House), guanidine hydrochloride (GuHCl; Fluka, AG) and 1,4-dithiothreitol (Merck) were used without further purification.

Buffers for calibration of pH meters were obtained from Radiometer A/S and Beckman.

c. Labelling with a DP-Group

Chymo, Chymogen or Sub (30-90 mg) was dissolved in 1 ml of 0.1 M Tris-HCl, pH=7.6, resulting in a protein concentration of 1-3 mM. AtrE solutions of this concentration were prepared at 4 °C from stock solutions of 0.01-0.10 mM active enzyme by concentrating with Amicon magnetically stirred cells (models 202 and 52) equipped with a PM 10 filter, followed by a further concentration with Minicon macrosolute concentrators (Type A-25, Amicon).

To achieve complete inhibition (> 99.9%), 20 µl of 0.5 M DFP in dry, peroxide-free isopropanol was added (final DFP concentration 10 mM) and the mixture was incubated at room temperature for about 6 h or, in the case of AtrE and Chymogen, for 20 h. Non-specific labelling was not observed under these conditions. Sometimes, e.g. at high concentrations of AtrE, a slight precipitate was formed. After inhibition this was removed by centrifugation.

The remaining DFP and its hydrolysis product were removed by dialysis at 4 °C against 140 ml buffer for at least 36 h, under continu-

ous stirring and frequent renewal. Finally, the sample was dialysed against 12 ml of buffer containing about 20% D_2O as internal standard for field-frequency locking. Buffers employed were 0.1 M Tris-HCl pH $\geq$ 7.6 and 0.1 M citric acid-sodium citrate pH < 7.6. Concentrations of phosphorylated proteins were measured by determination of the amount of phosphorus according to a modified method of Gerlach and Deuticke (Gerlach and Deuticke, 1963; Kienhuis and Baar, 1964). To improve the signal-to-noise ratio dialysed protein solutions were sometimes concentrated at 4 ^{o}C by means of Minicon macrosolute concentrators (Type A-25, Amicon). Usually, concentrations ranged from 1.5-3.0 mM.

d. Ageing and Denaturation

Unless stated otherwise, 0.5 ml of DP-enzyme was allowed to age at 36 ^{o}C in a dialysis tube to remove released low-molecular weight materials. After a specific time interval the sample was rapidly cooled to 4 ^{o}C to stop the reaction and brought to the conditions required for NMR measurements as described above.

For mass-spectrometric analysis of reaction products, ageing of 0.5 ml samples (mostly in a dialysis tube) was run to completion in closed glass capillaries under the same conditions but in the presence of about 50% $H_2{}^{18}O$ (introduced into the tube by dialysis).

Denaturations were carried out with 0.2 M SDS, 8 M urea or 6 M GuHCl , containing 10 mM 1,4-dithiothreitol. In the first case 1.0 M SDS in a buffer containing 20% D_2O was added to the protein solution (4 ^{o}C) and the mixture was slowly (4-8 h) brought to room temperature at which it was kept for at least 24 h before NMR measurements were done. In the other two cases the solutions were dialysed at 4-8 ^{o}C during 24 h and subsequently at room temperature for at least 48 h against 140 ml of buffer containing the denaturant, followed by dialysis for at least 24 h against 12 ml of the same solution containing D_2O. By following these denaturation procedures, additional ageing sometimes observed at the very beginning of denaturation was avoided.

e. NMR Spectrometry

^{31}P NMR spectra were recorded at a frequency of 40.5 MHz in the

Fourier Transform mode on a Varian XL-100-12 NMR spectrometer system; generally 5 mm cylindrical sample tubes (Wilmad 507 PP) containing 0.5 ml samples were used. Because of the limited amount of AtrE available, measurements with this enzyme were usually performed with cylindrical microtubes (Wilmad, 508 CP) with 0.2 ml samples. Proton noise decoupling was provided at high power by 90 Hz square wave modulated irradiation. A spectral width of 6 kHz, a 90^{o} pulse (pulse width 35 μs), an acquisition time of 1 s and a pulse delay of 2 s were applied. Data accumulation in the time domain and Fourier transformation of the free induction decay were carried out by a Varian 620/L-100 computer interfaced to the spectrometer. In order to enhance sensitivity the time domain data were exponentially weighted by using the optimal signal-to-noise filter (Cf. Ernst, 1966) with a time constant of 0.1 s, based on the narrowest line in the spectra of model compounds and denatured enzymes. Optimization of field homogeneity was performed with trimethyl phosphate, yielding line widths smaller than 0.4 Hz.

Dependent on the enzyme concentration 20,000-30,000 transients were accumulated for a spectrum. In some cases 50,000-80,000 transients were accumulated for the more dilute AtrE solutions. For the low-molecular weight model compounds (concentrations 1-10 mM) 100-500 transients were made. To calculate the chemical shift, 10-20 transients of a 85% phosphoric acid standard solution in a thin capillary, centred in a sample tube with water, were added. Shifts to higher frequencies (lower field) with respect to this external standard were taken as positive.

Results obtained with either external fluorine or internal deuterium field-frequency lock did not differ. In the latter case samples contained about 20% D_2O, unless urea or GuHCl was present. Then it amounted to at least 50%. If required for accurate comparison between various solvents, observed chemical shifts were corrected in the usual way for differences in magnetic susceptibility between solution and reference (Crutchfield et al., 1967; Strehlow, 1968). Spectra of denatured enzymes and model compounds were measured at 25.0 ^{o}C, the other spectra at 4.0 ^{o}C to avoid possible ageing (see below). Reproducibility was within 0.1 ppm for the proteins and within 0.05 ppm for the model compounds.

f. Mass Spectrometry

After completion of ageing the gaseous and liquid contents of the closed capillary were analysed for reaction products with a VG 7070 F mass spectrometer combined with a Varian Model 1400 gas chromatograph. Gas-chromatographic analysis was performed with a glass column (100x0.2 cm) filled with Porapak Q. For characterization of gaseous products 100 µl of the vapour above the liquid was injected and analysis was performed at a column temperature of 110 °C; for characterization of dissolved products 1-5 µl of liquid, freed from protein by dialysis, was injected and analysed at a column temperature of 80 °C raised to 130 °C at a rate of 4 °C/min. Data acquisition and spectral analysis were performed with a VG 2050 data system.

g. pH Measurements

Measurements of pH were performed with various Radiometer pH meters (No. 22 Type PHM 22q, No. 26 and PHM 64 Research pH meter). Calibration was performed shortly before use with standard buffers. Prior to the NMR experiment the pH of the protein solution was determined in the dialysate and immediately after completion of the experiment in the solution itself. NMR results were accepted if the difference between the two measurements was within 0.05 pH unit.

RESULTS

a. Native and Denatured DP-enzymes

Around pH 7.6 the ^{31}P NMR spectra of the DP-enzymes investigated showed a single line with a width at half height ($W_{1/2}$) between 10 and 20 Hz and with substantially different chemical shifts (Figure 1). The chemical shift did not depend on protein concentration, whereas $W_{1/2}$ showed a small increase at higher concentrations. In this region the chemical shift depended on pH according to a titration curve of a single titratable group with pK_a in the range 7.2-7.6 (Figure 2), whereas $W_{1/2}$ was not significantly affected by pH. The values of the parameters characterizing this titration are compiled in Table I. The chemical shift of DP-Chymogen showed a second titration curve at low

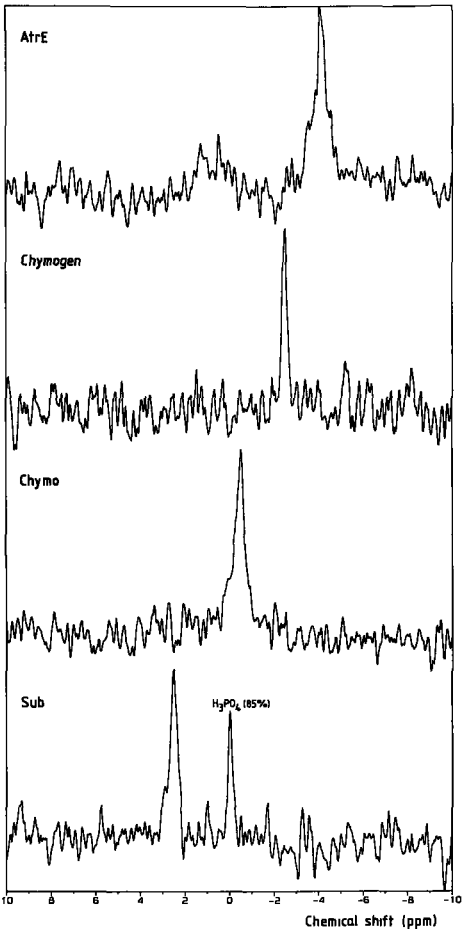

FIGURE 1: ^{31}P NMR spectra of DP-serine enzymes in buffered aqueous solution at 4 °C. AtrE = atropinesterase (pH = 7.76), Chymogen = α-chymotrypsinogen (pH = 7.52), Chymo = α-chymotrypsin (pH = 7.60), Sub = subtilisin A (pH = 7.65). H_3PO_4 reference peak is shown in the spectrum of Sub.

pH (Figure 2), the characteristic parameters of which are also given in Table I.

The variation in the chemical shift with pH was found to be reversible. At the lowest pH-values employed sometimes a slight precipitation occurred but this did not influence the chemical shifts. Spectra of native DP-Sub at pH below 4.5 could not be obtained because

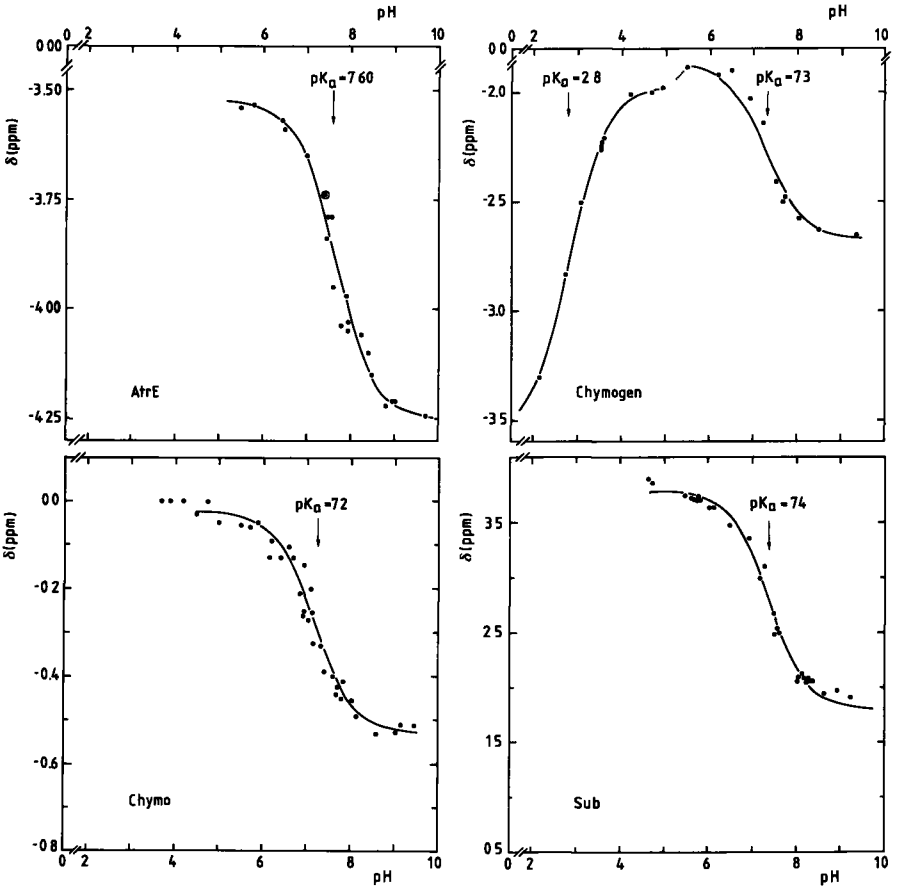

FIGURE 2: pH-Dependence of the chemical shift (δ) in the ^{31}P NMR spectra of DP-serine enzymes. Solid lines are theoretical curves calculated according to the Henderson-Hasselbach equation (Cf. Edsall and Wyman, 1958). For abbreviations, see legend to Figure 1.

the enzyme was rapidly denatured as appeared from a substantial increase in the viscosity of the solution (gelation) and the concomitant loss in the capacity to age (see below). Because of increased denaturation at lower pH, no measurements with native DP-AtrE were performed at pH < 5.

Differences in chemical shift may be due to differences in substitution at the phosphorus nucleus (attachment to different functional groups in the protein, loss of isopropyl groups) or to different

TABLE I: Characteristic parameters of DP-enzymes in aqueous solution as derived from the pH-dependence of the ^{31}P chemical shift. (1)

Parameter (2)	Chymotrypsin	Subtilisin	Atropinesterase	Chymotrypsinogen	
pK_a	7.2	7.4	7.6	7.3	2.8
$\delta(pK_a)$ (ppm)	-0.3	+2.8	-3.9	-2.3	-2.8
$\Delta\delta$ (ppm)	0.5	2.0	0.7	0.8	1.6

(1) Obtained from the titration curves in Figure 2.

(2) $\delta(pK_a)$ = chemical shift at pH = pK_a, $\Delta\delta$ = difference between the limiting values of the chemical shift at low and high pH. Estimated errors: pK_a < 0.1 pH unit, $\delta(pK_a)$ < 0.05 ppm, $\Delta\delta$ < 0.1 ppm.

interactions of the phosphoryl group with the immediate environment. Since phosphate mono-esters (pK_a's in the range 6-7; Cf. Sober, 1970) show an upfield shift with decreasing pH (Bock, 1976), the titration curves in Figure 2 do not reflect a primary phosphate. The data in Table II show that after denaturation the differences between the enzymes and the above-mentioned variation in the chemical shift with pH have disappeared, i.e. the differences between the non-denatured enzymes and the pH-dependence of the chemical shift resulted from interactions of the probe with the environment and not from differences in substitution.

To establish whether the signal of the denatured enzymes originated from a tertiary or a secondary phosphate ester, the two model peptides Gly-Ser(DP) and Gly-Glu-Ser(DP)-Gly-OEt, both phosphorylated at the hydroxyl group of the serine side chain, as well as diisopropyl hydrogen phosphate have been investigated under comparable conditions. The results for pH 3.2 and 9.3 are compiled in Table IIIA. Neither the chemical shift nor $W_{\frac{1}{2}}$ depended on the concentration. Since the differences between the corrections for magnetic susceptibility are negligible under the conditions used, uncorrected values of chemical shifts are given. The results at pH=7.5 were similar to those at pH=9.3, except that for GuHCl the upfield shift was 0.1-0.2 ppm smaller. Similarly it was found that results obtained at pH=3.5 did not differ from those at pH=3.2. Comparison of Tables II and IIIA shows that the signal of the proteins is due to a tertiary phosphate ester, i.e. to a DP-O-seryl structure.

TABLE II: ^{31}P chemical shifts (δ) of DP-enzymes in different aqueous systems. (1), (2)

System	δ (ppm)			
	Chymotrypsin	Subtilisin	Atropinesterase	Chymotrypsinogen
Buffer: low pH (3)	-0.0^{2}	$+3.8^{0}$	-3.5^{2}	-1.8^{7}
high pH (3)	-0.5^{5}	$+1.8^{0}$	-4.2^{5}	-2.6^{7}
Buffer with denaturant.				
pH = 3.5:				
0.2 M SDS	-3.1	-2.9	-2.8	-3.0
8.0 M urea	-3.6	-3.7	-3.6	-3.6
8.0 M urea + 0.2 M SDS	-3.3	-3.1	-3.0	-3.3
pH = 7.5:				
0.2 M SDS	-3.1	-2.8 (4)	-2.8	-3.1
8.0 M urea	-3.3	-3.2	-3.2	-3.2
8.0 M urea + 0.2 M SDS	-3.2	-2.8	-2.7	-3.1
6.0 M GuHCl (5)	-4.0 (6)	-4.1	-4.1	-4.0

(1) At room temperature, unless indicated otherwise. Standard error of the mean < 0.1 ppm.

(2) Upon denaturation the line widths of DP-enzymes (10-20 Hz) were reduced to values about equal to that of the model compounds under the same conditions (Table IIIA).

(3) Limiting values at 4 °C obtained from Figure 2 by extrapolation; estimated standard errors < 0.05 ppm.

(4) At pH > 5.5 there is always a second line upfield due to non-denatured DP-Sub-SDS complex. The titration curve of this line is identical to that of DP-Sub (Figure 2) but shifted to higher pH over about 0.5 pH unit ($pK_a \sim 7.9$).

(5) With 10 mM 1,4-dithiothreitol.

(6) A value of -3.2 ppm is observed at lower concentrations (~4 M) and exposures shorter than 36 h (Cf. Bock, 1976).

b. Native and Denatured MP-enzymes

Upon prolonged exposure of DP-Chymo, DP-Sub and DP-AtrE to 36 °C at pH=7.6, another line appeared in the spectrum with a position downfield relative to the first one and different for the three enzymes (Figure 3). Its intensity gradually increased at the expense of the original line which finally disappeared. This phenomenon was also observed at other pH-values within the titration range. It did not occur

TABLE IIIA: ^{31}P chemical shifts (δ) and mean line widths at half height ($\bar{W}_{\frac{1}{2}}$) of model compounds with a diisopropyl group bound to a serine side chain in different aqueous systems at room temperature.

System	δ(ppm) (1)		
	I	II	III
Buffer: pH = 3.2	-3.0	-3.2	-0.8
pH = 9.3	-2.9	-3.1	-0.8
Buffer with denaturant.			
pH = 3.2: 0.2 M SDS	-3.2	-2.6	-0.8
8.0 M urea	-3.6	-3.6	-1.4
8.0 M urea + 0.2 M SDS	-3.5	-3.0	-1.4
6 M GuHCl (2)	-3.2	-3.2	-1.0
pH = 9.3: 0.2 M SDS	-2.9	-2.7; -3.1 (3)	-0.8
8.0 M urea	-2.9	-3.1	-0.9
8.0 M urea + 0.2 M SDS	-2.9	-2.9	-0.9
6 M GuHCl (2)	-3.9	-4.3	-1.8
	$\bar{W}_{\frac{1}{2}}$ (Hz) (4)		
	I	II	III
All systems: pH = 3.2	5	5	4
pH = 9.3	5	6	4

(1) Model compounds: I = Gly-Ser(DP); II = Gly-Glu-Ser(DP)-Gly-OEt; III = diisopropyl hydrogen phosphate. Concentrations 1-10 mM. Standard error in δ < 0.1 ppm.

(2) With 10 mM 1,4-dithiothreitol.

(3) Chemical shift of a small second peak, which disappears at higher SDS concentrations and is, therefore, ascribed to free compound.

(4) Mean value of the different systems with and without denaturant at the pH indicated; standard error < 1 Hz.

with denatured DP-enzymes nor with DP-Chymogen. In contrast to the original line the position of the downfield line did not show any significant pH-dependence.

In order to determine the origin of this second line, the effect of denaturation has been investigated in the same way as for the first line (Table IV). Denaturation caused an upfield shift that yielded the same line for the three enzymes, which was, however, about 2.7 ppm downfield with respect to that of the denatured, freshly inhibited DP-enzymes (Tables II and IV). This difference in chemical shift under

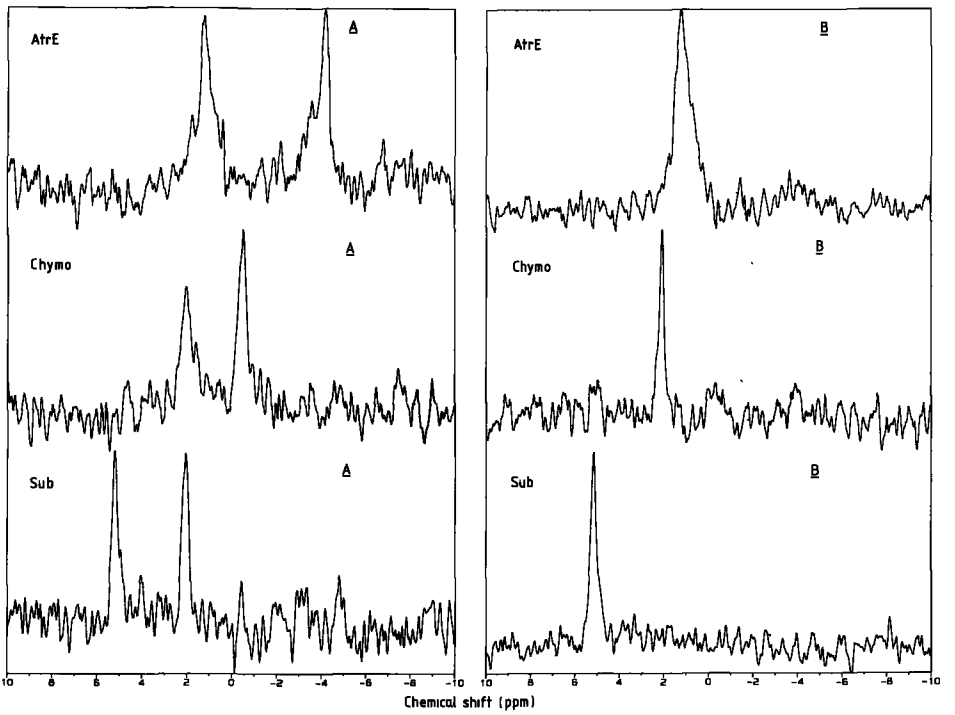

FIGURE 3: ^{31}P NMR spectra of partially (A) and completely aged (B) DP-serine enzymes in buffered aqueous solution at 4 ^{o}C. AtrE = atropinesterase (pH = 7.95), Chymo = α-chymotrypsin (pH = 7.80), Sub = subtilisin A (pH = 8.20).

the same denaturing conditions indicates that the second line must be ascribed to a ^{31}P nucleus with a different substitution and not to a conformational isomer as suggested by Gorenstein and Findlay (1976)*.

* Since the occurrence of conformational isomers has been questioned (Bock, 1976; Cohn and Rao, 1979; Porubcan et al., 1979) it should be mentioned that with DP-Chymo and DP-Sub, kept for some time at a pH around 5 at 4 ^{o}C, a second line was observed close to that of the aged enzyme. Upon denaturation this second line coincided completely with the DP-line for Chymo or, in the case of Sub, sometimes partly with the aged and partly with the non-aged enzyme. This points to the occurrence of slowly converting conformational isomers (Gorenstein and Findlay, 1976).

TABLE IIIB: Corrected ^{31}P chemical shifts (δ) and mean line widths at half height ($\bar{W}_{\frac{1}{2}}$) of model compounds with a phosphorylated serine side chain in solvents of different polarity and hydrogen-bonding capacity at room temperature.

Solvent	ε_o (1)	type (2)	δ(ppm) (3)		
			I	II	III
ethylacetate	6.0 (25 °C)	b			-1.1
+ 1 M phenol		a,b			-2.4
+ 5 M phenol		a,b	-4.8	-4.5	-3.6
acetic acid	6.2	a,b	-4.6		-1.9
aniline	6.9	a	-3.7		-2.6
pyridine	12.3 (25 °C)	b	-3.5		-1.7
ethanol	25.1	a	-4.3		-3.6
methanol	33.6	a	-4.2		-2.9
dimethylformamide	38.7	b	-3.6	-3.1	-2.7
+ 1 M phenol		a,b	-3.8		-3.1
+ 5 M phenol		a,b	-4.5	-4.1	-3.4
dimethylsulfoxide	46.7 (25 °C)	b	-3.7		-3.2
+ 5 M phenol		a,b	-4.4		-3.8
formic acid	58.5 (16 °C)	a,b	-5.2		-3.2
water: pH = 9.3	80.4	a,b	-3.5	-3.7	-1.4
pH = 3.2	80.4	a,b	-3.6	-3.8	-1.4
pH = 0.5	80.4	a,b	-4.0	-3.9	-2.7
formamide	109	a,b	-3.8	-4.0	-1.9
+ 1 M phenol		a,b	-4.0		-2.2
+ 5 M phenol		a,b	-4.4	-4.3	-2.6

	$\bar{W}_{\frac{1}{2}}$ (Hz) (4)		
	I	II	III
All solvents	7	6	5

(1) ε_o = static dielectric constant at 20 °C (unless stated otherwise) obtained from Riddick and Bunger (1970), Steffen (1970) and West (1974).

(2) Solvents have been classified, according to acids (a) and bases (b) in hydrogen bonding.

(3) Model compounds: I = Gly-Ser(DP), II = Gly-Glu-Ser(DP)-Gly-OEt, III = diisopropyl hydrogen phosphate. Concentrations 1-10 mM. Experimental values of δ have been corrected in the usual way for the difference in magnetic susceptibility between the reference and the sample (Crutchfield et al., 1967; Strehlow, 1968). Inaccuracy in $\delta < 0.1$ ppm.

(4) Average of $W_{\frac{1}{2}}$ over all solvents, except for compound I where formic acid and acetic acid have been excluded, since for these media $W_{\frac{1}{2}} = 40 \pm 2$ Hz. In general compound I shows a tendency of increasing $\bar{W}_{\frac{1}{2}}$ with strength of hydrogen bonding. Estimated error in $\bar{W}_{\frac{1}{2}}$ is about 1 Hz.

TABLE IV: ^{31}P chemical shifts (δ) of aged DP-enzymes in different aqueous systems and mean line widths at half height ($\bar{W}_{\frac{1}{2}}$) in buffer. (1)

System	δ(ppm)		
	Chymotrypsin (2)	Subtilisin (3)	Atropinesterase
Buffer (pH 3.5 - 9.5) (4)	+2.1	+5.2	+1.3
Buffer with denaturant.			
pH = 3.5: 0.2 M SDS	-0.5	-0.4	-0.4
8.0 M urea	-0.8	-0.8	-0.8
8.0 M urea + 0.2 M SDS	-0.6	-0.6	-0.7
pH = 7.5: 0.2 M SDS	-0.4	-0.4 (+5.3)	-0.4
8.0 M urea	-0.4	-0.4 (+5.0)	-0.4
8.0 M urea + 0.2 M SDS	-0.4	-0.3 (+5.1)	-0.4
6.0 M GuHCl (5)	-1.2 (6)	-1.2 (+4.9)	-1.2
	$\bar{W}_{\frac{1}{2}}$ (Hz) (7)		
	Chymotrypsin	Subtilisin	Atropinesterase
Buffer (pH 3.5 - 9.5) (8)	13	11	15

(1) At room temperature, unless stated otherwise.

(2) Only after denaturation of DP-chymotrypsinogen subjected to ageing conditions some aged zymogen may be observed. The values of δ and $\bar{W}_{\frac{1}{2}}$ for aged zymogen are not significantly different from those given for the enzyme.

(3) Within parentheses values for non-denatured aged subtilisin at the same conditions.

(4) Mean value of δ for aged enzyme at 4 ^{o}C in the pH-range indicated.

(5) With 10 mM 1,4-dithiothreitol.

(6) A value of -0.6 ppm is observed at lower concentrations ($\sim$4 M) and exposures shorter than 36 h.

(7) The values of $W_{\frac{1}{2}}$ of the denatured aged enzymes are not significantly different from those of the DP-enzymes under denaturing conditions.

(8) Mean value of $W_{\frac{1}{2}}$ for aged enzyme at 4 ^{o}C in the pH-range indicated.

Comparison of the data in Table IV with those of the model compounds in Table IIIA shows that the second line should be attributed to a secondary phosphate group, viz. to an MP-O-seryl structure. The phenomenon noted above therefore results from the conversion of a DP-group into an MP-group, i.e. from ageing.

c. Model Compounds in Non-aqueous Solvents

The data above indicate that under non-denaturing conditions differences in chemical shift between the various DP-enzymes as well as between the corresponding MP-enzymes result from different environments. To analyse the environmental contribution, the influence of various types of organic solvents on the chemical shift of the two phosphorylated model peptides and of diisopropyl hydrogen phosphate was investigated. The results are presented in Table IIIB, together with results obtained with phenol which was added as it forms strong hydrogen bonds with the phosphoryl oxygen (Cf. Joesten and Schaad, 1974). The corrected values of chemical shifts are compiled. A limited number of data has been obtained for the tetrapeptide since it is only soluble in a few solvents.

d. Kinetics of Ageing

From NMR spectra of DP-enzymes subjected to ageing for some time the fractions of remaining DP-enzyme were determined. In some cases (low protein concentrations) the aged samples were denatured before NMR experiments were carried out in order to improve the signal-to-noise ratio. Figure 4 shows the decrease in the fraction of DP-enzyme

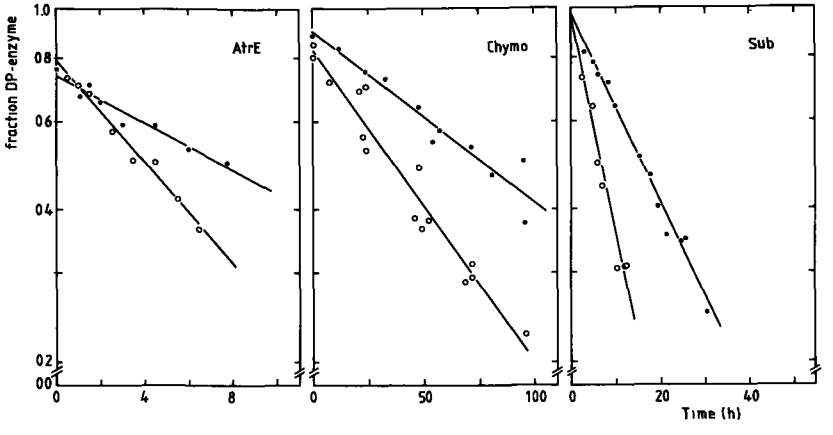

FIGURE 4: Semi-logarithmic plot of the decrease in the fraction of DP-enzyme with time, at 36 °C and different pH. The fractions of DP-enzyme were obtained from the NMR spectra. AtrE = atropinesterase at pH = 7.6 (●) and pH = 6.7 (○), Chymo = α-chymotrypsin at pH = 7.6 (●) and pH = 3.5 (○), Sub = subtilisin A at pH 7.6 (●) and pH = 5.5 (○). The straight lines were calculated by the method of least squares.

with time, at two pH-values. Apparently, the conversion of DP-enzyme into MP-enzyme occurs according to first-order kinetics. First-order rate constants of ageing (k_a) calculated from the slopes of such linear plots by the method of least squares are compiled in Table V. Results for Chymo agreed very well with those obtained by chemical analysis (Berends, 1964).

TABLE V: Rate constants of ageing (k_a) for different pH's at 36.0 °C.

Enzyme	pH	k_a (10^{-6} s^{-1})	
		NMR data (1)	Lit. data (2)
Chymotrypsin	8.7	0.8 ± 0.1	
	7.6	2.1 ± 0.2	
	7.5		1.7; 1.9 (3)
	3.5	3.9 ± 0.3	4.4
Subtilisin	8.7	2.0 ± 0.1	
	7.6	11.9 ± 0.4	
	5.5	27.2 ± 1.9	
Atropinesterase	7.6	14.7 ± 1.5	
	6.7	31.6 ± 1.7	

(1) With standard error.
(2) Berends, F. (1964).
(3) At 37 °C.

e. Mass-Spectrometric Characterization of Products

To determine whether loss of the isopropyl group proceeds by P-O or by C-O fission (Hudson, 1965; Kirby and Warren, 1967) and to investigate the mechanism of fission (S_N1 or S_N2, see discussion), the ageing reaction was run to completion in the presence of $H_2{}^{18}O$ in either a citric acid-sodium citrate buffer (0.1 M) or in 0.05 M sodium sulphate and the products formed were analysed by mass spectrometry. The results (Table VI) show that isopropanol was formed with an $^{18}O/^{16}O$ ratio equal to that of the solvent; furthermore different amounts of propene were found. Since it was observed that at low pH the presence of dialysis tube led to 10-20% exchange of ^{18}O between $H_2{}^{18}O$ and isopropanol, ageing experiments in dialysis tube were performed at pH > 5.5, where exchange was negligible.

TABLE VI: Results of mass-spectrometric analysis of products formed upon ageing of DP-enzymes in aqueous solution at 36.0 °C.

	Chymotrypsin	Subtilisin	Atropinesterase
Isopropanol (%) (1)	97 ± 13	42 ± 6	18 ± 14
Propene (%) (1)	1.2 ± 0.2	3.8 ± 0.6	11.3 ± 5.5
$^{18}O/^{16}O$ ratio (2)	0.99 ± 0.03	1.01 ± 0.01	0.98 ± 0.05

(1) The amount measured after complete ageing at 36.0 °C (± s.e.m.) expressed as percentage of the amount expected on the basis of the concentration of phosphorylated enzyme. Ageing was completed at pH = 5.7 for chymotrypsin and subtilisin, and at pH = 6.7 for atropinesterase in either 0.1 M citric acid-sodium citrate buffer or 0.05 M sodium sulphate. Since the results in these media did not differ significantly, the averaged values of both media are given. In some experiments also a small amount of acetone was found, presumably due to contamination.

(2) The ratio (± s.e.m.) of ($H_2{}^{18}O/H_2{}^{16}O$) and (^{18}O-isopropanol/^{16}O-isopropanol).

DISCUSSION

DP- and MP-enzymes can be considered to belong to the class of phosphate esters of the type RO(R'O)P(O)OR" where R is a proton, an alkyl group or an aromatic group. Due to appreciable differences in bonding between the phosphorus and the four substituents in which besides s and p orbitals also empty d orbitals of the phosphorus may participate, depending on the substitutents and the interactions with the environment (Ionin, 1968; Mavel, 1973), the ^{31}P chemical shifts of these compounds cover a range of roughly 30 ppm (Mark et al., 1967; Bock, 1976).

From theoretical considerations (Saika and Slichter, 1954; Karplus and Das, 1961) it can be concluded that the chemical shift of ^{31}P will mainly result from the paramagnetic contribution of the electrons in the valence shell orbitals to the screening constant σ (Letcher and Van Wazer, 1967; Ionin, 1968). For phosphate esters the average value of this contribution may be approximated by a sum of two negative terms, $\langle \sigma_{\pi}^{p} \rangle + \langle \sigma_{\pi}^{d} \rangle$, accounting for the contribution of the phos-

phorus p and d orbitals which participate in σ and π bonding, respectively (Letcher and Van Wazer, 1967). Various semi-empirical quantum mechanical treatments have been proposed to explain these contributions (Muller et al., 1956; Wagner, 1963; Gutowsky and Larmann, 1965; Letcher and Van Wazer, 1967; Purdela, 1971; Gorenstein and Kar, 1975). These treatments analyse the determinants which dominate the paramagnetic contributions, such as differences in electronegativity between the phosphorus and the substituent atoms, the σ-bond angles between the substituents and variations in π bonding, but the explanation of empirical data is still qualitative and restricted to particular compounds (Ionin, 1968; Mavel, 1973; Gorenstein, 1975). This is mainly due to limited incorporation of atomic orbitals and molecular geometry in the calculations and to incomplete understanding of the complex interplay between steric and electronic factors involved in bonding (Blackburn et al., 1971; Gorenstein, 1975). An interpretation of the chemical shifts of the phosphorylated enzymes can, therefore, only be qualitative and based on empirical data obtained with appropriate model compounds.

a. Chemical Shifts of Model Systems

A decrease in bond angle between alkoxy substituents in di and trialkylphosphates is accompanied with a downfield shift (Blackburn et al., 1964, 1971; Mark et al., 1967). Thermodynamic data on hydrogen bonding indicate that a smaller bond angle is also attended with some weakening of hydrogen bonding at the phosphoryl oxygen (Cf. Joesten and Schaad, 1974). The apparently decreased negative charge on this oxygen points to a strengthened phosphoryl bond due to a decreased electron release from other substituents towards ^{31}P (Bell et al., 1954; Halpern et al., 1955; Wagner, 1963; Hudson, 1965). As will be made plausible in the following, the reverse holds also: changes in the electronic charge distribution of alkyl phosphates which cause a downfield shift lead to a smaller O-P-O bond angle.

The data for model compounds I and II in Table IIIB show that hydrogen bonding (and maybe protonation in the presence of organic acids) at the phosphoryl oxygen causes a small but significant upfield

shift, similar to that for protonation in triisopropyl and analogous trialkyl phosphates (Cf. Olah and McFarland, 1971). In aqueous solution (Table IIIA), the upfield shift caused by urea at pH=3.2 and by GuHCl at pH=9.3 is, therefore, probably due to formation of hydrogen bonds with the phosphoryl oxygen.

Infrared and Raman studies have shown that hydrogen bonding at the phosphoryl oxygen leads to a decrease in the stretching frequency of this group, whereas that of the bonds between P and the other substituents becomes somewhat increased (Bell et al., 1954; Halpern et al., 1955). ^{1}H NMR studies showed a deshielding of the α-alkyl protons upon protonation of the phosphoryl oxygen in trialkyl phosphates, indicating a charge displacement from the alkyl groups towards the phosphorus (Olah and McFarland, 1971). This suggests that the p_{π}-d_{π} bonding contribution in the phosphoryl bond is appreciably decreased, whereas that in the other bonds is somewhat increased due to an inductively increased formal positive charge on ^{31}P (Wagner, 1963; Olah and McFarland, 1971). According to the valence shell electron pair repulsion theory (VSEPR) the decreased charge density of the phosphoryl bond and the slight increase in the charge density of the P-O bonds upon such hydrogen bonding yield a somewhat larger bond angle between the alkoxy groups than in the isolated molecule (Cf. Gillespie, 1972).

Similarly, the upfield shift due to protonation of the diisopropyl phosphate anion in aqueous solution (Table IIIB) will result from decreased orbital overlap between P and O^{-} as indicated by the increased P-O bond length (Cruickshank, 1961). Since the effect of urea and GuHCl on the chemical shift of the diisopropyl phosphate anion is about the same as for the tertiary phosphate esters (Table IIIA) it is concluded that the introduction of O^{-} does not lead to an enhanced overall hydrogen bonding at the unsubstituted oxygens.

Data for diisopropyl hydrogen phosphate in organic solvents (Table IIIB) show that hydrogen bonding in which the phosphoryl compound acts as proton donor also leads to an upfield shift. In this case the proton will lose electron density to the oxygen and the phosphorus (Kollman, 1977). Enhancement of this effect by stronger proton acceptors or by replacement of the hydrogen by a serine side chain

(Cf. Table IIIB) or another alkyl group (Cf. Olah and McFarland, 1971), enlarges the upfield shift. The decreased positive charge on ^{31}P resulting from such inductive charge displacements will decrease the π-bond character of the various bonds but mainly of the phosphoryl bond (Kirby and Warren, 1967; Letcher and Van Wazer, 1967). In terms of VSEPR the corresponding reduction in the electron density of this bond will lead to an increase in the O-P-O bond angle.

Summarizing, in di and trialkyl phosphate esters variations in the electronic charge distribution which lead to an upfield shift increase the O-P-O bond angle, i.e. decrease the crowding of the alkoxy groups. On the other hand, a decrease in the O-P-O bond angle leads to a downfield shift. In other words, for these phosphoryl compounds there is a one-to-one correspondence between chemical shift and O-P-O bond angle. The above analysis indicates that $p_\pi - d_\pi$ bonding of the phosphoryl bond is a main factor underlying this correspondence. This result supports other empirical correlations (Gorenstein, 1975) and theoretical investigations (Gorenstein and Kar, 1975) which also point to a relation between the chemical shift and O-P-O bond angle.

The bond angle between the alkoxy groups of secondary and tertiary phosphates in solution may also be determined by non-bonding interactions with the environment. The downfield shift observed for the tetrapeptide upon addition of SDS, which is not found for the smaller model compounds (Table IIIA), indicates that non-bonding interactions accompanying association of the peptide with the detergent lead to a decreased O-P-O bond angle.

b. Chemical Shifts of Phosphorylated Enzymes

The simple titration curves of the chemical shift for Chymo, Sub and AtrE (Figure 2) indicate the involvement of one single titratable group with pK_a 7-8. For Chymogen the titration curve is slightly different from that reported by Porubcan et al. (1979); it shows a somewhat less simple behaviour, which might be due to a second group titratable at lower pH.

After denaturation the chemical shifts of the DP-enzymes were no

longer dependent on pH and resembled those of the model DP-compounds which did not exhibit a pH-dependence either. Consequently, the pH-effect must be attributed to a similar titratable group which in the native tertiary structure resides in the vicinity of the DP-group. A $pK_a \geq 7.2$ (Table I) is too high for a carboxylic acid and points to a titratable histidine of a special kind, since it lies above the range 5.5-7.0 characteristic for most histidines. (Edsall and Wyman, 1959; Meadows, 1972; Brill, 1977). Such a special histidine is present in Chymo and its zymogen (His(57)) and in Sub (His(64)) (Kraut, 1977). These histidines are part of the charge-relay system, one of the essential structural elements of the catalytic site of these enzymes (Kraut, 1977). In unperturbed native serine proteases the histidine of the charge-relay system has $pK_a < 7.0$ (Cf. Cunningham and Brown, 1956; Glazer, 1967; Steitz and Shulman, 1982), but substitution of a DP-group at the active serine side chain leads to $pK_a \geq 7.2$ (Cf. Markley, 1979). The indication of a similar histidine at the active site of AtrE with pK_a=7.6 in the DP-enzyme but $pK_a < 7.0$ in the native enzyme (Cf. Berends et al., 1967; Stevens, 1969) is corroborated by fluorescence studies (Van der Drift et al., 1983[c]).

The increase in the chemical shift with decreasing pH indicates that protonation of the active-site histidine is accompanied by increased crowding of the substituents at the phosphorus. Since in Chymo and Sub protonation does not show an appreciable structural change of the active site (Mavridis et al., 1974; Cf. Huber and Bode, 1977; Matthews et al., 1977), increased crowding must be related to a direct interaction of the protonated histidine with the DP-group. According to X-ray data in Chymo, Chymogen and Sub the protonated Nε2 of the active-site histidine may form a hydrogen bond with either the oxygen of the P-O-serine bond or that of one of the isopropoxy groups (Matthews et al., 1977; Chambers and Stroud, 1979; Stroud, 1979). The increase in the pK_a of Chymo and Sub upon phosphorylation of the active serine, is consistent with hydrogen bonding (Cf. Jaffé et al., 1954). According to the above analysis of the data of the model compounds the increase in the partial positive charge on ^{31}P induced by such hydrogen bonding will lead to increased crowding. The sole loss of an iso-

propyl group upon ageing (see below) suggests that only the oxygen of the scissile isopropyl-O-phosphorus link is involved and that, consequently, the increased crowding depends on hydrogen bonding between the protonated histidine and the oxygen of the nearby isopropoxy group.

Other data agree with the occurrence such an interaction. The small upfield shift of the histidyl Cε1-^{1}H NMR line of protonated histidine in Chymogen and trypsinogen due to the presence of a DP-group and the concomitant shift of the pK_a characterizing titration of the aspartic acid carboxyl group of the charge-relay system to a higher value (Markley and Ibanez, 1978; Porubcan et al., 1978, 1979) point to increased electron density on the imidazolyl group. Hydrogen bonding with the protonated histidine as donor will lead to such an increase (Kollman, 1977). Likewise, the upfield shift of the ^{31}P line of DP-Chymogen at low pH accompanying protonation of the aspartic acid carboxyl group (pK_a=2.8, Figure 2) suggests a weakening of this hydrogen bonding due to an increase in the electronic density on the imidazolyl group. The reduction in the rate of ageing at low pH which is to be expected upon decreased hydrogen bonding (see below) is another indication for hydrogen bonding between the histidine and an isopropoxy group.

Since for AtrE the effect of pH on the chemical shift was qualitatively similar to that for the other DP-proteins and since the pK_a of the group involved shifted to an even higher value (Table I), it is concluded that also in AtrE the titratable active-site histidine may form a hydrogen bond with a nearby isopropoxy group when protonated, i.e. the position of this histidine relative to the DP-group is similar to that in the other DP-enzymes. The values of $\Delta\delta$ (Table I) suggest that for AtrE the decrease in the O-P-O bond angle upon protonation of the histidine is similar to that of Chymo and its zymogen rather than to that of Sub. If the values of $\Delta\delta$ were simply a measure of hydrogen bonding, they would parallel the corresponding values of pK_a (Table I) and - as appears from the analysis of the ageing data to be presented below - of k_a^m, the maximum rate of ageing expected when a fully protonated histidine is present and hydrogen bonding is maximal

(Table VII). Since such relations have not been found, the difference between Sub and the other DP-enzymes may not be attributed solely to a stronger hydrogen bonding with the histidine in the former enzyme but rather to a different interplay of this and other interactions between the DP-group and the protein.

At high pH, when this hydrogen bonding is absent, the chemical shift differs substantially for the various native DP-enzymes (Table II). For AtrE there is an upfield shift with respect to the DP-model peptides in buffer (Table IIIA), whereas the other enzymes show a downfield shift. This might be explained by different contributions of hydrogen bonding at the phosphoryl oxygen and non-bonding interactions.

Comparison with data of the model compounds (Tables IIIA,B) and of the denatured enzymes (Table II) shows that the upfield shift of AtrE in buffer can be entirely ascribed to hydrogen bonding at the phosphoryl oxygen, with non-bonding interactions between the DP-group and the protein being of minor influence. The value of the chemical shift at low pH indicates that this hydrogen bonding is not disrupted by the interaction of the isopropoxy group with the protonated histidine. This specific interaction between the phosphoryl oxygen and the protein suggests the presence of an oxy-anion hole in AtrE, similar to the other serine hydrolases.

The downfield shift at high pH with respect to the model peptides observed for the other three proteins results from non-bonding interactions between protein and DP-group which increase crowding of the phosphorus substituents. This crowding appears to depend on the structure of the active-site region, e.g. on the presence or absence of a primary binding pocket.

In DP- and MP-serine enzymes investigated so far one isopropyl group interacts with the entrance of the primary binding pocket and is more or less excluded from the solvent and out of reach of the histidine of the charge-relay system (Stroud et al., 1974; Chambers and Stroud, 1979; Kossiakoff and Spencer, 1981). In the phosphorylated zymogens Chymogen and trypsinogen such a non-bonding interaction with the protein will be much weaker because a fully developed and rigid

binding pocket adjacent to the active serine is lacking (Freer et al., 1970; Wright, 1973; Fehlhammer et al., 1977; Kossiakoff et al., 1977). Besides, in the native enzymes a stronger hydrogen bonding of the phosphoryl oxygen in the oxy-anion hole is expected than in the zymogens as a consequence of a more favourably oriented -NH of Gly(193) (Freer et al., 1970; Henderson, 1970; Wright, 1973; Stroud et al., 1974; Kossiakoff et al., 1977), which will lead to an upfield shift. The downfield shift of about 2 ppm in the titration curve of Chymo relative to that of Chymogen (Figure 2) is therefore probably due to non-bonding interaction of an isopropyl group with the primary binding pocket (Cf. Reeck et al., 1977). This applies also to DP-trypsinogen and DP-trypsin for which a similar phenomenon has been observed (Porubcan et al., 1979).

The downfield shift of MP-Chymo and MP-Sub with respect to diisopropyl hydrogen phosphate, a shift which largely disappears upon denaturation (Tables IIIA and IV), points also to increased crowding by non-bonding interactions in aged inhibited enzymes. Non-bonding interaction of an isopropyl group with a primary binding pocket adjacent to the active serine may thus lead to increased crowding of the substituents at the phosphorus. Such an increase in DP- and MP-enzymes results from a decrease in the O-P-O bond angle between the active serine and the non-hydrolysable isopropyl group.

The above considerations indicate that the O-P-O bond angle becomes smaller in in the order AtrE>Chymo>Sub as a result of an enhanced binding of the DP-group to the protein by hydrogen bonding with the active-site histidine or by interaction of one isopropyl group with the primary binding pocket, in addition to hydrogen bonding in the oxy-anion hole. This order is maintained for the MP-groups in the aged enzymes.

For Chymo, Sub and AtrE the differences between the chemical shifts of the DP-species at high pH (Table II) and the corresponding aged species (Table IV) are 0.0, 0.7 and 2.9 ppm larger than 2.7 ppm, respectively. A value of 2.7 ppm is expected (on the basis of Tables II, IV and the data of the model compounds in IIIA and IIIB) when one isopropyl group is lost without affecting interactions with the envi-

ronment that contribute to the chemical shift. In contrast to the DP-species, in aged inhibited enzymes the ^{31}P line did not show an appreciable pH-dependence. This (Cf. Jaffé et al., 1954), together with the above-mentioned numerical differences, the negligible effect of neutral and ionic hydrogen bond disrupting compounds on the chemical shift of non-denatured MP-Sub (Table IV) and the indications that the presence of O^- does not result in an enhanced hydrogen bonding suggests that in MP-enzymes neither appreciable hydrogen bonding between Nε2 of the active-site histidine and the phosphoryl substituent (Cf. Robillard and Shulman, 1974) nor significant Coulombic interaction between the negatively charged MP-group and a positive (protonated) histidine (Cf. Kossiakoff and Spencer, 1981) occurs. Therefore, the extra downfield shifts mentioned above suggest conformational changes upon ageing which lead to enhanced binding of the phosphoryl substituent in the order Chymo<Sub<AtrE due to an increase in the non-bonding interaction between the remaining isopropyl group and the protein, while hydrogen bonding with the histidine weakens or even disappears. Indications of a similar increase in non-bonding interactions resulting from ageing have also been obtained for phosphorylated cholinesterase (Amitai et al., 1982). The large increase in the non-bonding interaction upon ageing of AtrE and the difference in the chemical shift between MP-AtrE and MP-Chymo of 0.8 ppm and between MP-AtrE and MP-Sub of 3.9 ppm (Table IV) indicate the presence of a pocket-like structure nearby the active serine which interacts with the remaining isopropyl group in a way similar to Chymo rather than to Sub.

The increase in non-bonding interaction between the phosphoryl group and the protein upon ageing of DP-Sub and DP-AtrE may point to a larger stabilization of the leaving group in these processes than in ageing of DP-Chymo. This is consistent with the observation that the ageing reaction of DP-Chymo is more of the S_N2 type, and that of the other two enzymes more of the S_N1 type (see below).

c. Ageing of DP-Enzymes

In neutral and acidic solutions hydrolysis of non-cyclic trialkyl phosphates to secondary phosphate esters proceeds according to various

mechanisms (Cox and Ramsay, 1964; Kirby and Warren, 1967; Ingold, 1969). However, under the conditions employed in this investigation the corresponding (unimolecular) rate constant will be significantly smaller than the k_a observed (Table V) for the conversion of DP-enzymes into MP-enzymes (Barnard et al., 1961; Cox and Ramsay, 1964; Keyer, 1971). This fact and the absence of any appreciable conversion in denatured enzymes indicate that ageing is a catalytic process which depends on the native protein structure (Berends, 1964; Keyer, 1971). The increase in k_a with decreasing pH (Table V) points therefore to an intramolecular general acid-catalysed reaction in which the presence of a proton on a titratable group in the protein close to the phosphoryl substituent is essential. This suggests an analogy with the ageing of phosphylated* cholinesterases, which also requires the involvement of a protonated group (Keyer, 1971; Keyer et al., 1974).

In the absence of particular metal ions or special groups which may act as Lewis acids, intramolecular hydrogen bonding with a neighbouring proton donor, and perhaps a subsequent proton transfer, will underlie the internal general acid-catalysed hydrolysis of phosphate esters (Cf. Hudson, 1965; Kirby and Warren, 1967; Singleton, 1973). Ageing of the DP-enzymes will, therefore, require hydrogen bonding between the oxygen of the isopropoxy group to be released and an adjacent proton donor, similar to the mechanism proposed for ageing of phosphylated cholinesterases (Heilbronn-Wikström, 1965; Keyer, 1971). The above analysis of the NMR data indicates that in the enzymes investigated such a hydrogen bond may be formed with a protonated histidine as proton donor.

If protonation of the active-site histidine, which causes the chemical shift to increase with pH (Figure 2), is essential to the ageing reaction, a plot of the chemical shift (at 4 ^{o}C, Figure 2) versus k_a (at 36 ^{o}C, Table V) for pH-values in the titration range will be linear, as the pK_a of such a histidine does not differ appreciably for these temperatures (Cf. Robillard and Shulman, 1974; Markley,

* Phosphylated includes phosphinylated, phosphonylated and phosphorylated (Cf. Hudson and Keay, 1960).

1978; Porubcan et al., 1979; Steitz and Shulman, 1982). Such plots (Figure 5) are indeed consistent with a linear relationship.

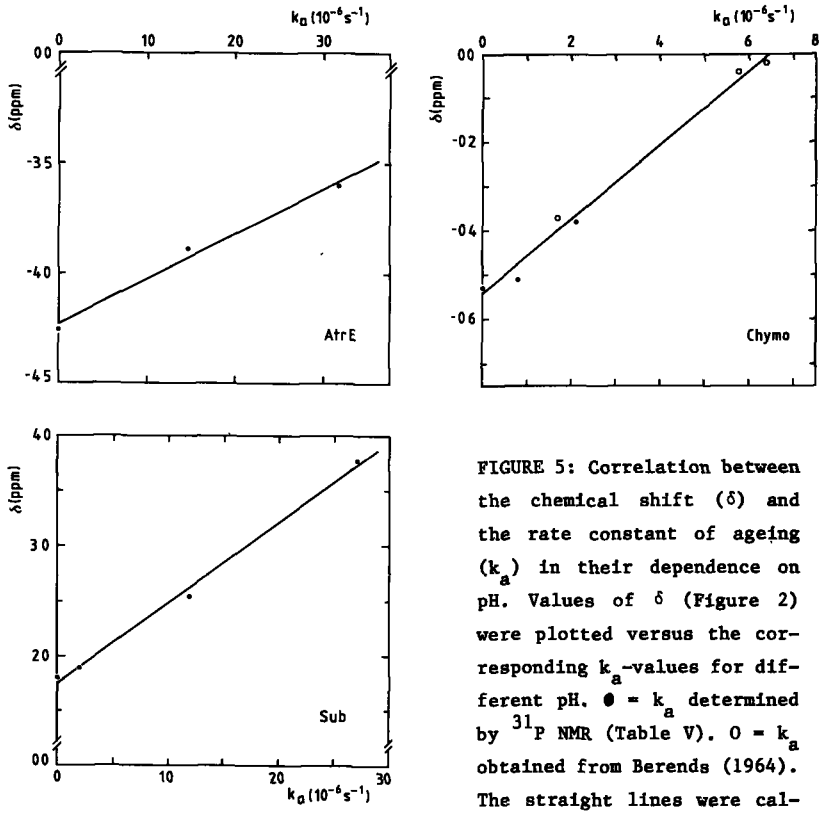

FIGURE 5: Correlation between the chemical shift (δ) and the rate constant of ageing (k_a) in their dependence on pH. Values of δ (Figure 2) were plotted versus the corresponding k_a-values for different pH. ● = k_a determined by ^{31}P NMR (Table V). O = k_a obtained from Berends (1964). The straight lines were calculated by the method of least squares, including the limiting value of δ at high pH where k_a = 0. For abbreviations, see legend to Figure 3. For Chymo only data for pH $\geq$ 4.5 have been used (see Discussion).

From these linear plots k_a^m, i.e. the maximum value of k_a expected for a fully protonated histidine in the otherwise unperturbed active site, can be estimated by using the values of the chemical shift at pH=5.0 (Figure 2). The k_a^m-values (Table VII) show an increase in the order Chymo<Sub<AtrE and suggest that the active-site region involved in ageing in AtrE resembles that in Sub more closely than that in Chymo. For Chymo, k_a at pH=3.5 is smaller (Table V) than the expected maximum value (Table VII), in agreement with other data which indicate

TABLE VII: Some characteristic quantities related to the ageing of DP-enzymes in aqueous solution at 36.0 °C.

Quantity (1)	Chymotrypsin	Subtilisin	Atropinesterase
k_a^m (10^{-6} s^{-1})	6.2	28.0	34.5
pK_a (2)	7.2	7.4	7.6
$\delta_{MP}-\delta_{DP}$ (ppm)	2.7	3.4	5.6

(1) k_a^m = maximum value of the rate constant of ageing obtained from the plots in Figure 5 for a fully protonated histidine at pH = 5.0. $\delta_{MP}-\delta_{DP}$ = difference in chemical shift between MP-enzyme (Table IV) and the corresponding DP-species at high pH (Figure 2)

(2) Based on Figures 2 and 5.

a decrease in k_a below pH 4-5 (Berends, 1964; Cf. Keyer, 1971). This may result from distortion of the active-site structure caused by protonation of particular groups at low pH. For AtrE, the value of k_a^m approaches that of DP-acetylcholinesterase (Cf. Berends, 1964).

The loss of an isopropyl substituent in hydrolysis may be envisaged to proceed by C-O fission, P-O fission, or both (Hudson, 1965; Kirby and Warren, 1967). Mass-spectrometric analysis of the products formed during ageing in the presence of $H_2{}^{16}O$ and $H_2{}^{18}O$ showed that isopropanol is formed with an $^{16}O/^{18}O$ ratio identical to that of the solution (Table VI), i.e. dealkylation in the DP-enzymes proceeds exclusively by C-O fission. Data obtained with Chymo phosphylated with various saligenin cyclic phosphorus compounds also point to C-O fission, but this reaction is favoured by interaction of an unprotonated Nε2 with the carbon atom of the bond involved (Toia and Casida, 1979). On the other hand, ageing of diphenyl phosphoryl Chymo is favoured by high pH; here it proceeds via P-O fission due to a nucleophilic attack of the imidazole group on the phosphoryl group (Wedler, 1968; Bender and Wedler, 1972). Apparently, the mechanism of ageing depends on the substituents at the phosphorus atom (Cf. Aldridge, 1975).

Fission of an alkyl-oxygen bond in phosphate esters proceeds by a nucleophilic substitution reaction in which a unimolecular (S_N1) or a bimolecular (S_N2) character may dominate dependent on the involvement

of the solvent (Hine, 1962; Breslow, 1969; Ingold, 1969; Badea, 1977). Ageing of DP-enzymes according to an S_N1 type reaction will lead to formation of an isopropyl carbenium ion which may react with water to yield isopropanol, may be captured by other nucleophilic reactants present in the protein or solution, or may loose a proton to give propene (Breslow, 1969; Badea, 1977). In ageing according to an S_N2 type reaction, attack of a solvent molecule displaces the phosphorylated enzyme from the secondary carbon atom and only isopropanol is formed. Table VI shows that invariably both propene as well as isopropanol were formed; no other products were found. This unambiguously proves that ageing in all three enzymes has at least some S_N1 character.

From data on the effect of temperature on the rate of ageing (Berends, 1964) it can be calculated that ageing of DP-Chymo is associated with an enthalpy of activation of 18.5 kcal/mole, while the entropy of activation is -25.4 cal/mole K. The value of the enthalpy is characteristic for S_N2 displacement by water at the saturated carbon atom (Hudson and Keay, 1956; Barnard et al., 1961). The value of the entropy is too large for a unimolecular reaction (Schaleger and Long, 1963) and corresponds with the value resulting from immobilization of a water molecule (Barnard et al., 1961; Kirby and Warren , 1967). Together with the data in Table VI this suggests that in the case of DP-Chymo the isopropanol formed results from ageing with a mainly bimolecular (S_N2) character.

The amount of propene increases in the sequence Chymo<Sub<AtrE, whereas the amount of isopropanol decreases (Table VI). In the same order an increase is seen in the difference between the amount of propene and isopropanol found and the total amount of products expected upon complete ageing (Table VI). Since there are no indications for binding sites with a high affinity for isopropanol in serine enzymes (Glazer, 1966), the result is only compatible with an enhanced unimolecular nature of ageing for which such a loss may be expected because of the high reactivity of the carbenium ion towards nucleophilic centres (Breslow, 1969; Badea, 1977). Replacement of the citrate buffer by sodium sulphate, which can be regarded as chemically almost inert with respect to carbenium ions (Cf. Badea, 1977), did not appreciably

decrease the deficit. Consequently, if the loss in isopropyl groups results from reaction of carbenium ions with nucleophilic sites on the protein, the S_N1 contribution to ageing of Sub and AtrE will be larger than is indicated by the amount of propene found. Such a loss has in fact been observed for the ageing of neurotoxic esterase inhibited with DFP (Clothier and Johnson, 1979). In the case of Chymo phosphylated with saligenic cyclic phosphorus compounds also ageing by C-O fission has been reported to give binding of released groups at the protein (Toia and Casida, 1979).

The data in Table VI in combination with the above considerations point to a shift in the ageing reaction from a mainly bimolecular reaction in the case of DP-Chymo to one with an appreciable unimolecular character when DP-Sub and DP-AtrE are concerned. This apparently leads to a substantial increase in k_a^m (Table VII). In other words, the larger k_a^m of Sub and AtrE compared with Chymo results from a larger ionizing power of the immediate environment of the scissile C-O bond in these enzymes.

The tertiary structure of DP-Chymo and DP-Sub suggests that in these enzymes the solvent-exposed isopropyl group which is supposed to be lost during ageing will not be subjected to different sterical constraints imposed by non-bonding interactions with the protein moiety and that an isopropyl carbenium ion formed will be accessible for solvation to the same extent in either protein. Besides, in all three cases the MP-enzyme anion per se will be an equally good leaving group because the negative charge developed will become involved in p_π-d_π bonding with the phosphorus in the same way (Kirby and Warren, 1967). Consequently, the difference in ionizing power between Chymo and the other enzymes results most likely from stabilization of this anion by hydrogen bonding and/or non-bonding interactions between the protein and the phosphoryl substituent.

Trialkyl phosphates show an increasing contribution to hydrolysis by the S_N1 mechanism with increasing electron release from the alkyl substituents towards the ester oxygens (Barnard et al., 1961; Cox and Ramsay, 1964; Hudson, 1965). Hydrogen bonding at the oxygen of the scissile C-O bond in DP-enzymes will promote this electron drift to-

wards the oxygen and therefore may facilitate ageing by the S_N1 mechanism (Breslow, 1969; Ingold, 1969). The pK_a-values of DP-Sub and DP-AtrE (Table VII) are larger than that of Chymo, pointing to weaker hydrogen bonding in the last-mentioned enzyme (Jaffé et al., 1954). This is consistent with a larger amount of S_N1 character in the ageing of the first two enzymes. Since the increase in the polarity of the scissile C-O bond by hydrogen bonding at the phosphoryl oxygen will be very small and because C-O fission by S_N1 is not affected by changing the substitution of the phosphorus in dialkylphosphonates (Hudson and Keay, 1956), the contribution of hydrogen bonding at other oxygens of the phosphoryl substituent to stabilization of the anion will be relatively small.

Like pK_a, the difference between the chemical shift of the DP-species at high pH (Table II) and that of the corresponding aged enzyme (Table IV) increases in the order Chymo<Sub<AtrE (Table VII). The parallelism between this increase in a measure for additional non-bonding interactions upon ageing (see b) and that in k_a^m (Table VII) is consistent with a substantial contribution to the S_N1 rate by stabilization of the anion by non-bonding interactions.

The above considerations suggest that the larger contribution of the S_N1 reaction to ageing of Sub and AtrE may result from an increased stabilization of the anion by hydrogen bonding with the histidine and non-bonding interactions between the remaining isopropoxy group and the protein in the transition state. As the analysis of the NMR data shows (see b), at least in the case of AtrE and Sub, the former interaction will be weakened whereas the latter becomes stronger in the course of the ageing reaction.

d. Comparison of Atropinesterase with Serine Proteases

Previous investigations by means of fluorescence (Van der Drift et al., 1983[c]) and ESR spectrometry (Van der Drift et al., 1981; 1983[a]) as well as kinetic methods (Van der Drift and Roos, 1983[b]) pointed to a structural resemblance of the active sites of AtrE and the serine proteases, e.g. the presence of a particular histidine and an apolar primary binding site. The present data support these results

and allow a more detailed comparison between the enzymes. The titration behaviour of the chemical shift indicates the presence of a particular histidine at the active site of AtrE with a pK_a=7.6 and, since it may form a hydrogen bond with the scissile C-O bond after protonation, with a position characteristic for a histidine in a charge-relay system. Like in Chymo and Sub this hydrogen bond is a prerequisite for the occurrence of ageing via C-O fission.

In AtrE and Sub ageing has more an S_N1 character than in Chymo where the S_N2 character dominates. Hydrolysis of phosphate esters by acid-catalysed unimolecular alkyl-oxygen fission proceeds through the ionic conjugate acid of the ester (Ingold, 1969). The unimolecular character of ageing via hydrogen bonding between the protonated histidine and the hydrolysable C-O bond therefore points to proton transfer from the histidine to the oxygen of this C-O bond at some stage of the reaction. This transfer is possible only if the histidine is in the conjugate acid form, i.e. present as a cationic acid. Thus the proton, which in the charge-relay system of Chymo and Sub is known to be involved in hydrogen bonding between Nδ1 of the histidine and the β-carboxyl group of the aspartic acid (Kraut, 1977), may reside on the histidine during ageing and does not migrate to the aspartic acid upon protonation of Nε2 (Cf. Blow et al., 1969; Hunkapiller et al., 1973). This agrees with other observations which indicate that upon protonation the charge-relay system in these enzymes is characterized by a positive histidine (Glazer, 1968; Bachovchin and Roberts, 1978; Markley, 1979; Hamilton and Zerner, 1981; Kossiakoff and Spencer, 1981). A positive histidine in the active site of AtrE involved in ageing therefore is consistent with the presence of a charge-relay system similar to Chymo and Sub.

The hydrogen bonding at the phosphoryl oxygen with the protein indicates the presence of an oxy-anion hole in AtrE, positioned similarly with respect to the active serine as in proteases of the prothrombin-related superfamily and the subtilisins.

Besides these hydrogen-bonding interactions there is a non-bonding interaction of the non-hydrolysable isopropyl group with the primary binding pocket in DP-Chymo and DP-Sub, which is not manifest in

DP-AtrE. However, the large increase in the chemical shift upon conversion of DP-AtrE into MP-AtrE points to an appreciable increase in non-bonding interactions between the non-hydrolysable isopropyl group and the protein. The chemical shift of MP-AtrE approximates that of MP-Chymo (Table IV). These results agree with the presence of a binding hole in which the remaining isopropyl group is inserted after ageing.

In conclusion the data obtained are consistent with the presence of a charge-relay system, an oxy-anion hole, and a primary binding site in the active-site region of AtrE. Since there is no homology between the primary structures of AtrE and the serine proteases, this structural similarity is a strong indication of convergent molecular evolution for these different types of hydrolases.

REFERENCES

Aldridge, W.N. (1975) Croat. Chem. Acta 47, 225.
Amitai, G., Ashani, Y., Gafni, A., and Silman, I. (1982) Biochemistry 21, 2060.
Bachovchin, W.W., and Roberts, J.D. (1978) J. Am. Chem. Soc. 100, 8041.
Badea, F. (1977) Reaction Mechanisms in Organic Chemistry, Abacus Press, Tunbridge Wells.
Barnard, P.W.C., Bunton, C.A., Llewellyn, D.R., Vernon, C.A., and Welch, V.A. (1961) J. Chem. Soc. 2670.
Bell, J.V., Heisler, J., Tannenbaum, H., and Goldenson, J. (1954) J. Am. Chem. Soc. 76, 5185.
Bender, M.L., and Wedler, F.C. (1972) J. Am. Chem. Soc. 94, 2101.
Berends, F. (1964) Ph.D. Thesis, University of Leiden.
Berends, F., Rörsch, A., and Stevens, W.F. (1967) in: Proceedings of the Conference on Structure and Reactions of DFP Sensitive Enzymes (Heilbronn, E., Ed.), p. 45, Försvarets Forskningsanstalt, Stockholm.
Blackburn, G.M., Cohen, J.S., and Lord Todd (1964) Tetrahedron Lett., 2873.
Blackburn, G.M., Cohen, J.S., and Weatherall, I. (1971) Tetrahedron 27, 2903.
Blow, D.M., Birktoft, J.J., and Hartley, B.S. (1969) Nature (London) 221, 337.
Bock, J.L. (1976) Ph.D. Thesis, Yeshiva University, New York.
Breslow, R. (1969) Organic Reaction Mechanisms 2nd Ed., W.A. Benjamin, Inc., New York.
Brill, A.S. (1977) Transition Metals in Biochemistry (Molecular Biology Biochemistry and Biophysics 26) Springer Verlag, Berlin.
Chambers, J.L., and Stroud, R.M. (1979) Acta Crystallogr. Sect. B. 26, 1861.
Clothier, B., and Johnson, M.K. (1979) Biochem. J. 177, 549.
Cohen, J.A., Oosterbaan, R.A., Warringa, M.G.P.J., and Jansz, H.S. (1955) Discuss. Faraday Soc. 20, 114.
Cohn, M., and Rao, B.D.N. (1979) Bull. Magn. Res. 1, 38.
Cox Jr., J.R., and Ramsay, O.B. (1964) Chem. Revs. 64, 317.
Cruickshank, D.W.J. (1961) J. Chem. Soc., 5486.
Crutchfield, M.M., Dungan, C.H., and Van Wazer, J.R. (1967) in P^{31} Nuclear Magnetic Resonance (Topics in Phosphorus Chemistry, Vol.5; Grayson, M. and Griffith, E.J., Eds.) p. 1, Interscience Publishers, New York.
Cunningham, L.W., and Brown, C.S. (1956), J.Biol.Chem. 221, 433.
Edsall, J.T., and Wyman, J. (1958) Biophysical Chemistry Vol. 1, Academic Press, New York.

Ernst, R. (1966) Adv. Magn. Res. 2, 1.
Fehlhammer, H. Bode, and Huber, R. (1977) J. Mol. Biol. 111, 415.
Freer, S.T., Kraut, J., Robertus, J.D., Wright, H.T., and Xuong, Ng.H. (1970) Biochemistry 9, 1997.
Gerlach, E., and Deuticke, B. (1963) Biochem. Z. 337, 477.
Gillespie, R.J. (1972) Molecular Geometry, Van Nostrand Reinhold Company Ltd., London.
Glazer, A.N. (1966) Biol. Chem. 241, 635.
Glazer, A.N. (1967) J. Biol. Chem. 242, 433.
Glazer, A.N. (1968) J. Biol. Chem. 243, 3693.
Gorenstein, D.G. (1975) J. Am. Chem. Soc. 97, 898.
Gorenstein, D.G., and Kar, D. (1975) Biochem. Biophys. Res. Comm. 65, 1073.
Gorenstein, D.G., and Findlay, J.B. (1976) Biochem. Biophys. Res. Comm. 72, 640.
Gutowsky, H.S., and Larmann, J. (1965) J. Am. Chem. Soc. 87, 3815.
Halpern, E., Bouck, J., Finegold, H., and Goldenson, J. (1955) J. Am. Chem. Soc. 77, 4472.
Hamilton, S.E., and Zerner, B. (1981) J. Am. Chem. Soc. 103, 1827.
Hartley, B.S. (1960) Ann. Rev. Biochem. 29, 45.
Heilbronn-Wikström, E. (1965) Svensk Kem. Tid. 77, 11.
Henderson, R. (1970) J. Mol. Biol. 54, 341.
Hine, J. (1962) Physical Organic Chemistry, Mc.Graw-Hill Book Company Inc., New York.
Huber, R., and Bode, W. (1977) in NMR in Biology (Dwek, R.A., Campbell, I.D., Richards, R.E., and Williams, R.J.P., Eds) p. 1, Academic Press, New York.
Hudson, R.F., and Keay, L. (1956) J. Chem. Soc., 2463.
Hudson, R.F., and Keay, L. (1960) J. Chem. Soc., 1859.
Hudson, R.F. (1965) Structure and Mechanism in Organo-Phosphorus Chemistry, Academic Press, New York.
Hunkapiller, M.W., Smallcombe, S.H., Whitaker, D.R., and Richards, J.H., (1973) Biochemistry 12, 4732.
Ingold, C.K. (1969) Structure and Mechanism in Organic Chemistry, 2nd Edition, Cornell University Press, Ithaca.
Ionin, B. (1968) J. Gen. Chem. USSR 38, 1618.
Jaffé, H.H., Freedman, L.D., and Doak, G.O. (1954) J. Am. Chem. Soc. 76, 1548.
Joesten, M.D., and Schaad, L.J. (1974) Hydrogen Bonding, Marcel Dekker Inc., New York.
Karplus M., and Das, T.P. (1961) J. Chem. Phys. 34, 1683.
Keyer, J.H. (1971) Ph.D. Thesis, University of Leiden.
Keyer, J.H., Wolring, G.Z., and De Jong, L.P.A. (1974) Biochim. Biophys. Acta 334, 146.
Kienhuis, H., and Baar, J.A.J. (1964) Internal report Prins Maurits Laboratory TNO, Rijswijk, The Netherlands.
Kirby, A.J., and Warren, S.G. (1967) The Organic Chemistry of Phosphorus (Reaction Mechanisms in Organic Chemistry, Vol. 5), Elsevier, Amsterdam.
Kollman, P.A. (1977) in Applications of Electronic Structure Theory (Modern Theoretical Chemistry, Vol. 4; Schaefer III, H.F., Ed.) p. 109, Plenum Press, New York.
Kossiakoff, A.A., Chamberş, J.L., Kay, L.M., and Stroud, R.M. (1977) Biochemistry 16, 654.
Kossiakoff, A.A., and Spencer, S.A. (1981) Biochemistry 20, 6462.
Kraut, J. (1977) Ann. Rev. Biochem. 46, 331.
Letcher, J.H., and Van Wazer, J.R. (1967) in P^{31} Nuclear Magnetic Resonance, (Topics in Phosphorus Chemistry, Vol. 5; Grayson, M., and Griffith, E.J., Eds.) p. 75, Interscience Publishers, New York.
Mark, V., Dungan, C.H., Crutchfield, M.M., and Van Wazer, J.R. (1967) in P^{31} Nuclear Magnetic Resonance (Topics in Phosphorus Chemistry, Vol. 5; Grayson, M., and Griffith, E.J., Eds.) p. 227, Interscience Publishers, New York.
Markley, J.L. (1978) Biochemistry 17, 4648.
Markley, J.L. (1979) in Biological Applications of Magnetic Resonance (Shulman, R.G., Ed.) p. 397, Academic Press, New York.
Markley, J.L., and Ibanez, I.B.(1978) Biochemistry 17, 4627.
Matthews, D.A., Alden, R.A., Birktoft, J.J., Freer, S.T., and Kraut, J., (1977) J. Biol. Chem. 252, 8875.
Mavel, G. (1973) in Ann. Reports on NMR Spectroscopy Vol. 5B, (Mooney, E.F., Ed.), p. 1, Academic Press, New York.

Mavridis, A., Tulinkski, A., and Liebman, M.N. (1974) Biochemistry 13, 3661.
Meadows, D.H. (1972) in Methods in Enzymology Vol. XXVI (Hirs, C.H.W. and Timasheff, S.N., Eds) p. 638, Academic Press, New York.
Muller, N., Lauterbur, P.C., and Goldenson, J. (1956) J. Am. Chem. Soc. 78, 3557.
Olah, G.A., and McFarland, C.W. (1971) J. Org. Chem. 36, 1374.
Oosterbaan, R.A., Kunst, P., and Cohen, J.A. (1955) Biochim. Biophys. Acta 16, 299.
Oosterbaan, R.A. et al. (1983) to be published.
Porubcan, M.A., Neves, D.E., Rausch, S.K., and Markley, J.L. (1978) Biochemistry 17, 4640.
Porubcan, M.A., Westler, W.M., Ibanez, I.B., and Markley, J.L. (1979) Biochemistry 18, 4108.
Purdela, D. (1971) J. Magn. Res. 5, 23.
Reeck, G.R., Nelson, T.B., Paukstelis, J.V., and Mueller, D.D. (1977) Biochem. Biophys. Res. Comm. 74, 643.
Riddick, J.A., and Bunger, W.B., (1970): Organic Solvents, 3th Edition (Techniques of Chemistry, Vol. II), Wiley Interscience, New York.
Robillard, G., and Shulman, R.G. (1974) J. Mol. Biol. 86, 541.
Rörsch, A., Berends, F., Bartlema, H.C., and Stevens, W.F.(1971), Proc. Koninkl. Nederl. Akademie van Wetenschappen, Series C, Vol. 74, No.2, 132.
Saika, A., and Slichter, C.P. (1954) J. Chem. Phys. 22, 26.
Schaffer, N.K., May, C.S., and Summerson, W.H. (1953) J. Biol. Chem. 202, 67.
Schaffer, N.K., May, C.S., and Summerson (1954) J. Biol. Chem. 206, 201.
Schaleger, L.L., and Long, F.A. (1963) Adv. Phys. Org. Chem.1, 1.
Singleton Jr., R. (1973) J.Chem.Ed. 50, 538.
Sober, H.A., Ed. (1970) Handbook of Biochemistry 2nd Edition, The Chemical Rubber Co., Cleveland.
Steffen, M. (1970) Ber. Bunsenges. Phys. Chem. 74, 505.
Steitz, T.A., and Shulman, R.G. (1982) Ann. Rev. Biophys. Bioeng. 11, 419.
Stevens, W.F. (1969) Ph.D. Thesis, University of Leiden.
Strehlow, H., (1968) Magnetische Kernresonanz und Chemische Struktur, 2.erw. Aufl., Dr. Dietrich Steinkopff Verlag, Darmstadt.
Stroud, R.M. (1979) quoted in Porubcan et al. (1979).
Stroud, R.M., Kay, L.M., and Dickerson, R.E. (1974) J. Mol. Biol. 83, 185, 209.
Toia, R.F., and Casida, J.E. (1979) Biochem. Pharmacology 28, 211.
Usdin, E. (1970) in Anticholinesterase Agents (Encyclopedia of Pharmacology and Therapeutics, Section 13, Vol. 1; Karczmar, A.G., Ed.) p. 249, Pergamon Press, Oxford.
Van der Drift, A.C.M., Moes, G.W.H., Van der Drift, E., and Rousseeuw, B.A.C., (1983[a]) This Thesis, Chapter 5; to be submitted for publication.
Van der Drift, A.C.M., and Roos, A.L.M. (1983[b]) This Thesis, Chapter 4; to be submitted for publication.
Van der Drift, A.C.M., Roos, A.L.M., and Moes, G.W.H. (1983[c]) This Thesis, Chapter 2; to be submitted for publication.
Van der Drift, A.C.M., Rousseeuw, B.A.C., and Van der Drift, E. (1981) Bull. Magn. Res. 2(1-4), 208.
Wagner, E.L. (1963) J. Am. Chem. Soc. 85, 161.
Wedler Jr., F.C.O. (1968) Ph.D. Thesis, Northwestern University.
West, R.C., Ed. (1976) Handbook of Chemistry and Physics 55th Edition, C.R.C. Press, Cleveland.
Wright, H.T. (1973) J. Mol. Biol. 79, 1,13.

SUMMARY

The present thesis deals with a physico-chemical investigation of atropinesterase (AtrE), a bacterial serine hydrolase isolated from Pseudomonas putida PMBL-1. This enzyme specifically catalyses the hydrolysis of the ester bond in (-)-atropine. In contrast to serine proteases it has no proteolytic activity and is therefore regarded as a true esterase. As AtrE does not show sequence homology with any other serine hydrolase it belongs to a separate superfamily of these enzymes. However, the absence of homology between enzymes of a comparable function does not preclude a close resemblance in the spatial organization of their active-site regions.

The objective of the investigation has been to characterize the conformation of AtrE, in particular to explore whether and, if so, to what extent the structure of its active-site region resembles that of the serine proteases. To this end attention has been focused on the exploration of those structural elements in the active-centre region of AtrE which are known to form the structural basis of the catalytic activity of serine proteases, i.e. a primary binding site near the active serine, a charge-relay system and an oxy-anion hole.

As direct characterization of the tertiary structure by X-ray diffraction was not feasible, indirect methods had to be applied. For the investigation of the overall conformation (size, shape and hydration) velocity and equilibrium sedimentation techniques performable in the analytical ultracentrifuge were used; for the characterization of the active-site region, various spectroscopic and kinetic methods were applied. This characterization has been performed in a comparison with serine proteases of a well-known active-site structure, viz. with α-chymotrypsin (Chymo) as a representative of the prothrombin-related proteases and with subtilisin A (Sub) representing the superfamily of subtilisins. For the spectroscopic investigations fluorescence, ESR and ^{31}P NMR spectrometry were applied. These techniques could be used because of the fact that suitable fluorescent, paramagnetic and nuclear magnetic reporter groups could be specifically attached to the side chain of the active serine residue in all enzymes. Reporter groups employed were: the fluorescent dansyl group, a sulphonylated

phenyl and naphthyl core both having a nitroxide spin label-containing substituent, and the diisopropyl phosphoryl (DP) group as a nuclear spin probe. The NMR study on the DP-enzymes was extended by an investigation of the "ageing" reaction, i.e. the spontaneous protein-assisted release of one isopropyl group. Information on the mechanism of this reaction was obtained by means of mass spectrometry. In the kinetic studies a comparison was made between enzymes of the reaction with dansyl fluoride and of the ageing in DP-enzymes by means of steady-state methods.

The hydrodynamic investigations (Chapter 1) show that AtrE is a globular protein consisting of a single polypeptide chain with a molecular weight of about 30,000. In aqueous solution under non-denaturing conditions it occurs predominantly as a dimer which hydrodynamically behaves as a rigid, impenetrable hydrated particle of ellipsoidal shape. Under denaturing conditions dissociation into monomers takes place. Indications were obtained that dimerization of AtrE results from side-by-side association of two ellipsoidal monomers rather than from end-to-end association. Analysis of the monomer-dimer equilibrium at various temperatures suggested a negligible temperature dependence of this process between 9 ^{o}C and 25 ^{o}C.

The comparative studies by means of the different spectroscopic techniques indicated that the active-site region of AtrE contains besides the active serine also other structural elements which characterize the active-site regions of serine proteases. Fluorescence (Chapters 2 and 3), ESR (Chapter 5) and to a somewhat lesser extent also ^{31}P NMR (Chapter 6) spectrometry pointed to the presence of a pocket-shaped rather apolar binding site near the active serine. The results indicated that in AtrE this apolar binding site is larger than in the two proteases. The inactivation of AtrE and *Chymo* by dansyl fluoride was studied in detail; both reactions were found to proceed via the formation of a reversible complex followed by a monomolecular sulphonylation step (Chapter 4). The thermodynamic parameters of both steps differed for the two enzymes in a manner consistent with a larger apolar binding pocket in AtrE. The pH-dependence of the fluorescence emission parameters of the dansyl group (Chapter 2) and of the ^{31}P chemical shift of the DP-group (Chapter 6) indicated the presence in

AtrE of a titratable group near the active serine with a $pK_a > 7$. Such a group with similar pK_a is present in the serine proteases where it is the histidine of the charge-relay system. The result therefore suggests that AtrE, too, contains such a histidine residue. DP-AtrE as well as DP-Sub were found to show ageing, as was already known for DP-Chymo. The rate of ageing of DP-AtrE was higher than that of the other DP-enzymes and approached that of DP-cholinesterase. Indications were obtained that in all cases the process was assisted by the protonated histidine at the active centre. Mass-spectrometric investigation of the dealkylation products (after ageing in $H_2{}^{18}O$) indicated an appreciably larger amount of S_N1 character of this process in AtrE and Sub than in Chymo. These results were indicative of the fact that the histidine in the active centre of AtrE has a position and properties similar to that in the charge-relay system of serine proteases. The pK_a of this histidine in inhibited AtrE, however, was somewhat higher than in labelled Chymo or Sub. The ^{31}P chemical shift of the DP-group in DP-AtrE (Chapter 6) revealed the occurrence of hydrogen bonding between the phosphoryl oxygen and the protein, which points to the presence of an oxy-anion hole in AtrE, similarly positioned with respect to the active serine as in the prothrombin-related serine proteases and in the subtilisins.

On the basis of these results it has been concluded that the active-site region of AtrE contains the same structural elements as the active centre of the serine proteases, viz. an apolar substrate binding pocket, a charge-relay system and an oxy-anion hole. Such a structural resemblance suggests that esterolysis by AtrE proceeds by essentially the same mechanism as hydrolysis by the serine proteases. In the process of ester hydrolysis the tropic acid moiety in (-)-atropine will require a specific binding site during acylation; a large apolar binding pocket in AtrE is therefore conceivable in view of the bulky size of this group and its mainly hydrophobic character. As, from an evolutionary point of view, AtrE is not related to any known serine protease, the above similarity between the tertiary structure of the active-site region of this esterase and members of the two superfamilies of serine proteases strongly suggests that the functional structure of serine hydrolases is the result of a convergent molecular evolution.

INLEIDING TOT DE SAMENVATTING VOOR NIET-VAKGENOTEN

Eiwitten of proteïnen zijn grote, in de natuur voorkomende moleculen die velerlei functies kunnen hebben. Zij zijn opgebouwd uit één of meer lange ketens van kleinere eenheden, de aminozuren. De verbinding tussen twee aminozuren in zo'n keten noemt men peptidebinding. Er zijn ongeveer 20 verschillende aminozuren bekend, waaronder serine, histidine en asparaginezuur.

De volgorde van de aminozuren in een eiwit wordt de primaire structuur genoemd. Wanneer zo'n keten van aminozuren net zoals bij een schroefveer rond een denkbeeldige as is gewonden spreekt men van secundaire structuur. De tertiaire (ruimtelijke) structuur ontstaat doordat de secundaire structuur weer op een speciale manier is opgevouwen. De functie van een eiwit wordt bepaald door zijn totale structuur. Bij een gehele of gedeeltelijke verstoring van deze structuur (denaturatie) is een eiwit meestal niet meer in staat zijn functie uit te oefenen.

Enzymen zijn eiwitten die de vorming of verbreking van bepaalde chemische verbindingen bewerkstelligen. Zo zijn er enzymen die specifiek peptidebindingen splitsen; dit zijn de z.g. proteasen, die door deze eigenschap eiwit-afbrekende enzymen zijn welke bij een groot aantal processen in de natuur een belangrijke rol spelen. Diverse spijsverteringsenzymen, zoals pepsine en trypsine, zijn proteasen, maar ook verschillende enzymen die betrokken zijn bij het ontstaan van bloedstolsels en het weer oplosbaar maken daarvan behoren tot de proteasen. Enzymen die specifiek de splitsing van esterbindingen bewerkstelligen noemt men esterasen (een esterbinding ontstaat wanneer een alcohol en een zuur een chemische binding aangaan). Soms kan een enzym meer dan één type binding helpen vormen of verbreken. Zo hebben sommige proteasen ook esterase-activiteit. Het gedeelte van een enzym dat rechtstreeks bij het proces van verbreken of vormen van bindingen is betrokken noemt men het actieve centrum. Bij de z.g. serine-enzymen wordt het actieve centrum gekenmerkt door de aanwezigheid van een bijzonder reactieve serine (de actieve serine) die essentieel is voor de werking van deze enzymen. Goed onderzochte serine-enzymen zijn de proteasen α-chymotrypsine (Chymo) en subtilisine A (Sub), die behalve de

peptidebinding tussen bepaalde aminozuren ook sommige esterbindingen kunnen splitsen.

Sommige proteasen hebben een onderling verschillende werking en ook hun primaire structuur vertoont verschillen. Toch lijken de aminozuurvolgorden nog zoveel op elkaar (d.w.z. vertonen homologie) dat aangenomen wordt dat ze van hetzelfde oer-enzym afstammen, maar zich tijdens de evolutie van het leven op aarde verschillend ontwikkeld hebben. De primaire structuur van Chymo vertoont echter geen homologie met die van Sub. Dit duidt erop dat deze enzymen, die een vrijwel gelijke functie bezitten, zich in de loop van de evolutie onafhankelijk van elkaar hebben ontwikkeld uit verschillende oer-enzymen. Chymo en Sub zijn daarom ingedeeld in twee verschillende groepen (superfamilies) van serine-proteasen waartussen, evolutionair gezien, geen verwantschap bestaat.

Uit onderzoek van de tertiaire structuur van Chymo en Sub blijkt dat de werking van deze enzymen berust op de aanwezigheid van een beperkt aantal structureel gelijksoortige elementen in het actieve centrum. Dit zijn: een "charge-relay"-systeem, een "oxy-anion"-holte en een bindingsholte die bepaalt welke peptide- of esterbinding gesplitst kan worden. Het eerste element wordt gevormd door een drietal aminozuren, t.w. een asparaginezuur, een histidine en de actieve serine, die in de primaire structuur ver van elkaar liggen, maar door de vouwing van de polypeptide keten in de tertiaire structuur zo dicht bij elkaar zijn gebracht dat zij elkaars eigenschappen sterk kunnen beïnvloeden. Dit element bewerkstelligt de eigenlijke splitsing van de chemische binding in het substraat. De twee andere elementen zijn instulpingen in het enzymoppervlak die elk een bepaald deel van het substraat zodanig binden dat de splitsing optimaal kan verlopen.

Behalve serine-proteasen bestaan er ook serine-esterasen. De manier waarop deze de splitsing van esterbindingen tot stand brengen lijkt waarschijnlijk erg veel op de wijze waarop de serine-proteasen werken. Over de tertiaire structuur van deze esterasen is veel minder bekend. Zo is niet bekend in hoeverre de structuur van het actieve centrum van deze enzymen overeenkomt met die van de proteasen. Het is zinvol om te trachten hier meer over te weten te komen omdat we op die manier wellicht beter gaan begrijpen hoe de werking van een enzym af-

hangt van zijn structuur. Verwacht mag worden dat deze kennis op den duur van nut zal zijn bij het ontwikkelen en verbeteren van industriële processen waarbij enzymen zijn betrokken en bij de ontwikkeling van nieuwe geneeskundige behandelingen. Deze interesse voor de relatie tussen de structuur en werking van een enzym is een belangrijke drijfveer geweest voor het in dit proefschrift beschreven onderzoek, waarbij op verschillende manieren is nagegaan of de tertiaire structuur van het serine-esterase "atropine-esterase" (AtrE) lijkt op die van de serine-proteasen. Hierbij werd een aantal eigenschappen van AtrE onderzocht, elk met een aparte techniek, waarbij ter vergelijking ook Chymo en Sub werden bestudeerd. Zoals uit de samenvatting blijkt geven de resultaten van deze onderzoekingen aan dat het actieve centrum van dit serine-esterase dezelfde structurele kenmerken bezit als het actieve centrum van de serine-proteasen.

SAMENVATTING

Atropine-esterase (AtrE) afkomstig uit de bacteriestam Pseudomonas putida PMBL-1 is een serine-enzym. Het splitst specifiek de esterbinding in (-)-atropine. In tegenstelling tot de serine-proteasen α-chymotrypsine (Chymo) en subtilisine A (Sub) vertoont het geen proteolytische activiteit. Het is derhalve een zuiver esterase.

Het is bekend dat de primaire structuur van AtrE geen homologie vertoont met die van andere, bekende serine-enzymen. Er lijkt evenmin overeenkomst te bestaan in de secundaire structuur. Dit wijst erop dat AtrE de representant is van een nieuwe superfamilie van serine-enzymen, die in een aparte evolutionaire ontwikkeling tot stand is gekomen.

Tussen Chymo en Sub, die elk één van de twee bekende superfamilies van serine-proteasen vertegenwoordigen, ontbreekt elke overeenkomst in de primaire en secundaire structuur; desondanks wordt het actieve centrum van deze enzymen door een beperkt aantal gelijksoortige structurele elementen gekenmerkt. Deze elementen, die essentieel zijn voor de katalytische activiteit en waarop de functionele overeenkomst tussen deze proteasen berust, zijn een "charge-relay"-systeem, een "oxy-anion"-holte en een bindingsholte die de specificiteit voor

het substraat bepaalt. Het is niet bekend of deze elementen ook in het actieve centrum van serine-esterasen voorkomen.

Het doel van het in dit proefschrift beschreven onderzoek was het nader karakteriseren van de tertiaire structuur van AtrE, in het bijzonder de structuur van het actieve centrum, ten einde vast te stellen in hoeverre dit esterase op dit punt overeenkomt met de serine-proteasen. Omdat als gevolg van het ontbreken van kristallen een directe karakterisering van de driedimensionale structuur m.b.v. röntgendiffractie niet mogelijk was, is het onderzoek uitgevoerd met indirecte methoden, t.w. hydrodynamische, spectroscopische en kinetische methoden.

Uit het hydrodynamische onderzoek, dat is uitgevoerd m.b.v. de analytische ultracentrifuge (Hoofdstuk 1), blijkt dat AtrE een globulair eiwit is bestaande uit één polypeptideketen met een molecuulgewicht van ongeveer 30.000. In oplossing komt het onder niet-denaturerende omstandigheden voornamelijk als dimeer voor. In hydrodynamisch opzicht gedraagt dit dimeer zich als een niet-doordringbaar, gehydrateerd ellipsoïdaal deeltje. Bij denaturatie treedt splitsing in monomeren op. Uit de splitsing onder invloed van natrium dodecyl sulfaat zijn aanwijzingen gevonden dat het dimeer bestaat uit twee ellipsoïdale monomeren, die naast elkaar liggen en niet in elkaars verlengde. De associatie lijkt weinig afhankelijk te zijn van de temperatuur.

De nadere karakterisering van de structuur van het actieve centrum is uitgevoerd met behulp van fluorescentie-, ESR- en ^{31}P NMR-spectrometrie. De toepassing van deze technieken was mogelijk door specifiek fluorescerende, paramagnetische of kernmagnetische "reporter"-groepen te koppelen aan de hydroxylgroep in de zijketen van de actieve serine. Hiervoor werden reporter-groepen gekozen die gevoelig zijn voor verschillende kenmerken van hun directe omgeving. Aangezien de gebruikte reporter-groepen bij andere serine-enzymen op dezelfde wijze konden worden ingebracht was het mogelijk om het actieve centrum van AtrE te vergelijken met dat van Chymo en Sub, o.a. op de mogelijke aanwezigheid van de drie genoemde structurele elementen. Bij het ^{31}P NMR-onderzoek werd tevens gebruik gemaakt van massaspectrometrie om de reactie te bestuderen waarbij de reporter-groep één van zijn alkylgroepen verliest ("veroudering") als gevolg van een speciale wissel-

werking met het eiwit. Daarnaast is tevens vergelijkend kinetisch onderzoek uitgevoerd van de reactie van Chymo en AtrE met een irreversibele remmer, om ook langs die weg inzicht te krijgen in de structuur van het actieve centrum.

Zowel uit het fluorescentieonderzoek (Hoofdstukken 2 en 3) als uit het onderzoek m.b.v. ^{31}P NMR en massaspectrometrie (Hoofdstuk 6) komen sterke aanwijzingen dat AtrE behalve de actieve serine ook eenzelfde speciale histidine in het actieve centrum heeft als Chymo en Sub waarbij dit aminozuur deel uitmaakt van het "charge-relay"-systeem. In geremd AtrE lijkt deze histidine iets gemakkelijker geprotoneerd te worden dan in geremd Chymo en Sub. Uit het fluorescentie- en ESR-onderzoek (Hoofdstuk 5) blijkt dat zich vlak bij de actieve serine in AtrE een apolaire bindingsholte bevindt die groter is dan die in Chymo en Sub. Gegevens verkregen uit het kinetische onderzoek (Hoofdstuk 4) zijn eveneens in overeenstemming met een grotere holte in AtrE dan in Chymo. De aanwezigheid van een bindingsholte vlakbij de actieve serine in AtrE volgt ook uit de resultaten van het NMR-onderzoek, waarin bovendien duidelijke aanwijzingen werden verkregen voor de aanwezigheid van een "oxy-anion"-holte.

De resultaten wijzen erop dat in het actieve centrum van AtrE dezelfde structurele elementen aanwezig zijn als in het actieve centrum van serine-proteasen. Dit duidt erop dat splitsing van de esterbinding door AtrE volgens hetzelfde mechanisme verloopt als de splitsing van peptidebindingen door proteasen. Dit zou betekenen dat er bij de serine-esterasen t.o.v. de serine-proteasen een convergente moleculaire evolutie heeft plaatsgevonden, d.w.z. de natuur heeft voor het uitvoeren van vergelijkbare functies in de loop der tijd sterk overeenkomstige structuren ontwikkeld.

NAWOORD

Gaarne wil ik op deze plaats uitdrukking geven aan mijn erkentelijkheid jegens allen die in de loop der tijd op enigerlei wijze hebben bijgedragen aan de totstandkoming van dit proefschrift. Slechts dankzij de morele en daadwerkelijke steun die ik van velen heb mogen ondervinden bij het uitvoeren van het experimentele werk, bij het verwerken van de resultaten en bij het verwoorden van de uitkomsten en het gereedmaken van het uiteindelijke manuscript, is het mogelijk geworden om op deze manier mijn academische vorming af te ronden. Hiervoor ben ik zeer dankbaar.

In het bijzonder ben ik dank verschuldigd aan vele medewerkers van het Medisch Biologisch Laboratorium TNO, van het Prins Maurits Laboratorium TNO en van de vakgroep "Magnetische Resonantie" van de Technische Hogeschool te Delft. Niet alleen hun inzet en toewijding in alle fasen van het onderzoek maar ook de stimulerende discussies die ik met hen mocht voeren zijn van essentiële betekenis geweest voor de voltooiing van dit gezamenlijke project. Ik hoop dat het verschijnen van dit proefschrift een nieuwe stimulans zal zijn voor samenwerking en onderlinge waardering zoals die gegroeid zijn tijdens dit gezamenlijk zoeken naar een oplossing voor één van de vele raadsels waarvoor de natuur ons nog steeds stelt.

Per correr miglior acqua alza le vele
Omai la navicella del mio ingegno
Che lascia dietro a sè mar sì crudele

Dante Alighieri: "La Divina Commedia",
Purgatorio (Canto Primo)

CURRICULUM VITAE

Na het behalen van het eindexamen gymnasium β aan het Openbaar Lyceum te Coevorden in juni 1959 begon de schrijver van dit proefschrift in oktober van hetzelfde jaar met zijn studie aan de Rijksuniversiteit te Leiden. Het kandidaatsexamen wijsbegeerte (met als bijvakken theoretische biologie en sterrenkunde) werd afgelegd in mei 1962, het kandidaatsexamen natuur- en scheikunde met wiskunde als bijvak (letter e) in juli 1963. De studie werd voortgezet onder leiding van de hoogleraren Dr. C.J.F. Böttcher, Dr. S.R. de Groot, Dr. P. Mazur en Dr. C. Visser. Het doctoraalexamen fysische chemie, met als bijvakken theoretische natuurkunde en wiskunde, werd behaald in oktober 1965.

Tot aan november 1969 was hij aanvankelijk als assistent later als hoofdassistent werkzaam op de afdeling Fysische Chemie II van de Rijksuniversiteit te Leiden. Zijn werkzaamheden bestonden daar uit het ontwikkelen van apparatuur om impedantiemetingen te kunnen doen aan sterkgeleidende, waterige oplossingen van eiwitten. Gedurende de periode november 1967 - april 1968 was hij in het kader van dit project werkzaam aan het Chelsea College of Science and Technology te Londen, hiertoe in staat gesteld door een beurs van de Wellcome Trust.

Tijdens zijn militaire diensttijd werd hij na een verkorte officiersopleiding gedetacheerd bij het Medisch Biologisch Laboratorium TNO te Rijswijk, waaraan hij sedert oktober 1970 is verbonden als wetenschappelijk medewerker van de afdeling Fysica. Zijn werkzaamheden hier betreffen de fysische chemie van biologische macromoleculen als ondersteuning en aanvulling van ander onderzoek in dit laboratorium. Een deel van het door hem in dat kader verrichte onderzoek wordt beschreven in dit proefschrift.